Vol. 146, February 1, 1983
Complete in one issue

ISSN 0003-2670

ANALYTICA CHIMICA ACTA

International journal devoted to all branches of analytical chemistry

ELSEVIER SCIENTIFIC PUBLISHING COMPANY

ANALYTICA CHIMICA ACTA

International journal devoted to all branches of analytical chemistry
Revue internationale consacrée à tous les domaines de la chimie analytique
Internationale Zeitschrift für alle Gebiete der analytischen Chemie

PUBLICATION SCHEDULE FOR 1983

	J	F	M	A	M	J	J	A	S	O	N	D
Analytica Chimica Acta	145	146	147	148	149	150/1 150/2	151	152	153/1	153/2	154	155

Scope. *Analytica Chimica Acta* publishes original papers, short communications, and reviews dealing with eve aspect of modern chemical analysis, both fundamental and applied.

Submission of Papers. Manuscripts (three copies) should be submitted as designated below for rapid and efficie handling:

Papers from the Americas to: Professor Harry L. Pardue, Department of Chemistry, Purdue University, West Lafayet IN 47907, U.S.A.

Papers from all other countries to: Dr. A. M. G. Macdonald, Department of Chemistry, The University, P.O. Box 36 Birmingham B15 2TT, England. Papers dealing particularly with computer techniques to: Professor J. T. Cle Universität Bern, Pharmazeutisches Institut, Sahlistrasse 10, CH-3012 Bern, Switzerland.

Submission of an article is understood to imply that the article is original and unpublished and is not being consider for publication elsewhere. Upon acceptance of an article by the journal, authors resident in the U.S.A. will be asked transfer the copyright of the article to the publisher. This transfer will ensure the widest dissemination of informati under the U.S. Copyright Law.

Information for Authors. Papers in English, French and German are published. There are no page charge Manuscripts should conform in layout and style to the papers published in this Volume. Authors should cons Vol. 132, p. 239 for detailed information. Reprints of this information are available from the Editors or from: Elsevi Editorial Services Ltd., Mayfield House, 256 Banbury Road, Oxford OX2 7DH (Great Britain).

Reprints. Fifty reprints will be supplied free of charge. Additional reprints (minimum 100) can be ordered. An ord form containing price quotations will be sent to the authors together with the proofs of their article.

Advertisements. Advertisement rates are available from the publisher.

Subscriptions. Subscriptions should be sent to: Elsevier Scientific Publishing Company, P.O. Box 211, 1000 A Amsterdam, The Netherlands.

Publication. *Analytica Chimica Acta* appears in 11 volumes in 1983. The subscription for 1983 (Vols. 145–155) Dfl. 1980.00 plus Dfl. 220.00 (postage) (total approx. U.S. $880.00). Journals are sent automatically by airmail to t U.S.A. and Canada at no extra cost and to Japan, Australia and New Zealand for a small additional postal charge. A earlier volumes (Vols. 1–144) except Vols. 23 and 28 are available at Dfl. 182.00 (U.S. $72.80), plus Dfl. 14.00 (U. $5.60) postage and handling, per volume.

Claims for issues not received should be made within three months of publication of the issue, otherwise they cann be honoured free of charge.

Customers in the U.S.A. and Canada who wish to obtain additional bibliographic information on this and oth Elsevier journals should contact Elsevier Science Publishing Company Inc., Journal Information Center, 52 Vanderb Avenue, New York, NY 10017. Tel: (212) 867-9040.

Reagents

MERCK

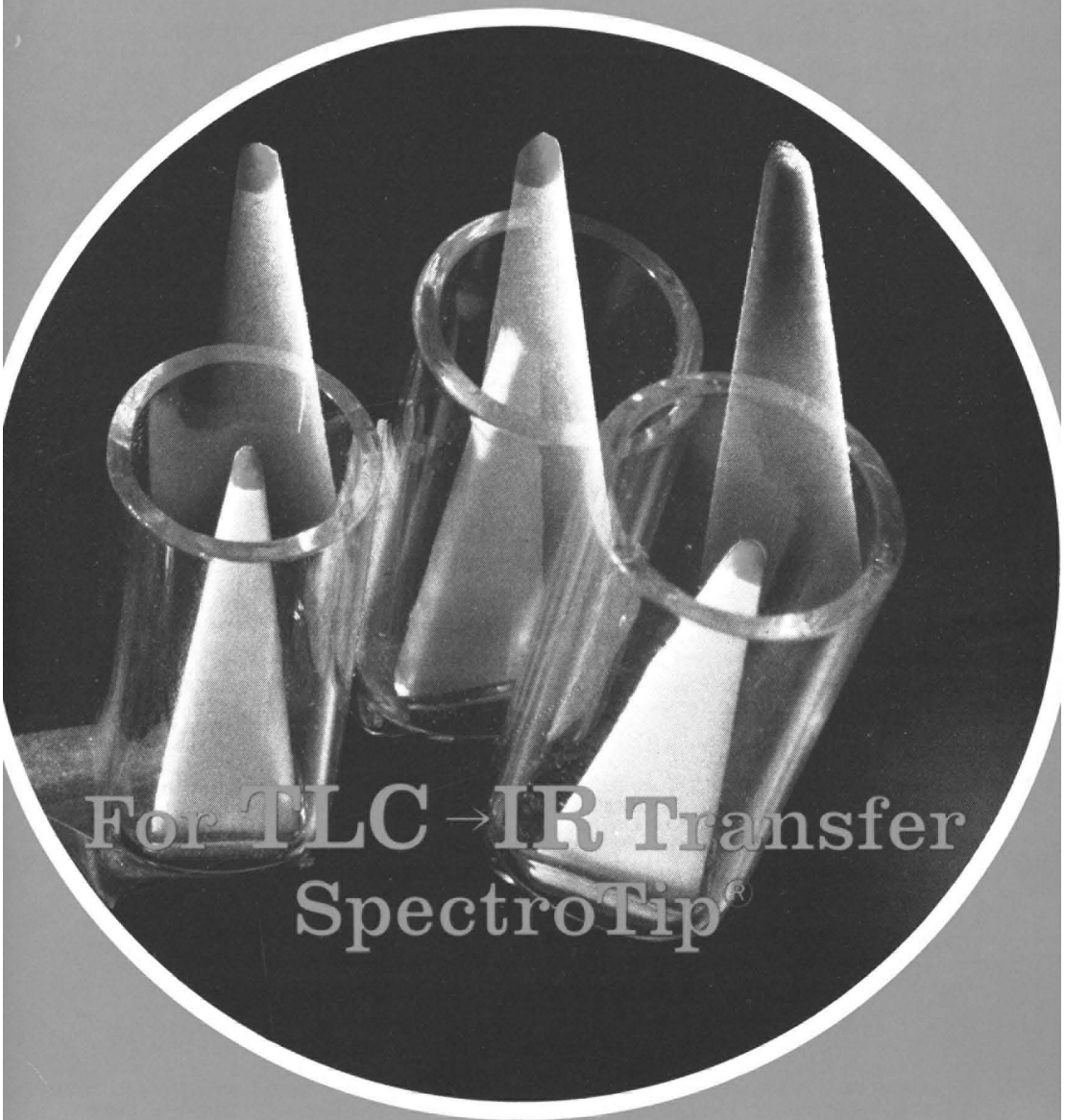

ıere are some fractions of thin-yer chromatograms which re-ıire further identification. The LC→IR transfer technique enables mple material to be transferred ıd concentrated in potassium omide, the concentration zone ing used directly to press the Br tablets.

15107 TLC-IR Transfer basic kit: 8 special cells, 8 stainless steel covers with a central hole, 1 working plate (holder for 8 cells), 1 funnel, 1 pair of tweezers, 1 dropper, 1 pack containing 39 SpectroTip® potassium bromide pyramids.

4909 SpectroTip® potassium bromide pyramids for spectroscopy Uvasol® 39 pieces (refill pack for TLC-IR Transfer basic kit).

Please send for our leaflet.

E. Merck, Darmstadt,
Federal Republic of Germany

426 E

ELECTROPHORESIS

A Survey of Techniques and Applications

edited by Z. DEYL, *Czechoslovak Academy of Sciences, Prague*

JOURNAL OF CHROMATOGRAPHY LIBRARY, 18

PART A: TECHNIQUES

Z. DEYL *(editor)*
F.M. EVERAERTS, Z. PRUSÍK *and*
P.J. SVENDSEN *(co-editors)*

"... provides a sound, state-of-the-art survey of its subject".

– Chemistry in Britain

"... the editors have set out to bring everything together into a coherent whole... they have succeeded remarkably well... the book is bound to be well liked and appreciated by readers".

– Journal of Chromatography

This first part deals with the principles, theory and instrumentation of modern electromigration methods. Both standard procedures and newer developments are discussed and hints are included to help the reader overcome difficulties frequently arising from the lack of suitable equipment. Adequate theoretical background of the individual techniques is given and a theoretical approach to the deteriorative processes is presented to facilitate further development of a particular technique and its application to a special problem. In each chapter practical realisations of different techniques are described and examples are presented to demonstrate the limits of each method.

CONTENTS:
Introduction. Chapters: 1. Theory of electromigration processes *(J. Vacík)*. 2. Classification of electromigration methods *(J. Vacík)*. 3. Evaluation of the results of electrophoretic separations *(J. Vacík)*. 4. Molecular size and shape in electrophoresis *(Z. Deyl)*. 5. Zone electrophoresis (except gel-type techniques and immunoelectrophoresis) *(W. Ostrowski)*. 6. Gel-type techniques *(Z. Hrkal)*. 7. Quantitative immunoelectrophoresis *(P.J. Svendsen)*. 8. Moving boundary electrophoresis in narrow-bore tubes *(F.M. Everaerts and J.L. Beckers)*. 9. Isoelectric focusing *(N. Catsimpoolas)*. 10. Analytical isotachophoresis *(J. Vacík and F.M. Everaerts)*. 11. Continuous flow-through electrophoresis *(Z. Prusík)*. 12. Continuous flow deviation electrophoresis *(A. Kolin)*. 13. Preparative electrophoresis in gel media *(Z. Hrkal)*. 14. Preparative electrophoresis in columns *(P.J. Svendsen)*. 15. Preparative isoelectric focusing *(P. Blanický)*. 16. Preparative isotachophoresis *(P.J. Svendsen)*. 17. Preparative isotachophoresis on the micro scale *(L. Arlinger)*. List of frequently occurring symbols. Subject Index.

1979 xvi + 390 pp. US $72.25/Dfl. 170.00
ISBN 0-444-41721-4

PART B: APPLICATIONS

Z. DEYL *(editor)*
A. CHRAMBACH, F.M. EVERAERTS *and*
Z. PRUSÍK *(co-editors)*

Part B is an exhaustive survey of the present status of the application of electrophoretic techniques to many diverse compounds. Those categories of compounds most suited to these separations, such as proteins and peptides, are dealt with in detail, while the perspectives of the applications of these techniques to other categories of compounds less commonly electrophoresed are given. Special attention is paid to naturally occurring mixtures of compounds and their treatment. This is the first attempt to cover the field on such a broad scale and the book will be valuable to separation chemists, pharmacologists, organic chemists and those involved in biomedical research.

CONTENTS: 1. Alcohols and phenolic compounds *(Z. Deyl)*. 2. Aldehydes and ketones *(Z. Deyl)*. 3. Carbohydrates *(Z. Deyl)*. 4. Carboxylic acids *(F.M. Everaerts)*. 5. Steroids and steroid conjugates *(Z. Deyl)*. 6. Amines *(Z. Deyl)*. 7. Amino acids and their derivatives *(Z. Deyl)*. 8. Peptides and structural analysis of proteins *(Z. Prusík)*. 9. Gel electrophoresis and electrofocusing of proteins *(edited by A. Chrambach)*. Usefulness of second-generation gel electrophoretic tools in protein fractionation *(A. Chrambach)*. Membrane proteins, native *(L.M. Hjelmeland)*. Membrane proteins, denatured *(H. Baumann, D. Doyle)*. Protein membrane receptors *(U. Lang)*. Steroid receptors *(S. Ben-Or)*. Cell surface antigens *(R.A. Reisfeld, M.A. Pellegrino)*. Lysosomal glycosidases and sulphatases *(A.L. Fluharty)*. Heamocyanins *(M. Brenowitz et al.)*. Human haemoglobins *(A.B. Schneider, A.N. Schechter)*. Isoelectric focusing of immunoglobulins *(M.H. Freedman)*. Contractile and cytoskeletal proteins *(P. Rubenstein)*. Proteins of connective tissue *(Z. Deyl, M. Horáková)*. Microtubular proteins *(K.F. Sullivan, L. Wilson)*. Protein hormones *(A.D. Rogol)*. Electrophoresis of plasma proteins: a contemporary clinical approach *(M. Engliš)*. Allergens *(H. Baer, M.C. Anderson)*. 10. Glycoproteins and glycopeptides (affinity electrophoresis) *(T.C. Bøg-Hansen, J. Hau,)*. 11. Lipoproteins *(H. Peeters)*. 12. Lipopolysaccharides *(P.F. Coleman, O. Gabriel)*. 13. Electrophoretic examination of enzymes *(W. Ostrowski)*. 14. Nucleotides, nucleosides, nitrogenous constituents of nucleic acids *(S. Zadražil)*. 15. Nucleic acids *(S. Zadražil)*. 16. Alkaloids *(Z. Deyl)*. 17. Vitamins *(Z. Deyl)*. 18. Antibiotics *(V. Betina)*. 19. Dyes and pigments *(Z. Deyl)*. 20. Inorganic compounds *(F.M. Everaerts, Th. P.E.M. Verheggen)*. Contents of "Electrophoresis, Part A: Techniques". Subject Index. Index of compounds separated.

1982 xiii + 462 pp. US $104.75/Dfl. 225.00
ISBN 0-444-42114-9

ELSEVIER
P.O. Box 211, Amsterdam
The Netherlands
52 Vanderbilt Avenue
New York, NY 10017, U.S.A.

ANALYTICA CHIMICA ACTA
VOL. 146 (1983)

ANALYTICA CHIMICA ACTA

International journal devoted to all branches of analytical chemistry

ELSEVIER SCIENTIFIC PUBLISHING COMPANY

Anal. Chim. Acta, Vol. 146 (1983)

Analytica Chimica Acta, 146 (1983) 1—8
Elsevier Scientific Publishing Company, Amsterdam — Printed in The Netherlands

COMPUTER DECOMPOSITION OF THE ULTRAVIOLET-VISIBLE ABSORPTION SPECTRUM OF THE METHYL VIOLOGEN CATION RADICAL AND ITS DIMER IN SOLUTION

JOYCE F. STARGARDT[a] and FRED M. HAWKRIDGE*

Department of Chemistry, Virginia Commonwealth University, Richmond, VA 23284 (U.S.A.)

(Received 14 June 1982)

SUMMARY

The first reduction of 1,1′-dimethyl-4,4′-bipyridinium dichloride (methyl viologen, MV^{2+}) results in the formation of both a monomeric, $MV^{+\cdot}$, and a dimeric $(MV^{+\cdot})_2$ product. The molar absorptivities and the wavelengths of maximum absorption for both reduction products can be determined by computer decomposition of the u.v.-visible absorption spectra resulting from the chemical and in situ electrochemical reduction of MV^{2+}. The FORTRAN computer program, SPECSOLV, is used to establish the spectral parameters of $MV^{+\cdot}$ and $(MV^{+\cdot})_2$.

The development in this laboratory of a gold electrode surface which has been electrochemically modified with 1,1′-dimethyl-4,4′-bipyridinium dichloride (methyl viologen, MV^{2+}) prompted this study. This modified gold surface exhibits measurable rates of heterogeneous electron transfer with several biological molecules [1—4]. The kinetics of the reaction of the electrochemically generated $MV^{+\cdot}$ with surface-adsorbed atomic hydrogen at gold and nickel electrodes has been recently reported [5]. This reaction does not result in the surface which is electroactive with biological molecules but was studied in an attempt to understand better the more complex reaction which does.

The purpose of this work is the assignment of accurate spectroscopic parameters so that monitoring of the species present in solution, $MV^{+\cdot}$ and $(MV^{+\cdot})_2$, during an electrode modification becomes possible.

As has been widely established, MV^{2+} undergoes two successive one-electron reduction steps to produce $MV^{+\cdot}$ and $MV^{\cdot}$, respectively. The formal potentials of these two reduction processes are —0.449 and —0.772 V vs. the normal hydrogen electrode (NHE), respectively [6—9]. The electrochemical modification of gold electrode surfaces with MV^{2+} is achieved by applying —0.720 V vs. NHE to the gold working electrode in pH 7.0 phosphate-buffered solution for 5—10 min [1—3]. This applied potential is sufficient

[a]Present address: Philip Morris U.S.A., PO Box 26583, Richmond, VA 23261, U.S.A.

to drive the first reduction step and produce the bright blue solution which contains the dimeric $(MV^{+\cdot})_2$ and monomeric $(MV^{+\cdot})$ species [10—14].

There are three solution reactions which involve $MV^{+\cdot}$ in aqueous solution which were of concern in this work. The first, oxidation of $MV^{+\cdot}$ by molecular oxygen, can be eliminated by rigorously deoxygenating sample solutions prior to electrochemical experiments. In the second, $MV^{+\cdot}$ concentrations can be altered by disproportionation; an equilibrium constant of 3.3×10^{-6} has been calculated for this reaction from the difference in the formal potentials for the two successive one-electron reduction steps for MV^{2+} [15] which indicates that loss of $MV^{+\cdot}$ by this process is negligible. A third reaction involves the dimerization of $MV^{+\cdot}$: $2\ MV^{+\cdot} \rightleftharpoons (MV^{+\cdot})_2$; the equilibrium constant for this reaction is $6.2(\pm 1.2) \times 10^2$ l mol^{-1} [16].

Both the monomeric and dimeric species have absorbance maxima in the uv.-visible absorbance region. Using 1,1′-diethyl-4,4′-bipyridinium dichloride as a "standard" viologen, Schwarz [14] assigned absorbance maxima at 731, 602, and 396 nm to the monomer and absorbance maxima at 556 and 368 nm to the dimer. These absorbance maxima were identified by diluting solutions containing the monomer and dimer.

Because the absorbance maxima of $MV^{+\cdot}$ and $(MV^{+\cdot})_2$ overlap in the u.v.-visible range, the decomposition of the spectrum from both components is required for the accurate determination of the concentrations of each species. The wavelengths of maximum absorption (λ_{max}) and the molar absorptivities (ϵ) at these wavelengths for both species were determined so that the concentrations of monomer and dimer can be calculated in a given solution. The FORTRAN program, SPECSOLV [17], was used to decompose spectra resulting both from the chemical reduction of MV^{2+} with dithionite and from the in situ electrochemical reduction of MV^{2+} at tin oxide optically transparent electrodes. The program decomposes spectra under the assumption that a spectrum contains gaussian and asymmetric gaussian component peaks.

EXPERIMENTAL

All electrode potentials are reported relative to the normal hydrogen electrode.

Reagents

Methyl viologen (1,1′-dimethyl-4,4′-bipyridinium dichloride; Aldrich) was recrystallized three times from ethanol. Sodium dithionite was reagent grade (MCB). Phosphate compounds (reagent grade; Mallinkrodt) were used to prepare pH 7.0 buffer solutions. Glycine (reagent grade; Fisher) and sodium hydroxide (reagent grade; Baker) were used to prepare pH 10.0 buffer solutions. All solutions were prepared in water which had been distilled, deionized, and then distilled again. Sodium chloride was reagent grade (VWR).

Apparatus

The electrochemical cell used in acquiring absorption spectra during the electrochemical reduction of MV^{2+} has been described [18]. Fluoride-doped tin oxide optically transparent electrodes (PPG Industries, Pittsburgh, PA) were used as the working electrodes; they exhibited a surface resistance of ca. 20 ohms square^{-1}. The Ag/AgCl, 1.0 M KCl, reference electrode used has been described [2]. A platinum wire auxiliary electrode was used in the optically transparent electrode cell.

The absorption spectra of dithionite-reduced MV^{2+} samples were obtained with a Beckman Acta MVII spectrophotometer. A Harrick rapid scanning spectrophotometer was used to obtain spectra during the electrochemical reduction of MV^{2+}. The wavelength axis of the latter instrument was calibrated before each experiment using a holmium oxide filter and the wavelength scan rate was calibrated to be 10.0 s between scans. All rapidly scanned spectra were recorded on a Houston Instruments 2000 X-Y recorder.

Procedures

The molar absorptivity of the absorption maximum at 257 nm of MV^{2+} was determined with standard solutions in pH 10.0 glycine buffer, 0.10 M. Solid samples of MV^{2+} which had been recrystallized from ethanol three times, dried at 120°C for 12 h, and then allowed to cool to room temperature in a desiccator were used to prepare the standard solutions. This procedure was repeated three times and the average value for the absorption maximum of MV^{2+} at 257 nm was used to determine the concentrations of all the MV^{2+} solutions.

Solutions of MV^{2+} in pH 10.0 glycine buffer, 0.1 M, were employed in the dithionite reduction experiments. Each sample was introduced into a 1.00-mm quartz cuvette and the absorption spectrum was recorded. Excess of solid sodium dithionite was then added to the cuvette, the cuvette was capped, and the mixture was agitated before the spectrum of the reduced MV^{2+} solution was obtained. A solution of pH 10.0 is sufficiently alkaline to permit quantitative reduction of MV^{2+} but not so alkaline as to result in decomposition. All samples were first deoxygenated with prepurified nitrogen which had been passed over hot (500°C) copper turnings and saturated with distilled water.

The chemical reduction of a solution containing MV^{2+} under these conditions produces an equilibrium mixture of both reduction products, i.e., $MV^{+\cdot}$ and $(MV^{+\cdot})_2$. The u.v.-visible absorption spectrum of the reduced sample is then decomposed into the component spectra for each species. These experiments were done for initial MV^{2+} concentrations of 0.380—0.995 mM.

The molar absorptivity values for the decomposed absorbance maxima obtained for each of the chemically reduced samples of MV^{2+} were then determined. Using the spectrally determined analytical concentration of MV^{2+} present in each sample solution prior to chemical reduction, the concentration of each reduction product, $MV^{+\cdot}$ and $(MV^{+\cdot})_2$, was calculated from

the previously reported equilibrium constant for the dimerization reaction [16] (see above). These calculated concentrations, the decomposed absorbance value for each absorbance maximum and the cell pathlength of 1.00 mm were then used to calculate the molar absorptivity for each species at each absorbance maximum. This calculation was done for the five different concentrations of MV^{2+} used in these experiments, and the average molar absorptivities were calculated for each reduction product at each absorbance maximum. The absorbance maxima for each species were calculated from average values determined from the decomposed spectra for each concentration of MV^{2+} employed. The spectral parameters were then used in the determination of the reduction product concentrations in the in situ electrochemical experiments.

The spectro-electrochemical experiments were done by vacuum-degassing MV^{2+} solutions and introducing them into the optically transparent electrochemical cell as described previously [18]. The initial potential, 0.430 V, was applied to the tin oxide electrode for 5 min before each experiment was started. The applied potential was then stepped to values sufficient to reduce MV^{2+}. The range of step potentials used here, —0.370 to —0.720 V, was selected to avoid generation of the neutral reduction product of MV^{2+} in significant quantities. After each potential step experiment, the initial potential was applied, with stirring, for sufficient time (ca. 5 min) to permit relaxation of the solution to initial conditions. After each potential step, absorption spectra were recorded from 340 to 420 nm over a 5 s period every 10 s, yielding nine absorbance spectra for each potential step.

Because the absorbing species are not uniformly distributed in solution, the thickness of the diffusion layer was used to calculate the normalized cell pathlength at a given point in time during each experiment [19]. The diffusion coefficient for MV^{2+} used in these calculations was 8.6×10^{-6} cm^2 s^{-1} [20].

Each absorption spectrum obtained during a potential step experiment was then manually digitized and decomposed using the SPECSOLV program. The concentrations of $MV^{+\cdot}$ and $(MV^{+\cdot})_2$ were then determined from the decomposed spectra using the ϵ values which had been determined in the chemical reduction experiments. These calculated concentrations were then used to calculate the equilibrium formation constant for the dimerization reaction. This calculation established the extent to which this equilibrium was maintained during the spectro-electrochemical potential-step experiments.

RESULTS AND DISCUSSION

The spectral parameters of $MV^{+\cdot}$ and $(MV^{+\cdot})_2$ were determined by chemical reduction of five solutions of MV^{2+} with sodium dithionite. Representative spectra for solutions containing MV^{2+} and the products of the dithionite

reduction reaction are shown in Fig. 1. The experimentally measured molar absorptivity of MV^{2+} at 257 nm, $(20.7 \pm 0.1) \times 10^3$ l mol^{-1} cm^{-1}, was used to determine the concentration of MV^{2+} in each solution. In reducing MV^{2+} solutions, it is necessary to use a minimum excess of dithionite in order to prevent the appearance of a large u.v. absorbance maximum at 314 nm which arises from the unreacted dithionite; this absorbance maximum is evident in trace B of Fig. 1. However, the existence of a small absorbance at 314 nm assures that the MV^{2+} has been completely reduced and that there is no residual oxygen in the sample which can react with the monomeric or dimeric radical species.

Decomposition of the reduced spectrum (i.e., trace B, Fig. 1) is accomplished by graphically determining the background (oxidized) spectrum and the spectrum of interest (reduced). In this work, the absorbance of each spectrum was measured at 5-nm increments for use in the computer program. The SPECSOLV program [17] initially subtracts the background spectrum from the spectrum of interest and then decomposes the corrected spectrum to obtain the gaussian and bi-gaussian best-fit absorption maxima within a selected tolerance level. Figure 2 shows representative decomposed spectra which were calculated from a corrected spectrum of a sample of MV^{2+} which had been reduced by dithionite. The absorbance maxima which were reproducibly resolved in all decomposition calculations are given in Table 1. The small but sharp absorbance maximum occurring at 385 nm varied and is not discussed here. The absorption maximum occurring at 405 nm is not real because SPECSOLV works best when one more peak than actually exists in the experimental spectrum is decomposed [17]. The absorbance maxima given in Table 1 agree fairly well with absorption maxima previously reported for the "standard" viologen, 1,1′-diethyl-4,4′-bipyridinium dichloride [14].

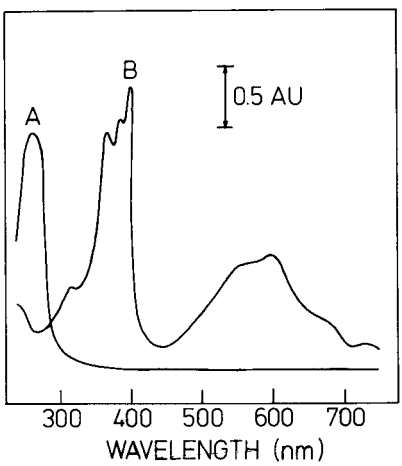

Fig. 1. Absorption spectra: A, spectrum of 1.0 mM MV^{2+} in pH 10.0 glycine buffer, 0.10 M; B, spectrum of the solution containing MV^{+} and $(MV^{+})_2$ after addition of excess of solid sodium dithionite to the solution that provided spectrum A.

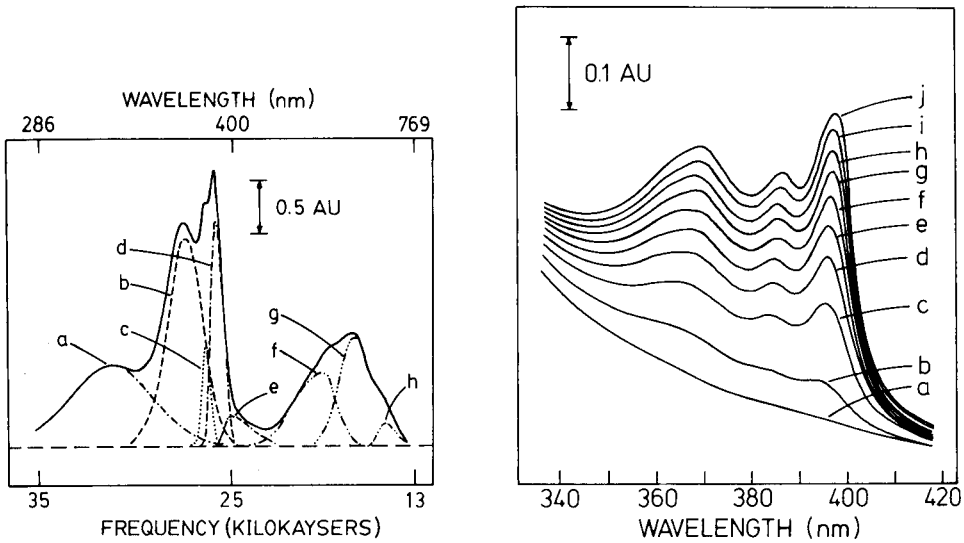

Fig. 2. Baseline-corrected absorption spectrum of reduced MV^{2+} solution and decomposed absorption maxima. The solution contained 0.995 mM MV^{2+} in pH 10.0 glycine buffer, 0.10 M. Sample reduced with an excess of solid sodium dithionite. (—) Original baseline-corrected spectrum. Decomposed spectra with peak assignment: (a, ····) 314 nm, excessive dithionite; (b, ----) 369.1 nm, $(MV^{+})_2$; (c, ····) 385 nm, unassigned peak; (d, ---) 395.7 nm, MV^{+}; (e, ----) 405 nm, artifact from SPECSOLV; (f, ·····) 537.1 nm, $(MV^{+})_2$; (g, ····) 604.4 nm, MV^{+}(h, ----) 675.1 nm, MV^{+}.

Fig. 3. Absorption spectra of the in situ electrochemical reduction of MV^{2+} at a tin oxide optically transparent electrode. The solution contained 1.0 mM MV^{2+} in pH 7.0 phosphate buffer, 0.10 M, and 0.10 M NaCl. Each spectrum was scanned in 5.0 s. The time at the start of recording each spectrum after application of —0.720 V to the tin oxide optically transparent electrode was: (a) —60 s; (b) 0 s; (c) 10 s; (d) 20 s; (e) 30 s; (f) 40 s; (g) 50 s; (h) 60 s; (i) 70 s; (j) 80 s.

TABLE 1

Spectral parameters determined from the decomposition of absorption spectra obtained on solutions of MV^{2+} reduced with sodium dithionite[a]

Species	λ_{max} (nm)	ϵ (10^4 l mol^{-1} cm^{-1})
MV^{+}	675.1(±1.5)	0.38(±0.01)
MV^{+}	604.4(±1.8)	1.69(±0.01)
MV^{+}	395.7(±0.4)	3.49(±0.01)
$(MV^{+})_2$	537.1(±6.2)	3.24(±0.05)
$(MV^{+})_2$	369.1(±1.8)	8.97(±0.03)

[a]Spectral parameters were calculated from results obtained in five separate experiments in which the analytical concentration of MV^{2+} was 0.380, 0.509, 0.615, 0.841, and 0.995 mM. Numbers in parentheses are standard deviations.

TABLE 2

Dimerization equilibrium constants calculated from potential step spectro-electrochemical experiments[a]

Applied potential (mV)	K (10^2 l mol^{-1})
−720	6.4(±1.8)
−620	7.3(±3.7)
−570	8.4(±3.2)
−520	7.3(±2.3)
−495	6.7(±0.7)
Average value:	7.2(±0.8)

[a]At each applied potential the equilibrium constant was calculated at the following times during the potential step experiment: 41, 51, 61, 71, and 81 s. Numbers in parentheses are standard deviations.

Typical results obtained for the optical monitoring of the reduction of MV^{2+} at tin oxide optically transparent electrodes are shown in Fig. 3. These results were obtained to determine the extent to which the reduction products obeyed the dimerization equilibrium constant which was previously reported [16]. This data analysis is subject to consideration of the non-uniform distribution of products as a function of distance from the electrode surface as described previously. Because the concentration of reduction products is greatest at the electrode surface, the position of the equilibrium for the dimerization would be shifted to the right compared to the equilibrium condition existing at various distances into solution. Nevertheless, the results shown in Table 2 indicate that the average equilibrium constant for the reduction products of MV^{2+} is in good agreement with the previously published value for the equilibrium constant, $6.2(\pm 1.2) \times 10^2$ l mol^{-1} [16].

The results of this work indicate that the concentrations of the reduction products of MV^{2+} can be established as functions of time and applied potential by using the spectral decomposition procedure described herein. The decomposed spectra shown in Fig. 2 also provide guidance in the selection of monitoring wavelengths in spectro-electrochemical experiments which are sensitive to the $MV^{+\cdot}$ and $(MV^{+\cdot})_2$ species alone.

The authors gratefully acknowledge numerous discussions with H. S. Gold in implementing the SPECSOLV program. This investigation was supported by NIH Grant GM 27208-02. F. M. H. gratefully acknowledges the support of the Department of Chemistry, The University of Delaware, in the form of a sabbatical during the preparation of this manuscript.

REFERENCES

1 H. L. Landrum, R. T. Salmon and F. M. Hawkridge, J. Am. Chem. Soc., 99 (1977) 3154.

2 J. F. Stargardt, F. M. Hawkridge and H. L. Landrum, Anal. Chem., 50 (1978) 930.
3 E. F. Bowden, F. M. Hawkridge and H. N. Blount, Bioelectrochem. Bioenerg., 7 (1980) 447.
4 C. D. Crawley and F. M. Hawkridge, Biochem. Biophys. Res. Commun., 99 (1981) 516.
5 E. F. Bowden and F. M. Hawkridge, J. Electroanal. Chem., 125 (1981) 367.
6 L. Michaelis and E. S. Hill, J. Gen. Physiol., 16 (1932) 859.
7 L. Michaelis and E. S. Hill, J. Am. Chem. Soc., 55 (1933) 1481.
8 R. M. Elofson and R. L. Edsberg, Can. J. Chem., 35 (1957) 644.
9 T. Osa and T. Kuwana, J. Electroanal. Chem., 22 (1969) 389.
10 A. W. Hofmann, Chem. Ber., 14 (1881) 1497.
11 E. Weitz and R. Ludwig, Chem. Ber., 55B (1922) 395.
12 E. Muller and W. Wiesemann, Chem. Ber., 69 (1936) 2157.
13 L. Michaelis, Biochem. Z., 250 (1932) 564.
14 W. M. Schwarz, Jr., Ph. D. Dissertation, The University of Wisconsin, Madison, WI (U.S.A.), 1961.
15 N. Winograd, H. N. Blount and T. Kuwana, J. Phys. Chem., 73 (1969) 3456.
16 R. N. F. Thorneley, Biochim. Biophys. Acta, 333 (1974) 487.
17 H. S. Gold, C. E. Reichsteiner and R. P. Buck, Anal. Chem., 48 (1976) 1540.
18 F. M. Hawkridge and T. Kuwana, Anal. Chem., 45 (1973) 1024.
19 A. J. Bard and L. R. Faulkner, Electrochemical Methods, Wiley, New York, 1980, p. 129.
20 E. Steckhan and T. Kuwana, Ber. Bunsenges. Phys. Chem., 78 (1974) 253.

Analytica Chimica Acta, 146 (1983) 9—14
Elsevier Scientific Publishing Company, Amsterdam — Printed in The Netherlands

THREE-DIMENSIONAL RANK ANNIHILATION FOR MULTI-COMPONENT DETERMINATIONS

C. J. APPELLOF and E. R. DAVIDSON*
Department of Chemistry, University of Washington, Seattle, WA 98195 (U.S.A.)
(Received 26th April 1982)

SUMMARY

The method of rank annihilation for multi-component determinations is extended to a three-dimensional data array. The possibility of improved sensitivity over the two-dimensional method is shown. An illustration using data of the type expected from a liquid chromatograph with a video-fluorimeter as detector is presented. Partial separation of the sample by the liquid chromatograph leads to improved sensitivity in the data analysis of the excitation or emission covariance matrices.

The technique of two-dimensional (2-D) rank annihilation has been used for the determination of fluorescent compounds in mixtures [1, 2]. The major advantage over other data-processing techniques is that a single compound in a mixture can be quantified without knowing what other compounds are in the mixture. Sensitivity criteria have been developed which indicate that the accuracy of determination of a compound concentration using 2-D rank annihilation depends on the spectral overlap of that compound with the other components of the solution [2]. In this paper, we show that by using three-dimensional (3-D) data, better accuracy should be obtained and possible spectral overlap problems avoided. The method is applied to data of the type expected from liquid chromatographic separation with video-fluorimetric detection (v.f./l.c.), but should apply equally well to other types of data.

THEORY

In 2-D rank annihilation [1, 2], the data processed is a two-dimensional emission—excitation matrix (EEM), M, the *ij* member of which is the fluorescence emission intensity of a solution at wavelength λ_i when excited by light of wavelength λ_j. For a dilute solution of r components, the EEM is a linear combination of standard EEM matrices.

$$M_{ij} = \sum_{p=1}^{r} \alpha_p x_{ip} y_{jp} \qquad (1)$$

where x_{ip} is the normalized, digitized emission spectrum for component p, y_{jp} is the normalized excitation spectrum, and the relative intensity α_p is proportional to the concentration. The rank of the matrix M should be equal to the number of independent components in the sample. Other sources of two-dimensional data, such as gas chromatography/mass spectrometry, also produce data of this form, and are amenable to the same data-processing schemes.

The determination of one compound in a multi-component solution by the method of rank annihilation proceeds by subtraction of a multiple of the standard EEM matrix N, for the pure solution, from the EEM matrix of the mixed solution to form a residual matrix $\mathbf{E} = \mathbf{M} - \beta\mathbf{N}$. Then, the covariance matrix, $\mathbf{D} = \mathbf{E}^T\mathbf{E}$, of E is formed and eigenvectors are established. When the proper multiple (β) of the standard matrix of the analyte has been subtracted from the mixture matrix, the lowest non-zero eigenvalue, ξ^2, of D should become zero. In practice, because of errors in the data, this eigenvalue does not become exactly zero, but does reach a minimum. At that point, the multiplier β of the standard matrix is equal to the concentration of this compound in the mixture, relative to its concentration in the standard solution.

As shown earlier [2], the accuracy of this determination is proportional to the fluorescence intensity of the analyte at unit concentration (α_1^0), and to the uniqueness of the analyte relative to the other components in the mixture. The uniqueness of the emission spectrum of the first compound in the mixture is defined [2] as

$$q_x = (1 - \mathbf{s}^T\mathbf{S}^{-1}\ \mathbf{s}) \tag{2}$$

where $s_p = \Sigma_i x_{ip} x_{i1} (p > 1)$ and $S_{pq} = \Sigma_i x_{ip} x_{iq}$ $(p, q > 1)$. The uniqueness of the excitation spectrum, q_y, is similarly defined. The uniqueness of either spectrum depends on the overlap of the analyte spectrum with the spectra of the other compounds in the mixture. If the spectrum of the analyte is very similar to a superposition of the other spectra, the uniqueness will be close to zero; if the spectrum is very different, the uniqueness will be close to one.

The error in the estimated concentration caused by errors in the measured data matrix is

$$\sigma^2(\beta) = (\partial^2\xi^2/\partial\beta^2)^{-1}\ \sigma^2\ (\mathbf{M}) \tag{3}$$

if the error in the data matrix does not depend on wavelength [3]. At the minimum of ξ^2,

$$\partial^2\xi^2/\partial\beta^2 = 2\ (\alpha_1^0)^2\ q_x q_y \tag{4}$$

so the sensitivity of the analysis by rank annihilation, which is defined here as $\partial^2\xi^2/\partial\beta^2$, is proportional to $q_x q_y$.

This paper presents an extension of this two-dimensional data-processing technique to the problem of processing a three-dimensional array of data

obtained, for example, from liquid chromatographic separation with video-fluorimetric detection (v.f./l.c.) [4]. These data are in the form of an array M_{ijk}, which measures the fluorescence emission intensity at wavelength λ_i when the sample collected at elution time t_k is excited by light with wavelength λ_j. For dilute solutions, this array, like its two-dimensional counterpart, is a linear combination of products of one-dimensional spectra:

$$M_{ijk} = \sum_{p=1}^{r} \alpha_p x_{ip} y_{jp} z_{kp} \tag{5}$$

where z_{kp} is the h.p.l.c. profile of compound p.

To start the calculation, the three covariance matrices $C(x)$, $C(y)$, and $C(z)$ are eigen-analyzed, where

$$C_{ii'}(x) = \sum_{jk} M_{ijk} M_{i'jk}$$

$$C_{jj'}(y) = \sum_{ik} M_{ijk} M_{ij'k} \tag{6}$$

$$C_{kk'}(z) = \sum_{ij} M_{ijk} M_{ijk'}$$

For error-free data, the number of non-zero eigenvalues of each matrix should be equal to the number of components in the sample. In practice, because of errors in the data, an estimate must be made of the number of eigenvalues which are large compared to zero. This number is then used as an estimate of the number of detectable components in the sample. Then, a procedure analogous to 2-D rank annihilation is followed. Some of a standard 3-D data array N for one component is subtracted from the mixture array: $E_{ijk} = M_{ijk} - \beta N_{ijk}$. Then one of the covariance matrices of E is formed and eigen-analyzed. The value of β which makes the lowest non-zero eigenvalue a minimum is the concentration of this component in the sample relative to its concentration in the standard solution. To reduce the calculations involved, the original data array and the standard array can be transformed to a reduced space as described earlier [1, 4].

As before [2], the accuracy of the calculated concentration will depend on how sensitive the lowest eigenvalue is to changes in concentration near the minimum. In two dimensions, this depends on the intensity of the standard at unit concentration and the uniqueness of the standard emission and excitation spectra (Eqn. 3). For three-dimensional data, there are three covariance matrix eigenvalues that could be examined, and these give three different sensitivity criteria:

$$\partial^2 \xi^2(x)/\partial \beta^2 = 2(\alpha_1^0)^2 \, q_x q_{yz} \tag{7}$$

$$\partial^2 \xi^2(y)/\partial \beta^2 = 2(\alpha_1^0)^2 \, q_y q_{xz} \tag{8}$$

$$\partial^2 \xi^2(z)/\partial \beta^2 = 2(\alpha_1^0)^2 \, q_z q_{xz} \tag{9}$$

The q's with a single subscript are the same uniqueness indices which are cal-

culated for 2-D data, and just depend on the overlap of the standard emission, excitation, and chromatograms with those of the other components in solution. However, the doubly subscripted q's are calculated from two-dimensional overlaps. For q_{yz} in Eqn. (7) for instance,

$$q_{yz} = (1 - s^T[yz]\ S^{-1}[yz]\ s[yz]) \tag{10}$$

where $s_p(yz) = (\sum_j y_{jp} y_{j1})(\sum_k z_{kp} z_{k1})$

and $S_{pq}(yz) = (\sum_j y_{jp} y_{jq})(\sum_k z_{kp} z_{kq})$ $(p, q > 1)$

The factor q_{yz} in Eqn. (7) will always be larger than q_y in Eqn. (4) and q_{xz} in Eqn. (8) will be larger than q_x in Eqn. (4), so the use of 3-D processing may provide better sensitivity than a 2-D processing if the signal intensity is the same.

It is usually the case that the lowest eigenvalue of one of the three covariance matrices is less sensitive to errors in the data than the other two. Therefore, the concentration corresponding to the minimum of that eigenvalue is more accurate than that determined by the other two. In extreme cases, when the spectrum of the analyte totally overlaps the spectra of the other components in one of the dimensions (e.g., the emission spectrum), a change in the subtracted concentration will have no effect on the lowest eigenvalue of the corresponding covariance matrix. In that case, one of the other covariance matrices must be used to determine the true concentration of the standard. In this way, a 3-D array gives more flexibility in choosing the most appropriate covariance matrix, and in the extreme case, can provide results when a 2-D procedure would fail completely.

Equation (9) can be evaluated only if all of the components in the solution are known. Because rank annihilation is designed to work without this knowledge, an alternative formula must be used to estimate the sensitivity. For noise-free data, when the minimum of the lowest eigenvalue has been found, the uniqueness can be calculated from the overlap of the eigenvector corresponding to this eigenvalue with the corresponding eigenvector from the standard analyte spectrum. For instance, if there are K components in the mixture, the Kth eigenvalue should reach a minimum; and for a standard with normalized spectral vectors x, y, and z,

$$q_x = \sum_i x_i v_{iK} \tag{11}$$

where $\mathbf{v}_K$ is the Kth eigenvector of the emission covariance matrix of E. To calculate q_{yz}, it is necessary to form the covariance matrix:

$$D_{(jk)(j'k')}(yz) = \sum_i E_{i(jk)} E_{i(j'k')} \tag{12}$$

This matrix has a row index of (jk) and a column index of $(j'k')$. For a K-component mixture, the Kth eigenvalue of this matrix will reach a minimum for the same choice of β. The Kth eigenvector, $\mathbf{w}_K$, can be used to compute

$$q_{yz} = \sum_{jk} y_j z_k w_{(jk)\,K} \tag{13}$$

The uniqueness indices q_y, q_{xz}, q_z, and q_{xy} can be calculated in a similar way.

RESULTS AND DISCUSSION

The excitation and emission spectra for perylene, fluoranthene, tetracene and 9,10-dimethylanthracene were obtained by eigenanalysis of EEM's taken with a video-fluorimeter [2]. Then, h.p.l.c. elution profiles for each compound were simulated as strongly overlapping Gaussian peaks and random noise was added. The noise had a uniform distribution with a maximum magnitude which was 10% of the root-mean-square value of the data array. Table 1 lists the true relative concentrations of the components in the simulated data, as well as the concentrations calculated by rank annihilation.

Table 2 compares the uniqueness indices calculated by Eqn. (2) to those calculated by Eqn. (10). As can be seen, the 3-D indices for excitation and emission are larger than the corresponding 2-D index. Even a partial h.p.l.c. separation into overlapping peaks improves the sensitivity. Table 2 also compares the 3-D uniqueness indices calculated by Eqn. (10) to those calculated by Eqns. (11—13). The difference between these last two columns of Table 2 is caused by the random noise.

When the uniqueness indices in this table are considered, it can be seen, for example, that to obtain the most sensitive determination of fluoranthene, the lowest non-zero eigenvalue of the excitation covariance matrix should be minimized. It is also seen that because of the large overlap put into the h.p.l.c. simulation, the h.p.l.c. covariance matrix is predicted to give the least sensitive results. These predictions are supported by Table 1.

TABLE 1

Relative concentrations of compounds for the simulated data matrix

	True	Calculated	Error
Perylene	5.638	5.691[a]	+0.053
		5.694[b]	+0.056
		5.729[c]	+0.091
Fluoranthene	1.122	1.140[a]	+0.018
		1.177[b]	+0.055
		1.236[c]	+0.114
Tetracene	11.13	11.12[a]	—0.01
		11.10[b]	—0.03
		11.15[c]	+0.02
9,10-Dimethyl-anthracene	22.26	22.27[a]	+0.01
		22.29[b]	+0.03
		22.28[c]	+0.02

[a]Calculated from excitation covariance matrix. [b]Calculated from emission covariance matrix. [c]Calculated from h.p.l.c. covariance matrix.

TABLE 2

Square of uniqueness indices for the simulated data matrix

	2-D	3-D	
		True[a]	Calculated[b]
Perylene	0.0677	0.1827[c]	0.1708[c]
		0.1962[d]	0.2107[d]
		0.2251[e]	0.2098[e]
Fluoranthene	0.0750	0.2915[c]	0.2775[c]
		0.1016[d]	0.0938[d]
		0.0918[e]	0.0829[e]
Tetracene	0.1274	0.2536[c]	0.2527[c]
		0.3055[d]	0.2718[d]
		0.0729[e]	0.0821[e]
9,10-Dimethyl-anthracene	0.2647	0.5615[c]	0.5527[c]
		0.4257[d]	0.4237[d]
		0.1960[e]	0.2066[e]

[a]Eqns (7)—(9) and Eqn. (10). [b]Eqns. (7)—(9) and (11)—(13). [c]Calculated for excitation covariance matrix. [d]Calculated for emission covariance matrix. [e]Calculated for h.p.l.c. covariance matrix.

The authors thank Leon Hershberger and Chu-Ngi Ho for providing the experimental data. This work was supported by NIH grant number GM-22311.

REFERENCES

1 C. N. Ho, G. D. Christian and E. R. Davidson, Anal. Chem., 50 (1978) 1108.
2 C. N. Ho, G. D. Christian and E. R. Davidson, Anal. Chem., 52 (1980) 1071.
3 I. W. Warner, G. D. Christian and E. R. Davidson, Anal. Chem., 49 (1977) 564.
4 L. W. Hershberger, J. B. Callis and G. D. Christian, Anal. Chem., 51 (1979) 1444.

Analytica Chimica Acta, 146 (1983) 15—27
Elsevier Scientific Publishing Company, Amsterdam — Printed in The Netherlands

AN EVALUATION OF AUTOMATED SPECTRUM MATCHING FOR SURVEY IDENTIFICATION OF WASTEWATER COMPONENTS BY GAS CHROMATOGRAPHY—MASS SPECTROMETRY

W. M. SHACKELFORD* and D. M. CLINE

U.S. Environmental Protection Agency, Environmental Research Laboratory, Athens, GA 30613 (U.S.A.)

L. FAAS and G. KURTH

Computer Science Corporation, Falls Church, VA (U.S.A.)

(Received 25th June 1982)

SUMMARY

An automated system for extracting spectra and matching them against a library of reference spectra was assembled and tested on 20000 g.c.-m.s. data files over a period of 2.5 years. The files were for actual field samples and were surveyed for all compounds rather than for a target list. No prior assumptions about sample content could be made. The reliability of spectrum matching is shown to be enhanced from the use of retention data accumulated in an historical library. An overall reliability of 71% is shown for matched spectra in field samples as demonstrated by re-processing of sample extracts.

The use of gas chromatography/mass spectrometry (g.c.-m.s.) with computer-controlled data acquisition and reduction has become the recommended practice for identification of organic pollutants in environmental samples [1, 2]. As can be noted for many samples, however, comparatively few components in any given sample will be a member of some preselected list (such as priority pollutants) [3, 4].

In this study, the probability based matching (PBM) system [5, 6] was used to augment and, in many cases, supplant conventional efforts in component identification so that large numbers of components could be tentatively identified in the most cost-effective way. The goals of this study were: (a) to define the effectiveness of spectrum matching on field samples, and (b) to determine the reliability of the answers generated by spectrum matching. Sample extracts corresponding to selected data files that were processed by the computer were re-examined for the specific compounds identified by spectrum matching [7]. These confirmatory data demonstrate the confidence that can be placed in matching results.

Although previous studies [5—8] have evaluated the use of search systems, the spectra used for unknowns in those studies were known to be of high quality. In this study, the unknown spectra in almost every case were truly

unknowns in that neither was there prior knowledge of the sample contents available nor was there any guarantee that the spectra submitted for matching were uncontaminated.

Over the 2.5-year duration of this study, some 225 000 spectra were submitted for spectrum matching. Over 30% of the spectra submitted were matched with spectra in the reference library to a degree sufficient that the unknown was considered to be tentatively identified and entered into an historical library.

EXPERIMENTAL

Data used in this study were obtained from a comprehensive study of wastewater from industrial and publicly owned treatment works sponsored by the Effluent Guidelines Division of the U.S. Environmental Protection Agency. Some 4000 samples were taken over a broad range of industrial processes and g.c.-m.s. data were obtained for 114 specific organic compounds (priority pollutants) at twenty different laboratories across the country. All raw g.c.-m.s. data were saved on magnetic tape for survey evaluation. The extract of each extractable fraction from each sample was also sent to the Environmental Research Laboratory, Athens, GA, for confirmation of the survey results. Detailed descriptions of the experimental procedures can be found elsewhere as noted.

Computer system [3]

The computer system consists of four main parts: inventory, spectrum extraction, spectrum matching, and historical library. Because of the number of g.c.-m.s. data files involved (some 22000) a rather elaborate data management system was used for inventory of both the data files and extracts. The INFORM (United Computing Systems, Kansas City, MO) system allows cross-referencing, sorting, and search/retrieval so that correlations of the data by analytical technique, laboratory, or other descriptive parameter are conveniently made.

Spectra were extracted by using the program CLEANUP [9], which was obtained from T. C. Rindfleisch at Stanford University. As reported by the originators of CLEANUP [9], components eluting within two scans of each other cannot, for the most part, be separated. Thus, for complicated data files, many of the extracted spectra are contaminated by one or more other compounds.

Matching an unknown spectrum with a reference spectrum involves two steps, a spectrum match by PBM and a retention data match with the historical library. The spectrum matching program, PBM, was obtained from F. W. McLafferty at Cornell University. A version of PBM evaluated and described previously [5] was used with modifications by Atwater [10] and our group. Modifications such as spectrum subtraction [10], spectrum tilting [10], and reliability ranking [10] were not employed. Both spectrum sub-

traction and spectrum tilting require operator intervention to a greater degree than was desired in this study. Reliability ranking was supplanted by the use of retention data and the use of another ranking factor explained below. The historical library concept has been used in several laboratories [11—15] and was used in this study to add confidence to a given spectrum match by the application of retention data.

Each file examined contained one or more internal standards. Retention data relative to the nearest internal standard were collected for each spectrum chosen for matching. In the acid and base/neutral fractions, only anthracene-d_{10} was used as an internal standard; in the purgeable fractions both bromochloromethane and 1,4-dichlorobutane were used.

To initialize the historical library, several commonly found homologous series were run at two laboratories to generate retention data. Thus, for such series as methyl esters of fatty acids, alkanes, alkylbenzenes, ketones, and others, retention data greatly aided initial identification attempts.

Hardware [3]. For all ADP functions, either a Digital Equipment Corporation PDP 11/70 or PDP 11/34 computer was used. Magnetic discs and tapes were used for both temporary and permanent data storage.

Laboratory procedures [1]

The procedures applied in the twenty laboratories followed a common protocol that has been continuously updated since March 1977 [1]. A purgeable fraction and base/neutral- and acid-extractable fractions for each sample taken in the field were examined by packed column g.c.-m.s. One internal standard, anthracene-d_{10}, was added to the final extract of the acid and base/neutral fraction. Two internal standards, bromochloromethane and 1,4-dichlorobutane, were added to the purgeable fraction. During the whole of the study, two g.c. column liquid phases were used for the purgeable fraction (0.2% Carbowax 1500 and 1% SP-1000), two liquid phases were used for the acid extracts (Tenax GC and 1% SP-1240 DA), and three liquid phases were used for the base/neutral extracts (1% SP-2250, 3% SP-2250, 3% SP-2250 DB). In two sets of data, capillary columns were used for chromatography. One laboratory employed a 0.3-mm i.d., 30-m glass capillary coated with OV-17 for both acid and base/neutral fractions, whereas a second laboratory processed a group of samples using a 0.25-mm i.d., 30-m fused silica capillary coated with SE-54. Column performance was checked by the chromatography of test compounds (benzidine, pentachlorophenol) and g.c.-m.s. performance was required to meet the specifications set forth by Eichelberger et al. [16].

The g.c.-m.s. systems included a Finnigan 3200, Finnigan 4000, Finnigan OWA, Hewlett-Packard 5985, Hewlett-Packard 5982, Hewlett-Packard 5993B, and DuPont Dimaspec. Computers employed in acquisition included Systems Industries System 150, Finnigan Incos, and Hewlett-Packard data systems.

To confirm the tentative identifications made by spectrum matching, selected extracts were chosen and re-processed using glass capillary column g.c.-m.s. at a single laboratory. Because the vast majority of samples had

originally been processed using packed column g.c.-m.s., the expected improvement in chromatographic resolution in the re-examination was deemed a positive influence in determining the presence or absence of a matched component. Capillary columns used in the confirmatory study included Carbowax (0.5-mm i.d., 50-m), SE-30 (0.5-mm i.d., 50-m) and CP SIL-5 (0.25-mm i.d., 25-m).

Confirmation proceeded in two steps. The extract was subjected to capillary column g.c.-m.s. and each of the compounds tentatively identified by spectrum matching was sought in the data from the re-examination. Standards of each of the compounds found in the re-examination were then added to the extract for a second g.c.-m.s. experiment. Confirmation was made on the basis of co-elution with the standard as well as by comparison of the mass spectrum of the unknown with that of the standard.

Reference library [17, 18]

Three reference libraries were evaluated for this study. The Wiley Library of Mass Spectra contains 30476 spectra of 30476 compounds. The EPA-NIH Library contains 34363 compounds, many of which are in the Wiley Library also. Finally, the EPA master data base that contains over 40000 spectra of about 32000 compounds was available locally. Because all three libraries contained spectra unique to each, the libraries were combined.

RESULTS AND DISCUSSION

Matching effectiveness

The success of the matching program can be gauged by the number of correct and incorrect answers returned from a known set of data. In this work, however, the estimation of matching success depends upon several unknown factors which complicate matters somewhat. First, spectra were chosen by a computer algorithm that, although having built-in allowances for noise and column bleed, could not distinguish between many common chromatography artifacts and the compounds of interest. For instance, if an instrument had a poorly conditioned septum, the algorithm found the resulting silicone peaks as if they were sample components. Neither the matching program nor the data analysis could specifically identify spectra of this sort for the most part, although the chemical class of silicones was obvious. Also, if sample components eluting at the end of the temperature program appeared to be broad peaks not unlike column bleed artifacts, the CLEANUP program would ignore them in many cases.

A second complicating factor was that only in a very few cases, even with standards, were all the components separated by the chromatograph to such an extent that pure spectra were obtained for all components. In cases of contamination, the analyst must make the decision whether one or more components are present. This decision, in all but the most obvious of cases (Fig. 1), was found to be difficult.

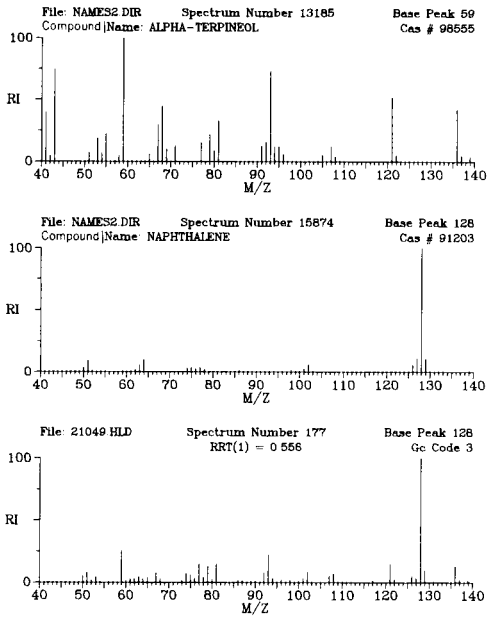

Fig. 1. Spectrum of two components not separated by CLEANUP but both identified by PBM.

Finally, in this study the matches were reconfirmed by capillary g.c.-m.s. In no case was there any guarantee that components in the extract would not degrade over time. In fact, degradation of some components was seen to occur at the confirming laboratory during the time period between the initial and confirmatory studies.

Table 1 summarizes, by gas chromatographic column and fraction type, the overall effectiveness of the automated system. It is important to note that all spectra sent to the matching program were chosen by the CLEANUP algorithm. Thus, even though there are errors of omission and commission in the choosing of spectra, these errors should be constant across the various

TABLE 1

Comparison of g.c. columns and fraction type with matching efficiency

Column	Fraction type	Spectra matched (%)	
		Samples	Standards
0.2% Carbowax 1500 on Carbopak C (packed)	Purgeable	57	70
SP-1240 DA (packed)	Acid	27	77
3% SP-2250 (packed)	Base/neutral	26	71
SE-54 fused silica (capillary)	Acid-base/ neutral (combined)	65	85

data sets. The information to be gained from Table 1 is twofold. First, it is apparent from the data shown that the capillary column chromatography results in a greater fraction of matched spectra than with the packed columns. Second, the compounds present in the fraction make a decided difference in the matching efficiency. Note that the purgeable fraction, though chromatographed on a packed column, yielded 57% matchable spectra. It is believed that this efficiency is due to the preponderance of compounds with distinctive spectra such as low-molecular-weight halogenated compounds. For most samples, the base/neutral and acid fractions contained a large number of obviously unresolved components. Because the possible set of answers was in no way thought to be a subset of the reference library, discrimination to false positive results by PBM was tested severely.

The data on standards showed very little difference among the matching efficiencies for the packed columns. The acid fraction contained only 11 compounds, whereas the purgeable and base/neutral fractions contained 31 and 42 compounds respectively. With standards also, the capillary column showed an appreciable advantage in providing matchable spectra.

The data in Table 1 should be viewed not as an absolute indication of spectral matching ability, but rather as a relative measure of experimental factors that improve matching ability. For instance, if the possible set of sample components is limited, as in the purgeable fraction, the rate of component matching will be higher. Likewise, the better the chromatographic resolution, the better will be the matching efficiency. The values in this table reflect the leniency of component recognition by CLEANUP as much as the matching ability of PBM. In order to insure that components were not missed by CLEANUP, spectra were accepted that turned out to be artifacts.

Extracts containing compounds found frequently by the matching system were sent to the confirming laboratory for study. There were 827 compounds to be confirmed in the 436 extracts sent for study. Because many of the compounds were found in more than one extract, each occurrence of a compound was confirmed. Of the total of 2373 occurrences to be confirmed, 71% were found in the initial re-examination by capillary column g.c.-m.s. The occurrence of the new results with PBM at this point corresponds to matching at the Class II level as defined by Pesyna et al. [5] (identical compound, stereoisomer, or positional isomer). Of those confirmed at the Class II level, 91% were additionally confirmed at the Class I level (identical compound or stereoisomer) by co-injection of standards.

The extracts used for the confirmation had been stored for periods of time up to 2.5 years, and no data exist for the great majority of compounds for stability in dichloromethane extracts. Although a concerted effort was made to insure correct documentation for each sample through quality control procedures, it is apparent that errors are present that cause wrong assignment of an extract to the wrong g.c.-m.s. data file. Because about 8% of the extracts re-examined showed no correspondence with either the PBM results or the reconstructed gas chromatogram of the original sample, we estimate this to be the upper limit of documentation errors.

TABLE 2

Comparison of retention data with K and K_{max} for selected compounds

Compound (CASRN)	Number of occurrences	G.c. column	S.d.[a]	K		K/K_{max}	
				Median	Range	Median	Range
2-Butanone [78-99-3]	67	0.2% Carbowax 1500	±0.062	36	62–20	0.57	0.86–0.41
1,1,2,2-Tetrachloroethane [79-34-5]	93	0.2% Carbowax 1500	±0.007	65	99–25	0.65	1.00–0.26
α-Pinene [80-56-8]	82	0.2% Carbowax 1500	±0.067	67	89–42	0.74	1.00–0.48
2-Chlorophenol [95-57-8]	18	SP-1240 DA	±0.043	52	78–38	0.56	0.79–0.41
Benzoic acid [65-85-0]	298	SP-1240 DA	±0.035	66	100–22	0.74	1.00–0.38
Stearic acid [57-11-4]	66	SP-1240 DA	±0.053	88	138–44	0.63	0.95–0.30
α-Terpineol [98-55-5]	224	3% SP-2250	±0.041	72	97–38	0.74	1.00–0.38
Diethylphthalate [84-66-2]	222	3% SP-2250	±0.012	75	113–36	0.66	1.00–0.32
Cholesterol [57-88-6]	79	3% SP-2250	±0.055	111	193–41	0.54	1.00–0.19
α-Picoline [108-89-4]	21	SE-54 FSCC	±0.007	59	74–43	0.64	0.80–0.46
Nitrobenzene [98-95-3]	20	SE-54 FSCC	±0.004	73	83–45	0.82	0.89–0.47
Fluorenone [486-25-9]	10	SE-54 FSCC	±0.001	87	95–55	0.92	1.00–0.58

[a]Standard deviation of the relative retention.

The 9% of the identified target compounds that was not confirmed by co-injection of standards was found to be more or less equally divided between errors in determining the correct isomer and errors in identification by PBM that were also made by manual identification.

Although it is difficult to assess quantitatively the effectiveness of the matching system because of the unknown variables in this work, it is safe to say that a minimum of 65% (91% of 71%) of those matches accepted by the system were correct even for specific isomers. As will be demonstrated below, this is a greater overall reliability than has been predicted in other work [5, 10] for similar match qualities.

Match quality

Table 2 illustrates, for selected compounds on four types of chromatographic column, the range of match quality parameters (K and K/K_{max}) that were accepted for tentative identification purposes. As can be seen, the range of K values was in many cases greater than a factor of two. Likewise, the range of K/K_{max} values is as great as a factor of five. Examination of the standard deviation of the relative retention, however, shows that the retention data in this work are defined within rather narrow limits. It is the retention data coupled with the match quality that lead to efficient matching. As demonstrated in the retention data column, the fused silica capillary column data show that much tighter retention data windows are possible with capillary column chromatography for use in corroboration of matches.

Use of relative retention times improves matching efficiency, also, in that as more corroborating evidence is acquired, a greater number of tentative identifications can be made with the same spectral information. Table 3 illustrates the increase in matching efficiency (tentative identifications/spectra matched) as more relative retention times were entered in the historical library.

Figure 2 demonstrates the effect of retention data corroboration on the confidence that can be placed in the K value for match quality. The data of Atwater [10] were used to show the reliability of K in distinguishing the correct match for a given spectrum. Plots of data from this study show much higher reliability at lower K values than those of Atwater [10]. This higher reliability is due to the use of retention data as part of the matching process.

TABLE 3

Increase of matching efficiency with the growth of the historical library

Number of compounds in historical library	Date	Matching efficiency (%)
620	December 79	18
945	July 80	23
1553	September 81	31

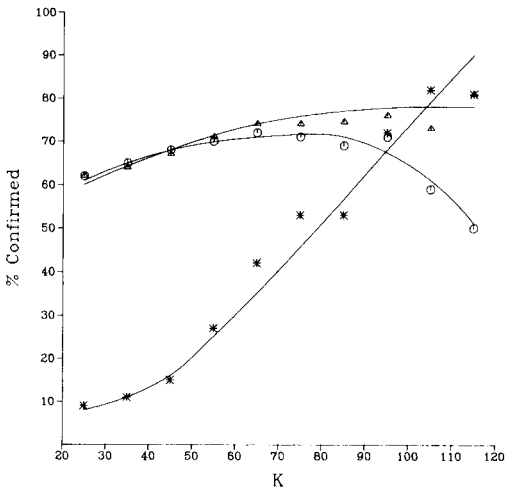

Fig. 2. Relation of PBM matches confirmed to overall match quality K. (0) All compounds; (△) carboxylic acids deleted; (*) data of Atwater [10].

At $K > 95$, however, an anomaly was seen. Instead of the reliability increasing, it began to decrease, unlike the finding of Atwater [10]. Examination of the matches with high K values for compounds that had been sent for confirmation showed that a large fraction of the unconfirmed answers were carboxylic acids. Further examination showed that, for fatty acids of C_{11} or greater, only 32% were confirmed although most had K values in excess of 100. Likewise, aromatic carboxylic acids had only a 37% confirmation rate. All results for carboxylic acids were then removed from consideration and the data were plotted. As can be seen in Fig. 2, the remaining data follow closely the data of Atwater [10] at $K > 95$.

The reason for the poor confirmation rate for the carboxylic acid spectra is not known, although it is believed that sample degradation is in some measure responsible. In Fig. 3 the relation of match reliability to compound class is shown. Whereas one would expect the ambiguity of matching results among alkanes and alkylbenzenes to cause poor reliability, it appears that stability of the compounds during storage has a great influence on reliability in this work. Esters of carboxylic acids had a much greater reliability in matching than the acids themselves.

In Fig. 4 the relation of reliability to ΔK is shown. At low ΔK, the reliabilities are similar to those of Atwater [10] and at high ΔK matches in this work have much higher reliabilities because of the retention data corroboration. The ΔK plot did not show the anomalous decrease at low ΔK corresponding to that at high K seen in Fig. 2. The reason is that the ΔK value is a measure of the difference between the unknown and the reference and as such is not as greatly influenced by the molecular weight as K is. For instance, as molecular weight increases, the highest possible K value increases generally because there will be more peaks in the spectrum. The calculated K value

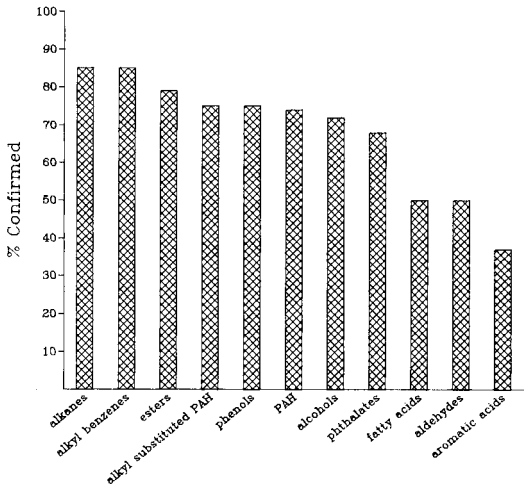

Fig. 3. Relation of PBM matches confirmed to compound class.

may be larger than 100, denoting an excellent match, and yet ΔK can be large also, denoting some question in the match. The set of compounds that predominated in the $K \geqslant 95$ regions did not, moreover, predominate in the $\Delta K \leqslant 15$ region. The carboxylic acids of high molecular weight (>184) that showed such a poor confirmation rate were evenly distributed with ΔK values up to 100, even though their K values had been concentrated in the $\geqslant 95$ categories.

Observations like those above led to the use of K/K_{max} as the ranking value rather than K alone. In this way, high K values with large ΔK values

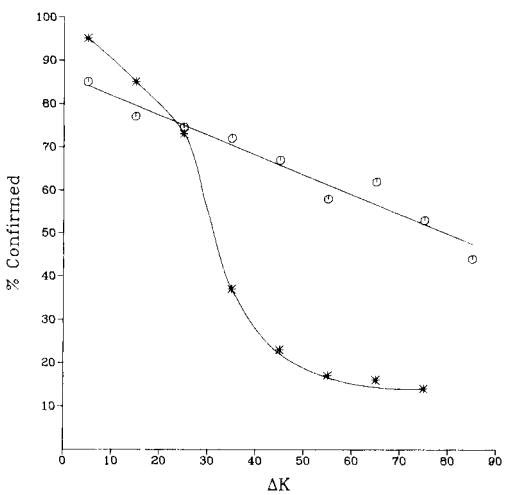

Fig. 4. Relation of PBM matches confirmed to match deficiency, ΔK. (○) All compounds; (*) data of Atwater.

were not given undue weight over small K values with small ΔK values. In Fig. 5, the relation of K/K_{max} to the rate of confirmation at constant K ranges is displayed. The positive slope of each line indicates the utility of K/K_{max} as a ranking factor.

Spectrum quality

For the most part, the reference spectra available for matching are of known quality [19]. The quality of spectra input for matching, however, is generally unknown when submitted in automated fashion. In order to make some measure of the quality of the spectra that had been tentatively identified by the matching software, a quality index [19] was calculated for approximately 25% of the matched spectra. In Table 4 results of applying the quality index calculations to the above set of spectra are compared to those of a previous study by Speck et al. [19]. As can be seen, spectra matched in this work appear to be of lower overall quality than those in reference libraries. If Table 4 is examined closely, however, one can see that the individual quality factors (QF1—QF7) compare quite well except for QF6. In fact, with the exception of this quality factor, the spectra of this study show quality factors of equal or better value than the reference libraries.

The factor, QF6, is a measure of the number of peaks present in the spectrum compared to the number of peaks expected from the molecular formula. Apparently, the spectrum extraction program was unable to separate the small peaks of the spectra from the background on the average. Such points as isotopic ratio accuracy (QF5), high-molecular-weight impurities (QF3), and illogical neutral losses (QF4) all appear to be well within reference

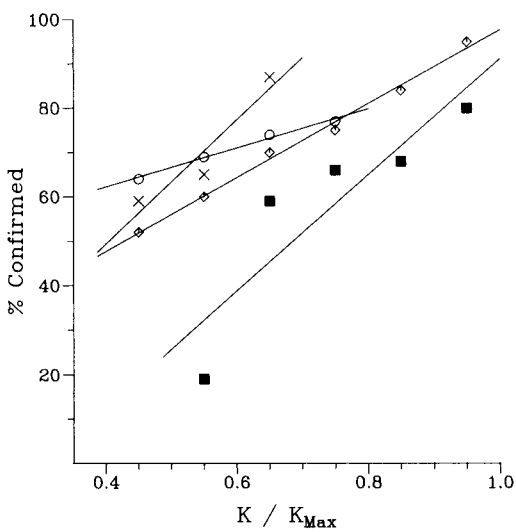

Fig. 5. Plot of K/K_{max} versus confirmation rate at constant K ranges. (×) K = 20—40; (○) K = 41—60; (◇) K = 61—80; (■) K > 80.

TABLE 4

Comparison of quality indices and quality factors for spectra from several sources

Quality factor	Reference library A	Reference library B	Reference library C	Literature [19]	Present work
QF1	1.0(0.0)[a]	0.909(0.0)	0.900(0.0)	0.927(0.0)	0.900(0.0)
QF2	0.995(0.65)	0.962(4.5)	0.972(4.1)	0.999(0.05)	1.000(0.0)
QF3	0.988(0.95)	0.976(1.9)	0.990(0.89)	0.985(1.4)	0.954(3.2)
QF4	0.979(1.1)	0.964(1.9)	0.976(1.5)	0.975(1.8)	0.970(1.3)
QF5	0.965(0.65)	0.971(0.56)	0.955(1.2)	0.942(1.5)	0.977(0.45)
QF6	0.848(13.7)	0.873(10.3)	0.873(10.6)	0.748(24.9)	0.671(28.2)
QF7	0.931(3.8)	0.968(1.4)	0.953(1.8)	0.886(6.9)	0.926(0.23)
QI[b]	0.756(21.2)	0.689(22.6)	0.691(22.4)	0.579(40.3)	0.505(51.0)

[a] Values in parentheses represent percent of spectra showing QF < 0.5. [b] $QI = \Pi_{N=1}^{7} QF_N$.

spectrum quality. Thus, the spectrum extraction program appears to have delivered accurate spectra even though the threshold for peak detection seems to have been high in some cases.

Conclusions

The use of an automated spectrum matching system for survey identification by g.c.-m.s. is quite feasible with little intervention. The reliability of matching when an historical library of retention data is used in conjunction with the spectrum library is at least 65% including matching specific isomers. In this study, 71% overall reliability was achieved when specific isomer resolution was not required. Use of retention data greatly enhances the reliability of lower quality matches, but has little effect on high quality matches. Both positive and negative points of the match must be considered before reliability is assigned.

Valuable discussions with Professors F. W. McLafferty and J. McGuire are gratefully acknowledged. The assistance of Barbara Atwater Fell in bringing PBM up on our PDP 11/70 system is appreciated as is the help of In Ki Mun and David Martinsen with the quality index program and Drew Sauter with the assembly of the total package. We thank Bruce Bartel and Susan Sims for generating the statistical reports necessary for this work, and Laura Folwell for her help in collation of results.

REFERENCES

1 Federal Register, 44 (233) 69532—69552, December 3, 1980.
2 L. H. Keith and W. A. Telliard, Environ. Sci. Technol., 13 (1979) 416.
3 W. M. Shackelford, D. M. Cline, L. O. Burchfield, L. Faas, G. R. Kurth and A. D. Sauter, in L. H. Keith (Ed.), Advances in the Identification and Analysis of Organic Pollutants in Water, Ann Arbor Science Publishers, Ann Arbor, 1981.

4 W. M. Shackelford and L. H. Keith, Frequency of Organic Compounds in Water, EPA-600/4-76-062, December 1976.
5 G. M. Pesyna, R. Venkataraghavan, H. E. Dayringer and F. W. McLafferty, Anal. Chem., 48 (1976) 1362.
6 F. W. McLafferty, R. H. Hertil and R. D. Villwock, Org. Mass Spectrom., 9 (1974) 690.
7 F. P. Abramson, Anal. Chem., 47 (1975) 45.
8 G. T. Rasmussen and T. L. Isenhour, J. Chem. Inf. Comput. Sci., 19 (1979) 179.
9 R. G. Dromey, M. J. Stefik, T. C. Rindfleisch and A. M. Duffield, Anal. Chem., 48 (1976) 1368.
10 B. L. Atwater, Ph.D. Thesis, Cornell University, Ithaca, NY, 1980.
11 H. Nau and K. Biemann, Anal. Chem., 46 (1974) 426.
12 C. C. Sweely, N. D. Young, J. F. Holland and S. C. Gates, J. Chromatogr., 99 (1974) 507.
13 B. E. Blaisdell, Anal. Chem., 49 (1977) 180.
14 D. S. Smith, M. Achenback, W. J. Yaeger, P. J. Anderson, W. L. Fitch and T. C. Rindfleisch, Anal. Chem., 49 (1979) 1623.
15 S. Lewis, C. N. Kenyon, J. Meili and A. L. Burlingame, Anal. Chem., 51 (1979) 1275.
16 J. E. Eichelberger, L. E. Harris and W. R. Budde, Anal. Chem., 47 (1975) 995.
17 Registry of Mass Spectral Data (Enlarged Version), Wiley, New York, 1981.
18 EPA/NIH Mass Spectral Data Base, NSRDS-NBS 63.
19 D. D. Speck, R. Venkataraghavan and F. W. McLafferty, Org. Mass Spectrom., 13 (1978) 209.

Analytica Chimica Acta, 146 (1983) 29—35
Elsevier Scientific Publishing Company, Amsterdam — Printed in The Netherlands

INTERACTIVE FRAGMENT DISPLAY PROGRAM FOR INTERPRETATION OF MASS SPECTRA

JOHN FIGUERAS

Research Laboratories, Eastman Kodak Company, Rochester, NY 14650 (U.S.A.)

(Received 24th July 1982)

SUMMARY

A computer program accepts a structure entered by means of a graphics tablet, creates a fragment pool by cleaving selected bonds one, two, and three at a time, and keeps a record of the structures of the fragments. Subsequent input of a given fragment mass enables display of the structures of fragments with the given mass.

A central task in the interpretation of mass spectra is discovering, within a hypothesized structure, substructures with masses which would account for observed mass peaks. Inspired guesswork, knowledge of precursors, familiarity with the chemistry involved in the ionization chamber of the spectrometer [1], and experience will often lead to quick identification of peaks in the spectrum. With complex or unfamiliar molecules, interpretation may involve much trial and error and hand calculation of fragment masses. The computer program described here considerably eases the assignment of substructures to mass peaks in the spectrum.

The program permits graphical input of an organic chemical structure and will display substructures derived from that input in response to subsequent input of mass peaks that appear in an experimental mass spectrum. Figure 1 shows an example of output for 16-methyl-16-dehydropregnenolone acetate. Atoms of substructures are highlighted (they appear in inverse video on the CRT of the terminal). Figure 1(a) shows the substructure produced for a peak at m/z 311, which is one mass unit larger than the observed base peak at mass 310 (the program did not produce a fragment at mass 310). Thus, the base peak corresponds to neutral loss of a molecule of acetic acid from the parent structure. A trial input of m/z 107 produced the two structures in Fig. 1(b, c). The time required to generate these answers was short: manual entry of the structure required 2 min, processing required 2 s, and responses to requests for substructure display were practically instantaneous. Thus, the program is fast enough to be used in an interactive mode.

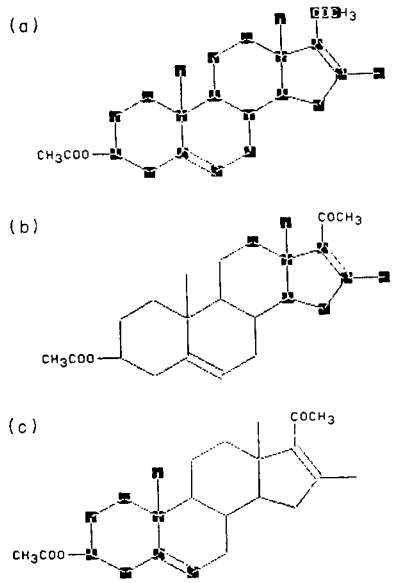

Fig. 1. Highlighted substructures correspond to fragments satisfying input mass requirements: (a) m/z 310 (base peak); (b) and (c) are two fragments for m/z 107.

THE COMPUTER PROGRAM

The fragment display program called MASH (mass spectroscopist's helper) is written in ANSI 66 FORTRAN and implemented on an IBM 3033 computer under the time share option. (Two machine-language subroutines are used for efficient setting and reading of specific bits in a 32-bit computer word.) The program contains fewer than 500 FORTRAN statements but requires 120K bytes of memory for fragment data and a rather large subroutine for structure entry. Graphics are implemented on a Hewlett-Packard 2647A terminal with a graphics tablet for input (HP9111A or Summagraphics Bit Pad One). The local BASIC intelligence of the terminal is used to transmit data between the graphics tablet and the host computer. The terminal is interfaced to the host on a 1200 baud line.

Bit Pad One must be configured for particular use with the HP2647A terminal, which does not incorporate the standard Hewlett-Packard Interface Bus (HPIB) for which Summagraphics did the original tablet design. The fix is supplied by Summagraphics but must be specified when ordering Bit Pad One.

Program operation will be discussed under the headings (1) structure input, (2) fragment generation, (3) data storage, and (4) display. The overall operation of the program is outlined initially. The program takes graphics input data from which it derives a connection table. The connection table identifies the atoms in a structure and their linkages to other atoms. The connection table is sent to a fragment generator, which records the frag-

ments formed from all possible cleavages taken one, two, and three at a time, subject to a few restrictions. Fragment compositions are stored in a list keyed to molecular masses (m/z) of the fragments. Redundancy is avoided, thus reducing the amount of memory required to store fragment information and sparing the user the annoyance of repeatedly retrieving the same substructure during output. The fragment compositions are retrieved from the storage list (stack) to create the highlighted atom display that defines the substructure. Fragments are selected by the user when a mass peak is input.

Structure input

The structure input subroutine facilitates building of conventional chemical structure diagrams on the CRT in the terminal. Structure building is done by operations selected from a menu, by use of a cursor controlled by the stylus of the graphics tablet. The tablet is used as a pointing and selecting device rather than as a drawing device [2]. The menu contains the following items.

(1) BUILD. Carbon atoms can be linked together and multiple bonds established.

(2) RINGS. Saturated or aromatic rings can be formed in linked, fused, or spiro structures; ring sizes are 3—8.

(3) HETEROATOMS. Any atom can be replaced by B, N, O, S, P, or Se, all of which appear on the menu; atoms not on the menu can be entered through the keyboard.

(4) SUBSTITUENTS. Atom strings entered from the keyboard can be placed in the structure diagram as required. This routine allows flexible and free definition of substituent groups, connectives, or even whole molecules. It is backed by an interpreter that will accept common conventions for representing structures, such as -COOH for carboxyl and -$CONHCH_3$ for *N*-methylamide. Other conventions, such as use of parentheses for chain branching and use of subscripts for replication, are also recognized.

(5) AUGMENT ATOM. Charges and hydrogen atoms which require suppression of explicit bonds can be placed directly at an atom.

(6) DELETE BONDS. Incorrectly placed bonds can be removed.

(7) DELETE ATOMS. Incorrectly placed atoms can be removed.

(8) ABORT. Two options are available; the user can clear the screen completely and enter a new structure or replace the current copy of the structure with a copy as it existed before the last menu operation.

(9) EXIT. On exit, the graphics representation of structure is converted into a connection table. A simple example of a connection table is shown in Fig. 2.

Fragment generation

Bonds available for cleavage are located by a scan of the connection table and are put onto a bond-cleavage list. Only single bonds and aromatic bonds

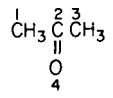

From	To	Bond Order
1	2	1
2	3 4	2 1
3	–	–
4	–	–

Fig. 2. Connection table for acetone. The table shows connections going one way. Numbering sequence is arbitrary.

are eligible for this list. By means of a cycle perception routine, bonds eligible for cleavage are classified as cyclic or acyclic. This classification is used for avoiding redundant fragment compositions, as discussed later. The connection table is converted so that it shows connections between atoms going both ways (the table in Fig. 2 shows connections only once and there is no redundancy); the redundant form of the connection table facilitates searching in the cleavage subroutine. The cleavage routine produces fragments that result from one, two, or three simultaneous bond cuts. The routine simulates a walk through the structure starting from the cleavage point and notes the atoms encountered. The record of encountered atoms is stored in a vector V, called a fragment map; if atom I is encountered during the walk, V(I) is turned "on". In the implementation, chains of atoms are traced through the connection table, with appropriate backtracking when branch points are encountered, and with due allowance for the possibility that traverses may loop back because of rings.

To simulate a multiple cleavage, the routine starts from an atom at one of the bond cuts and makes the walk within boundaries set by the other cuts. Thus a triple cleavage is equivalent to a single cleavage in which the walk is restricted by two boundaries determined by the other cleavages. One aspect of this process is that it is directed: the direction is always away from the bond cut. The directed nature of the delineation of fragment composition has two consequences. First, if a nonredundant bond list is used (one on which the bond appears from atom *a* to atom *b* but not vice versa), only half of the possible fragments will be generated by the program. This is handled by recording both the fragment map V and its complement. Second, in a triple cut (*I*, *J*, *K*), the walk from cut *K* might go in the wrong direction, away from *I* and *J* (see Fig. 3). In this case, the composition of the fragment

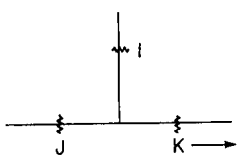

Fig. 3. A "wrong way" cut for cut *K*. Only atoms to the right of *K* will appear in the fragment map, and boundary conditions imposed by cuts *I* and *J* will be ineffective.

will not be bounded by I and J, so that the resulting fragment will not be one characteristic of a triple cleavage. In the program, a test is made to ensure that the atom set created by cut K is bounded by cuts I and J, and if it is not, the bond at K is reversed (from and to are interchanged) and the cleavage is repeated. In this case, taking the complement of the original fragment map will not work because there might be atoms beyond cuts I and J that would be incorrectly included.

Completely random generation of bond cuts to a depth of three represents a substantial combinatorial problem. In the sample case (Fig. 1), the total number of possible cleavages of 26 bonds (excluding multiple bonds) is $C_1^{26} + C_2^{26} + C_3^{26} = 2951$ for one, two, or three simultaneous bond breaks. This number can be reduced considerably (to 235) by restrictions on allowed cleavages and by simple rules based on experience (heuristics).

First, multiple cleavage cannot occur at a single carbon atom unless it carries a non-carbon substituent attached by a double or single bond. This restriction prevents formation of carbenes but allows certain neutral losses that require multiple cleavage at carbon, such as the loss of carbon monoxide from a phenol.

Second, triple cleavage of a structure (or fragment) is not attempted if the structure (or fragment) contains no branch points. Triple cleavage of an unbranched structure cannot produce a fragment set that is different from the set produced by separate single and double cleavages.

Third, no cleavage or combination of cleavages is allowed if it results in a single ring cut. For example, the set of cleavages in Fig. 4(a) is allowed, but the set in Fig. 4(b) is not. In Fig. 4(a), each ring has two cuts, which result in two fragments with lower molecular masses that are accessible only by a triple cleavage. In Fig. 4(b), one ring has a single cut; this does not produce smaller fragments, and the fragments obtained are equivalent in molecular mass to those obtainable at a lower (double) cleavage level.

Data storage

The fragment map V described above is a record of the atoms in a given fragment. This record, with atom coordinates, is required later to display a fragment structure. Many fragment maps must be stored; a compact record for storage is obtained by translating the V vectors into bit maps. The bit maps are arranged in the minimum number of 32-bit words (standard word length in the IBM 3033 computer) that will span the molecule; up to eight words can be used, which would allow a maximum of 256 atoms. A machine-language program (see above) allows efficient transfer of information from

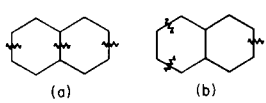

Fig. 4. (a) "Good" cleavages; all rings have more than one cut. (b) "Bad" cleavages; the ring on the right has a single cut.

V to the bit maps; for every V(I) = 1, bit I in the bit map is turned on. The bit maps are stored on a stack indexed by a vector DIR, which is used as a directory file based on fragment molecular masses. For example, a value DIR(89) = 145 denotes that 145 is the first storage position on the stack that contains a bit map for a fragment with a molecular mass of 89. A given fragment is added to the stack when its bit map is copied into the stack. An additional word adjacent to the bit map is used to contain the stack index (address) of the next fragment having the same molecular mass. If there is no other fragment beyond the current one, the address word will contain zero. To reclaim all fragments with a common molecular mass, one enters the stack at the position indicated by DIR(IWT), where IWT is the required molecular mass of the fragment, and traces through the list of fragments that are linked together by the associated address words. The trace terminates when a zero address word is encountered or when eight maps at a common molecular mass have been retrieved, whichever comes first. A limit of eight for storage depth keeps the amount of storage under control and prevents the tiresome reappearance of fragments that are basically the same, for example, loss of a methyl group from a structure containing many methyl groups. However, the imposition of a limit poses the risk that fragments of interest might not be recorded because the limit would be exceeded. Yet, if no limit were placed on each mass category, fragments of interest might be lost because all available storage was occupied by many repetitions of small fragments. To what extent the performance of the program is compromised, if at all, by the imposition of a limit must be settled by experience.

Before a bit map is added to the stack (if there is room for it) it is compared with the stored bit maps at the common molecular mass, and the new bit map is added to the stack only if it is different from the others. The stack is dimensioned to 40 000 words (160 Kbytes). At the greatest molecular mass allowed by the program (1000), the program can store about 800 fragments. At this extreme, the worst case (multiplicity of eight for all fragments) would allow storage of fragments corresponding to about 100 different mass peaks.

Display

The structure created during structure entry remains on the screen and is used to receive highlighting characters for delineating substructures of fragments, in response to input of various fragment masses (or mass peaks from an observed spectrum). In this phase of the program, the molecular mass of the input fragment is used as an index for the directory DIR to search the stack for the bit maps corresponding to the input mass. As each bit map is retrieved, its content is interpreted to retrieve the indices of the atoms of the fragment. These indices are used to retrieve coordinates of the atoms appearing on the screen, and an inverse highlight is placed at each of the retrieved atoms. The required atom coordinates are supplied by the subroutine used for structure entry, at the time the original structure is created on the screen. Previous highlights are turned off before the current set is displayed.

The possibility that a given mass peak may appear as a consequence of hydrogen migration is accommodated in the program by a simple expedient. After a mass M is submitted for search by the user, the program looks in the directory DIR for mass M, and also for M + 1 and M − 1, and reports the presence of these augmented or diminished masses if found. The user can then access the fragment displays appropriate to the changed (±1) masses; these fragments then constitute possible "explanations" for the observed mass peak, allowing for the possibility of hydrogen migration.

The program fails, of course, when cleavages occur that fall beyond the specifications of the computer-model because of rearrangements, cleavage to a depth greater than three, or the presence of impurities. Failure of the program to generate an observed peak is therefore a warning to the user that something unusual is occurring that is not explicable in terms of simple cleavages and hydrogen transfer.

Limited experience has been gained with this program, but it appears that substantial saving in time is made possible, particularly with large molecules. A version of the program is now under development for application to high-resolution mass spectra.

The program described herein is available from the author on request.

The author is indebted to Richard Phillips for the two machine-language subroutines and to Craig Shelley, who wrote the cycle perception routine.

REFERENCES

1 F. W. McLafferty, Interpretation of Mass Spectra, 2nd edn., Benjamin-Cummings, Reading, MA, 1973.
2 W. J. Howe and T. R. Hagadone, ACS Symposium Series No. 84, Am. Chem. Soc., Washington, DC, 1978.

Analytica Chimica Acta, 146 (1983) 37—43
Elsevier Scientific Publishing Company, Amsterdam — Printed in The Netherlands

DETERMINATION OF TRACES OF METALS BY ANODIC STRIPPING VOLTAMMETRY AT A ROTATING GLASSY CARBON RING-DISC ELECTRODE

Part 2. Comparison between linear anodic stripping voltammetry with ring collection and various other stripping techniques

C. BRIHAYE and G. DUYCKAERTS*

Laboratoire de Chimie analytique, Université de Liège au Sart Tilman, B6, B-4000 Liège (Belgium)

(Received 27th July 1982)

SUMMARY

Linear anodic stripping voltammetry (a.s.v.) with ring collection is compared with differential pulse a.s.v. at a hanging mercury drop electrode and with linear or differential pulse a.s.v. at a mercury film rotating electrode. Sensitivity, detection limits, resolution, base-line, the concentration range covered, the influence of organic compounds in the sample, and operational ease are discussed. The main conclusions are as follows: differential pulse a.s.v. at a hanging mercury drop electrode is best suited for determining heavy metal concentrations of the order of $\mu g\ l^{-1}$; the differential pulse mode at the rotating disc electrode or the d.c. mode at the rotating ring-disc electrode are required for sub-$\mu g\ l^{-1}$ concentrations; the limits of detection for the determination of cadmium, lead and copper are in the 2—5 $ng\ l^{-1}$.

In the first part of this work [1], the principles of trace analysis by means of anodic stripping voltammetry (a.s.v.) with collection were reviewed, the applicability of the theory for a.s.v. at a plane mercury film electrode was discussed, and calibration curves, detection limits, precision and accuracy were reported. This second part is devoted to a comparison of this analytical method with the various other a.s.v. techniques used for the determination of heavy metals in sea water at pH 2. This comparison is applied to the following methods:

(a) the hanging mercury drop electrode with differential pulse a.s.v. (HMDE-d.p.a.s.v.);

(b) the rotating mercury film disc electrode with linear a.s.v. (RDE-d.c.a.s.v.);

(c) the rotating mercury film disc electrode with differential pulse a.s.v. as described by Valenta et al. [2] (RDE-d.p.a.s.v.);

(d) the rotating mercury film ring-disc electrode with linear a.s.v. (RRDE-d.c.a.s.v.).

The comparison deals with the following points: sensitivity, detection limits,

resolution, base-line shape, concentration range, influence of organic compounds in solution, and operational ease.

EXPERIMENTAL

The rotating ring-disc electrode and the bipotentiostat used have been described [1]. In differential pulse a.s.v., the voltammograms were recorded with a modular Brucker E310. The HMDE was a Metrohm E410 electrode. The potentials were measured against an Ag/AgCl (0.1 M KCl) electrode. The samples of sea water from the North Sea (Belgian coast) were filtered through 0.45-μm Millipore filters.

RESULTS AND DISCUSSION

Sensitivity

The criterion of sensitivity, Σ, is the slope of the calibration curve $i_p = f(C)$ [3] under the following conditions: same electrode surface, same rotation speed for the rotating electrodes, and maximal potential scan rate (i.e., RRDE-d.c. 3 V min^{-1}, RDE-d.c. 3 V min^{-1}, RDE-d.p. 0.6 V min^{-1}, and HMDE-d.p. 0.3 V min^{-1}). Table 1 gives the values of Σ obtained for the four methods.

The d.p.a.s.v. mode at the HMDE is the least sensitive of the four methods. It can be used for the determination of concentrations of the order of 1 μg l^{-1}. The use of the RDE or RRDE provides a sensitivity 4—10 times greater than that with the HMDE. The most sensitive method is the differential pulse mode at the rotating thin mercury film electrode (RDE-d.p.a.s.v.), which provides a sensitivity 2—5 times higher than linear a.s.v. with the RDE or RRDE.

Detection limits

The detection limit is defined as the concentration giving a signal equal to 3 times the background deviation. The values presented in Table 2 were obtained by analysing a sample of sea water under the following conditions: t_{dep} = 1 h, electrode surface 0.21 cm^2, rotation speed for rotating electrodes (ω) 1500 rpm. These experimental values may be different from those found in the literature because the background can be affected by the presence of organic material in solution. It immediately appears that the lowest values

TABLE 1

Sensitivity Σ(μA cm^{-2} μg^{-1}) for the four methods under comparison[a]

	RRDE-d.c.a.s.v.[b,d]	RDE-d.c.a.s.v.[b,d]	RDE-d.p.a.s.v.[c,d]	HMDE-d.p.a.s.v.[b,e]
Cd	2	4	12	0.6
Pb	2.5	5	10	0.6
Cu	2	4	6	0.4

[a]Rotation speed (ω) = 1500 r.p.m. [b]Deposition time = 5 min. [c]Deposition time = 6 min. [d]$[Hg^{2+}]$ added = 1.63×10^{-5} M. [e]No Hg^{2+} added.

TABLE 2

Detection limits ($\mu g\ l^{-1}$) for the four methods under comparison

	RRDE-d.c.a.s.v.	RDE-d.c.a.s.v.	RDE-d.p.a.s.v.	HMDE-d.p.a.s.v.
Cd	0.005	0.02	0.002	0.02
Pb	0.005	0.02	0.002	0.05
Cu	0.005	0.02	0.004	0.05

are obtained with the rotating ring-disc electrode and the rotating disc electrode in the d.p.a.s.v. mode.

Resolution

The resolution depends on the width at half-height ($W_{1/2}$) of the dissolution or collection peaks. Values of $W_{1/2}$ were obtained by determining lead in a sea-water sample by means of the four methods under the following conditions: mercury film thickness (d) 0.03 μm, ω = 1500 rpm, mercury drop diameter 0.086 cm; scan rate 3 V min^{-1} for RRDE-d.c.a.s.v. and RDE-d.c.a.s.v., 0.6 V min^{-1} for RDE-d.p.a.s.v. and 0.3 V min^{-1} for HMDE-d.p.a.s.v. The thin mercury film electrodes showed the same resolution ($W_{1/2}$ = 40 mV regardless of the mode of voltammetry), which was better than the resolution obtained with the HMDE ($W_{1/2}$ = 60 mV). This results from the more favourable diffusion conditions in the thin mercury film.

Base-line shape

The shape of the base-line can influence the measurement of the peak heights, especially when sub-$\mu g\ l^{-1}$ concentrations have to be determined. The error on the measurement of this height often comes from ignorance of the shape of the base-line. It is not always possible to record this shape by applying a potential scan without electrolysis. Indeed, it can happen that the base-line changes with electrolysis time in a natural medium such as sea water, because of the presence of organic matter. In order to reduce this source of error to a minimum, it is advisable to use a method that shows a base-line as monotonous as possible with a slope independent of the scan rate. In d.p.a.s.v., the base-line appears as a curve, the curvature of which is turned towards the anodic current axis; this curvature is more pronounced with a mercury film electrode than with an HMDE. The base-line in linear a.s.v. with mercury film disc electrode approximates a straight line with a slope which is a function of the potential scan rate. In a.s.v. with collection, the base-line of the ring current is a straight line with almost zero slope which is independent of the potential scan rate. All these data are summarized in Fig. 1. It follows from this comparison that a.s.v. with collection allows the most accurate peak-height measurement, especially when the concentration is low.

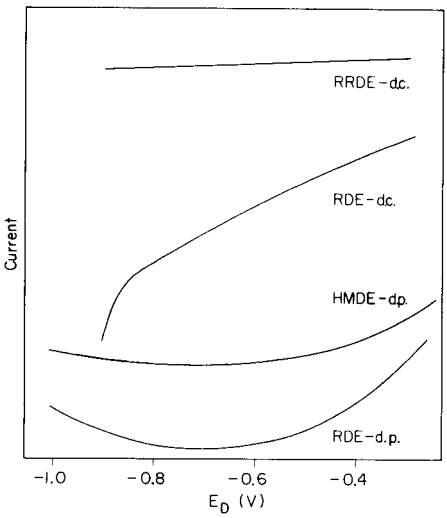

Fig. 1. Base-line shapes for the following methods: RRDE-d.c.a.s.v., RDE-d.c.a.s.v., HMDE-d.p.a.s.v. and RDE-d.p.a.s.v.

Concentration range

If the detection limit defines the lower limit of the use of a method, the upper limit of concentration is fixed by the formation of intermetallic compounds or by the solubility of the metal in mercury. As the amount of mercury is low on mercury film electrodes, these phenomena appear, other things being equal, at lower concentrations than with a hanging mercury drop electrode. Therefore, in determination by a.s.v., it is better to use a mercury film electrode when the elements to be determined are at concentrations lower than 1 $\mu g\ l^{-1}$ and a hanging mercury drop electrode when the concentrations are higher. In simultaneous determinations of Cd, Pb and Cu in sea water by a.s.v. with collection, there was no observable mutual influence between the three elements up to concentrations of 25 $\mu g\ l^{-1}$, for deposition times of 5 min. The lines $i_{p,R} = f(C)$ were not modified by the presence of the other elements at any concentration up to 25 $\mu g\ l^{-1}$. Furthermore, these relations were straight lines passing through the origin. In d.p.a.s.v. at the RDE, a non-linear dependence appears in cases of amalgam saturation for example, for copper [4].

Influence of organic compounds in solution

The influence of organic compounds depends on their nature, particularly their complexing or adsorption properties [5—11].

Complexing organic matter. Metal ions in solution can be distributed between free or solvated ions, labile complexed ions (i.e., electroactive ions) and complexed nonlabile ions which cannot be reduced during the deposition step. The different methods compared here show the same behaviour

with regard to complex formation, because the nature of the electrode does not play any role. It should be recalled, however, that when the mercury film electrode is formed in situ, it is necessary to add Hg^{2+} ions to the solution in a much higher concentration than that of the Pb^{2+}, Cd^{2+} and Cu^{2+} ions in sea water. Comparisons of the global dissociation constants for complexes between Hg^{2+}, Cd^{2+}, Pb^{2+} and Cu^{2+} ions and a series of complexing agents (e.g., aminocarboxylic acids, amines, amino acids, organic acids and thiols) shows that Hg^{2+} ions generally form complexes more stable than those of other heavy metals. Therefore, Hg^{2+} ions can displace other elements from their complexes and thus increase the electroactive ion concentration. This characteristic of mercury(II) ions has recently been brought to light [12], and the present experimental results confirm the earlier warning. Thus, for a sea-water sample at pH 2, a RRDE plated with mercury in situ, indicates slightly higher concentrations than those measured with a hanging mercury drop electrode. Yet, when the sample solutions initially contain the same number of Hg^{2+} ions, but are analysed one hour later, the concentrations indicated by the two methods are the same, within experimental error. These results are grouped in Table 3. Consequently, the possible presence of Hg^{2+} ions must be mentioned when results obtained by different methods are compared.

Organic matter adsorbable on the electrode. Adsorbable organic matter can exercise diverse influences on stripping peaks. Certain studies have shown that their main role is in the reduction (electrolysis) phase, which can cause variations in peak heights and potentials. The effects produced by these substances depend on their chemical structure, their environment, the electrolysis potential, and the type of electrode used. If the surfactants present do not have adsorption peaks or waves, and if their action is constant (i.e., independent of metal ion concentration), the standard addition method furnishes a concentration representative of the real solution concentration. Otherwise, the appearance of an adsorption peak (or wave) can invalidate redissolution peak-height measurements when the potentials of the two peaks are close. Such a situation is presented in Fig. 2: this is a sea-water sample at pH 2.1 measured at the RRDE. The upper voltammogram, re-

TABLE 3

Effect of mercury(II) ions on the cadmium, lead and copper concentrations ($\mu g\ l^{-1}$) observed in three samples (A—C) of sea water

	Cd			Pb			Cu		
	A	B	C	A	B	C	A	B	C
HMDE	0.07	0.05	0.11	0.68	0.56	0.80	1.03	0.59	1.07
HMDE + Hg^{2+}	0.10	0.05	0.14	0.92	0.69	1.23	1.18	0.79	1.56
RRDE	0.11	0.06	0.16	0.81	0.72	1.31	0.98	0.84	1.74

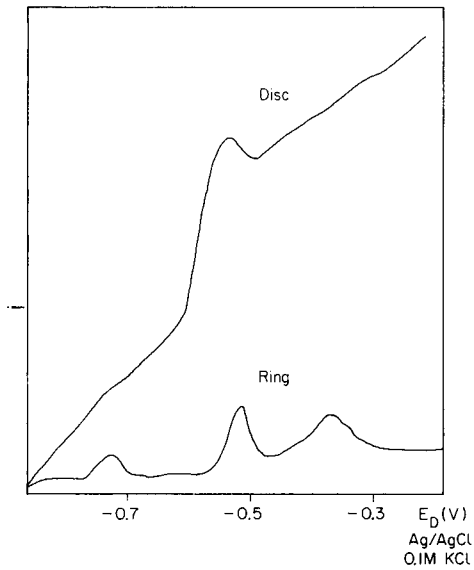

Fig. 2. Influence of adsorbable organic matter on the voltammogram for the analysis of sea water by a.s.v. with collection.

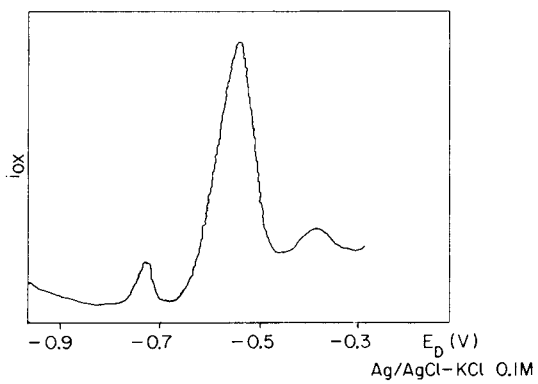

Fig. 3. Influence of adsorbable organic matter on the voltammogram for the analysis of sea water with a rotating mercury film electrode by d.p.a.s.v.

corded at the disc, shows the presence of an adsorption peak near the lead redissolution peak at —0.55 V. Nevertheless, the ring collection peak (lower voltammogram) is not affected by the presence of the adsorption peak. Moreover, the same sample was analysed (under the same experimental conditions) with a mercury-plated RDE in the differential pulse mode: this voltammogram also shows an adsorption peak near the lead redissolution peak (Fig. 3). This example shows that the use of the RRDE electrode allows the elimination of adsorption peaks, which is quite significant in natural water analysis.

Ease of use

Incontestably, the easiest method to use is d.p.a.s.v. with a hanging mercury drop electrode. Mercury-plated disc electrodes are more delicate to use, because they demand an extremely precise polishing step before mercury plating. Generally, as these electrodes do not turn during the potential scan, they can tolerate a certain eccentricity. This is not so for the rotating ring-disc electrode, because it must turn to ensure transport of the electroactive species to the ring. Therefore, the RRDE requires the most precise construction; moreover, the active surface must be absolutely planar. If there exists any discontinuity in the insulation between disc and ring, transport of active species toward the ring will be under turbulent conditions, causing a decrease in collection efficiency. Accordingly, the electrodes can be classed in order of decreasing ease of use: HMDE > RDE > RRDE.

Conclusions

The above comparison allows the following conclusions to be drawn. First, the hanging mercury drop electrode used in the differential pulse mode is the best adapted for the measurement of traces of metals at $\mu g\ l^{-1}$ concentrations. Yet, for lower concentrations, the differential pulse mode with the disc electrode (RDE-d.p.a.s.v.) and the linear mode with the ring-disc electrode (RRDE-d.c.a.s.v.) are better. In effect, these two methods have the same detection limits; the RDE-d.p.a.s.v. method is more sensitive, but the ring-disc electrode gives the best base-line, allowing the most exact measurements of peak height. In addition, this base-line is not influenced by adsorbable organic matter.

Anodic stripping voltammetry with collection seems to be particularly useful for the measurement of heavy metals in low concentrations from natural sources, even if it is less sensitive than the RDE with the differential pulse mode of stripping.

REFERENCES

1 C. Brihaye and G. Duyckaerts, Anal. Chim. Acta, 143 (1982) 111.
2 P. Valenta, L. Mart and H. Rützel, J. Electroanal. Chem., 82 (1977) 327.
3 H. Kaiser, Pure Appl. Chem., 34 (1973) 35.
4 L. Mart, Thesis, RWTH Aachen (1979).
5 E. A. Schonberger and W. F. Pickering, Talanta, 27 (1980) 11.
6 P. L. Brezonik, P. A. Brauner and W. Stumm, Water Res., 10 (1976) 605.
7 Z. Lukaszewski, M. K. Pawlak and A. Ciszewski, J. Electroanal. Chem., 103 (1979) 217.
8 Z. Lukaszewski and M. K. Pawlak, J. Electroanal. Chem., 103 (1979) 225.
9 T. A. O'Shea and K. H. Mancy, Anal. Chem., 48 (1976) 1603.
10 G. E. Batley and T. M. Florence, J. Electroanal. Chem., 72 (1976) 121.
11 T. M. Florence and G. E. Batley, J. Electroanal. Chem., 75 (1977) 791.
12 R. K. Skogerboe, S. A. Wilson, J. G. Osteryoung, T. M. Florence and G. E. Batley, Anal. Chem., 52 (1980) 1960.

Analytica Chimica Acta, 146 (1983) 45—50
Elsevier Scientific Publishing Company, Amsterdam — Printed in The Netherlands

ANODIC STRIPPING VOLTAMMETRY OF HEAVY METALS WITH A FLOW INJECTION SYSTEM

JOSEPH WANG*, HOWARD D. DEWALD and BENJAMIN GREENE
Department of Chemistry, New Mexico State University, Las Cruces, NM 88003 (U.S.A.)
(Received 29th July 1982)

SUMMARY

The design and operation of an anodic stripping voltammetric system based on the flow injection technique are described. A flow cell with a wall-jet glassy carbon disk electrode and a 500-μl sample volume are employed. The system allows trace metals at the $\mu g\ l^{-1}$ level to be quantified simultaneously at a rate of ten samples per hour. A low differential pulse background current allows a detection limit for lead of about 3×10^{-9} M (0.3 ng) with a 3-min deposition time. Deposition is done in the presence of oxygen in the sample solution, but the carrier solution is oxygen-free.

Flow injection techniques are fast, precise and versatile [1, 2]. The use of electrochemical transducers for detection in flow systems is growing rapidly [3]. Constant-potential amperometry is usually employed because of its low background current level. This detection mode has been used to determine arsenic and iodide [4], meptazinol [5], phenol [6], and ascorbic acid, L-dopa, epinephrine and hexacyanoferrate(II) [7]. In addition, different potential step waveforms, such as reverse-pulse [8, 9] or triple-pulse [10] amperometry, have been incorporated as a means of detection in flow systems.

Current interest in quantifying heavy metals has resulted in an increasing demand for the adaptation of the most sensitive electroanalytical technique, anodic stripping voltammetry (a.s.v.), to automated measurements. For this purpose, a.s.v. flow cells have been incorporated with environmental monitoring systems [11, 12], and with automated systems for discrete samples based on the AutoAnalyzer principle [13].

This paper reports the use of a.s.v. as a sensitive detection mode for a flow injection procedure. In this adaptation of a.s.v., one must consider the nature of the process (deposition followed by potential scanning), which dictates the use of larger sample volumes and lower flow rates, as compared to those employed in amperometric detection. The wall-jet detector used in this study maintains high sensitivity even at low volume flow rates because of the narrow inlet nozzle that yields high linear flow rates. The operation of the system was optimized to achieve the desired balance between high sensitivity, rapid injection rate, and minimum carry-over effects. In the following

sections, the flow injection a.s.v. system is characterized and its performance is discussed.

EXPERIMENTAL

Instrumentation

Carrier and sample reservoirs were 400- and 250-ml Nalgene beakers, respectively, fitted with plexiglass covers. Flow of the electrolytic carrier solution was maintained by an FML Lab pump Model RPP (Fluid Metering, Oyster Bay, NY). The sample injection valve was a Rheodyne Model 7010 with a 500-μl sample loop. The connecting tubing (0.5-mm i.d.) was teflon. The length of tubing between the valve and the detector was 9 cm. An additional sample reservoir (connected via a T-connector to the sample tubing, close to the valve) was used in the carry-over experiments.

The electrochemical wall-jet detector was described previously [14]. The working electrode was a planar glassy carbon disk (0.25-cm diameter) onto which a solution stream was directed from an inlet nozzle (0.34-mm diameter). The glassy carbon disk was polished by an 1-μm alumina slurry, until a mirror-like surface was obtained. All potentials are reported with respect to the Ag/AgCl reference electrode. Current—voltage data were recorded with a Princeton Applied Research Model 174 polarographic system and a Houston Omniscribe strip-chart recorder.

Chemicals

All solutions were prepared from deionized water and analytical-grade chemicals. Stock solutions (10^{-3} M) of metal ions were prepared by dissolving the pure metal or its nitrate salt in nitric acid and diluting to volume with water. The 1×10^{-3} M mercury plating solution was prepared by dissolving mercury(II) nitrate. The stock solutions were stored in polyethylene bottles and diluted as required for standard addition purposes. All samples were prepared in 0.1 M potassium nitrate supporting electrolyte.

Procedure

The mercury film was deposited at the beginning of each day and yielded reproducible results. For this purpose, 10 ml of the Hg^{2+} solution and 190 ml of the supporting electrolyte solution were introduced into the carrier reservoir (giving a final Hg^{2+} concentration of 5×10^{-5} M). The carrier solution was purged with nitrogen for 10 min and passed through the detector at a rate of 0.25 ml min^{-1} for 20 min, with a potential of −1.0 V imposed on the working electrode. The potential was then switched to 0.0 V and held there for 2 min to dissolve any contaminants which may have codeposited with the mercury. Following this conditioning, the electrode was ready for use in an analytical run.

Background and sample determinations were done as follows. The deaerated carrier solution was pumped continuously at a flow rate of

0.2 ml min^{-1}. The valve was turned from the load position, in which the loop had been filled by gravity flow of the sample, into the inject position. After 15 s (a sufficient time for the solution to reach the detector) the deposition potential was applied for 3 min. The pump was then stopped and after 15 s the metals were stripped from the mercury film by applying a differential pulse ramp. Immediately after stripping had begun, the valve was returned to the load position. The potential scan was terminated at 0.0 V and after 30 s, during which solution flow was maintained, the system was ready for the next injection. For a 10 mV s^{-1} scan rate during the stripping step, the complete deposition/stripping cycle lasted 6 min, thus allowing ten injections per hour. The mercury film was removed at the end of a day by holding the electrode at +0.4 V for 10 min.

RESULTS AND DISCUSSION

Manifold procedure and carry-over studies

To allow application of a 3-min deposition (which suffices for measurement at the $\mu g\ l^{-1}$ level) from a 500-μl sample volume, flow rates around 0.2 ml min^{-1} were used. Under these conditions, dispersion of the sample plug is limited [2, 15], and the carrier reaches the detector a few seconds before the end of the deposition step. (For a dispersion lower than 1.2, all the sample is passed through the cell during deposition.) Thus, a medium-exchange procedure [16] is employed which possesses several advantages, e.g., deposition from a nondeaerated sample followed by stripping to the deaerated exchange (carrier) solution [17]. It should be noted that the use of the medium-exchange procedure corrects only for the background current interference of oxygen, and not for its other interferences. These include the precipitation of metal hydroxides by hydroxyl ions formed during the reduction of oxygen in basic or neutral media, and chemical oxidation of metals in the amalgam. In this study, the first interference was eliminated by using an acidic solution (pH 5), while the second did not affect the sensitivity and precision. The base-line of the voltammograms shown below indicates that re-aeration of the carrier while passing through the teflon tubing is minimized under the conditions used.

Flow systems for processing discrete samples are characterized by the interaction of two adjacent samples. This carry-over may increase in systems with relatively large sample volumes compared to the volume of the separating carrier stream. In amperometric detection, carry-over is usually examined with sequential solutions of the same compound, differing in concentration. The multi-element capability of a.s.v. permits carry-over to be studied with sequential solutions of different ions. Figure 1 illustrates the performance of the system with sequential injections of 1×10^{-7} M Pb^{2+} and 3×10^{-7} M Cd^{2+} solutions. These data show the absence of carry-over effects, indicating satisfactory performance of the system at ten injections per hour. The small lead and cadmium peaks in the cadmium and lead runs, respectively, are due

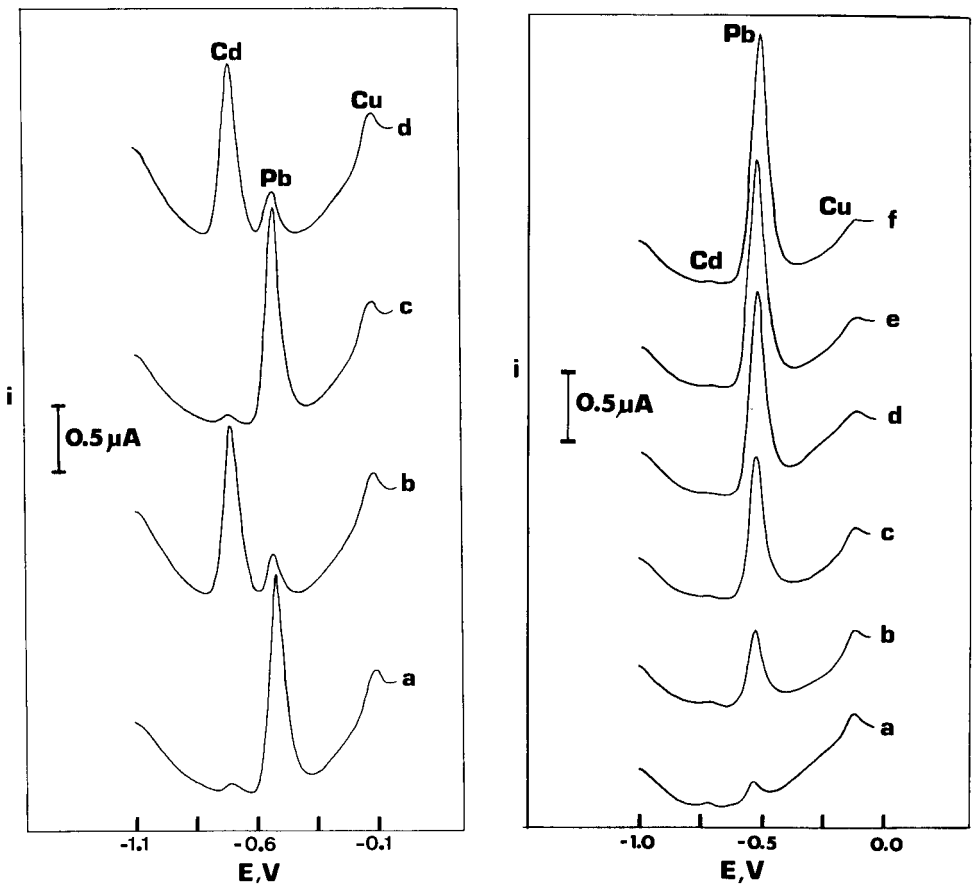

Fig. 1. Carry-over between sequential samples: (a, c) 1.0×10^{-7} M Pb^{2+} solution; (b, d) 3×10^{-7} M Cd^{2+} solution. Deposition period and potential, 3 min at −1.1 V. Flow rate, 0.18 ml min^{-1}. Differential pulse scan rate, 10 mV s^{-1}; amplitude, 50 mV; repetition time, 0.5 s. Supporting electrolyte, 0.1 M KNO_3. The peak at −0.1 V is due to Cu^{2+} present in the blank solution.

Fig. 2. Stripping voltammograms obtained after successive injections of Pb^{2+} solutions of ascending concentrations: (a) blank level (8×10^{-9} M); (b—f) successive concentration increments of 2.5×10^{-8} M. Conditions as in Fig. 1 except that the deposition potential was −1.0 V.

to impurities in the blank solution (not shown). Together with the Cu^{2+} impurity, three ions can be determined simultaneously at the $\mu g\ l^{-1}$ level. Tests were also made with sequential injections of 2.5×10^{-8} M and 1.0×10^{-7} M Pb^{2+} solutions; the carry-over found was negligible (not shown). Different system parameters such as tube diameter or solution viscosity may affect the carry-over and dispersion, thus requiring proper adjustment of procedure parameters such as flow rate or deposition time.

Detection limits, precision and stability

Differential pulse stripping voltammograms, obtained after successive injections of Pb^{2+} solutions of ascending concentration (2.5—12.5 × 10^{-8} M) are shown in Fig. 2. The well-defined sharp peaks allow convenient measurement at the $\mu g\ l^{-1}$ level. The Pb^{2+} blank level (voltammogram a) was 8 × 10^{-9} M. Based on the signal-to-background characteristics of the response, the detection limit for lead (using 3-min deposition) would be near 3 × 10^{-9} M (0.3 ng). Thus, subnanogram quantities of trace metals can be detected in nondeaerated samples using the medium-exchange method and the differential pulse mode that decrease or eliminate the oxygen and double-layer charging background components, respectively. Even better detectability would be obtainable by using longer deposition periods, i.e., lower injection rate. The data of Fig. 2 yielded a linear calibration plot. Least-squares treatment of these data yielded the equation I(nA) = (119 ± 17) $C(10^{-8}$ M) + 1736 ± 1418 nA with S_{yx} = 1352 nA and r = 0.972. A similar calibration experiment for Cd^{2+} (six injections from 2.5 to 15 × 10^{-8} M) yielded the equation I(nA) = (35 ± 1.8) $C(10^{-8}$ M) + 188 ± 177 nA with S_{yx} = 190 nA and r = 0.995 (conditions as in Fig. 1). If the flow rate is not adjusted to suit the deposition time and sample volume employed (i.e., the carrier flows through the detector during a larger fraction of the deposition period), deviations from linearity are observed.

The performance of the system was tested over an uninterrupted 72-min period of operation. During this period, a series of 12 injections of 1.5 × 10^{-7} M Pb^{2+} solution was studied. The mean peak current found was 1.19 μA with a range of 1.10—1.31 μA (n = 12) and a relative standard deviation of 6%. This precision is similar to that reported for other types of flow systems for a.s.v. [13]. Some experiments were done with the same film over more than 6 h of continuous operation, yielding stable results throughout. Similar stability was reported for an a.s.v. environmental warning system [12].

As in the medium-exchange procedure, the carrier stream can be selected to minimize interferences such as overlapping peaks or high background (e.g., hydrogen evolution) currents. The preliminary stages of sample treatment, as frequently required in stripping methods, usually lend themselves to automation with the components available for flow injection systems.

This work was supported by a grant from the U.S. Department of the Interior through the New Mexico Water Resources Research Institute.

REFERENCES

1 J. Růžička and E. H. Hansen, Anal. Chim. Acta, 99 (1978) 37.
2 J. Růžička and E. H. Hansen, Flow Injection Analysis, Wiley-Interscience, New York, 1981.
3 E. Pungor, Z. Fenér, G. Nagy, K. Tóth, G. Horvai and M. Gratzl, Anal. Chim. Acta, 109 (1979) 1.
4 J. A. Lown, R. C. Koile and D. C. Johnson, Anal. Chim. Acta, 116 (1980) 33.

5 H. K. Chan and A. F. Fogg, Anal. Chim. Acta, 111 (1979) 281.
6 R. C. Koile and D. C. Johnson, Anal. Chem., 51 (1979) 741.
7 A. N. Strohl and D. J. Curran, Anal. Chem., 51 (1979) 1045.
8 P. Maizota and D. C. Johnson, Anal. Chim. Acta, 118 (1980) 233.
9 J. Wang and H. D. Dewald, Talanta, 29 (1982) 901.
10 S. Hughes, P. L. Meschi and D. C. Johnson, Anal. Chim. Acta, 132 (1981) 1.
11 A. Zirino, S. H. Lieberman and C. Clavell, Environ. Sci. Technol., 12 (1978) 73.
12 J. Wang and M. Ariel, Anal. Chim. Acta, 99 (1978) 89.
13 J. Wang and M. Ariel, Anal. Chim. Acta, 101 (1978) 1.
14 J. Wang and H. D. Dewald, Anal. Chim. Acta, 136 (1982) 77.
15 P. L. Meschi and D. C. Johnson, Anal. Chim. Acta, 124 (1981) 303.
16 I. Shain and S. L. Phillips, Anal. Chem., 34 (1962) 262.
17 E. B. Buchanan, Jr. and D. D. Soleta, Talanta, 29 (1982) 207.

Analytica Chimica Acta, 146 (1983) 51—59
Elsevier Scientific Publishing Company, Amsterdam — Printed in The Netherlands

THE INFLUENCE OF LONG-CHAIN AMINE AND AMMONIUM SALTS ON THE ANODIC STRIPPING VOLTAMMETRY OF THALLIUM, LEAD, TIN, CADMIUM AND INDIUM[a]

A. CISZEWSKI and Z. LUKASZEWSKI*
Institute of General Chemistry, Technical University of Poznań, 60-965 Poznań (Poland)
(Received 2nd January 1982)

SUMMARY

The influence of n-nonylamine, di-n-hexylamine, tetrabutylammonium chloride, and cetyltrimethylammonium bromide (CTMA) on the anodic stripping peaks for Tl, Pb, Sn, Cd and In in 0.1 M hydrochloric acid, 0.1 M acetic acid and 0.05 M oxalic acid is described. The effects of these surfactants on the peaks increase in the sequence Tl < Pb < Cd < In < Sn, in accordance with increasing ionic potential. The thallium, lead and cadmium peaks are only depressed to different degrees, whereas the indium and tin peaks may be depressed strongly or enhanced spectacularly. Enhancement is observed mainly in 0.05 M oxalic acid; without surfactant, the indium and tin peaks are strongly depressed in this medium, but addition of surfactant restores normal deposition and stripping relationships. Peak heights are enhanced only by the unsymmetrical surfactants (CTMA and the amines); the symmetrical ammonium salts cause only peak damping. Some possible analytical uses of the effects of cationic surfactants are outlined.

The influence of surfactants on anodic stripping voltammetric peaks mainly involves change of peak heights and of peak potentials. An analytical application of the effects was proposed by Kemula and Głodowski [1] who used, as an example, the determination of cadmium in the presence of indium, with the addition of gelatin. Neeb and Kiehnast [2] worked out methods for the determination of thallium in the presence of significant amounts of bismuth by adding the cationic active inhibitor Eulan NK (3,4-dichlorobenzyltriphenylphosphonium chloride), and thallium in the presence of copper, bismuth and antimony by adding nonionic Triton X-100. Łukaszewski et al. [3] described a method for the determination of thallium or lead in cadmium salts, based on inhibiting the electrochemical activity of cadmium with a suitable compound. The present paper is an extension of the earlier work [3, 4]. Only a detailed knowledge of the changes in peak heights and peak potentials in the presence of surfactants allows efficient utilization of electrochemical masking effects. Thus systematic investigations in this field seem justified.

The peaks of thallium, lead and tin, as well as of cadmium and indium,

[a]This paper is dedicated to Professor Wiktor Kemula on the occasion of his 80th birthday.

are located close to each other, so that their simultaneous determination is difficult or even impossible. These elements were therefore investigated. Changes valuable from the analytical point of view were sought by testing different cationic surfactants in supporting electrolytes with various complexing abilities.

EXPERIMENTAL

Apparatus and reagents

Radelkis OH102 and OH105 polarographs were used with hanging mercury drop electrodes and thermostated measuring cells (Radiometer). A saturated calomel electrode (SCE) was the reference electrode.

The cationic surfactants n-nonylamine (Fluka), di-n-hexylamine, cetyltrimethylammonium bromide (Koch-Light), and tetrabutylammonium chloride (BDH), as well as aqueous 20% solutions of tetrapropylammonium hydroxide (Fluka) and tetraethylammonium hydroxide (Merck), were used as received. Stock solutions were prepared as 1% or 0.05 M solutions in 0.1 M sulfuric acid.

Supporting electrolyte solutions were prepared from super-pure grade reagents except for oxalic acid which was of analytical-reagent grade. The supporting electrolytes used were 0.1 M hydrochloric acid, 0.1 M acetic acid and 0.05 M oxalic acid. Standard solutions of thallium(I), lead(II), cadmium(II), indium(III) and tin(IV) were prepared by dissolving the purest metals available. All solutions were prepared in water triple-distilled from quartz.

Procedure

A given volume of the surfactant-free solution under test was introduced into the measuring cell. Dissolved oxygen was removed by bubbling oxygen-free nitrogen through the solution for 15 min, and then the nitrogen stream was directed over the solution surface. A surfactant was introduced into this deoxygenated solution. At an appropriate potential (usually −1.0 V vs. SCE), cathodic deposition was allowed to proceed for 2 min from the stirred solution, then the stirrer was stopped and the deposition was continued for 1 min. The stripping voltammetric curve was recorded at a scan rate of 0.25 V min^{-1}. Each measurement was made with a new drop.

RESULTS

The dependence of the peak heights for thallium, lead, tin, indium and cadmium on the deposition potential (i_{pa} vs. E_e) in surfactant-free 0.1 M acetic acid and in 0.05 M oxalic acid was examined, to choose the optimum deposition potentials for these ions. The metal ion concentrations tested were 2 μM for cadmium and lead, and 4 μM for the remaining metals. The results obtained are shown in Fig. 1. Corresponding results for 0.1 M hydrochloric

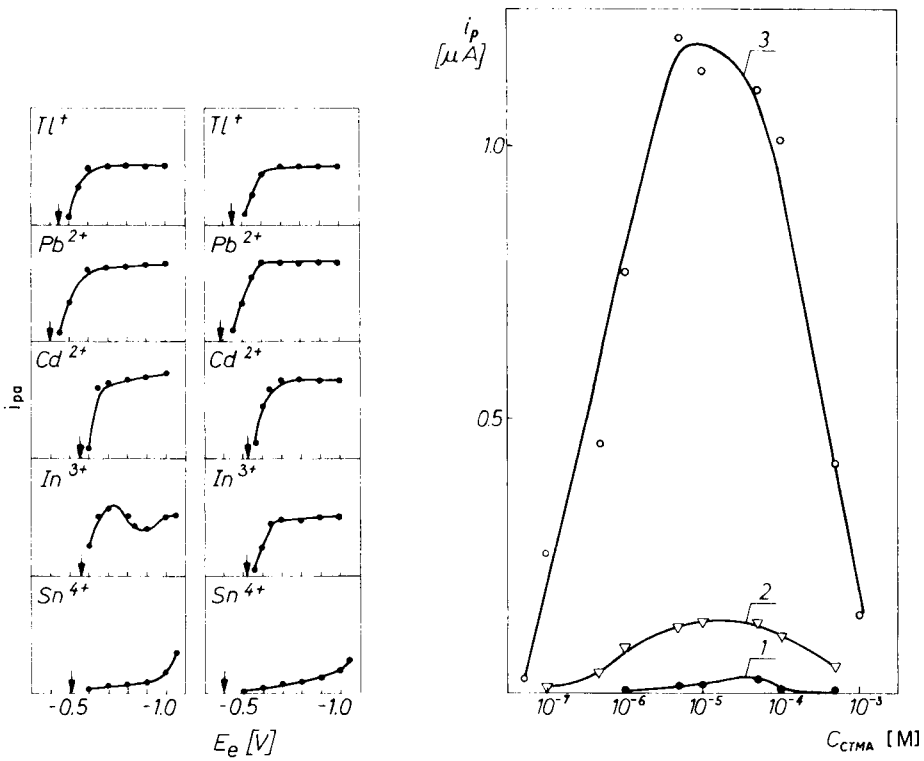

Fig. 1. Peak height vs. deposition potential for Tl, Pb, Cd, In and Sn in 0.05 M oxalic acid (left side) and in 0.1 M acetic acid (right side). The concentration of Pb(II) or Cd(II) was 2 μM, and 4 μM for the other ions; deposition time t_e = 2 min. Peak potentials are indicated by arrows.

Fig. 2. Peak height for tin(IV) vs. concentration of CTMA in 0.05 M oxalic acid for different concentrations of tin(IV): (1) 0.1 μM; (2) 1.0 μM; (3) 10 μM. E_e = —0.75 V vs. SCE, t_e = 3 min.

acid have been reported by Neeb and Kiehnast [5]. On the basis of these data [5] and the data in Fig. 1, the most suitable deposition potentials were selected.

Further tests were designed to examine the effects of the cationic surfactants n-nonylamine (NA), di-n-hexylamine (DH), tetrabutylammonium chloride (TBA), and cetyltrimethylammonium bromide (CTMA) on the peak heights and peak potentials for thallium, lead, tin, cadmium and indium. The electrolytes used were 0.1 M hydrochloric acid or acetic acid, or 0.05 M oxalic acid. The deposition conditions were identical to those applied in the previous investigations. The concentrations of metal ions varied from 1 μM to 4 μM, being chosen to provide peaks of similar height in surfactant-free solutions. The concentrations of cationic surfactants were varied from 0.0001% to 0.01% or 0.05% (w/v). The peak heights obtained were recalcu-

lated to heights relative to the value of the peak height in a surfactant-free solution. The shifts of peak potentials were also examined. The results are listed in Tables 1—3.

The very different behaviour of the peaks of indium and tin in the presence of the various surfactants, particularly in the oxalic acid solutions, indicated further studies on the voltammetric behaviour in this supporting electrolyte. Tin and CTMA were used to check whether or not the increase in peak height depended on the concentration of the metal ion. The results presented in Fig. 2 show that the nature of the effect is similar for different tin(IV) concentrations.

In the case of indium, only some of the surfactants increased the peak heights (Table 3), thus tetrapropylammonium hydroxide (TPA) and tetraethylammonium hydroxide (TEA) were also examined and the surfactant concentration range was extended. The results (Fig. 3) demonstrate that the relative peak heights depend on the concentration of the cationic surfac-

TABLE 1

Effect of cationic surfactants on the relative peak heights (h) and peak potentials (V vs. SCE) of the metal ions in 0.1 M HCl[a]

Surfactant	Conc. (%)	Tl		Pb		Sn		Cd		In	
		h	$-E_p$	h	$-E_p$	h	$-E_p$	h	$-E_p$	h	$-$
—	—		0.45		0.40		0.42		0.60		
NA	0.0001	1.00	0.45	1.00	0.40	0.44	0.42	1.00	0.60	0.63	
	0.0005	1.00	0.45	1.00	0.40	0.35	0.41	1.00	0.60	0.54	
	0.001	1.00	0.45	1.00	0.40	0.22	0.41	1.00	0.60	0.45	
	0.005	1.00	0.45	1.00	0.40	0.10	0.40	0.99	0.60	0.17	
	0.01	1.00	0.45	0.99	0.40	0.03	0.40	0.93	0.60	0.04	
DH	0.0001	1.00	0.45	1.00	0.40	0.56	0.40	1.00	0.60	0.50	
	0.0005	1.00	0.45	1.00	0.40	0.45	0.40	0.97	0.60	0.27	
	0.001	1.00	0.45	0.95	0.40	0.21	0.40	0.94	0.59	0.14	
	0.005	1.00	0.45	0.90	0.40	0.10	0.39	0.90	0.59	0.05	
	0.01	1.00	0.45	0.88	0.39	0.05	0.39	0.86	0.58	—	
TBA	0.0001	1.00	0.45	1.00	0.40	0.16	0.40	0.90	0.59	0.16	
	0.0005	1.00	0.45	1.00	0.40	0.10	0.39	0.72	0.59	0.08	
	0.001	1.00	0.45	1.00	0.40	0.08	0.38	0.68	0.58	0.04	
	0.005	1.00	0.45	1.00	0.40	—	—	0.56	0.58	—	
	0.01	1.00	0.45	1.00	0.40	—	—	0.50	0.57	—	
CTMA	0.0001	1.00	0.45	1.00	0.40	0.11	0.42	1.00	0.60	1.25	
	0.0005	1.00	0.45	1.00	0.40	0.16	0.42	1.00	0.60	1.30	
	0.001	1.00	0.45	1.00	0.40	0.20	0.42	1.00	0.60	1.36	
	0.005	1.00	0.45	0.99	0.40	0.23	0.42	1.00	0.60	1.83	
	0.01	1.00	0.45	0.99	0.40	0.25	0.42	1.00	0.60	2.03	

[a]Concentrations were 1 μM for Tl(I), Pb(II) and Cd(II), 2 μM for In(III), and 4 μM for Sn(IV). Deposition potential $E_e = -1.0$ V vs. SCE. Deposition time $t_e = 2$ min.

TABLE 2

Effect of cationic surfactants on the relative peak heights (h) and peak potentials of the metal ions in 0.1 M acetic acid[a]

Surfactant	Conc. (%)	Tl		Pb		Sn		Cd		In	
		h	$-E_p$	h	$-E_p$	h	$-E_p$	h	$-E_p$	h	$-E_p$
—	—		0.45		0.36		0.40		0.54		0.52
NA	0.0001	1.00	0.45	1.00	0.36	0.10	0.40	0.95	0.54	0.80	0.52
	0.0005	1.00	0.45	1.00	0.36	—	—	0.55	0.54	0.15	0.52
	0.001	1.00	0.45	0.95	0.36	—	—	0.42	0.54	0.04	0.52
	0.005	1.00	0.45	0.81	0.36	—	—	0.31	0.55	—	—
	0.01	1.00	0.45	0.75	0.36	—	—	0.25	0.55	—	—
DH	0.0001	1.00	0.45	1.00	0.36	0,06	0.40	0.90	0.54	0.50	0.52
	0.0005	1.00	0.45	1.00	0.36	—	—	0.73	0.54	0.30	0.52
	0.001	1.00	0.45	1.00	0.36	—	—	0.50	0.54	0.21	0.52
	0.005	1.00	0.45	0.98	0.36	—	—	0.42	0.54	0.15	0.52
	0.01	1.00	0.45	0.92	0.36	—	—	0.30	0.54	0.10	0.52
TBA	0.0001	1.00	0.45	1.00	0.36	0.10	0.40	0.98	0.54	0.50	0.52
	0.0005	1.00	0.45	1.00	0.36	—	—	0.78	0.54	0.32	0.52
	0.001	1.00	0.45	0.95	0.36	—	—	0.52	0.54	0.21	0.52
	0.005	1.00	0.45	0.90	0.36	—	—	0.15	0.55	0.10	0.52
	0.01	1.00	0.45	0.80	0.36	—	—	0.10	0.55	—	—
CTMA	0.0001	1.00	0.45	1.00	0.36	0.09	0.40	0.45	0.54	0.20	0.52
	0.0005	1.00	0.45	1.00	0.36	—	—	0.10	0.55	0.17	0.52
	0.001	1.00	0.45	1.00	0.36	—	—	0.26	0.56	0.10	0.52
	0.005	1.00	0.45	0.98	0.36	—	—	0.42	0.60	0.02	0.52
	0.01	1.00	0.45	0.96	0.36	—	—	0.60	0.60	—	—

[a]Concentrations were 2 μM for Tl(I), Pb(II) and Cd(II), and 4 μM for In(III) and Sn(IV). Deposition potential and time as in Table 1.

tant. In the presence of 0.1 mM CTMA, which has the strongest effect, the dependences of indium peak height on the deposition potential, the deposition time and the indium concentration were investigated. The results, compared to measurements in CTMA-free solutions, are shown in Fig. 4.

DISCUSSION

Tables 1—3 show that the influence of the cationic surfactants on the anodic stripping peaks, especially on the peak height, increases in the order Tl < Pb < Cd < In < Sn. The sequence of indium and tin is uncertain in the hydrochloric acid solution. The above sequence corresponds to the increasing ionic potential (ion charge and ion radius ratio). The values of the ionic potential after acceptance of ion radius [6] are: Tl^+ 0.74, Pb^{2+} 1.59, Cd^{2+} 2.02, In^{3+} 3.26 and Sn^{4+} 5.97. Loshkarev and Kryukova [7] reported a relationship between the effect of a surfactant on a polarographic wave and the radius and charge of the ion undergoing reduction.

TABLE 3

Effect of cationic surfactants on the relative peak heights and peak potential of the metal ions in 0.05 M oxalic acid[a]

Surfactant	Conc. (%)	Tl		Pb		Sn		Cd		In	
		h	$-E_p$	h	$-E_p$	h	$-E_p$	h	$-E_p$	h	$-E_p$
—	—		0.45		0.40		0.51		0.56		0.5
NA	0.0001	1.00	0.44	1.00	0.39	1.60	0.51	1.00	0.56	1.10	0.5
	0.0005	1.00	0.44	1.00	0.39	2.20	0.50	0.96	0.56	1.83	0.5
	0.001	1.00	0.44	0.99	0.39	2.60	0.49	0.94	0.55	2.83	0.5
	0.005	1.00	0.44	0.99	0.39	8.80	0.48	0.74	0.54	8.40	0.5
	0.01	1.00	0.44	0.98	0.38	12.6	0.44	0.57	0.52	9.33	0.5
	0.05	0.99	0.43	0.60	0.36	11.0	0.43	0.10	0.47	6.33	0.5
DH	0.0001	1.00	0.44	0.99	0.40	1.50	0.51	0.95	0.55	1.20	0.5
	0.0005	1.00	0.44	0.95	0.39	2.00	0.49	0.77	0.55	1.66	0.5
	0.001	1.00	0.44	0.90	0.39	6.00	0.49	0.73	0.55	1.80	0.5
	0.005	1.00	0.44	0.88	0.39	6.40	0.48	0.43	0.54	3.80	0.5
	0.01	0.99	0.44	0.83	0.38	8.90	0.47	0.30	0.53	4.00	0.5
	0.05	0.99	0.44	0.80	0.37	7.20	0.45	0.04	0.52	2.00	0.5
TBA	0.0001	1.00	0.44	1.00	0.40	2.00	0.50	0.94	0.56	0.92	0.5
	0.0005	1.00	0.44	0.99	0.40	4.28	0.49	0.82	0.56	0.88	0.5
	0.001	1.00	0.44	0.97	0.40	3.00	0.48	0.62	0.55	0.81	0.5
	0.005	1.00	0.44	0.95	0.40	2.85	0.47	0.10	0.54	0.61	0.5
	0.01	0.99	0.44	0.95	0.39	2.71	0.46	0.06	0.53	0.36	0.5
	0.05	0.99	0.44	0.91	0.38	2.57	0.45	0.03	0.52	0.09	0.5
CTMA	0.0001	1.00	0.44	1.00	0.41	23.0	0.50	0.91	0.56	3.20	0.5
	0.0005	1.00	0.44	1.00	0.41	31.0	0.50	0.90	0.56	7.23	0.5
	0.001	1.00	0.44	1.00	0.41	50.0	0.49	0.83	0.56	7.88	0.5
	0.005	1.00	0.44	1.00	0.42	48.0	0.49	0.79	0.57	14.0	0.5
	0.01	0.99	0.44	1.00	0.41	36.0	0.50	0.70	0.57	12.0	0.5
	0.05	0.99	0.44	1.00	0.42	30.0	0.50	0.75	0.58	8.46	0.5

[a]Concentrations were 2 μM for Pb(II) and Cd(II), and 4 μM for Tl(I), In(III) and Sn(IV). Deposition potential and time as in Table 1.

The changes in the peak potential are more complicated. In most cases (Tables 1—3), the shifts are insignificant. The shifts observed in the peaks of tin, indium and cadmium are usually in the range 20—50 mV in the anodic direction. The greatest shifts (80—90 mV) are caused by n-nonylamine for the peaks of cadmium and tin in solutions of oxalic acid. The cathodic shift of the cadmium peak by 60 mV in acetic acid solution containing CTMA is worth noting.

The surfactants tested tended simply to depress the peaks of thallium, lead and cadmium to different degrees. In some experiments, the peak heights for indium and tin were increased significantly whereas in others they were decreased. These differences are connected with the supporting electrolyte used and with the nature of the surfactant. In 0.1 M acetic acid, all the tested surfactants depressed the peaks for indium and tin; in 0.1 M hydrochloric

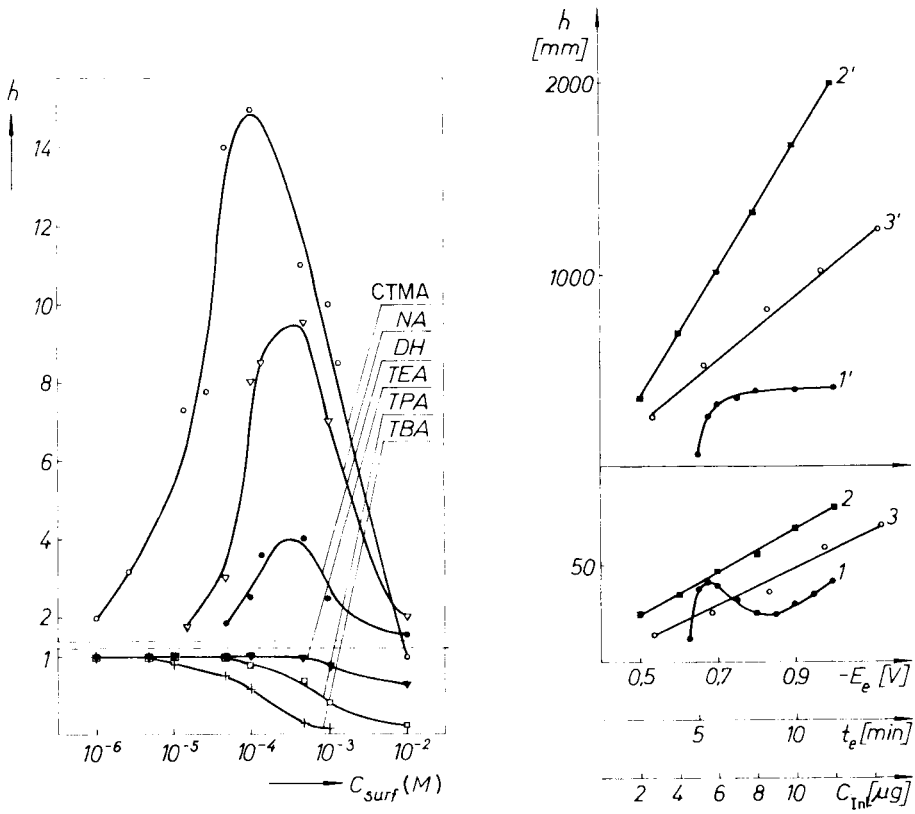

Fig. 3. Effect of symmetrical (TEA, TPA, TBA) and unsymmetrical (NA, DH, CTMA) cationic surfactants on the relative peak height of indium (4 µM) in 0.05 M oxalic acid. E_e = —0.85 V vs. SCE, t_e = 2 min.

Fig. 4. Dependence of the stripping peak for indium (4 µM) on the deposition potential (1, 1') and deposition time (2, 2'), and dependence of the peaks on indium(III) concentration (3, 3'), without CTMA (1, 2, 3) and with 0.1 mM CTMA (1', 2', 3'). Supporting electrolyte was 0.05 M oxalic acid. Deposition potential (curves 2, 2', 3, 3'), —0.85 V vs. SCE; deposition time (curves 1, 1', 3, 3'), 2 min. The peak heights in curves 1', 2' and 3' were recalculated from data obtained at different sensitivities of the polarograph.

acid, CTMA enhanced the indium peak while other surfactants depressed it. In 0.05 M oxalic acid, the indium and tin peaks increased significantly in most cases (Table 3 and Fig. 3); only symmetrical tetraalkylammonium salts caused a lowering of the indium peak. In the same supporting electrolyte, introduction of 0.1 mM CTMA caused a significant increase of the indium peak and a change in the dependence of the indium peak height on the deposition potential and deposition time (Fig. 4). In the absence of CTMA, the dependence of the indium peak height on the deposition potential is abnormal (curve 1, Fig. 4), as is also observed in Fig. 1. Addition of CTMA

caused a change in the dependence (curve 1′, Fig. 4) with a significant increase in the indium peak (compare curves 3 and 3′). In surfactant-free solution, the plot of peak height vs. deposition time does not pass through the origin, suggesting an unusual mechanism of deposition. In the presence of CTMA, the indium peak height increased proportionally to the deposition time (curve 2′), and the deposition mechanism appeared to be normal.

The peaks for indium and tin in all three supporting electrolytes in the absence of surfactants were significantly lower than would be expected considering the concentration and charge of these cations. The addition of surfactant did not increase the peaks above the expected values. For example, in 0.05 M oxalic acid in the absence of surfactant, the tin peak (4 μM) was characterized by a current of only 6.4 nA whereas the lead and cadmium peaks (2 μM), which also correspond to the transfer of two electrons on stripping, were characterized by currents of 127 and 129 nA, respectively. Thus a tin stripping peak, recalculated for 1 μM tin(VI) was 40 times lower than expected. Introduction of 0.001% CTMA caused a 50-fold increase in the peak height for tin (Table 3), i.e. the peak then obtained was comparable in height with the lead and cadmium peaks. A similar situation occurred in all investigated cases of peak increase under the influence of a surfactant. It was shown earlier that in the two-stage anodic stripping cycle, the main effect of surfactant is on the cathodic process [4]. When peak heights were increased by addition of surfactant, the relationship between peak enhancement and surfactant concentration always passed through a maximum. This indicates that the higher surfactant concentrations inhibit the cation reduction.

The difference in the effects of unsymmetrical cationic surfactants which enhanced the indium peak (CTMA, NA and DH), and symmetrical ammonium salts (TEA, TPA and TBA) which depressed the indium peak (Fig. 3) is of interest. The stronger surface activity of unsymmetrical surfactants does not explain their different effects on the indium peaks.

From the analytical point of view, the introduction of cationic surfactants does not allow the simultaneous determination of thallium, lead and tin in any of the supporting electrolytes examined. The insignificant effects of all these surfactants on the peak height and potential of thallium and lead mean that the main advantage to be gained by their addition is the depression of the tin peak, which is low itself. This is possible in 0.1 M hydrochloric acid in the presence of TBA and in 0.1 M acetic acid in the presence of all the surfactants tested. The increase in the tin peak in the presence of CTMA in 0.05 M oxalic acid may have some analytical utility. The height of the tin peak was enhanced about 40-fold, reaching values comparable with the lead peak (for equal concentrations). Under such conditions, the lead and tin peak potentials differed by 90 mV (−0.41 and −0.50 V vs. SCE, respectively). However, the potential of the thallium peak was −0.44 V, so that thallium would interfere in the determination.

In the supporting electrolytes considered, the peaks of indium and cadmium

are very close together. The complete damping of indium by di-n-hexylamine in 0.1 M hydrochloric acid without any very significant effect on the cadmium peak suggests the possibility of determining cadmium in the presence of indium. The peaks of lead and cadmium usually are sufficiently far apart that overlapping is not a problem unless a very large amount of cadmium is present. The introduction of CTMA in a 0.1 M acetic acid electrolyte results in a significant separation of these peaks (−0.36 and −0.60 V vs. SCE) with simultaneous depression of the cadmium peak so that lead can be determined [3].

This work was supported by Research Program MR-I-32.

REFERENCES

1 W. Kemula and S. Głodowski, Rocz. Chem., 36 (1962) 1203.
2 R. Neeb and I. Kiehnast, Naturwissenschaften, 57 (1970) 37.
3 Z. Łukaszewski, M. K. Pawlak and A. Ciszewski, Talanta, 27 (1980) 181.
4 Z. Łukaszewski, M. K. Pawlak and A. Ciszewski, J. Electroanal. Chem., 103 (1979) 217.
5 R. Neeb and I. Kiehnast, Fresenius Z. Anal. Chem., 241 (1968) 142.
6 Spravochnik khimika, Gosudarstvennoye nauchno-tekhnicheskoye izdatelstvo khimicheskoy literatury, Leningrad—Moscov, 1963, p. 382.
7 M. A. Loshkarev and A. A. Kryukova, J. Phys. Chem., 23 (1949) 1457.

Analytica Chimica Acta, 146 (1983) 61—69
Elsevier Scientific Publishing Company, Amsterdam — Printed in The Netherlands

POLAROGRAPHIC DETERMINATION OF TRACES OF ANTIMONY IN SILICON

P. LANZA

Chemical Institute "G. Ciamician", University of Bologna, Via Selmi, 2, 40126 Bologna (Italy)

(Received 30th November 1981)

SUMMARY

Methods based on differential pulse polarography and differential pulse anodic stripping voltammetry are described for the determination of low concentrations of antimony in silicon. The importance of reduction of the various oxidation states of antimony formed during dissolution of the sample is discussed. Results are greatly improved by addition of potassium iodide as a catalyst in the reduction of Sb(V) and Sb(IV) to Sb(III) by means of sulfur dioxide. Satisfactory results were obtained for commercial samples with antimony concentrations in the range 0.1—200 $\mu g\ g^{-1}$.

Antimony, like phosphorus and arsenic, is utilized as a dopant in high-purity silicon for electronic devices. Reliable, sensitive and not too expensive chemical methods for determining low concentrations of such elements in silicon are therefore of interest. Differential pulse polarography (d.p.p.), anodic stripping voltammetry or better differential pulse anodic stripping voltammetry (d.p.a.s.v.) are among the most suitable techniques for this kind of problem. These techniques are well known for their high sensitivity and have been used previously for the determination of traces of copper [1] and arsenic [2] in silicon. The present work was initiated to investigate the possibility of applying such voltammetric techniques to the determination of antimony in silicon so as to provide a rapid, simple method with sufficient sensitivity to eliminate the need of preconcentration or chemical separations.

The polarographic behaviour of antimony is well known [3]. Antimony(III) gives well shaped d.c. polarographic waves in several electrolytes and few problems arise in analytical applications. In contrast, antimony(V) only gives poorly defined waves in highly concentrated hydrochloric acid solutions. These waves have, however, been used to quantify antimony by d.c. polarography. However, the use of d.p.p. is hindered, especially at low antimony concentrations, because the antimony(V) reduction potential is too near the oxidation potential of mercury. Batley and Florence [4] reported that both antimony(III) and antimony(V) give excellent stripping peaks at the hanging mercury drop electrode (HMDE) in 4 M hydrochloric

acid, but this uncommon behaviour could not be fully explained. Because the polarographic behaviour of antimony depends very much on its oxidation state, it is necessary to transform the element present in the sample to the more suitable form, antimony(III).

The dissolution of silicon generally requires an oxidizing medium such as hydrofluoric acid with nitric acid or hydrogen peroxide. As is known [5, 6], however, the dissolution of the samples in mineral acids produces solutions in which antimony may be present in various oxidation states; Sb(V), Sb(III) and even Sb(IV) can be formed in variable ratios, depending on the experimental conditions. In particular, antimony(IV) forms a very stable oxide (Sb_2O_4), which behaves as an Sb(V)—Sb(III) mixture in solution [7]. It was therefore necessary to establish the best conditions for transforming antimony in the sample to antimony(III), which seems to be the better oxidation state for polarographic determinations.

EXPERIMENTAL

Instrumentation and reagents

An AMEL (Milan) Model 472 Multipolarograph was used to record polarograms; this instrument is suitable for conventional d.c. polarography, d.p.p., a.s.v. and d.p.a.s.v. A conventional DME electrode (Hg flow, $m = 2.63$ mg s^{-1} in 0.1 M KCl, open circuit) was used in the three-electrode configuration with a platinum ring as an auxiliary electrode and a saturated calomel reference electrode. The drop time ($t = 2$ s) was regulated by an electromagnetic knocker AMEL synchronized with the polarograph. For d.p.a.s.v., a Metrohm Type EA 410 HMDE was used. The cell for anodic stripping measurements was located in a reproducible position on a constant-speed AMEL 291/LF magnetic stirrer, which was automatically controlled by the polarograph.

Analytical-grade reagents were used without further purification.

Antimony(III) standard solution was prepared by dissolving Sb_2O_3 in concentrated hydrochloric acid and diluting to give a 1000 ppm antimony solution in 2 M HCl. Antimony(V) standard solutions were prepared either by dissolving the appropriate quantity of potassium pyroantimonate ($KSb(OH)_6$) in water or by oxidizing the Sb_2O_3 solutions in hydrochloric acid with bromine or nitric acid. Stock solutions were standardized in the usual way. Dilute solutions were freshly prepared by appropriate dilution.

The polarographic behaviour of antimony

The polarographic behaviour of antimony in solutions which appeared suitable for practical application was re-examined. By d.c. polarography, Sb(III) gives fairly well developed waves in 0.1—4 M hydrochloric acid solutions, while Sb(V) produces a wave only in the more concentrated acid (Fig. 1).

By d.p.p., Sb(III) in 0.1 M HCl solution gives a peak at −0.19 V (vs. SCE). At the 1 μg ml^{-1} level (8.21×10^{-6} M), the peak current is 4.40 μA. In the

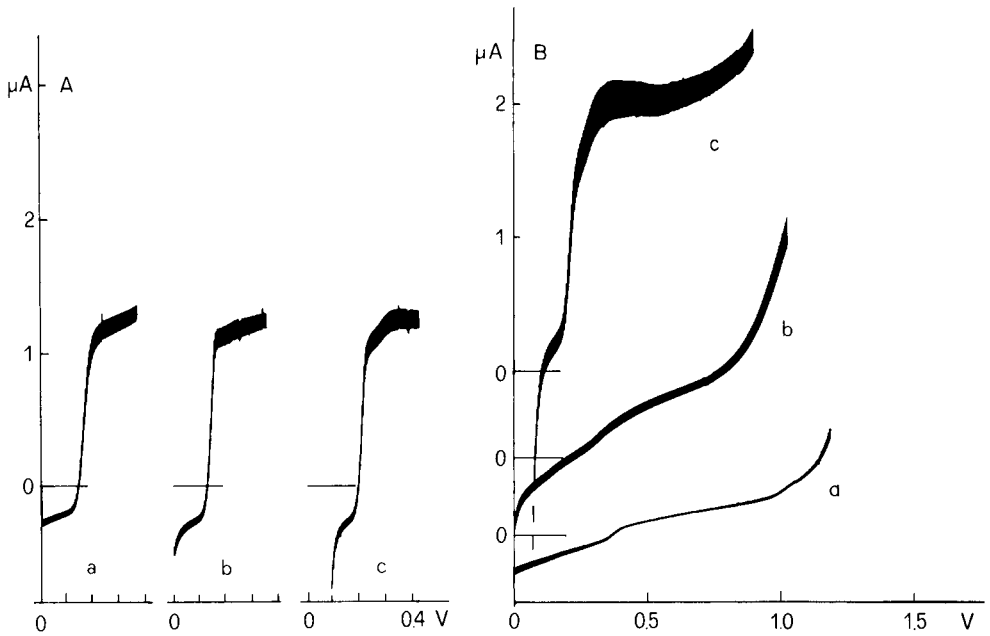

Fig. 1. D.c. polarograms for 10 ppm solutions of (A) Sb(III) and (B) Sb(V) in (a) 0.1 M HCl, (b) 1 M HCl, (c) 4 M HCl.

range tested (0—50 μg ml^{-1}), the peak current is proportional to the concentration. The peak current rises with increasing acid concentration, but the peak becomes gradually overlapped by the mercury oxidation current (Fig. 2A). At the 10 μg ml^{-1} level, Sb(V) gives no usable peaks in 0.1—1 M HCl; in 4 M HCl, a poorly shaped peak is formed (Fig. 2B).

With d.p.a.s.v., 0.1 μg ml^{-1} Sb(V) (8.21×10^{-7} M) in 4 M HCl gives a peak at —0.21 V. With the particular geometrical conditions of the cell used, a stirring rate of 400 rpm and a pre-electrolysis time of 72 s, the peak current was 12.2 μA. Under the same conditions, with a pre-electrolysis time of 600 s, 1 ng ml^{-1} Sb(V) gave a peak current of 0.4 μA. In more dilute hydrochloric acid, as observed by Batley and Florence [4], lower peaks were obtained (Fig. 3A). Antimony(III), under the same conditions, gave higher peaks than Sb(V) (Fig. 3B).

Preliminary studies of the sample treatment and reduction process

Powdered silicon is dissolved in teflon vessels with hydrofluoric acid plus nitric acid. After complete dissolution, the matrix is eliminated as hexafluorosilicic acid and silicon tetrafluoride by evaporation in a filtered air flow. The residue, containing the antimony and other impurities, is dissolved in reagents convenient for polarography. The procedure has been described in detail in previous papers [1, 2].

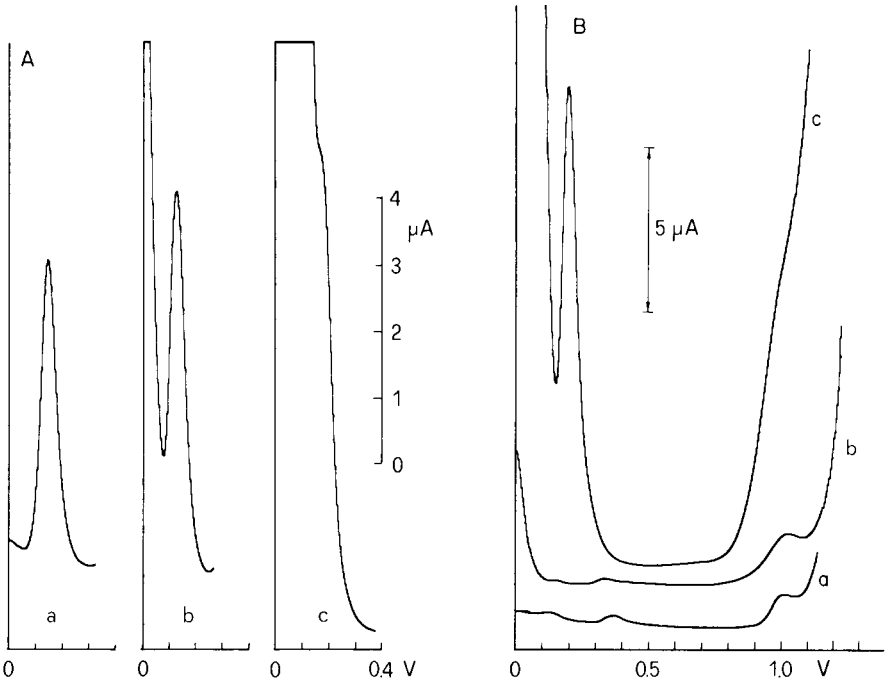

Fig. 2. Differential pulse polarograms for 1 ppm solutions of (A) Sb(III) and (B) Sb(V) in (a) 0.1 M HCl, (b) 1 M HCl, (c) 4 M HCl. Conditions: pulse amplitude —50 mV, scan rate 2 mV s^{-1}, drop time 2 s.

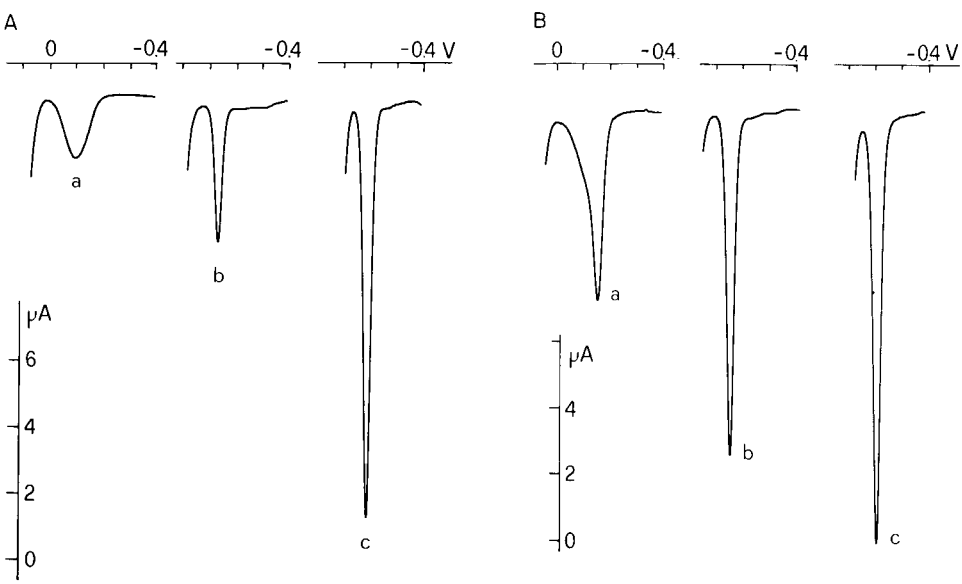

Fig. 3. D.p.a.s. voltammograms for 0.1 ppm solutions of (A) Sb(V) and (B) Sb(III) in (a) 0.1 M HCl, (b) 1.0 M HCl, (c) 4 M HCl. Conditions: pre-electrolysis potential —0.4 V vs. SCE, pre-electrolysis time 72 s, pulse amplitude +10 mV, scan rate 2 mV s^{-1}.

Study of the Sb(V) → Sb(III) reduction process and of the stability of the reduced solutions. Of the many reduction procedures available for antimony-(V), that based on the use of sulfurous acid seemed to be the most suitable. The reduction proceeds readily in hydrochloric acid solutions and the excess of sulfur dioxide is easily removed by passing nitrogen. However, some difficulties were encountered in obtaining quantitative reduction under conditions compatible with subsequent polarography.

In preliminary tests of the reduction process, portions (0.25 ml) of standard 100 μg ml^{-1} Sb(V) solution were introduced into 25-ml volumetric flasks. To each flask 2.5 ml of 1 M HCl and 5 ml of about 5% (w/v) sulfurous acid solution were added and the mixture was diluted to volume with doubly-distilled water. The flasks were thermostated at 50° C. At various times, each flask was cooled quickly to room temperature, the solution was placed in the polarographic cell, the excess of sulfur dioxide was removed by a prolonged nitrogen bubbling, and d.p.p. was then applied. Reference points were obtained in the same way by using standard Sb(III) solutions. The results are shown in Fig. 4; the dashed curve relates to an experiment in which aliquots of a reacting solution were withdrawn at various times from the same vessel.

These results (Fig. 4) are obviously unsatisfactory and seem to depend on the type of the standard Sb(V) solution used. The measurements made with aqueous $KSb(OH)_6$ solutions gave fairly good, reproducible results, and reduction was extensive after about 1 h. However, antimony(V) prepared by oxidizing Sb(III) in hydrochloric solutions with bromine or nitric acid gave generally low, erratic values. This behaviour might be due to re-oxidation of

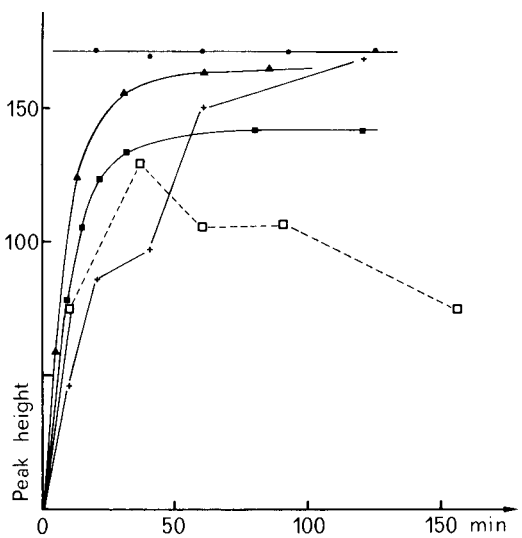

Fig. 4. Reduction of antimony(V) in 0.1 M HCl, at 50°C with SO_2. (•) Reference values obtained with Sb(III); (▲) Sb(V) from $KSb(OH)_6$; (■) Sb(V) from Sb_2O_3 oxidized with bromine, (+) Sb(V) from Sb_2O_3 oxidized with nitric acid; (□) As curve (+), but with aliquots withdrawn from the same vessel (see text). Peak heights were measured in arbitrary units.

the Sb(III) to the polarographically inactive Sb(V), which was therefore examined in some detail.

In systematic experiments, the behaviour of acidic Sb(III) solutions was observed with and without sulphur dioxide addition, at room and higher temperatures. The observations led to the following conclusions. First, Sb(III) in dilute or concentrated hydrochloric acid, in the absence of catalytic substances, is stable towards oxidation by atmospheric oxygen. Secondly, acidic Sb(III) solutions, containing small quantities of catalytic substances, (e.g., chlorine, bromine, nitrogen oxides), can be oxidized by air even if SO_2 is present in some excess (see Fig. 4, dashed curve). Thirdly, high SO_2 concentrations prevent the oxidation by oxygen. The reactions appear to be as follows:

$$\text{Sb(III)} \xrightarrow[(NO_2, Cl_2, Br_2)]{O_2} \text{Sb(V)} \quad (1); \qquad \text{Sb(III)} \xleftarrow[(I^-)]{SO_2} \text{Sb(V)} \quad (2)$$

Some substances with apparent catalytic activity are mentioned in parentheses. The uncontrolled air contact during the introduction of the solutions into the polarographic cell and the deaeration, and the varying sulphur dioxide and trace catalyst concentrations are some factors which could explain the erratic results.

This difficulty was largely overcome by adding to the solutions some potassium iodide, which, although present at trace level, acts as a powerful catalyst for the reduction reaction (2) without introducing serious interference in the subsequent polarographic analysis. The effect of iodide was checked by comparing the results of numerous experiments made with and or without addition of potassium iodide. As an example, reductions were tested for 1 μg ml^{-1} Sb(V) solutions, as $KSb(OH)_6$, in 0.1 M HCl with 1% (w/v) SO_2 solution at 70°C for 45 min. When iodide was not added, the mean peak height obtained was 154 mm (s.d. = 13.2, r.s.d. = 8.6%, N = 17), whereas when 10^{-5} M iodide was present, the mean peak height was 172 mm (s.d. = 4.3, r.s.d. = 2.5%, N = 13). The value expected from Sb(III) was 172 ± 2. Thus the trace of iodide produces significant improvements in both accuracy and precision.

Recovery of antimony from the residue of the sample solution

Preliminary experiments on the recovery of the antimony in the residue of the sample solution, after the elimination of the silicon matrix, gave very erratic results. This led to a systematic study of the conditions. First, solutions containing 2.5—25 μg of antimony(III) in 25 ml of 0.1, 1.0 and 4.0 M HCl were heated under reflux in teflon vessels for times up to 2 h; no losses of antimony were observed by d.p.p. or d.p.a.s.v. Second, solutions containing 2.5—25 μg of antimony(III) or (V) were mixed with 4 ml of 6 M hydrofluoric acid and 2 ml of concentrated (65%) nitric acid and dried in a glycerol bath at 120°C, with air flow. The residue was dissolved in 25 ml of 4 M HCl by heating under reflux for 30 min. Measurements by d.p.a.s.v., which allows

a direct determination of both Sb(III) and Sb(V), showed recoveries of 50—80%. Similar low recoveries were obtained when the latter experiment was repeated with the addition of 80—100 mg of very pure powdered silicon; the silicon was completely dissolved at reflux temperature, the solution was evaporated to dryness, and the residue was dissolved with 4 M HCl as before.

The apparent antimony losses can reasonably be ascribed to the different oxidation states of antimony produced by oxidative sample treatments [5, 6]. Reduction with sulfur dioxide after the dissolution stage with hydrochloric acid effectively improved the recoveries, because Sb(V) and Sb(IV) were converted to the active trivalent state, particularly when iodide was present as catalyst. Thus when sample residues which were simply dissolved with 4 M HCl in teflon vessels, without reduction with sulphur dioxide before application of d.p.a.s.v., the mean recovery was 76.9% (r.s.d. = 14.6%, N = 12). When d.p.a.s.v. was applied after the reduction process, the mean recovery was 97.3% (r.s.d. = 2.7%, N = 6). Anodic stripping was used because it allows the determination of Sb(V) as well as Sb(III). When d.p.p. was used in 0.1 M HCl after reduction with SO_2, the mean recovery was 88.1% (r.s.d. = 6.2%, N = 10), and when iodide was added as catalyst, the mean recovery improved to 99.2% (r.s.d. = 1.8%, N = 7).

Recommended procedure

Dissolve 10—100 mg of powdered silicon with 4 ml of 6 M hydrofluoric acid and 2 ml of concentrated nitric acid in teflon test tubes. For complete dissolution, maintain the covered tubes in a thermostated bath at 120°C for about 30 min. Evaporate the solution to dryness at 120°C with the aid of a filtered air flow. In this way, the silicon matrix is completely eliminated as silicon tetrafluoride or hexafluorosilicic acid. Antimony, in mixed oxidation states, remains in the residue with most other impurities.

Add to the residue in the teflon tubes 2.5 ml of 1.0 M HCl, close the tubes with teflon plugs and maintain at 120°C for 20 min to dissolve the residue. Cool to room temperature, transfer the solutions to 25-ml volumetric flasks, add 0.25 ml of 10^{-3} M potassium iodide solution and 5 ml of 5% (w/v) sulfur dioxide solution, and dilute to the mark with distilled water. Maintain the closed flasks at 70°C for 30 min. Cool, transfer the solution to a suitable polarographic cell, and deaerate for at least 20 min with a fast nitrogen flow before starting the polarographic measurements.

Samples containing more than about 5 $\mu g\ g^{-1}$ antimony are conveniently measured by d.p.p. Samples with lower antimony contents are better measured by d.p.a.s.v. In the latter case, after dissolution of the residue and reduction of the antimony as described above, the solution is diluted to the mark with 5 M HCl, instead of water, to give a final hydrochloric acid concentration of ca. 4 M.

Calibration graphs for the appropriate ranges of concentration are constructed by adding various amounts of standard Sb(III) or Sb(V) solution to 50—100 mg of pure silicon and processing as described for the samples.

TABLE 1

Analysis of silicon samples[a]

Sample	D.p.a.s.v.			D.p.p.		
	Sb found ($\mu g\ g^{-1}$)	R.s.d. (%)	N	Sb found ($\mu g\ g^{-1}$)	R.s.d. (%)	N
Alfa-Ventron Co. No. 00469	0.13	5	9	—		
Merck Art. 12497	2.75	5	11	—		
SGS-ATES (Milan)	215	5	9	213	2.0	9

[a]Results are given as the mean and relative standard deviation of results for N separate samples.

RESULTS AND DISCUSSION

The proposed method was used for determining antimony in two commercial samples of silicon and in antimony-doped silicon slices for electronic purposes (SGS-ATES, Milan). Results are shown in Table 1.

It is clear that both d.p.p. and d.p.a.s.v. are valuable for determining antimony in silicon. Anodic stripping permits the analysis of samples with much lower antimony contents. Unfortunately, as a result of the treatment for sample dissolution, antimony takes variable oxidation states and a reduction process is necessary even if d.p.a.s.v. is used, in order to obtain the best results, because the uncontrolled Sb_2O_4 formation can affect the accuracy of the results. Differential pulse polarography is less sensitive than d.p.a.s.v., but it provides greater precision because, unlike d.p.a.s.v., it is not dependent on critical parameters, such as drop reproducibility and stirring conditions. The relative standard deviation is adequate for most cases.

With the described procedure for d.p.p., silicon samples with antimony contents down to about 5 $\mu g\ g^{-1}$ can be analysed. The use of smaller volumes of solution and polarographic microcells (ca. 5 ml) would permit the analysis of silicon samples with antimony contents of 0.5—1 $\mu g\ g^{-1}$ by processing about 100 mg of silicon, without preconcentration stages, if no interfering elements were present. Among the common elements, copper can interfere if present in more than 20-fold amounts (molar ratio). Iron and lead do not interfere. When d.p.a.s.v. is used, samples with 0.1—0.2 $\mu g\ g^{-1}$ antimony can be analysed. However, at very low concentration, losses can occur by adsorption of antimony on glass surfaces.

This work was supported by Consiglio Nazionale delle Ricerche, under a contract related to the Progetto Finalizzato Per La Chimica Fine e Secondaria.

REFERENCES

1 P. Lanza and M. T. Lippolis, Anal. Chim. Acta, 87 (1976) 27.
2 P. L. Buldini, D. Ferri and P. Lanza, Anal. Chim. Acta, 113 (1980) 171.
3 I. M. Kolthoff and J. J. Lingane, Polarography, Vol. II, Wiley—Interscience, New York, 1965.
4 G. E. Batley and T. M. Florence, J. Electroanal. Chem., 55 (1974) 23.
5 T. H. Maren, Anal. Chem., 7 (1947) 487.
6 M. G. Tamba and N. Vantini, Analyst, 97 (1972) 542.
7 N. Konopik and J. Zwiauer, Monatsh. Chem., 83 (1952) 189.

Analytica Chimica Acta, 146 (1983) 71—86
Elsevier Scientific Publishing Company, Amsterdam — Printed in The Netherlands

CATHODIC STRIPPING VOLTAMMETRIC DETERMINATION OF TRACE AMOUNTS OF PENICILLINS

ULF FORSMAN

Department of Analytical Chemistry, Institute of Chemistry, University of Uppsala, P.O. Box 531, S-751 21 Uppsala (Sweden)

(Received 25th June 1982)

SUMMARY

The cathodic stripping voltammetric behaviour of four penicillins is described. After conversion to the corresponding penicilloic acid by alkaline hydrolysis, accumulation is performed at a hanging mercury drop electrode at −0.10 V vs. SCE in a pH 4.6 buffer containing excess of copper(II). During the accumulation, the penicilloic acid is further degraded and a copper complex of penicillamine is formed. This complex is subsequently reduced at about −0.4 V in the stripping step. After accumulation for 1 min or 10 min, 1×10^{-9} or 2×10^{-10} M penicillin, respectively, may be detected. Cathodic stripping voltammetry conducted in absence of copper(II), at pH 4.6 or 9.2, yields a stripping peak corresponding to the reduction of a mercury complex of penicillamine. At pH 9.2, an additional peak, regarded as the reduction of a penamaldic acid complex with mercury is obtained. This complex degrades with time which makes its stripping peak less valuable for the determination of traces. The mercury complex peak disappears in presence of copper(II). The anodic stripping voltammetric behaviour in presence of copper(II) is also reported. Two anodic film stripping peaks are obtained, at + 0.08 and + 0.13 V.

Numerous methods for quantifying penicillins have been described in the literature. Disregarding all microbiological methods, spectrophotometric [1, 2] and titrimetric techniques [3, 4] seem to predominate. However, few methods are sensitive enough for trace determinations. Ampicillin can be detected fluorimetrically at concentration levels lower than 0.05 μg ml^{-1} (10^{-7} M) [5]. A spectrophotometric method based on the coloured complex formed in penicillin solutions treated with imidazole and mercury(II) chloride can be used down to 0.5 μg ml^{-1} [2]. In addition, this reaction has been utilized in an h.p.l.c. post-column derivatization system [6].

Recently it was reported that penicilloic acid obtained by alkaline hydrolysis of benzylpenicillin gives rise to anodic polarographic waves at a dropping mercury electrode [7]. This reaction was applied in a flow-injection system for quantifying penicilloic acid in penicillin preparations [8]. The electrode reaction product, a mercury complex, is adsorbed at the electrode surface. Application of cathodic stripping voltammetry (c.s.v.) to the determination of traces of penicilloic acid is therefore a possibility. Previously the technique of c.s.v. has been shown to be extremely sensitive in the deter-

mination of penicillamine [9], cysteine and cystine [10]. These substances were accumulated at a hanging mercury drop electrode (HMDE) in the form of a mercury or a copper complex. When the copper complex was employed, the determination was done in the presence of excess of Cu(II) and a detection limit of 2×10^{-9} M was reported after a 1-min accumulation. A similar c.s.v. procedure for the determination of thiocyanate as a copper(I) complex was recently reported [11]. Cyanide has also been determined by stripping analysis in the presence of Cu(II) [12]. In this case, an anodic potential scan was used, and the oxidation peaks obtained were evaluated. In the present paper, the stripping voltammetric behaviour of penicillins after their alkaline hydrolysis to penicilloic acid is investigated, in both the absence and presence of copper(II) ions.

EXPERIMENTAL

Apparatus and reagents

A PAR-174 polarograph was used together with a Hewlett-Packard 7044A X-Y recorder. The PAR instrument contains a 10× amplification in the differential pulse (d.p.) mode. All d.p. current values reported here refer to these amplified values. The current sampling interval of the PAR instrument was changed from 16.7 ms to 20 ms in order to optimize discrimination against 50-Hz noise. The working electrode was a Metrohm E290 hanging mercury drop electrode (HMDE). A drop with a surface area of 2.7 mm^2 was used unless otherwise stated. A saturated calomel electrode, together with a diaphragm tube containing the buffer solution (described below), was used as a reference. In the following, all potentials are referred to this electrode combination. Stirring was done magnetically at a speed of 200 rpm.

Benzylpenicillin potassium, ampicillin sodium, cloxacillin sodium and phenoxymethylpenicillin potassium (all from ASTRA Pharmaceuticals AB, Södertälje, Sweden) were used as received. Penicilloic acid was prepared by alkaline hydrolysis of the penicillin as described previously [7].

Stock solutions (1×10^{-3} M) of penicillamine (Fluka) were prepared in deoxygenated water. All penicilloate and penicillamine solutions were freshly prepared. Stock solutions (1×10^{-1}—1×10^{-4} M) of copper(II) and mercury(II) nitrate were prepared from analytical-grade chemicals (Merck).

Mercury used in the HMDE was Merck, suprapur. For the dropping electrode, double-distilled mercury (Kebo) was used. The pH 4.6 acetate buffer consisted of 0.05 M sodium acetate and 0.05 M acetic acid in triply distilled water. The copper ion content of the buffer, measured by anodic stripping voltammetry, was found to be $<1 \times 10^{-8}$ M. The pH 9.2 borate buffer consisted of 0.01 M disodium tetraborate-10-hydrate and 0.1 M KNO_3 in triply distilled water.

Procedure

Penicilloic acid and copper(II) nitrate solutions were added to 10 ml of deoxygenated buffer solution with 10-μl syringes. Deposition was performed under stirring followed by a 30-s rest period. The potential scans were typically done at a potential sweep rate, v, of 10 mV s^{-1} in the differential pulse (d.p.) mode and 20—200 mV s^{-1} when a linear potential scan was employed. A new drop was used for every scan. The pulses in d.p. mode were applied every 0.5 s with a pulse amplitude of 50 mV. The sampled d.c. polarograms were recorded with a drop time of 2 s and a potential sweep rate of 5 mV s^{-1}. All experiments were done at room temperature (22 ± 1°C).

RESULTS AND DISCUSSION

Degradation of penicilloic acid by mercury

Mercury(II) ions convert benzylpenicilloic acid (BPA) initially to a mercury complex of penamaldic acid and finally to a penicillamine complex [13]. The lifetime of the penamaldic acid complex is dependent on pH. A

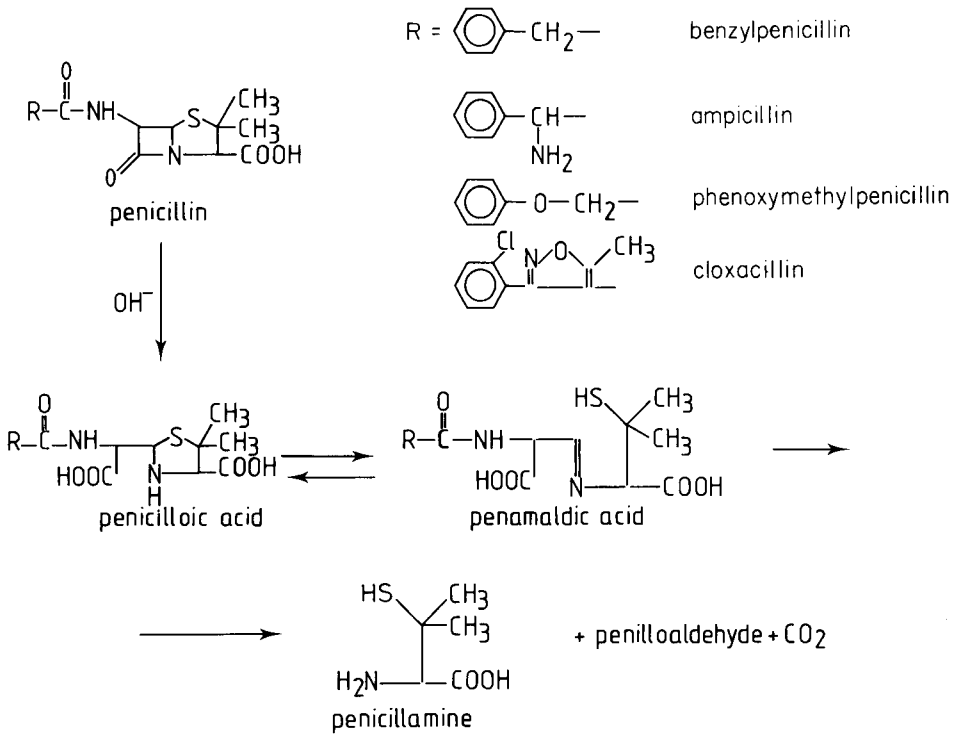

half-life of 4 to 5 min was reported at pH 7.4, but is shorter in more acidic media [14]. In the present study, the formation of the penicillamine complex was verified with the aid of d.c. polarography at pH 4.6. In the

absence of Hg(II), BPA gives rise to several poorly separated waves (Fig. 1, curve b). (A detailed discussion concerning the polarographic behaviour of BPA can be found in a previous paper [7].) When BPA is mixed with an equimolar amount of Hg(II), the polarogram in Fig. 1, curve c, is obtained. An identical polarogram is found in a 1:1 mixture of penicillamine and Hg(II).

At pH 4.6 penicillamine yields an anodic wave at about −0.3 V with the formation of a mercury complex [9, 15]. The reversibility of the reaction [15] suggests that the cathodic wave at −0.28 V in Fig. 1 corresponds to the reduction of a mercury penicillamine complex formed by the reaction between BPA and Hg(II) in the solution. The wave at +0.1 V is only observed at pH values below 6, and will be discussed in detail in a later paper.

The penicillamine complex is found also when BPA is electrolysed at +0.2 V at a mercury pool electrode. The polarogram obtained in the final solution after electrolysis was identical to those obtained from BPA or penicillamine in mixtures with Hg(II). (Fig. 1, curve c).

Cathodic stripping voltammetry at pH 4.6 in absence of copper(II) ions

In Fig. 2 is shown a linear potential scan cathodic stripping voltammogram (l.s.c.s.v.) of 4×10^{-7} M BPA at pH 4.6. Accumulation was done at −0.10 V and a single stripping peak at −0.30 V was obtained. This peak potential is in

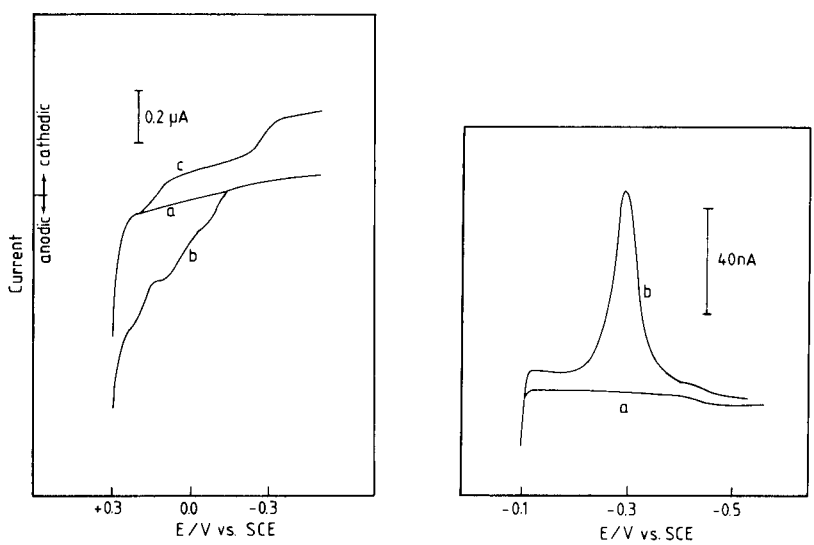

Fig. 1. Sampled d.c. polarograms of: (a) acetate buffer pH 4.6; (b) 5×10^{-5} M BPA; (c) with 5×10^{-5} M $Hg(NO_3)_2$ added.

Fig. 2. Linear scan c.s.v. of: (a) acetate buffer pH 4.6; (b) 4×10^{-7} M BPA. Accumulation for 1 min at −0.10 V; $v = 20$ mV s^{-1}.

good agreement with the one reported for c.s.v. of penicillamine when the d.p. mode was employed [9]. Considering that a mercury complex of penicillamine is formed from BPA on its reaction with mercury, it is concluded that the stripping peak corresponds to the reduction of such a complex. The shape of the stripping peak is affected by the surface concentration of the mercury penicillamine complex. With increasing surface concentrations, the peak width at half the peak height decreases. This results in an S-shaped plot when the peak height is recorded for the bulk concentration range 2×10^{-7}—6×10^{-6} M after a 1-min accumulation. The same relationship was previously reported for c.s.v. of penicillamine, when a differential pulse potential ramp was employed [9].

Intermolecular attraction forces between adjacent molecules in the adsorbed state can result in such effects on the peak shape [16]. At pH 4.6 the carboxy and the amino group of the penicillamine molecule are oppositely charged, while at alkaline pH, the amino group is neutral. Because the peak width of the stripping peak obtained from penicillamine is unaffected by the surface concentration at pH 9.2, it is assumed that attraction between these functional groups is important. Hydrogen bonding of mercury(II) cysteinate in the adsorbed state was previously suggested [17]. The peak area, does, however, increase linearly with concentration. This area, which reflects the amount of adsorbed mercury penicillamine complex, should mainly be determined by the mass transport of BPA to the electrode surface during the accumulation period.

When the bulk concentration exceeds about 3×10^{-6} M, the slopes of both the peak height and peak area plots decrease drastically when a 1-min accumulation time is employed. An integrated peak area of 75 μC cm^{-2} was obtained from a 1×10^{-5} M solution. This value is in close agreement with the maximum coverage of 80 μC cm^{-2} reported for mercury(II) cysteinate [17].

Accumulation at potentials between 0.0 and +0.2 V sometimes yielded a second peak, negative to the one at −0.30 V. An increase in peak height of this second peak was always followed by a decrease of the first peak. The origin of this new peak is not clear, but its irreproducible character indicates that analytical utilization of the peak is limited. An accumulation potential of −0.10 V where only the peak at −0.30 V is obtained, is the most advantageous for c.s.v. in the absence of Cu(II), at pH 4.6.

Cathodic stripping voltammetry at pH 9.2 in the absence of copper(II) ions

The d.c. polarographic behaviour of BPA at alkaline pH is quite different from that in acidic medium [7]. Only one anodic wave ($E_{1/2}$ = −0.25 V) is observed at pH 9.2. Cyclic voltammetry yields an anodic peak at −0.22 V, and a cathodic one at −0.27 V. It was suggested that the electrode reaction product of BPA at pH 9.2 under polarographic and cyclic voltammetry conditions is a mercury complex of penamaldic acid [7] (see above). Experimental verification of this suggestion, for instance via bulk electrolysis, is

difficult, because of degradation of the complex with time. The conclusion concerning the nature of the product, therefore relies mainly on literature data [14, 18]. However, in cyclic voltammetry, several scan cycles performed in a row, at the same mercury drop, yields the same peak couple. This reversible behaviour is possible if the anodic reaction product is the mercury penamaldic acid complex, because of the proposed equilibrium between the penamaldic and penicilloic acids [19, 20]. If an open ring structure, with a free sulfhydryl group predominated after the first scan cycle, the anodic peak obtained in the second cycle would most probably be situated at a more negative potential. The peak potentials of penicillamine and penicillenic acid, which both contain a free —SH group, are —0.55 V [7] (pH 9.2), and —0.54 V [21] (pH 6.4), respectively.

Figure 3 shows the cathodic voltammetric response of BPA at pH 9.2 after accumulation for 1 min at +0.05 or —0.10 V. The peak obtained at —0.24 V is considered as the reduction of the mercury penamaldic acid complex, while the peak at —0.55 V corresponds to the mercury penicillamine complex. The appearance of the penicillamine complex peak depends on both the accumulation potential and the time. After accumulation at +0.05 V, both peaks are observed, and the penamaldic acid peak is predominant for accumulation times less than 30 s. With increasing time, the penicillamine complex peak increases at the expense of the penamaldate peak. After accumulation at —0.10 V, mainly the penamaldate peak appears. However, the peak does not grow with increased accumulation time. After a

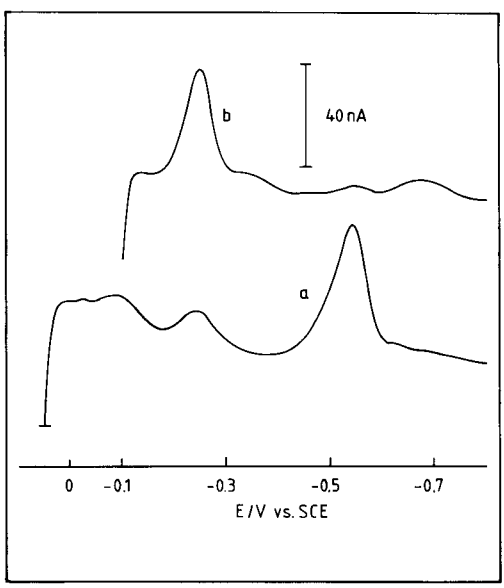

Fig. 3. Linear scan c.s.v. of 4×10^{-7} M BPA at pH 9.2. Accumulation for 1 min at: (a) +0.05 V; (b) —0.10 V. $\upsilon = 20$ mV s^{-1}.

5-min accumulation, the peak has vanished and is replaced by a broad peak at about −0.7 V. This peak does not correspond to the penicillamine complex, but suggests the formation of additional degradation products. After addition of 2×10^{-7} M penicillamine to a 1×10^{-6} M BPA solution, only the penicillamine complex peak was observed after accumulation at −0.10 V. It is assumed that the penicillamine complex is more strongly adsorbed than the penamaldic acid complex, and that the former complex therefore is preferentially accumulated. After addition of 2×10^{-6} M Hg(II) to a 5×10^{-7} M BPA solution, the penamaldate peak decreased with time after the addition; simultaneously the penicillamine complex peak appeared. These results are explained by the formation of the penicillamine complex as the final product from the reaction between BPA and Hg(II) in the solution.

Degradation of the penamaldic acid complex to other products, essentially the penicillamine mercury complex, is considerably slower at pH 9.2 than at pH 4.6. However, in the alkaline buffer, the degradation of the penamaldate complex during the time of analysis makes the peak obtained from this complex less valuable for trace determinations.

Cathodic stripping voltammetry in the presence of copper(II) ions

At pH 9.2, the stripping peaks from the mercury complexes of penamaldic acid and penicillamine are lost on addition of copper(II) ions. Instead, a single peak at −0.65 V is obtained. At pH 4.6, the peak at −0.30 V is replaced by a peak at about −0.4 V. This latter situation is illustrated in Fig.4A,

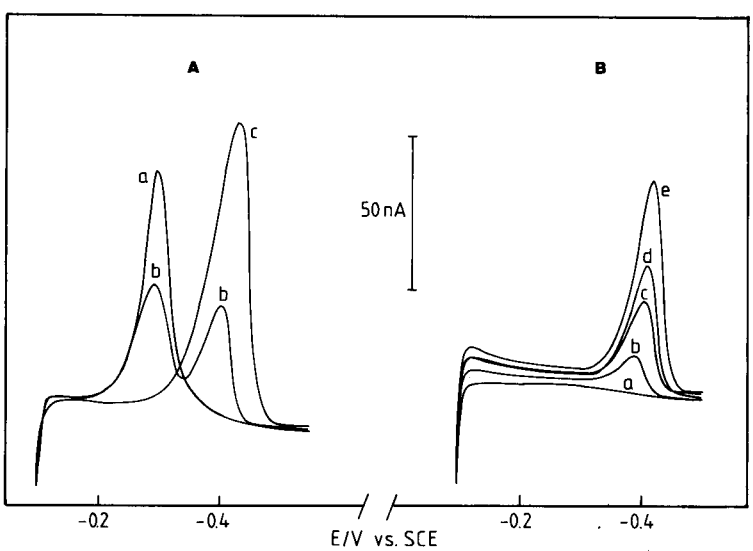

Fig. 4. (A) Linear scan c.s.v. of (a) 4×10^{-7} M BPA; (b) 1×10^{-7} M Cu(II) added; (c) 4×10^{-7} M Cu(II) added. (B) Linear scan c.s.v. of (a) blank; (b) 4×10^{-8} M; (c) 8×10^{-8} M; (d) 1.2×10^{-7} M; (e) 2×10^{-7} M BPA, all with 1×10^{-6} M Cu(II) added. Accumulation for 1 min at −0.10 V, pH 4.6, $v = 20$ mV s^{-1}.

where the stripping peaks of 4×10^{-7} M BPA, after successive additions of copper(II), are shown. The second peak is observed even when the Cu(II) concentration is only a quarter that of the BPA. At equimolar levels, only the second peak is observed. In the following paragraphs, attention is focused on this new peak obtained in pH 4.6 buffer containing copper(II) ions, because it was found to be the most advantageous one for c.s.v. of trace amounts of penicillins.

The nature of the electrode reaction product obtained during the accumulation in the presence of Cu(II) was investigated with the aid of cyclic voltammetry. Figure 5(a) shows the cyclic voltammogram of 1×10^{-6} M BPA in the presence of 1×10^{-5} M Cu(II). The scan was initiated at −0.10 V in the anodic direction after a 20-s accumulation time. This voltammogram should be compared with the one from 1×10^{-5} M penicillamine in the presence of 2×10^{-5} M copper(II) (Fig. 5b). Disregarding the different sensitivities on the current axes, the traces are very similar. Evidently the same product is formed from BPA during the accumulation period as is formed at the electrode surface in the penicillamine copper solution. Penicillamine is known to form a copper complex in copper(II)-containing solutions [22]. The

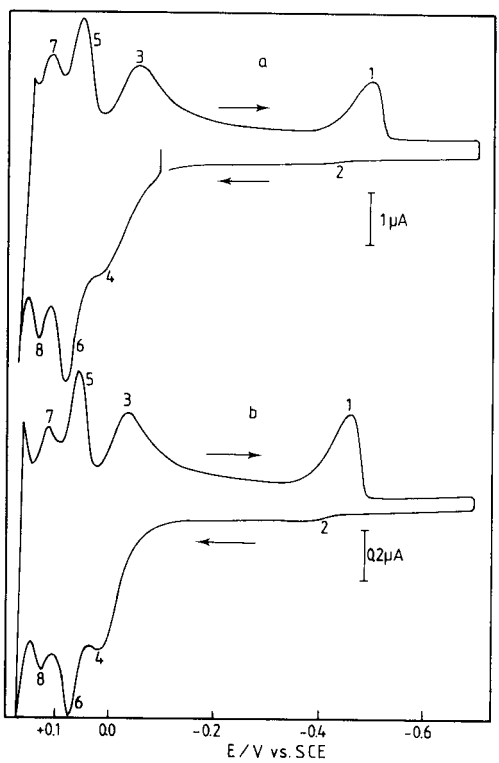

Fig. 5. Cyclic voltammetry of (a) 1×10^{-6} M BPA and 1×10^{-5} M Cu(II) after 20-s accumulation at −0.10 V; $v = 200$ mV s^{-1}. (b) 1×10^{-5} M penicillamine and 2×10^{-5} M Cu(II); $v = 50$ mV s^{-1}, $E_{start} = -0.70$ V.

complex is reduced about 0.1 V negative to the reduction potential of the mercury complex, and may be accumulated at the mercury electrode [9]. The cathodic peak 1 (Fig. 5) is considered to correspond to the reduction of the adsorbed copper penicillamine complex, to copper amalgam and the free thiol:

$$CuRS_{(ads)} + H^+ + e^- \rightleftharpoons Cu_{(Hg)} + RSH_{(sol)} \quad (1)$$

The small peak 2 at about −0.35 V is the diffusion-controlled formation of the complex as this reaction proceeds to the left. Peaks 3 and 4 are the formation and oxidation of copper amalgam because of the excess of Cu(II) ions. It is suggested that peak 6 corresponds to an oxidation process in which the adsorbed copper complex is converted to an adsorbed mercury complex of penicillamine; this will be discussed in detail in a later paper. Peak 5 then represents the reverse reaction. The peaks 7 and 8 at +0.13 V represent an oxidation and reduction process of the mercury complex formed at +0.08 V during the anodic scan. This peak couple is in accordance with the d.c. wave at +0.10 V (Fig. 1), only observed at pH values below 6. Peaks 5—8 will be discussed in detail elsewhere.

It is concluded that a copper complex of penicillamine is formed from BPA during the accumulation at pH 4.6, when Cu(II) is added. The stripping peak obtained at −0.4 V is therefore considered to originate from the reduction of this complex as in reaction 1. The amount of Cu(II) required in order to obtain exclusively the copper complex stripping peak is very low. Thus c.s.v. of BPA based on the accumulation and reduction of the mercury complex requires solutions with extremely low contents of copper(II) ions. This is a requirement that can be very difficult to fulfil. However, the copper complex may readily be used for quantitative purposes and BPA can thus be measured with c.s.v. also in the presence of excess of copper(II). This is exemplified in Fig. 4B, where stripping peaks of $4-20 \times 10^{-8}$ M BPA in the presence of 1×10^{-6} M Cu(II) are shown. The copper complex stripping peaks increase linearly with the potential sweep rate, when examined between 5 and 200 mV s^{-1}. This is in accordance with the stripping of a film from the surface of an electrode [23]. The integrated peak area is unaffected by v.

Effect of excess of copper(II) on the reduction peak

The peak current, i_p, of the copper complex stripping peak, was previously investigated for penicillamine as a function of the Cu(II) excess, when the differential pulse mode was employed [9]. It was found that i_p increased as the Cu(II) excess was raised up to a limit after which i_p was practically constant. The influence of the excess of copper(II) on the reduction peak obtained from BPA was examined by using a linear potential scan. Figure 6 shows the peak height, peak area and peak width of the peak obtained from 1×10^{-7} M BPA as a function of the excess of copper(II). The width was measured at half the peak height.

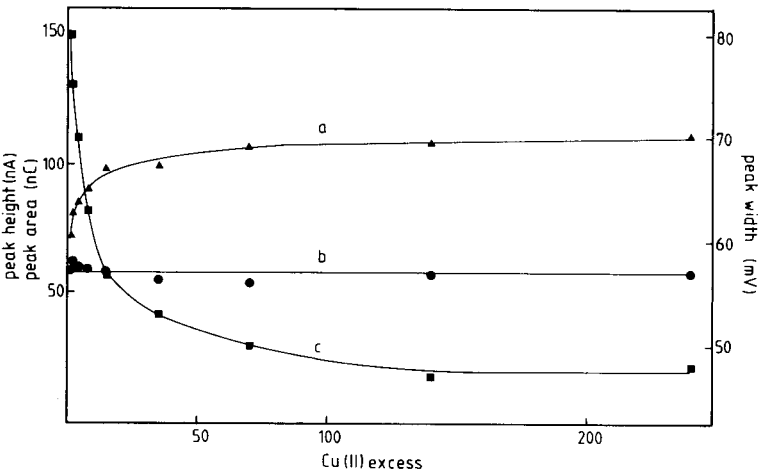

Fig. 6. Linear scan c.s.v. of 1×10^{-7} M BPA in presence of different molar excesses of Cu(II), after accumulations for 1 min at −0.10 V (v = 100 mV s^{-1}): (a) peak height; (b) peak area; (c) peak width.

The peak height increases rapidly for low excesses of copper ion, while at higher excesses, i_p is only marginally affected (curve a, Fig. 6). The peak area, however, is independent of the excess of copper(II) (curve b). Finally, the peak width decreases as the excess of copper(II) increases (curve c). Copper amalgam will be formed at the electrode during the accumulation, when excess of copper(II) ion is present. As previously reported [9, 10], the influence on the peak height from the excess of Cu(II) is due to this amalgam formation. The constant value obtained for the peak area shows that the amount of copper penicillamine complex accumulated is independent of the excess. The altered peak shape obtained with increasing excess (Fig. 6) is therefore assumed to arise from changes in the kinetics of the reduction process.

Reduction of excess of copper(II) ions during the accumulation will decline once the stirring has stopped, because of depletion of copper(II) in the immediate vicinity of the electrode. However, during the potential scan, a contribution to the background current from this reduction may be observed when a linear potential scan is employed. In the presence of less than about 2×10^{-6} M Cu(II), the background is essentially of capacitive origin. Above this value, the contribution from Cu(II) reduction does, however, increase rapidly.

When the differential pulse mode is used, both current and noise levels in the potential region of the stripping peak are unaffected by copper(II) concentrations up to at least 10^{-5} M.

A copper(II) concentration of 10^{-6}—10^{-5} M is usually most convenient. There is no gain in using higher levels. When extremely low BPA concentrations ($<10^{-9}$ M) are to be measured, a Cu(II) level of 10^{-7}—10^{-6} M is preferred. This case is further discussed below.

Accumulation potential

The influence of the accumulation potential, E_{acc}, on the stripping peak area and peak height is shown in Fig. 7. The peak shape, here represented by the peak height, is dependent on the presence of copper amalgam at the electrode, as described above (Fig. 6). When accumulation is done at potentials positive to the normal potential of the Cu(II) reduction, essentially no amalgam is formed during the accumulation. At E_{acc} negative to about 0.0 V, however, copper amalgam will be formed during the accumulation, and the stripping process will proceed at a copper amalgam electrode. In accordance with Fig. 6, higher and narrower stripping peaks will result. For E_{acc} more negative than −0.1 V, the amount of amalgam formed during the accumulation is practically independent of the potential. A constant peak height is then obtained. When E_{acc} approaches the stripping potential, the amount of adsorbed copper complex naturally approaches zero. It should be noted that at potentials positive to the anodic peak 6 in Fig. 5, a mercury complex is accumulated and not the copper one. However, during the cathodic potential scan, the adsorbed mercury complex will be converted to the copper analogue when copper(II) is present. The extent of this conversion is dependent on the Cu(II) concentration and on the scan rate [9]. Under the conditions used for the data of Fig. 7, complete conversion is obtained, and only the copper complex stripping peak is recorded.

Other penicilloates

Penicilloates obtained by alkaline hydrolysis of ampicillin, cloxacillin and phenoxymethylpenicillin were also investigated. After accumulation at −0.10 V, all these penicilloates gave rise to a stripping peak at the potential

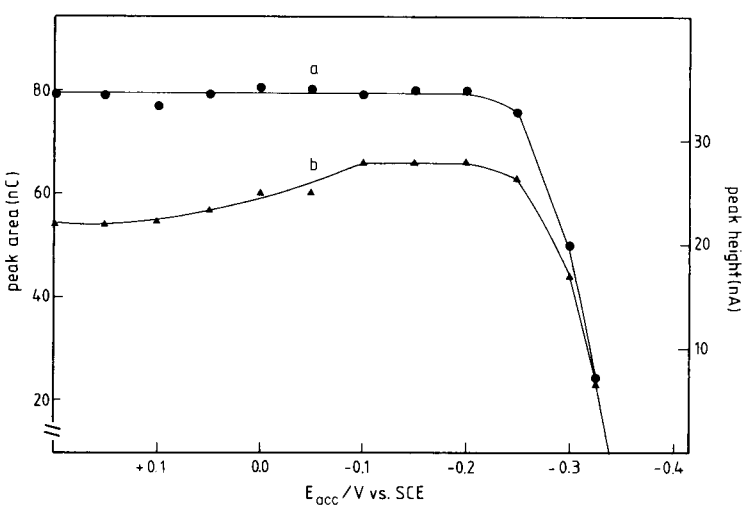

Fig. 7. Peak area (a) and peak height (b) of 2×10^{-7} M BPA in presence of 3×10^{-6} M Cu(II) as a function of accumulation potential. $v = 20$ mV s^{-1}; electrode area 1.9 mm^2.

of the mercury penicillamine complex, when measurements are done in the absence of Cu(II). On addition of Cu(II), all the penicilloates exhibit the voltammetric pattern shown in Fig. 4, and the measurements are then done on the basis of the copper penicillamine complex, regardless of which penicilloate is under investigation.

The similarities of the cathodic stripping voltammetric behaviour of different penicilloates is not surprising. That part of the molecule which reacts with mercury is the sulphur-containing 5-membered ring, connected to the hydrolysed β-lactam ring. This part is found in any penicilloate, regardless of the side-chain.

Calibration graphs and accumulation time

The cathodic stripping peak of the copper complex increases linearly with penicilloic acid concentration for all four penicillins investigated when a constant copper(II) ion concentration is present. When the differential pulse mode is employed after an accumulation time of 1 min, and the parameters specified in the experimental section are used, the graphs obtained for 2×10^{-9}—1×10^{-7} M penicilloate solution in the presence of 2×10^{-6} M copper(II) give the following typical values: slope $1.6 \pm 0.2 \times 10^{7}$ μA M^{-1}, intercept <10 nA, $R^2 > 0.9995$. In Fig. 8 the differential pulse cathodic stripping voltammograms (d.p.c.s.v.) of low levels of hydrolysed ampicillin are shown. The shapes of these traces are typical for all the investigated penicilloates. At penicilloic acid concentrations higher than 10^{-7} M, the peak height vs. concentration slope slowly decreases as previously reported for penicillamine and cysteine at this pH [9, 10]. The concentration at which linearity no longer prevails, depends to some extent on the Cu(II) concentration as will be discussed below and can be extended above 10^{-7} M by increasing the Cu(II) level to values exceeding 2×10^{-6} M.

When a linear sweep potential scan is used, either the peak height or the peak area may be evaluated. The peak height is linear with penicilloic acid concentration up to the same limit as when the d.p. mode is used. For the peak area, however, linearity prevails even when the peak height no longer changes linearly with concentration. When BPA was examined between 2×10^{-8} and 7×10^{-7} M after a 1-min accumulation, in presence of 2×10^{-6} M Cu(II), the peak height gave a linear plot up to about 10^{-7} M BPA solution, while the peak area was linear within the entire investigated interval ($R^2 = 0.9995$). The extended linear range obtained when peak areas are evaluated can be understood from the results reported in Fig. 6. When the BPA concentration increases, the excess of Cu(II) decreases. When the molar excess is less than 10—20, the peak width increases rapidly, so that peaks are lower than those obtained with higher Cu(II) excesses. Evaluation of peak area is restricted to the concentration interval accessible with the linear sweep mode. For a 1-min accumulation, the lower limit is about 10^{-8} M.

Above 4×10^{-6} M penicilloate, the current, and the peak area, approach constant values when accumulation is done for 1 min in presence of

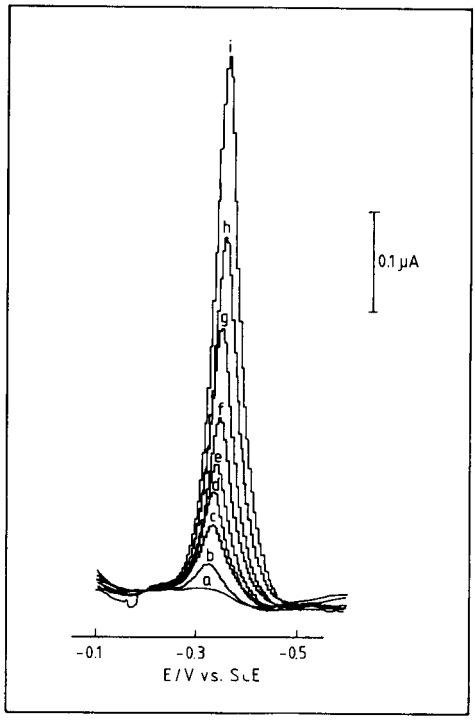

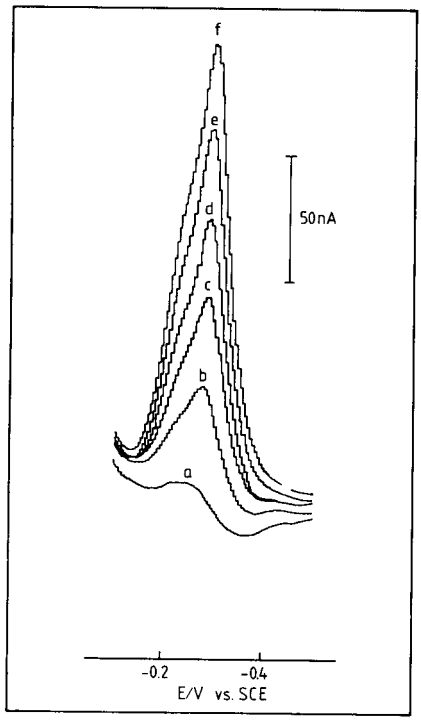

Fig. 8. Differential pulse c.s.v. of hydrolysed ampicillin in presence of 2×10^{-6} M Cu(II) after accumulation for 1 min at −0.10 V: (a) acetate buffer; (b) 2×10^{-9}; (c) 4×10^{-9}; (d) 6×10^{-9}; (e) 8×10^{-9}; (f) 1×10^{-8}; (g) 1.5×10^{-8}; (h) 2×10^{-8}; (i) 3×10^{-8} M.

Fig. 9. Differential pulse c.s.v. of BPA in presence of 1×10^{-7} M Cu(II) after accumulation for 10 min at −0.10 V: (a) acetate buffer; (b) 2×10^{-10}; (c) 4×10^{-10}; (d) 6×10^{-10}; (e) 8×10^{-10}; (f) 1×10^{-9} M.

1×10^{-5} M Cu(II). The mercury drop is becoming saturated with the accumulated copper penicillamine complex, and the peak splits, yielding another sharp peak, positive to the initial one. The charge involved in the reduction at saturation is about 60 μC cm^{-2}, which indicates the presence of a monolayer of the complex at the mercury surface [11].

The peak current increases linearly with accumulation time up to about 10 min, for 2×10^{-8} M BPA in the presence of 1×10^{-6} M Cu(II). By extending the accumulation time further, the increase in peak height is slightly less than predicted by the initial linear relationship.

Very low levels of penicilloic acid may be quantified by employing long accumulation times. In Fig. 9 are shown stripping peaks from BPA solutions between 2×10^{-10} and 1×10^{-9} M, obtained after accumulation for 10 min in presence of 10^{-7} M Cu(II). The figure demonstrates the high sensitivity of the c.s.v. method. As expected, an increased stirring rate also enhances the stripping current. The more efficient mass transport to the electrode results in an increase in the amount of copper penicillamine molecules accumulated.

The relative standard deviation for five repetitive determinations of 1×10^{-8} M BPA in presence of 10^{-6} M Cu(II) was $<3\%$. For five determinations of 1×10^{-9} M BPA in presence of 10^{-7} M Cu(II), the r.s.d. was $<5\%$. A 1-min accumulation was used in all cases.

Anodic stripping in the presence of copper(II) ions

Anodic potential scans conducted after an accumulation at −0.10 V, are shown in Fig. 10. As Cu(II) is present, the oxidation peak of copper amalgam is initially observed (curve a). After addition of BPA, two anodic film stripping peaks appear at +0.08 and +0.13 V (curves b and c). These peaks have the same origin as peaks 6 and 8 in the cyclic voltammograms of Fig. 5. The peak heights of these film stripping peaks increase linearly with sweep rate, while the copper amalgam peak increases proportionally to $v^{1/2}$. Measurement of the anodic film stripping peaks becomes quite uncertain at high excesses of copper(II) because the peaks will drown in the sloping part of the copper amalgam peak.

The peak heights of the two anodic film stripping peaks were investigated between 8×10^{-8} M and 6×10^{-7} M BPA in the presence of 2×10^{-6} M

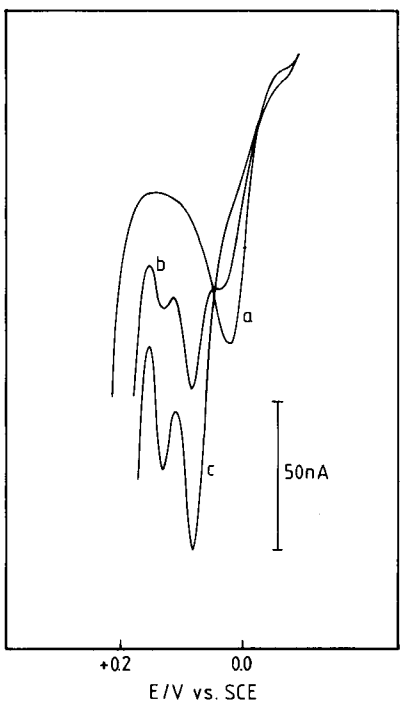

Fig. 10. Linear sweep anodic stripping voltammograms after accumulation for 1 min at −0.10 V (v = 20 mV s^{-1}): (a) 1×10^{-6} M Cu(II) in acetate buffer; (b) 2×10^{-7} M BPA added; (c) 5×10^{-7} M BPA added.

Cu(II). The plot obtained for the peak at +0.08 V was linear up to about 3×10^{-7} M BPA and then the slope decreased. The peak at +0.13 V increased linearly (R^2 = 0.9991) within the entire interval. However, neither of the plots passed the origin, but instead crossed the x-axis at 4×10^{-8} and 1×10^{-7} M, respectively. As a consequence of the formation of the copper penicillamine complex, the copper amalgam oxidation peak decreases linearly with increasing BPA concentration.

The analytical utilization of the anodic film stripping peaks for the determination of penicilloic acid is limited if a large excess of Cu(II) is present, because the size of the copper amalgam peak inevitably limits the lowest detectable concentration of BPA. The anodic stripping behaviour of cysteine and penicillamine in presence of copper ions will be discussed in detail in a later paper.

Interferences

Penicillamine and cysteine will interfere because these substances give rise to a stripping peak at the same potential as the penicilloic acids. Among the metal ions, lead(II) yields a reduction peak close to the cathodic stripping potential of the copper penicillamine complex. The peak from 5×10^{-8} M BPA is only affected if the lead(II) concentration exceeds 10^{-6} M. The presence of 10^{-4} M iron(III) or 5×10^{-6} M mercury(II) or zinc(II) does not influence the stripping peak. Strongly adsorbing species such as proteins influence the c.s.v. of BPA. Thus 2×10^{-4}% (w/v) albumin gives a slight distortion, whereas 10^{-3}% of the protein completely eliminates the peak from 2×10^{-8} M BPA in presence of 10^{-6} M Cu(II). Among the halides, 10^{-3} M bromide reduces the cathodic stripping current obtained from 4×10^{-8} M BPA and 10^{-6} M Cu(II) by about 7%; 10^{-2} M chloride gives a 15% reduction of the peak current. However, when an accumulation potential of −0.20 V is applied instead of −0.10 V, the interference from these anions is diminished.

Conclusions

Cathodic stripping voltammetry of penicilloic acid is extremely sensitive when the measurements are done in the presence of copper(II) ions. During the accumulation, a copper complex of penicillamine is formed. Evaluation of the reduction peak of this complex makes it possible to determine bulk concentrations of penicilloic acid lower than 10^{-9} M. In the absence of Cu(II), the pH dependence of the degradation of the penicilloic acid molecule on reaction with mercury results in quite different voltammetric patterns at acidic and alkaline pH values. The penicillamine mercury complex is rapidly formed at pH 4.6. This product is stable at the electrode and may serve for quantitative purposes. The mercury penamaldate peak, which occurs at pH 9.2, has an advantage in that it is unique for penicilloic acid, and does therefore indicate the presence of this substance. Yet, the peak is labile and does not appear when long accumulation times are employed or when

penicillamine is present. Both the mercury complex peaks reported are lost when Cu(II) is added. The presence of this metal ion therefore will influence the detection limits of these peaks.

The four different penicilloates investigated here all exhibit the same cathodic stripping behaviour at pH 4.6. It is therefore most probable that other penicilloates will also be suitable for cathodic stripping analysis.

REFERENCES

1 A. O. Niedermayer, F. M. Russo-Alesi, C. A. Lendzian and J. M. Kelly, Anal. Chem., 32 (1960) 664.
2 H. Bundgaard and K. Ilver, J. Pharm. Pharmacol., 24 (1972) 790.
3 J. F. Alicino, Ind. Eng. Chem. Anal. Ed., 18 (1946) 619.
4 B. Karlberg and U. Forsman, Anal. Chim. Acta, 83 (1976) 309.
5 W. J. Jusko, J. Pharm. Sci., 60 (1971) 728.
6 D. Westerlund, J. Carlqvist and A. Theodorsen, Acta Pharm. Suec., 16 (1979) 187.
7 U. Forsman and A. Karlsson, Anal. Chim. Acta., 128 (1981) 135.
8 U. Forsman and A. Karlsson, Anal. Chim. Acta, 139 (1982) 133.
9 U. Forsman, J. Electroanal. Chem., 111 (1980) 325.
10 U. Forsman, J. Electroanal. Chem., 122 (1981) 215.
11 R. Bilewicz and Z. Kublik, Anal. Chim. Acta, 123 (1981) 201.
12 H. Berge and P. Jeroschewski, Z. Anal. Chem., 228 (1967) 9.
13 D. W. Hughes, A. Vilim and W. L. Wilson, Can. J. Pharm. Sci., 11(1976) 97.
14 C. H. Schneider and A. L. de Weck, Helv. Chim. Acta., 49 (1966) 1689.
15 M. Jemal and A. M. Knevel, J. Electroanal. Chem., 95 (1979) 201.
16 E. Laviron, J. Electroanal. Chem., 52 (1974) 395.
17 M. T. Stankovich and A. J. Bard, J. Electroanal. Chem., 75 (1977) 487.
18 H. T. Clarke, J. R. Johnson and R. Robinson, The Chemistry of Penicillins, Princeton Univ. Press, NJ, 1949, p. 427.
19 M. A. Schwartz, J. Pharm. Sci., 58 (1969) 643.
20 B. B. Levine, Nature, 187 (1960) 940.
21 M. Jemal and A. M. Knevel, Anal. Chem., 50 (1978) 1917.
22 J. J. Vallon and A. Badinand, Anal. Chim. Acta, 42 (1968) 44.
23 Kh. Z. Brainina, Talanta, 18 (1971) 513.

Analytica Chimica Acta, 146 (1983) 87—95
Elsevier Scientific Publishing Company, Amsterdam — Printed in The Netherlands

DETERMINATION OF SOME CEPHALOSPORINS BY DIFFERENTIAL PULSE POLAROGRAPHY AND LINEAR SCAN VOLTAMMETRY[a]

ARI IVASKA* and FREDRIK NORDSTRÖM
Department of Analytical Chemistry, Åbo Akademi, 20500 Turku 50 (Finland)
(Received 6th May 1982)

SUMMARY

Methods for the determination of cefadroxil, cephalexin and cephapirin are described. Differential pulse polarograms of cephalexin and cefadroxil show a distinct peak at −1.25 to −1.3 V (vs. Ag/AgCl) at pH 1—2. The peak can be obtained immediately after dissolution of the solid sample and is stable for several hours. The calibration graphs have two linear portions with a break around 4×10^{-5} M; for cefadroxil, the graph is linear down to 2×10^{-6} M; and for cephalexin down to 10^{-5} M, the upper limit being around 10^{-3} M in both cases. At a glassy carbon electrode, cefadroxil gives an anodic oxidation wave at +0.8 V (vs. Ag/AgCl) at pH 7.3; this wave was used for linear scan voltammetry. Cephapirin gives a stable peak on differential pulse polarography at pH 7—8.5. At pH 7.3, the calibration graph is linear over the range 10^{-3}—5×10^{-7} M. The methods were tested on commercial samples and good agreement was found between the results obtained and the values given by the manufacturer. Mechanisms are discussed.

Polarography and other voltammetric methods are becoming increasingly important in the determination of compounds of pharmaceutical interest. The techniques themselves are simple and reliable, and the electrochemical reactions, either reduction or oxidation, often provide selectivity for the compound sought in the presence of degradation products, metabolites and the raw materials in the manufacturing process.

Cephalosporins are closely related to the penicillin family and are used for patients allergic to penicillin. Cephalosporins are electrochemically active; there are several studies on their polarographic properties [1—11] and polarography has also been used in studying their degradation [12—14]. Hall [3] stated that polarographic methods are generally applicable to all cephalosporins containing a leaving group at the 3-position. Fogg et al. [10], using differential pulse polarography (d.p.p.), found that cephalosporins containing an unsubstituted 3-methyl group but no reducible groups, did not give peaks at the dropping mercury electrode. Fogg et al. [11] and Squella et al. [8] devised methods for the determination of cephalexin, a cephalosporin having an unsubstituted 3-methyl group, based on polarographic measurement of one of its degradation products after intensive hydrolysis, in pH 7.4 buffer

[a]This paper was presented in part at Euroanalysis IV, Helsinki, Finland, August 1981.

for 1 h at 100°C [11] or in 5 M HCl for 15 min at 80°C [8]. Yet Benner [2] and Siegerman [6] reported that cephalexin gives a d.c. polarographic wave [2] and a d.p.p. peak [6] at −1.25 V vs. SCE in 0.125 M sulphuric acid which provide linear relationships between the current and concentration in the range 1—70 μg ml^{-1}. Benner [2] also reported a wave at −0.85 V vs. SCE in 0.25 M sodium hydroxide but the wave was stable only after hydrolysis. Siegerman [6] also used this peak analytically without mentioning stability. Both authors gave the linear range as 1—100 μg ml^{-1}. Hall et al. [7] reported that Δ^3deacetoxycephalothin, which has an unsubstituted 3-methyl group, produced a wave at low pH values but the wave merged into the electrolyte discharge at pH values above 3.2.

This paper is concerned with the polarographic properties of cefadroxil (I), cephalexin (II) and cephapirin (III); methods are described for their polarographic and voltammetric determinations.

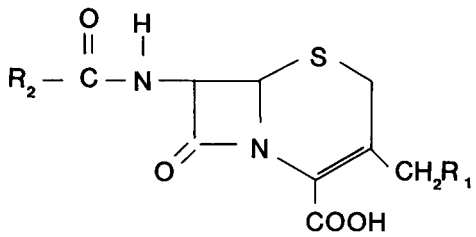

Cefadroxil R_1 = -H; R_2 = 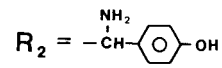 I

Cephalexin R_1 = -H; R_2 = 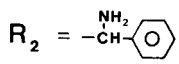 II

Cephapirin R_1 =  ; R_2 = 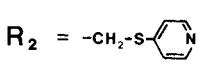 III

EXPERIMENTAL

Apparatus

A PAR 174A polarograph (E.G. and G. Princeton Applied Research) was used with either a 303 SMDE or 1743 drop timer in the three-electrode mode. The working electrode was a dropping mercury electrode or a glassy carbon electrode. The auxiliary electrode was a platinum wire and a saturated Ag/AgCl electrode was used as the reference electrode. All potentials in this work are measured against this reference electrode. Lithium chloride replaced potassium chloride if potassium ions interfered. In the d.p.p. mode, conditions included a drop time of 1 s, a pulse amplitude of 50 mV and a scan rate of 5 mV s^{-1}. Cyclic polarograms were recorded at a scan rate of 100 mV s^{-1}. The surface of the glassy carbon electrode was polished with aluminium oxide to a mirror finish and was washed with methanol and mechanically dried and cleaned with soft tissue paper before every run in order to obtain as reproducible results as possible. Solutions were deaerated with a flow of nitrogen for 10 min before measurements.

Reagents

Cephalosporin samples were kindly provided by Lääke Oy Pharmaceutical Works (Turku, Finland) who also guaranteed their purity. Cephalexin was provided as its monohydrate, cefadroxil as such and cephapirin as its sodium salt. All other chemicals were of analytical grade. Britton—Robinson universal buffer was used. The stock buffer solution was 0.04 M in boric, orthophosphoric and acetic acid and the pH was adjusted with 1 M sodium hydroxide.

Procedures

The polarographic properties of cefadroxil (I), cephalexin (II) and cephapirin (III) were studied in 5 M, 1 M and 0.1 M HCl, Britton—Robinson buffer pH 2—10, and 0.1 M and 1 M NaOH in order to find the optimum pH range for quantitative work. To avoid interferences from potassium and sodium ions, polarograms were also taken in 0.1 M LiOH, 0.1 M tetramethylammonium bromide and in 0.1 M $LiNO_3$, the pH being adjusted with phosphoric acid, acetic acid and lithium hydroxide. Dimethylformamide was tested as the solvent in an attempt to broaden the potential range of the mercury electrode, but showed no advantages over water, in which all the compounds studied were soluble. Solutions of the cephalosporins were always prepared immediately before the electrochemical measurements.

When repeated anodic scans were done to assess reproducibility, the potential was always held for 1 min at the final potential before returning to the initial potential, to ensure that the electrode surface was always polarized the same way before each scan. Reproducible results also required washing of the electrode surface with methanol before each scan.

RESULTS AND DISCUSSION

Cathodic reduction of cefadroxil and cephalexin

Cefadroxil and cephalexin were found to have rather similar polarographic properties. Both compounds gave a d.p.p. peak at around −1.25 V vs. Ag/AgCl electrode in 1 M HCl but this peak decreased with time. The decrease was faster, the higher the acid concentration. In 0.1 M HCl and in Britton—Robinson buffer pH 2, the peak was stable at room temperature for several hours, and so could be used analytically. The peak appeared immediately after dissolution of the sample, without any particular hydrolysis procedure. The changes in the polarograms with pH are shown in Fig. 1. As can be seen, the d.p.p. peak is shifted to more negative potentials and decreases with increasing pH, merging with the electrolyte discharge at pH values over 3, as was found earlier [7] for a similar compound. The peak potential shifts by about −30 mV between 1 and 2. Similar behaviour was observed for cefadroxil. The difference in the peak potentials between cephalexin and cefadroxil is about 30 mV, those of cefadroxil being more positive. In neutral and alkaline solutions, cephalexin and cefadroxil undergo rapid hydrolysis. In 0.1 M NaOH, a new peak appeared rather quickly at

—0.76 V (vs. Ag/AgCl); this is obviously the peak recommended by Benner [2] and Siegerman [6] for analytical work. Cephalexin degradation has been studied extensively by Fogg et al. [12, 13]. Based on the present results, the stable d.p.p. peaks at around —1.25 V in 0.1 M HCl and at around —1.3 V in Britton-Robinson buffer pH 2 can be used to quantify cephalexin and cefadroxil.

Polarography in the d.c. mode was used to check the relationship between the square root of the mercury height (corrected for back-pressure) and the limiting current of a solution of 2.2×10^{-4} M cephalexin. The non-linearity found suggests that the current is not fully diffusion-controlled, but it was rather difficult to measure the wave height because of its proximity to the electrolyte discharge.

At concentrations of cephalexin exceeding 10^{-3} M, the d.p.p. peak almost merged with the electrolyte discharge. At lower concentrations, the d.p.p. peak moved to less negative potentials and became clearer. An adsorption prepeak appeared at concentrations exceeding 10^{-4} M. For cefadroxil, there was no distinct prepeak, only a small change in the background current; with 10^{-3} M cefadroxil, the d.p.p. peak can be distinguished from the electrolyte discharge so that this compound is easier to determine than cephalexin.

The d.p.p. peak potential of cephalexin shifted by about —90 mV over the range 10^{-4}—10^{-3} M at pH 2. This shift is in good agreement with the value of —89 mV given by Kolthoff and Lingane [15] for the shift in the hydrogen discharge wave for a 10-fold change in concentration of an unreducible weak acid. The shift in the peak potential was less than —90 mV over the range 10^{-5}—10^{-4} M cephalexin. This suggests that at low concentrations the acid exists in the anionic form rather than in the undissociated

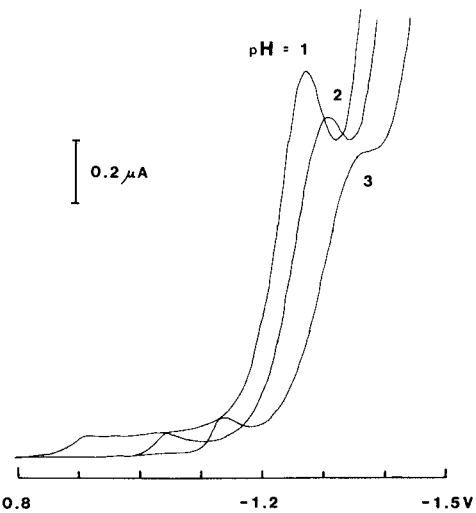

Fig. 1. Differential pulse polarograms of 2×10^{-4} M cephalexin solutions of pH 1 (0.1 M HCl), pH 2 and pH 3 (Britton—Robinson buffers).

form assumed in deriving the equation for catalytic hydrogen discharge. For cefadroxil, the shift was around −70 mV over the 10^{-4}—10^{-3} M range.

The logarithmic plot, ln $[i/(i_l - i)]$ vs. $-E$, where i_l is the limiting current and E is the potential, calculated with values from a d.c. polarogram of a 2.9×10^{-5} M solution of cephalexin in 0.1 M HCl, was linear within experimental error. A value of $\alpha n = 1.04$ was calculated from the slope. On cyclic polarograms of 10^{-4} M cephalexin and cefadroxil solutions only the cathodic wave was observed, indicating an irreversible reaction. The d.p.p. peak currents of 10^{-4} M cephalexin and cefadroxil solutions were approximately the same as the peak current of a cephalothin solution of the same concentration. Cephalothin undergoes a 2-electron reduction [7], and the d.p.p. peaks of cephalexin and cefadroxil are probably also caused by a 2-electron reduction where one molecule of cephalexin or cefadroxil catalyses the reduction of two hydrogen ions.

The calibration graph for cephalexin consisted of two linear branches with a break around 4×10^{-5} M (ca. 15 μg ml^{-1}). The lower part was linear down to 1×10^{-5} M (ca. 4 μg ml^{-1}); the upper limit was 10^{-3} M (ca. 0.4 mg ml^{-1}) and the practical detection limit was around 5×10^{-6} M (ca. 2 μg ml^{-1}). For cefadroxil, the calibration graph was linear down to 2×10^{-6} M (ca. 0.7 μg ml^{-1}) and the upper limit was just over 1×10^{-3} M; the plot showed a break at the same concentration as cephalexin, again indicating a change in the reaction mechanism. The slopes of the lower and upper portions of the calibration graph were 1 and 0.65, respectively. A similar break in the calibration graph for cephalexin at about the same concentration was reported by Benner [2]. These breaks are particularly important when standard addition methods are considered.

In repeated determinations of cephalexin in 0.1 M HCl, the standard deviation was 0.6% ($n = 10$) for 6×10^{-4} M and 1.3% ($n = 10$) for 2×10^{-5} M cephalexin. Similar values were observed for cefadroxil.

The proposed method was tested in the assay of commerical cephalexin capsules nominally containing 500 mg of cephalexin monohydrate. Each capsule was dissolved in 100 ml of 0.1 M HCl and the solution was diluted (1 + 49) with 0.1 M HCl for d.p. polarography. The results were evaluated from a calibration graph obtained with solid cephalexin standards (480—550 mg). The average value of ten capsules was 534 mg with a relative standard deviation of 2%.

Cathodic reduction of cephapirin

Cephapirin (III) has a substituted methyl group in the 3-position and should therefore have a distinct d.p.p. peak at −1 V vs. SCE in the pH range 2—4 [3, 10]. However, the d.p.p. peak in this pH range was found to be distorted and a distinct peak appeared only for concentrations lower than 5×10^{-5} M. In 1 M HCl, the peak was distinct but unstable with time. Cephapirin contains a pyridine group in the 7-position side-chain, and heterocyclic nitrogen compounds are known to cause catalytic hydrogen reduction [16, 17]. Thus, it

is difficult to determine cephapirin in acidic solutions because of overlapping of the catalytic hydrogen wave and the cephapirin reduction wave. This is demonstrated in Fig. 2 where the addition of 5×10^{-5} M cephapirin is seen to shift the catalytic hydrogen peak from 10^{-3} M nitric acid to more positive potentials; doubling the concentration of nitric acid doubled the peak current, but the peak potential remained unchanged. Increasing the cephapirin concentration had little effect on either the peak potential or the current.

In nearly neutral solutions, cephapirin gave a distinct d.p.p. peak at −1.22 V vs. Ag/AgCl (Britton–Robinson buffer pH 7.3). As shown in Fig. 3, the peak height decreased with increasing pH. A distinct peak was also obtained in 0.1 M LiOH at −0.46 V vs. Ag/AgCl, but this was obviously caused by a hydrolysis product; at room temperature, the peak increased during the first 20 min and then decreased while a new peak increasing, with time, appeared at −0.75 V. Several other peaks were also found at potentials similar to those at which cephalexin and cefadroxil degradation products have their peaks. The d.p.p. peak of cephapirin at pH 7.3 was quite stable; it decreased only by 10% after 20 h at room temperature and so is suitable for analytical work.

The d.c. polarogram of cephapirin solution at pH 7.3 showed a strong polarographic maximum of the first kind, which could be eliminated by making the solution 0.003% in Triton X-100. The limiting current was

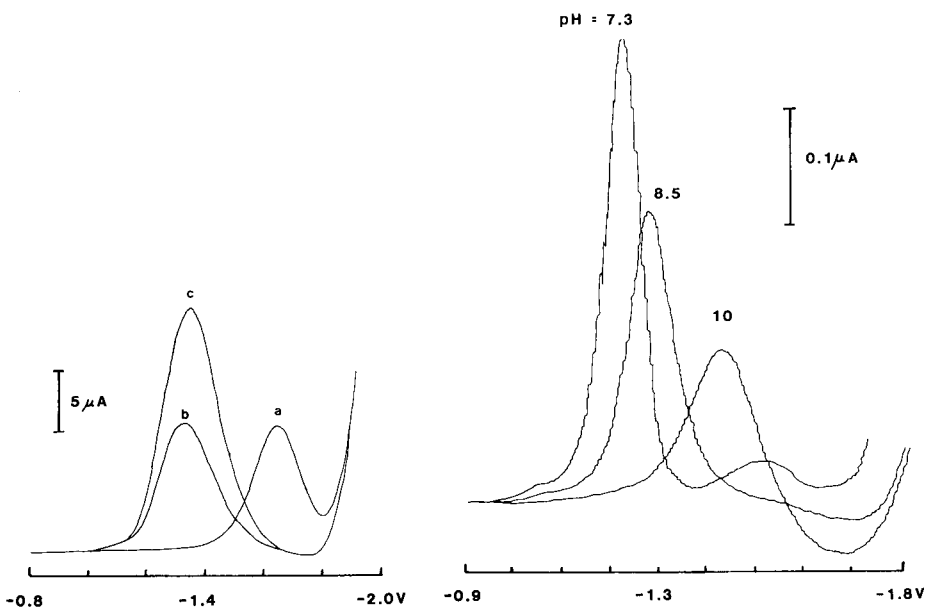

Fig. 2. Differential pulse polarograms for: (a) 10^{-3} M HNO_3; (b) 10^{-3} M HNO_3 + 5×10^{-5} M cephapirin; (c) 2×10^{-3} M HNO_3 + 5×10^{-5} M cephapirin. All solutions contained 0.1 M $NaNO_3$.

Fig. 3. Differential pulse polarograms of 1×10^{-4} M cephapirin solution in Britton–Robinson buffer at different pH values.

linearly related to the square root of the corrected mercury column height, indicating diffusion-control. Reduction of cephapirin is irreversible; a cyclic polarogram of 1.4×10^{-4} M cephapirin at pH 7.3 showed only the cathodic wave. The plot ln $[i/(i_l - i)]$ vs. $-E$ from a d.c. polarogram of 2×10^{-4} M cephapirin in the presence of 0.003% Triton X-100 was linear, and an αn value of 1.1 was calculated from the slope of the line. Cephapirin is obviously reduced in a 2-electron reduction where the substituent at the 3-methyl group is eliminated as proposed by Hall et al. [7].

At concentrations higher than 10^{-4} M, the polarographic maximum affected the d.p.p. peak so that it was followed by a dimple which deepened with increasing concentration. At lower concentrations the peak was symmetric. It was found, however, that when the peak current was measured from the extrapolated base line, a linear relationship was obtained between the peak current and concentration even in the absence of the maximum suppressor. The calibration plot was linear over the concentration range 5×10^{-7}—1×10^{-3} M (ca. 0.2—400 μg ml^{-1}). The precision was also good; the relative standard deviation of ten determinations at the 10^{-4} M level was 0.5%, and even at the 10^{-5} M level it was 0.7%.

Cephapirin is commercially available as its sodium salt in ampoules; it is dissolved in water and then given intramuscularly, because cephapirin is not absorbed when given orally. To test the proposed method for the determination of cephapirin, ampoules containing 500 mg of cephapirin were assayed. The contents of each ampoule were first dissolved in 100 ml of water and then diluted (1 + 99) with Britton—Robinson buffer pH 7.3 for polarography. The results were similar to those obtained with commercial cephalexin samples. The average of five determinations was 535 mg with a relative standard deviation of 4%.

Anodic oxidation of cefadroxil

Of the compounds studied, only cefadroxil gave a distinct anodic wave at the glassy carbon electrode. The linear sweep voltammograms of 2×10^{-4} M cefadroxil solutions at different pH values are shown in Fig. 4. The 7-position side-chain with the aromatic—OH group is obviously where the anodic oxidation takes place. As can be seen in Fig. 4, the wave is shifted to less positive potentials with increasing pH while the current decreases; this is in accordance with the fact that phenolic compounds undergo a 2-electron oxidation at low pH values and a 1-electron oxidation at high pH values [18]. The reproducibility of the wave was better in neutral and alkaline than in acidic solutions and therefore pH 7.3 was chosen for further work. The anodic wave is also stable against hydrolysis.

A diffusion-controlled current was indicated by the linear relationship found between the current and the square root of the sweep rate. In cyclic voltammograms, only the anodic oxidation wave was obtained, indicating an irreversible reaction.

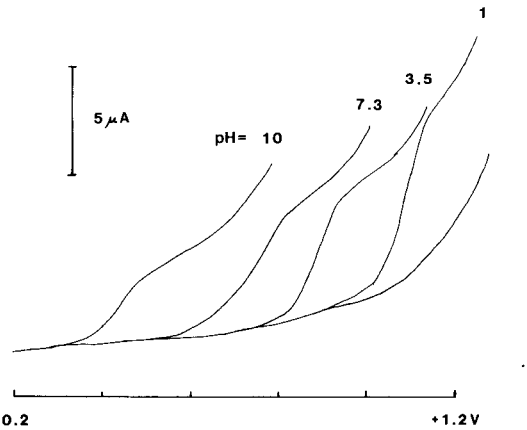

Fig. 4. Linear sweep voltammograms of a 2×10^{-4} M solution of cefadroxil at different pH values. Sweep rate 10 mV s^{-1}. The background current at pH 1 is also shown.

A linear relationship was found between current and concentration in the range 2×10^{-6}—4×10^{-4} M cefadroxil (ca. 0.8—200 μg ml^{-1}). Above this limit the calibration plot became slightly curved; 1×10^{-6} M may be regarded as the detection limit.

Because the oxidation reaction was studied at a glassy carbon electrode, the reproducibility depended strongly on how the electrode surface was cleaned. When the cleaning procedure recommended in the Experimental section was used, the relative standard deviation was 9% (n = 5) for 10^{-4} M cefadroxil if the current was measured at constant potential. Because the anodic wave studied is near the electrolyte decomposition wave, it was somewhat difficult to measure the peak current and the potential also changed slightly from run to run. When a new voltammogram was constructed each time by subtracting the background voltammogram from the actual voltammogram and the maximum current was measured, the precision of the method was improved, the relative standard deviation then being 5% at the 10^{-4} M level.

Conclusions

The methods described in the literature for determinations of cephalexin are tedious. The colorimetric method of Kirschbaum [19] takes at least 1.5 h. Barbhaiya and Turner [20] have described a spectrofluorimetric method which takes about 1 h. The polarographic methods [8, 11] for determination of cephalexin require hydrolysis, taking an overall time of >1 h. In one of his methods, Benner [2] used 0.125 M H_2SO_4 as supporting electrolyte and the samples were assayed without hydrolysis. An alternative polarographic determination is described above for cephalexin and cefadroxil. The method is based on the d.p.p. peaks at −1.25 V (vs. Ag/AgCl) at pH 1, the measurements being made immediately after dissolution and deaeration. No chemical methods seem to be available for cephapirin which is normally determined

by microbiologial methods. The overall time needed for determination of the drugs by the above methods is 10—15 min. If small sample volumes are used, the deaeration time may even be shortened. The sensitivity of the procedures described is comparable with those of earlier methods.

The authors are grateful to Mr. L. Liponkoski, Lääke Oy Pharmaceutical Works, Turku, Finland, who provided all the sample materials needed.

REFERENCES

1 I. F. Jones, J. E. Page and C. T. Rhodes, J. Pharm. Pharmacol., 28 (1968) Suppl., 45S.
2 E. J. Benner, Antimicrob. Agents Chemother., (1970) 201.
3 D. A. Hall, J. Pharm. Sci., 62 (1973) 980.
4 M. Ochiai, O. Aki, A. Morioto, T. Okada, K. Shinozaki and Y. Asahi, J. Chem. Soc., Perkin Trans. 1, (1974) 258.
5 E. C. Rickard and G. C. Cooke, J. Pharm. Sci., 66 (1977) 379.
6 H. Siegerman, in A. J. Bard (Ed.), Electroanalytical Chemistry, Vol. 11, Marcel Dekker, New York, 1979, p. 315.
7 D. A. Hall, D. M. Berry and C. J. Schneider, J. Electroanal. Chem., 80 (1977) 155.
8 J. A. Squella, L. J. Nunez-Vergara and E. M. Gonzales, J. Pharm. Sci., 67 (1978) 1466.
9 L. J. Nunez-Vergara, J. A. Squella and E. M. Gonzalez, J. Assoc. Off. Anal. Chem., 62 (1978) 556.
10 A. G. Fogg, N. M. Fayad, C. Burgess and A. McGlynn, Anal. Chim. Acta, 108 (1979) 205.
11 A. G. Fogg, N. M. Fayad and R. N. Goyal, J. Pharm. Pharmacol., 32 (1980) 302.
12 A. G. Fogg, N. M. Fayad and C. Burgess, Anal. Chim. Acta, 110 (1979) 107.
13 A. G. Fogg and N. M. Fayad, in W. F. Smyth (Ed.), Electroanalysis in Hygiene, Environmental, Clinical and Pharmaceutical Chemistry, Elsevier, Amsterdam, 1980, p. 233.
14 A. G. Fogg and M. J. Martin, Analyst, 106 (1981) 1213.
15 I. M. Kolthoff and J. J. Lingane, Polarography, Interscience, New York, 2nd edn., 1952, p. 243.
16 E. Knobloch, Collect. Czech. Chem. Commun., 12 (1947) 407.
17 M. P. Strier and J. C. Cavagnol, J. Am. Chem. Soc., 79 (1957) 4331.
18 F. J. Vermillon and I. A. Pearl, J. Electrochem. Soc., 111 (1964) 1392.
19 J. Kirschbaum, J. Pharm. Sci., 63 (1974) 923.
20 R. H. Barbhaiya and P. Turner, J. Pharm. Pharmacol., 28 (1976) 791.

Analytica Chimica Acta, 146 (1983) 97—108
Elsevier Scientific Publishing Company, Amsterdam — Printed in The Netherlands

A PYROLYTIC CARBON FILM ELECTRODE FOR VOLTAMMETRY
Part 1. Preparation and General Characterization

KENT LUNDSTRÖM

Department of Analytical Chemistry, University of Uppsala, P.O. Box 531, S-751 21 Uppsala (Sweden)

(Received 16th November 1981)

SUMMARY

The preparation of a pyrolytic carbon film material is described. The stationary silica tube used in the deposition process contains only the graphite substrates of a suitable form and size for direct electrode mounting. The deposition conditions were studied systematically at temperatures below 1150°C. The carbon material produced exhibits favourable qualities as an electrode material. The voltammetric behaviour is exemplified with cyclic voltammetry on *o*-dianisidine (3,3'-dimethoxybenzidine) in 1 M H_2SO_4 and on hexacyanoferrate(II) in 2 M KCl. The results show a satisfactory combination of good electrode kinetics with small reproducible residual currents. Submicromolar levels of *o*-dianisidine can be determined by differential pulse voltammetry. Dopamine in 0.04 H_2SO_4—0.01 M Na_2SO_4 exhibits quasi-reversible behaviour with no severe poisoning effects. Characteristic microstructural features of the carbon film material are discussed.

Solid electrodes based on carbon are currently in widespread use in voltammetry and in amperometric detectors, primarily because of their applicability to oxidations of organic compounds over an extended potential range. Many different carbon materials are employed, both all-carbon varieties such as glassy carbons or pyrolytic graphite, as well as several composites such as the carbon pastes. Several reviews on this topic, with fairly complete compilations of materials frequently used together with a brief summary of their electrochemical qualities, are available [1—5]. The more fundamental aspects of carbon as an electrode material have been discussed comprehensively by Randin [6].

Improvements in certain respects are, however, still desirable, especially in those cases where the use of carbon pastes is ruled out. For glassy carbon, the frequent alternative choice in electroanalytical applications, shortcomings reported have included high and often irreproducible residual currents in linear sweep voltammetry, as well as substantial and slowly decaying background response on the application of a potential pulse. The magnitude and appearance of this pulse response effectively prohibit measurements at submicromolar levels by means of pulse techniques in quiescent solutions. The present interpretation of this slow relaxation behaviour on changing the potential, sweep or pulse, involves sluggish redox equilibria of

0003-2670/83/0000-0000/$03.00

oxygen-containing functional groups at the surface. It is also widely recognized that the source of the glassy carbon material is of vital importance, which indicates that there are unidentified causes of the anomalous behaviour.

The present paper calls attention to a promising line of development available for carbon electrodes which previously has aroused only modest interest among electrochemists, namely, the coating of a suitable substrate with a very thin deposit of pyrolytic carbon. Such an approach can confer unusual qualities to the electrode. The preparation of pyrolytic carbons involves thermal decomposition of a hydrocarbon gas with deposition onto a heated refractory substrate placed in the pyrolysis chamber, to produce a dense and resistant carbon material. Techniques based on either a stationary tube reactor or a fluid bed can be used. Owing to the technical importance of this broad category of carbons, extensive research has been directed towards the many aspects of their preparation, structure and properties. The final product is critically dependent on conditions prevailing during the process; temperature, flow rate and partial pressure of the carbon source gas and the geometry of the reaction chamber are the most influential parameters. Massive deposits, hitherto used as an electrode material under the designation pyrolytic graphite, are obtainable under a narrow range of conditions [7]. The fundamental aspects of the production of pyrolytic carbon films, which is the type of material exploited in the work reported here, have been comprehensively reviewed by Bokros [8].

Beilby et al. [9] published the first report on a pyrolytic carbon film electrode, fabricated essentially as described by Grisdale et al. [10]. Natural gas, diluted with nitrogen to 25%, was decomposed at 1025°C in a rotating combustion tube containing the ceramic rods to be coated and a layer of sand to ensure an even deposit. A defined electrode surface was obtained by force-fitting the rods into machined teflon tubes. Charge-transfer rates similar to those obtained at a platinum electrode were found when chronopotentiometry was tested on the hexacyanoferrate(II)/(III) system, while residual currents were very low. Surprisingly, this promising initial report seems not to have been followed up. More recently, another interesting type of carbon film material, designated LTIC (low-temperature isotropic carbon), was evaluated with the aid of linear sweep voltammetry (l.s.v.) by Hepler et al. [4]. This material is produced by fluid bed technology under conditions which result in an isotropic structure, having remarkable strength. A thin-layer electrochemical detector based on this material was later described [11]. Earlier, Epstein et al. [12] characterized the l.s.v. behaviour of an electrochemically oxidized LTIC electrode. Two more reports on pyrolytic carbon film electrodes have appeared [13, 14]. However, these approaches differ in essential points (deposition technique, conditions and type of substrate) from the present work.

EXPERIMENTAL

Preparation of electrodes

Equipment. The pyrolytic carbon films were deposited in a stationary quartz tube situated horizontally in a resistively-heated tube furnace (450 mm long) which provided a uniformly heated 300-mm zone. A platinum/platinum—10% rhodium thermocouple was located in the middle of the furnace outside the quartz tube; heating was controlled and regulated with standard equipment (thyristor-based regulator) capable of a temperature constancy within ±5°C. The quartz tube was made of transparent Vitreosil (99.8% SiO_2) equipped with ground B19 joints; its inner diameter was 20.5 mm, outer diameter 24 mm, and total length, 600 mm. It was consistently positioned so that the middle portion was heated. Gases were supplied through glass and metal tubing, with short connections of PVC tubing (wall thickness 3 mm) as needed, and a PVC outlet tube. Gas flow rates were checked with meters based on the variable area principle ("Shorate", Brooks), previously calibrated with a soap-bubble meter.

Deposition parameters. All carbon films utilized were obtained under the following conditions. The temperature of pyrolysis was 1100°C. The carbon source gas was 10 ± 0.5% methane in argon (gas chromatography quality) and the flow rate was 260 ± 5 cm^3 min^{-1}. The time of deposition was 8 h or longer. Inert conditions were maintained with nitrogen as soon as the methane supply was interrupted and also during heating-up periods. After deposition was complete, purging with nitrogen for about 60 min was allowed before the furnace was turned off. Nitrogen was purified as described by Sawyer and Roberts [2]. Carbon material deposited on the wall of the quartz tube was burned off at roughly 700°C in an oxygen atmosphere between runs.

Substrate. A batch of short graphite rods (spectrographic quality, 6 mm diameter, 30 mm long) were first polished with silicon carbide paper (600 grit) and then polished to a mirror finish against a filter paper heavily impregnated with graphite from previous use. The rods were firmly held perpendicular to the support by means of a plastic guide during this handling in order to minimize rounded edges.

Procedure. A preliminary run with a long graphite rod extending over the entire heated zone established the proper positions and provided a useful check on the entire system. Under the recommended conditions, a lustrous grey deposit, almost metallic in appearance, should result and there should be no signs of soot formation. Sets of four rods, held together with preformed stiff kanthal wire in such a way that the edges of the polished surfaces were free (two backwards), were carefully placed in the predetermined positions in the quartz tube. Normally four sets were treated in each run.

Electrode assembly. During the initial stages of this work, when many deposits were tested, the sides of the graphite rods were carefully coated with ceresin wax applied with a small brush. The rod must be prewarmed

(e.g., by holding the hot brush against the rod for a moment) otherwise the wax film will not adhere. This wax film proved to be convenient and dependable for aqueous test solutions. A few tight turns of copper wire on the upper part of the rods provided electrical contact (d.c. resistance less than 1 ohm) and a glass tube served as shaft.

In the later stages of the work, the rods were mounted with heat-shrinkable teflon tubing (Habia AB, S-74100 Knivsta, Sweden) extending over the glass shaft. Shrinking was done under nitrogen, because the temperature required (ca. 320°C) can otherwise allow formation of surface oxides [15]. Edges defining the active electrode surface were carefully trimmed with a surgical scalpel. Electrical contact with copper wire, as described above, was fixed under the teflon tubing. No special precautions were observed for storing the coated rods, but prior to electrode assembly (and later as required) the deposited carbon film was cleaned carefully with a non-abrasive paper tissue soaked in dichloromethane followed by another soaked in ethanol. All results reported were obtained with the electrode surfaces as deposited; polishing procedures expose reactive sites on the microlevel, e.g., unsaturated carbon valences, with immediate consequences for the surface chemistry [16, 17].

Voltammetry

Equipment. A PAR 174A polarograph was used with a Hewlett-Packard X-Y recorder (model 7044A). The RC time constant of the sample-and-hold circuitry for the differential pulse mode was changed to that of the normal pulse mode (i.e., 15 ms). The geometric area of the working electrode (described above) was 0.28 cm^2. The reference electrode for aqueous test solutions was a saturated calomel electrode (SCE) placed in a salt bridge containing 0.5 M $NaNO_3$; for partly or completely non-aqueous solutions, a silver wire was used as quasi-reference. A platinum foil (10 × 20 mm) served as the auxiliary electrode. Conventional Metrohm cells thermostatted at 25.0 ± 0.2°C were employed; solution volumes were always 10 ml.

Procedures. The following instrumental parameters for differential pulse voltammetry (d.p.v.) were used throughout: pulse amplitude 50 mV, pulse repetition 0.5 s, scan rate 10 mV s^{-1}, low-pass filter in the off position. The offset function was used as required. Current setting was normally in the range 1—10 μA; in the differential pulse mode of the PAR 174A instrument, this setting includes an internal ten-fold amplification. Reported currents (text and figures) in this paper are the true values obtained by dividing the apparent current responses by ten. This practice has not always been followed in published works. Linear scan parameters are stated in the text as required.

Solutions were not deaerated. The pyrolytic carbon film electrode was always conditioned by a sweep over the potential range of interest; sometimes further electrolysis for a few minutes at the positive limit of the sweep was applied. Care was taken not to expose the electrode to extreme anodic

or cathodic potentials. When a suitable background current had been established, aliquots from a sample stock solution were added by means of a microliter syringe (not less than 25 μl) to give the desired concentrations.

Reagents. All chemicals were of analytical-reagent grade and were used as received; stock solutions (10^{-3} M) were prepared freshly. Triple-distilled water (from all-quartz equipment) was used throughout. Sulfuric acid was Aristar grade (BDH).

RESULTS AND DISCUSSION

Character of the prepared film

Under the conditions recommended above, the deposit obtained was lustrous grey, almost metallic, in appearance. Besides the four principal deposition parameters [8], attention must also be paid to other factors which can affect the product to a significant degree. These parameters include the purity of gases employed and of the substrate surface. However, once initial difficulties had been overcome, the given procedure proved to be dependable with a remarkable conformity in electrochemical qualities from batch to batch. Full characterization of the deposited film in terms of crystallite size and orientation of unit crystallites was not attempted. However, from the deposition conditions, it seems likely that a multitude of strong covalent cross-linkages within and between crystallites (i.e., the small structural units of graphitic nature) causes strong intermolecular cohesion [18] and so favourable mechanical properties. In accordance with earlier observations [19], it was not possible to dissolve the pyrolytic deposit in hot sulphuric acid/potassium dichromate solution despite immersion for several hours.

Examination of the surface with a microscope indicated that a replicate of the substrate surface was obtained. No marked growth features could be discerned. Owing to the difficulty of polishing the graphite substrate surface to a complete mirror finish, minor flaws were also apparent in the deposited film. A possible remedy would be to polish a deposited film and then repeat the coating process. Because polishing exposes edge orientation, a final deposition is essential in order to retain the advantages of the recommended film. The use of glassy carbon as substrate might also solve the problem of surface flaws.

Long-term tests of stability have not so far been undertaken, but preliminary results are promising. In some cases, several months elapsed between preparation of a carbon film and its voltammetric usage, but there were no differences in performance compared to that of a newly deposited film. As long as the electrode was not exposed to potentials where high current densities were encountered (see below), no decline in voltammetric behaviour on prolonged use was noted. When linear sweep voltammetry was examined in a medium of acetonitrile (Burdick & Jackson, pesticide grade) with 5 mM sodium perchlorate as supporting electrolyte, the potential sweep could be

extended to 1.80 V vs. SCE before the residual current exceeded 1 μA (scan rate 10 mV s^{-1}).

Initial tests of analytical performance

o-*Dianisidine in 1 M sulphuric acid.* As an initial example of the performance of the pyrolytic carbon film electrode (PCFE), the cyclic voltammetry of *o*-dianisidine (3,3'-dimethoxybenzidine) in 1 M H_2SO_4 is shown in Fig. 1. This particular system was selected because it provides an opportunity to compare the electrode performance with that of the LTIC electrode [4] and of graphite paste materials. As judged from conventional cyclic voltammetric criterion at scan rates up to 50 mV s^{-1}, reversible behaviour is displayed at the graphite-Nujol paste, while the same reaction proceeds quasi-reversibly at the LTIC material [4]. From Fig. 1, it is clear that the reaction is only quasi-reversible at the PCFE, with an E_p value of 34 mV at a scan rate of 10 mV s^{-1}. From the qualitative treatment outlined by Adams [1] of Nicholson's approach to the evaluation of rate constants from the degree of separation of anodic and cathodic peaks in a cyclic voltammogram, an apparent constant of 7×10^{-3} cm s^{-1} can be estimated. This value lies in the

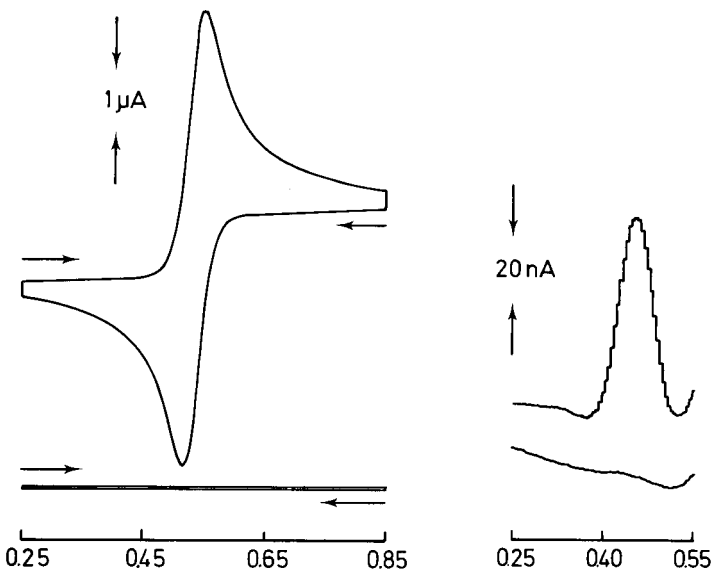

Fig. 1. Cyclic voltammogram for 1.1×10^{-4} M 3,3'-dimethoxybenzidine in 1.0 M H_2SO_4; scan rate 10 mV s^{-1}. The cyclic background trace recorded at the same sensitivity is shown beneath. Electrolysis for 15 s was allowed at the switching potential in both cases before the reverse scan.

Fig. 2. Differential pulse voltammogram of 2.5×10^{-7} M 3,3'-dimethoxybenzidine in 10 mM H_2SO_4. Background trace is shifted for clarity.

same range as that reported for the LTIC material [4]. As in the case of graphite paste and LTIC, fouling of the PCFE surface did not interfere and reproducibility of peak currents was excellent, ±0.3% for 10^{-4} M *o*-dianisidine (n = 10; 10 mV s^{-1}). From data reported by Hepler et al. [4], a response factor of 163.6 μA mM^{-1} cm^{-2} at 10 mV s^{-1} could be calculated for the graphite-Nujol paste, and the corresponding value for the PCFE comes surprisingly close, 158.7 μA mM^{-1} cm^{-2}.

The residual current is small (ca. 0.05 μA at 10 mV s^{-1}) over the entire potential range included in Fig. 1. This indicates a differential capacitance of roughly 20 μF cm^{-2}, which is about the same as that of the well-defined basal plane surface as judged from the potential sweep criterion [17]. At approximately 1.4 V vs. SCE, the residual current amounted to 1 μA and the extrapolated cut-off limit was normally about 1.5 V.

The favourable residual current combined with adequate charge transfer kinetics enables measurements at the submicromolar level to be obtained by differential pulse voltammetry (d.p.v.). Figure 2 shows a voltammogram obtained from the oxidation of 2.5×10^{-7} M *o*-dianisidine in 10 mM H_2SO_4. A linear increase in peak currents over a ten-fold concentration range was established (0.264 A M^{-1}) and adsorbed reactant could not be found when the electrode was transferred to a separate cell containing only the supporting electrolyte. A change in acidity from 1 M to 10 mM sulphuric acid roughly halved the magnitude of the residual current and this was of vital importance for measurements at the sensitivity setting employed for these tests. For the PCFE used, a response factor of 943 nA μM^{-1} cm^{-2} was calculated. It was also beneficial to interrupt the potential sweep at approximately 0.55 V beyond the voltammetric peak in order to retain the flat (albeit somewhat sloping) background indicated in Fig. 2, otherwise a small interfering peak appeared in the background trace. In such a case the flat baseline could be restored by cleaning with dichloromethane (see Experimental).

As will be discussed later in this series, d.p.v. measurements at submicromolar levels are not possible with glassy carbon electrodes, largely because of the unfavourable residual current. Results comparable to those reported above for the PCFE have, however, been obtained at a graphite-nujol paste electrode for a number of easily oxidized organic compounds, including *o*-dianisidine [20]. A more extensive evaluation of the PCFE for d.p.v. will be reported later in this series. It may be noted that, after a PCFE has been subjected to oxidizing potentials around 1.5 V or higher for some time in aqueous medium, the kinetics for the *o*-dianisidine system is somewhat improved, but such treatment causes an appreciable increase in the linear scan residual current, typically 0.2 μA at 10 mV s^{-1}. More important, the d.p.v. measurements reported above are impossible with such an electrochemically maltreated electrode, because of increased background. Essentially the same behaviour is also apparent when the surface is polished with fine alumina.

Hexacyanoferrate(II) in 2 M potassium chloride. This widely used test system behaves quasi-reversibly at graphite paste and LTIC electrodes [4]. At the PCFE, its behaviour is similar (Fig. 3) with an 80 mV peak separation in a cyclic voltammogram recorded at 10 mV s^{-1}. The residual current for the PCFE is significantly better than that reported for the LTIC material in this medium [4], and compares favourably even with that for graphite paste. This system shows excellent reproducibility of peak currents; the relative standard deviation was 0.22% (n = 10) for 10^{-4} M hexacyanoferrate(II) at 10 mV s^{-1}.

Dopamine in 0.04 M H_2SO_4—0.01 M Na_2SO_4. Electrochemical detection for continuous monitoring of flowing streams (e.g., column effluents) is of great interest at present. An important sphere of application is in the determination of biogenic catecholamines. While principles and designs vary [4, 21—23], a crucial point is always the performance of the electrode material Pyrolytic carbon film offers interesting properties in this regard. An indication of the favourable kinetics obtainable is illustrated in Fig. 4A for dopamine in a medium which has been used as a mobile phase in an h.p.l.c. separation with electrochemical detection [24]. This system was also evaluated for the LTIC material [4]. With the PCFE in the as-deposited state, without any cleaning with dichloromethane, the kinetic behaviour is rather sluggish and qualitatively resembles that of LTIC and carbon paste [4].

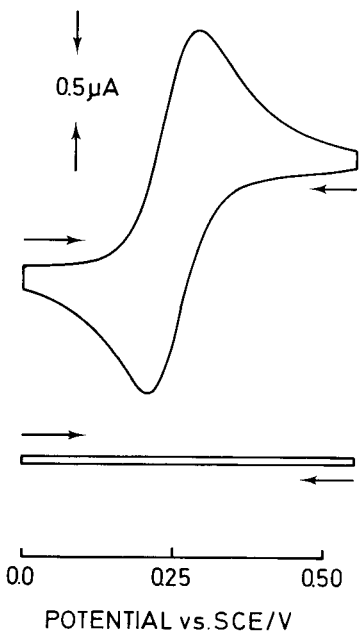

Fig. 3. Cyclic voltammogram recorded at 10 mV s^{-1} for 1.0×10^{-4} M hexacyanoferrate(II) in 2 M KCl. The background trace is also shown. Electrolysis for 15 s was allowed at the switching potential in both cases before the reverse scan.

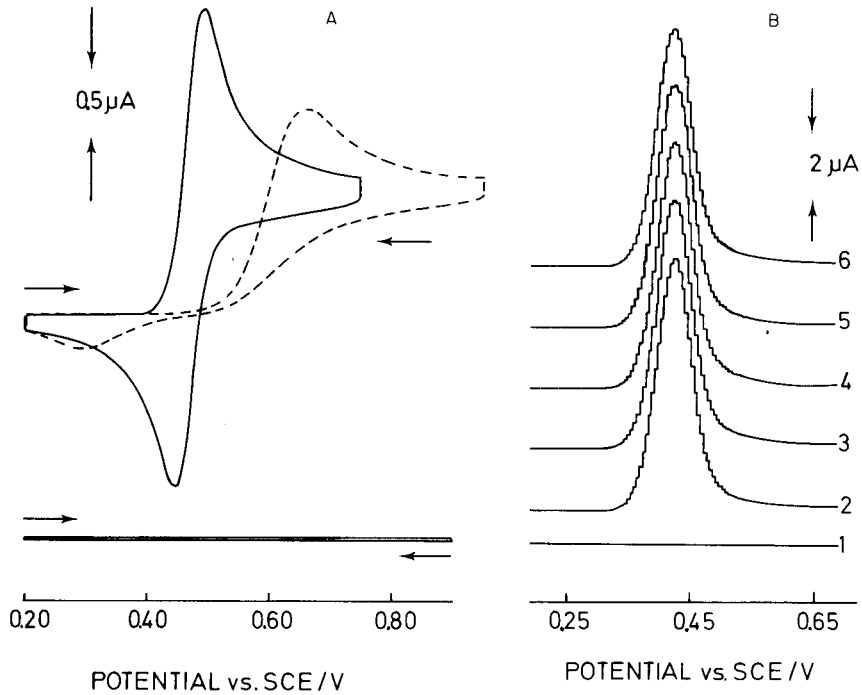

Fig. 4. Oxidation of 5×10^{-5} M dopamine in 0.01 M H_2SO_4—0.04 M Na_2SO_4. (A) Cyclic voltammograms recorded at 10 mV s^{-1}; the broken line corresponds to the as-deposited state and the solid line is after pre-electrolysis (see text); the background trace is shown beneath; electrolysis for 15 s was allowed at the switching potential before the reverse scan. (B) Sequentially recorded differential pulse voltammograms from the same solution.

Pre-electrolysis at 1.3 V vs. SCE for 5 min vastly improved the electrode kinetics as shown in Fig. 4A. This activation effect is in accordance with the observations of Wightman et al. [25] who evaluated the basal plane surface of a well-ordered structure of pyrolytic graphite. Similar observations on "anodic activation" have been reported for other carbon electrodes [9, 26, 27]. However, cleaning of the PCFE with dichloromethane was found to produce almost the same degree of improvement, so that desorption of accumulated species seems a more likely explanation in this case. The general need for initial cleaning of the deposited film is emphasized by these findings. Despite very thorough cleaning, however, pre-electrolysis for a short time was essential in arriving at the result shown in Fig. 4A.

Also of prime importance is the small susceptibility towards poisoning effects even at a concentration of 5×10^{-5} M, as demonstrated in Fig. 4B where the six voltammograms shown were recorded with only brief stirring between runs. Both carbon paste and LTIC suffer from a more pronounced effect [4]. Fouling is reported to be undetectable when related catecholamines (adrenaline and noradrenaline) are oxidized in 1 M H_2SO_4 at a

glassy carbon electrode using d.p.v. [28]. In this case, the lower end of the linear range was 10^{-5} M and the voltammogram was less well-developed.

Significance of the results

The unusual properties of the pyrolytic carbon film which provide the very good performance outlined above will be discussed in detail elsewhere [29]. Here only a brief discussion will be offered, to put this carbon film material in perspective compared with other all-carbon materials used for electrodes.

A turbostratic structure with a preferred orientation of the unit crystallites along the plane of the substrate should result from the conditions recommended for deposition [8]. This implies a certain number of exposed unsaturated carbon valences with contributions from crystallite edges as well as defects within basal planes [7, 18]. These are essentially the same surface conditions as are displayed by any as-deposited variety of pyrolytic carbon, including the pyrolytic graphite which has long been used in electrochemistry [7]. The more recent LTIC material is unusual among pyrolytic carbons in that the individual crystallites are randomly orientated, which means pronounced isotropic bulk properties [30]. Glassy carbons, being also macroscopically isotropic, expose significant numbers of such sites in a similar fashion [31].

In general, the number of such prismatic edges exposed at the surface of the bulk carbon significantly influences its surface properties and so its characteristics as an electrode [6]. Any polishing procedure inevitably causes significant edge exposure and produces a distinct levelling effect between different sorts of carbon [16, 17]. Exposed edges tend to combine instantaneously with any suitable reagent, usually atmospheric oxygen [15]. True surface compounds normally result, which in the case of oxygen can only be desorbed as CO_2 and CO under vacuum at temperatures approaching 1000°C [15]. These varying surface states involving oxygen functionalities create well-known complex problems in carbon electrode methodology. It is widely accepted that the electrocatalytic properties of an oxygenated surface are essential to the attainment of adequate electrode kinetics [6, 32].

An essential aspect of the improved performance of the PCFE is the favourable surface state resulting from the conditions of deposition. This is evident from the detrimental effects of polishing and of extremes of anodic treatment. The following three features of the deposition process may provide the unusual surface state of the deposited film. First, complete dehydrogenation is not achieved at the comparatively low temperature (1100°C) used in the deposition process and a substantial amount of hydrogen is likely to remain in the deposited material [8, 10, 33]. Because the hydrogen is bonded covalently to carbon atoms at sites where unsaturated carbon valences might otherwise occur, subsequent oxygen attack is prevented. Secondly, the carbon film is exposed to atmospheric oxygen only after cooling to room temperature, so that only so-called "basic" surface

oxides are formed [15, 33]. Thirdly, according to Cullis and Norris [34], some silicon is likely to be present on the surface because a quartz tube served as combustion chamber. The hydrogen-rich atmosphere assured by the decomposition of the hydrocarbon gas may promote formation of silicon carbide [35]. Silicon-alloyed pyrolytic carbons are known to display increased resistance to oxidation [34].

The following observation favours the first of the three features outlined above as an explanation for the surface state. It was found that heat-treatment in the normal atmosphere at roughly 320°C caused no observable detrimental effects. This temperature lies well within the range where "acidic" surface oxides [15, 33] can be formed by direct oxidation with atmospheric oxygen, or via the conversion of basic oxides. Further, several months of storage in a normal laboratory atmosphere did not change the character of the surface. Hence, a comparatively unreactive surface state is indicated in accordance with the character of a hydrogenated carbon surface [33].

Conclusions

The developed PCFE offers significant improvements in anodic voltammetry, especially as regards residual current behaviour. The linear scan residual currents compare well with those reported for a pyrolytic graphite basal plane surface of great perfection [17], which is remarkable because such a surface is virtually free from functional groups. This favourable residual current behaviour is combined with adequate electrode kinetics, which is not the case for the highly perfected basal plane surface [6, 25, 36]. Current responses displayed are similar to those of glassy carbon or carbon paste. This situation provides excellent possibilities for differential pulse voltammetry, which will be reported in subsequent parts. The electrodes can be prepared in the laboratory by means of a comparatively simple yet dependable procedure; and because many units can be produced in one run, the cost and effort is reasonable.

The author thanks Prof. B. Nygård for his valuable advice and Dr. M. Richardson from the Inorganic Department of this Institute for technical advice on furnaces and for the loan of equipment.

REFERENCES

1 R. N. Adams, Electrochemistry at Solid Electrodes, Dekker, New York, 1969, pp. 19—42.
2 D. T. Sawyer and J. L. Roberts, Jr., Experimental Electrochemistry for Chemists, Wiley-Interscience, New York, 1974, pp. 60—79.
3 E. Pungor, Z. Fehér and M. Váradi, Crit. Rev. Anal. Chem., 9 (1980) 97.
4 B. R. Hepler, S. G. Weber and W. C. Purdy, Anal. Chim. Acta, 102 (1978) 41.
5 W. E. van der Linden and J. W. Dieker, Anal. Chim. Acta, 119 (1980) 1.
6 J.-P. Randin, in A. J. Bard (Ed.), Encyclopedia of Electrochemistry of the Elements, Vol. VII, Dekker, New York, 1976, pp. 1—291.

7 A. W. Moore, in P. L. Walker, Jr. and P. A. Thrower (Eds.), Chemistry and Physics of Carbon, Vol. 11, Dekker, New York, 1973, p. 69.
8 J. C. Bokros, in P. L. Walker, Jr. (Ed.), Chemistry and Physics of Carbon, Vol. 5, Dekker, New York, 1969, pp. 1—118.
9 A. L. Beilby, W. Brooks, Jr. and G. L. Lawrence, Anal. Chem., 36 (1964) 22.
10 R. O. Grisdale, A. C. Pfister and W. van Roosbroeck, Bell. Syst. Tech. J., 30 (1951) 271.
11 B. R. Hepler, S. G. Weber and W. C. Purdy, Anal. Chim. Acta, 113 (1980) 269.
12 B. D. Epstein, E. Dalle-Molle and J. S. Mattson, Carbon, 9 (1971) 609.
13 W. J. Blaedel and G. A. Mabbot, Anal. Chem., 50 (1978) 933.
14 E. Sutzkover, C. Zur and M. Ariel, J. Appl. Electrochem., 9 (1979) 495.
15 H. P. Boehm, Adv. Catal. Relat. Subj., 16 (1966) 179.
16 H. Harker, J. B. Horsley and D. Robson, Carbon, 9 (1971) 1.
17 J.-P. Randin and E. Yeager, J. Electroanal. Chem., 36 (1972) 257.
18 G. M. Jenkins, in P. L. Walker, Jr. and P. A. Thrower (Eds.), Chemistry and Physics of Carbon, Vol. 11, Dekker, New York, 1973, pp. 189—242.
19 A. R. Ford and E. Greenhalgh, in L. C. F. Blackman (Ed.), Modern Aspects of Graphite Technology, Academic Press, London, 1970, p. 275.
20 W. M. Chey, R. N. Adams and M. S. Yllo, J. Electroanal. Chem., 75 (1977) 731.
21 P. T. Kissinger, Anal. Chem., 49 (1977) 447A.
22 K. Brunt, Pharm. Weekbl., 113 (1978) 689.
23 R. J. Rucki, Talanta, 27 (1980) 147.
24 R. M. Riggin, R. L. Acorn and P. T. Kissinger, Clin. Chem., 22 (1976) 782.
25 R. M. Wightman, E. C. Palk, S. Borman and M. A. Dayton, Anal. Chem., 50 (1978) 1410.
26 L. Bjelica, R. Parsons and R. M. Reeves, Croat. Chem. Acta, 53 (1980) 211.
27 W. J. Blaedel and J. Wang, Anal. Chem., 53 (1981) 78.
28 J. Ballantine and A. D. Woolfson, Int. J. Pharm., 3 (1979) 239.
29 K. Lundström, Ph.D. Thesis, University of Uppsala, 1981.
30 J. C. Bokros, R. J. Akins, H. S. Shim, A. D. Havbold and N. K. Agarwal, Chem. Technol., 7 (1977) 40.
31 J.-P. Randin and E. Yeager, J. Electroanal. Chem., 58 (1975) 313.
32 R. E. Panzer and P. J. Elving, Electrochim. Acta, 20 (1975) 635.
33 B. R. Puri, in P. L. Walker, Jr. (Ed.), Chemistry and Physics of Carbon, Vol. 6, Dekker, New York, 1970, pp. 191—282.
34 C. F. Cullis and A. C. Norris, Carbon, 9 (1971) 517.
35 J. L. Kaae and T. D. Golden, J. Am. Ceram. Soc., 54 (1971) 605.
36 I. Morcos and E. Yeager, Electrochim. Acta, 15 (1970) 953.

Analytica Chimica Acta, 146 (1983) 109—115
Elsevier Scientific Publishing Company, Amsterdam — Printed in The Netherlands

A PYROLYTIC CARBON FILM ELECTRODE FOR VOLTAMMETRY
Part 2. Oxidative Differential Pulse Voltammetry of Selected Organic Molecules

KENT LUNDSTRÖM

Department of Analytical Chemistry, University of Uppsala, P.O. Box 531, S-751 21 Uppsala (Sweden)

(Received 16th November 1981)

SUMMARY

The carbon film electrode is evaluated for oxidative differential pulse voltammetry of organic compounds. Applications are indicated for dopamine, tryptophan, aniline and retinyl acetate in aqueous and organic media. Well-defined voltammograms are obtainable and the low residual current permits measurements at 10^{-7} M levels.

Differential pulse voltammetry at solid electrodes has not achieved widespread application for the determination of oxidizable compounds. The main reason is that the required inertness of the electrode itself is seldom attained, but only approached to varying degrees by the solid electrode materials available. In addition to the capacitive currents induced on the application of a pulsed potential ramp, other processes are initiated and these are characterized by extremely slow relaxation behaviour. Owing to the way that currents are sampled and displayed in the differential pulse mode, a substantial background current is inevitable. The common interpretation of these processes involves a complex and sluggish redox behaviour of certain oxygen-containing functional groups formed on the surface of the electrode material (see, e.g., refs. 1—5). Both glassy carbon [1—4] and platinum [5] are known to display pronounced behaviour of this kind. Frequently, it is the magnitude and shape of such background responses which prevents measurements at concentration levels otherwise attainable with the differential pulse technique, rather than a poor signal to noise ratio [5]. An additional complicating factor is the often poor reproducibility of this background, which prevents the successful application of correction procedures. The notorious difficulties encountered in restoring an identical surface state after renewal of a "poisoned" electrode surface are especially important in this regard.

In the case of glassy carbon, which is a frequent choice in various electroanalytical applications [6], determinations at levels approaching 10^{-6} M are normally not possible by differential pulse voltammetry (d.p.v.). Some examples of the performance of the glassy carbon electrode in organic

0003-2670/83/0000-0000/$03.00

analysis using oxidative d.p.v. [7—11] illustrate this point. An exception is a claimed detection limit of 2×10^{-8} M for polynuclear aromatic hydrocarbons in acetonitrile [12]. The utility of a more successful solid electrode is exemplified in a report by Chey et al. [13], who described applications of oxidative d.p.v. at a carbon paste electrode. This electrode, when carefully prepared, is characterized by a very small and uniform residual current at modest potentials in aqueous medium. Analytically meaningful measurements are therefore feasible at levels around 5×10^{-7} M for some organic compounds and in favourable cases even lower levels are attainable [13]. It is unfortunate that the successful use of carbon paste is confined to aqueous medium.

In the present report, the potentialities of a new pyrolytic carbon film electrode (PCFE) [14] in d.p.v. are demonstrated. This electrode material is characterized by a residual current behaviour similar to that of a well-prepared carbon paste, because of its unusual surface state. Because the electrode kinetics are also favourable [14], it was expected that this PCFE would allow the inherent sensitivity of the differential pulse technique to be more fully exploited even in the solutions that are incompatible with the carbon paste electrode. To provide a general idea of applicability, selected representatives of the different classes of organic compounds amenable to oxidative voltammetry were surveyed; compounds were also chosen so that comparisons with literature data would be possible. Choice of solutions likewise reflected common usage. It is shown below that determinations at the submicromolar level are possible; because traditional d.p.v. parameters are used throughout, the vital role of the new electrode material is clearly demonstrated.

EXPERIMENTAL

Instrumentation, equipment, procedures and quality of reagents were all identical to those described earlier [14]. Briefly, a PAR 174A polarograph was used, with the RC time constant of the sample-and-hold circuitry for the d.p.v. mode changed to 15 ms. Other equipment was conventional. The PCFE had a geometric area of 0.28 cm^2. The following d.p.v. parameters were used throughout: pulse amplitude 50 mV; pulse repetition 0.5 s, scan rate 10 mV s^{-1}; and low-pass filter in the off position. The offset function was used as required. Current settings as indicated on the polarograph in the range 1—10 μA were normally used. In the d.p.v. mode of the PAR 174A instrument these settings include an internal tenfold amplification. The currents reported (text and figures) are the true values which have been obtained by dividing the apparent current responses by this amplification factor of ten. This practice is not always followed in published work.

RESULTS AND DISCUSSION

Numerous voltammetric investigations of biologically important organic molecules have been reported in recent years [15, 16]. Many of these compounds are amenable to anodic oxidation and carbon is regarded as the electrode material of choice. The sensitivity attainable is of major concern in many applications. The analytical performance of the new PCFE in this area is demonstrated for some model compounds in the following paragraphs.

Dopamine

The three d.p. voltammograms reproduced in Fig. 1 are for 5×10^{-7} M dopamine in pH 7.4 phosphate buffer containing 0.9% sodium chloride. A

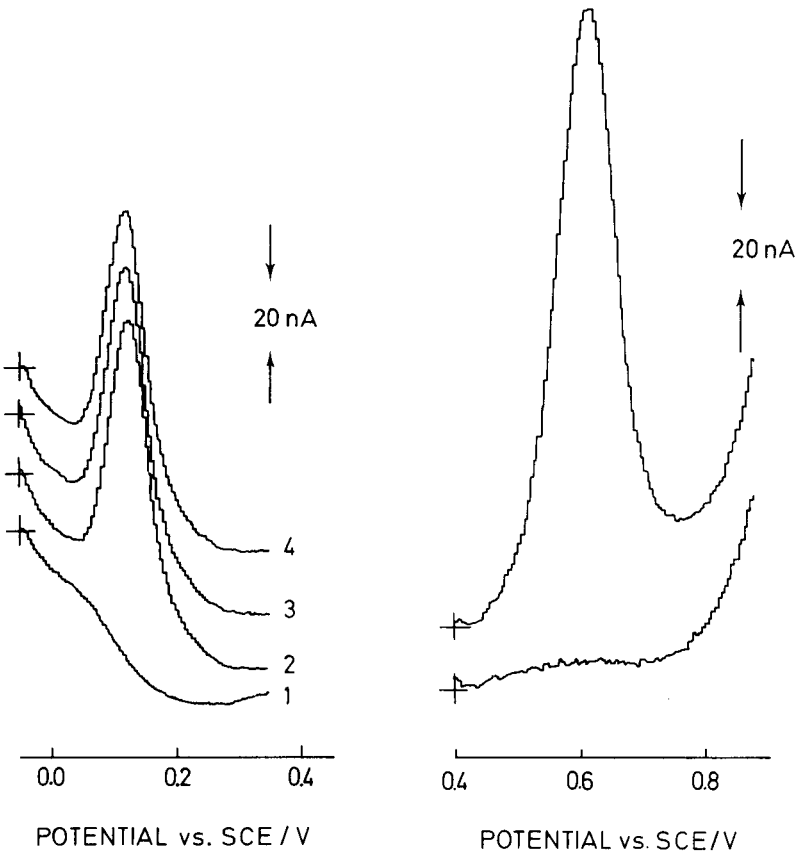

Fig. 1. Sequentially recorded differential pulse voltammograms of 5×10^{-7} M dopamine in pH 7.4 phosphate buffer containing 0.9% NaCl. Curve 1 is the background. See text for further details.

Fig. 2. Differential pulse voltammogram of 9.2×10^{-7} M tryptophan in 0.1 M phosphate buffer pH 7.4. The background trace is displaced for clarity.

similar sensitivity of measurement by d.p.v. has hitherto been reported only when the more sophisticated differential double-pulse voltammetric technique was applied at a platinum electrode which prior to the measurement had been chemically modified via chemisorption of iodide [17]. This essential pre-treatment involving chemisorption of iodide resulted in a favourable residual current over a confined potential range where the surface state remained electrochemically inert. A differential capacity of about 20 μF cm^{-2} was reported for such a surface.

The residual current encountered at the PCFE in this medium and potential range is extremely small and even challenges that found with carbon paste electrodes. When linear scan voltammetry was used, the residual current was less than 0.04 μA at 10 mV s^{-1}. This indicates a differential capacitance of roughly 14 μF cm^{-2}. The voltammograms (Fig. 1) were recorded consecutively with only brief stirring between runs; it can be seen that poisoning of the electrode surface is not a major problem. A calibration graph over the range 5×10^{-7}—5×10^{-6} M was rectilinear with a slope of 0.172 A M^{-1}. When the electrode was moved to a separate cell containing only the supporting electrolyte, the normal background trace was once again recorded with no traces of adsorbed reactant discernable. These results supplement the earlier discussion of the d.p.v. of dopamine [14].

Tryptophan

A well developed d.p. voltammogram is obtained for 9.2×10^{-7} M tryptophan in pH 7.4 phosphate buffer, though the peak half-width is rather large at 110 mV (Fig. 2). The residual current curve, included in the figure, indicates the potential limit for d.p.v. in this medium and also the expected detection limit for tryptophan. No poisoning effects could be ascertained between successive runs. Further addition from the stock solution resulted in a linear increase of the peak-current over a ten-fold concentration range (0.209 A M^{-1}). In research on amino acids [18], and on nucleotides and related substances [19], the pyrolytic graphite electrode is most often used. Brabec and Dryhurst [20] pointed out that it was becoming difficult to obtain a quality adequate for electrochemical purposes.

Aniline

The oxidation of aniline at the PCFE in 50% ethanolic Britton-Robinson buffer pH 1.9 is illustrated in Fig. 3. Aniline was selected because the aromatic amines constitute a large and important group which is frequently determined by voltammetric techniques at solid electrodes. When an organic solvent is a major component of the medium, as here, there is a considerable decline in the performance of carbon paste electrodes and other materials must be used. The favourable residual current and the absence of discernible poisoning effects allowed measurements at the 10^{-7} M level, as illustrated in Fig. 3. A few minutes of pre-electrolysis at 0.90 V (vs. Ag [14]) was mandatory in establishing this background, otherwise a somewhat more

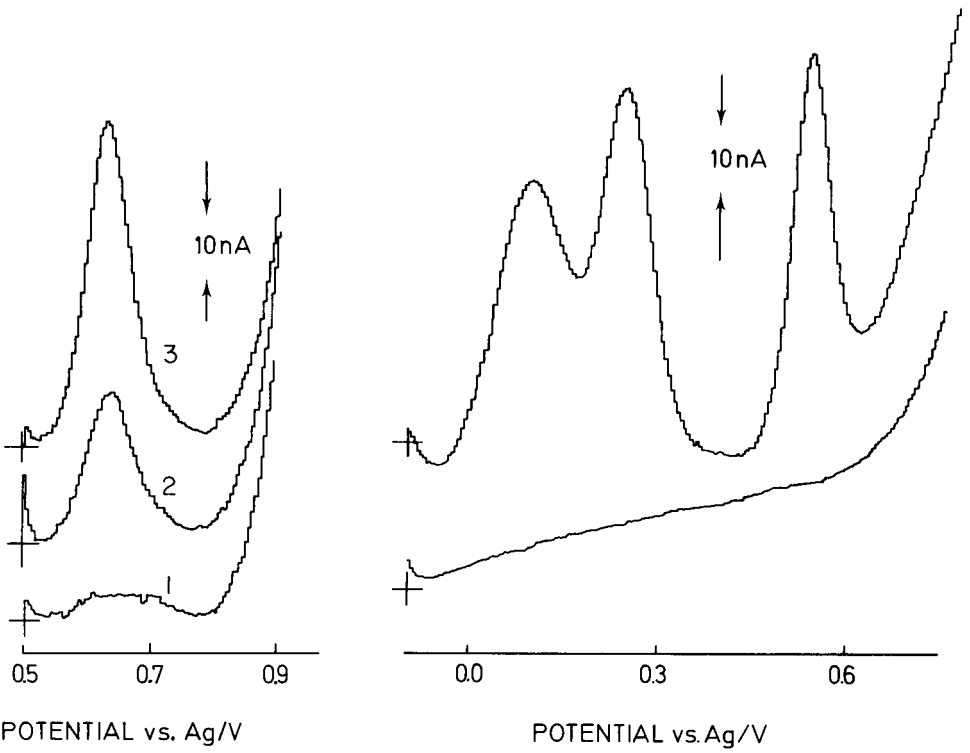

Fig. 3. Differential pulse voltammograms of aniline at low levels in 50% ethanol—Britton-Robinson buffer, pH 1.9: (1) background; (2) 1.02×10^{-7} M; (3) 2.49×10^{-7} M aniline.

Fig. 4. Differential pulse voltammogram from a mixture of 5.2×10^{-7} M retinyl acetate and 1.7×10^{-6} M α-tocopherol in 1:1 ethanol—n-hexane. See text for further details. Potential is given versus a silver electrode [14].

sloping appearance was found. A calibration graph covering 10^{-7}—10^{-6} M aniline showed a slope of 0.193 A M^{-1}.

In order to provide some frame of reference, a recent study of the voltammetric determination of the three monochloroanilines [7] may be cited. A glassy carbon electrode was used in essentially the same medium as above and a detection limit of 1.6×10^{-6} M was stated for d.p.v. (extrapolated value), whereas amperometric detection in a wall-jet configuration after h.p.l.c. separation made determinations of the 5×10^{-7} M level feasible.

Instability at the high sensitivity settings used is clearly evident from Fig. 3, as well as other figures in this paper. The more extensive filtering frequently used in the d.p.v. mode, 110 ms time constant, should obviate these problems, but only at the expense of a distorted voltammogram. The figures thus illustrate the fact that, in addition to electrode performance, factors such as instrumental capabilities, shielding and cell design must also be considered at this low level of concentration.

Vitamins E and A

The final example provided is the oxidation of α-tocopherol and retinyl acetate, i.e., unesterified vitamin E and the acetate ester of vitamin A. These two fat-soluble vitamins are oxidized in a 1:1 mixture of ethanol and hexane. The determination of vitamin A by linear scan voltammetry (l.s.v.) has been reported [21, 22]; retinyl acetate displayed three oxidation peaks when oxidized at a carbon paste electrode or a glassy carbon electrode. This is also true under the present conditions and the well developed d.p.v. peak at 0.55 V (vs. Ag [14]) shown in Fig. 4 corresponds to the first oxidation peak for 5.2×10^{-7} M retinyl acetate; the second peak merges with the background. From Fig. 4 and the earlier l.s.v.-work, the detection limit is improved by almost two orders of magnitude. Further, this particular medium enables the frequently mandatory extraction step to be included in a sample preparation without any evaporation of the extraction medium (hexane) prior to the final voltammetric measurement. Degradation losses of vitamin A are particularly difficult to avoid during such handling. A further asset of the medium is the near elimination of electrode poisoning; this is also valid for glassy carbon. The tocopherol used was heavily degraded and gave two incompletely resolved d.p.v. peaks which, however, were adequately resolved from the vitamin A peak (Fig. 4). Intact tocopherol corresponds to the second peak at 0.25 V. Further details of this application will be reported separately. For the present purpose, the behaviour illustrates the spacing required for resolution of d.p.v. peaks.

Conclusions

The above examples indicate the usefulness of the PCFE for organic anodic voltammetry. Thus, d.p.v. measurements at submicromolar levels are possible because of the small residual current combined with adequate electrode kinetics. The qualities of available glassy carbon do not permit such measurements. The ability to cover both aqueous and nonaqueous media is a useful attribute of the PCFE compared to carbon paste electrodes. There is also a surprisingly small susceptibility to poisoning of the electrode surface; this aspect must be further investigated before any final conclusions can be reached. Although the carbon paste electrode offers a convenient solution to this notorious problem for discontinuous measurements, in that a new surface can be conveniently generated as needed, the PCFE surface can be regenerated simply by cleaning with dichloromethane and application of suitable voltages. Future applications of the PCFE include an evaluation for organic reductions.

REFERENCES

1 W. J. Blaedel and R. A. Jenkins, Anal. Chem., 45 (1974) 1952.
2 J.-P. Randin and E. Yeager, J. Electroanal. Chem., 58 (1975) 313.
3 J. W. Dieker, W. E. Van der Linden and H. Poppe, Talanta, 25 (1978) 151.
4 L. Bjelica, R. Parsons and R. M. Reeves, Croat. Chim. Acta, 53 (1980) 211.

5 W. F. Sokol and D. H. Evans, Anal. Chem., 53 (1981) 578.
6 W. E. Van der Linden and J. W. Dieker, Anal. Chim. Acta, 119 (1980) 1.
7 J. P. Hart, M. R. Smyth and W. F. Smyth, Analyst, 106 (1981) 146.
8 H. K. Chan and A. G. Fogg, Anal. Chim. Acta, 109 (1979) 341.
9 J. Ballantine and A. D. Woolfson, Int. J. Pharm., 3 (1979) 239.
10 A. G. Fogg and D. Bhanot, Analyst, 105 (1980) 868.
11 O. Podlaha, Å. Eriksson and B. Toregård, J. Am. Oil Chem. Soc., 55 (1978) 530.
12 J. F. Coetzee, G. H. Kazi and J. C. Spurgeon, Anal. Chem., 48 (1976) 2170.
13 W. M. Chey, R. N. Adams and M. S. Yllo, J. Electroanal. Chem., 75 (1977) 731.
14 K. Lundström, Anal. Chim. Acta,
15 R. L. McCreery, Crit. Rev. Anal. Chem., 7 (1978) 89.
16 W. F. Smyth (Ed.), Polarography of Molecules of Biological Significance, Academic Press, London, 1979.
17 R. F. Lane and A. T. Hubbard, Anal. Chem., 48 (1976) 1287.
18 V. Brabec, J. Electroanal. Chem., 116 (1980) 69.
19 W. T. Bresnahan, J. Moiroux, Z. Samec and P. J. Elving, Bioelectrochem. Bioenerget., 7 (1980) 125.
20 V. Brabec and G. Dryhurst, J. Electroanal. Chem., 89 (1978) 161.
21 S. S. Atuma, J. Lindqvist and K. Lundström, Analyst, 99 (1974) 683.
22 S. S. Atuma, K. Lundström and J. Lindqvist, Analyst, 100 (1975) 827.

Analytica Chimica Acta, 146 (1983) 117—124
Elsevier Scientific Publishing Company, Amsterdam — Printed in The Netherlands

OXIDATIVE VOLTAMMETRY AND LIQUID CHROMATOGRAPHY WITH ELECTROCHEMICAL DETECTION OF 1-[5-(TETRADECYLOXY)-2-FURANYL]ETHANONE AND 5-(TETRADECYLOXY)-2-FURANCARBOXYLIC ACID AND ESTERS AT A CARBON PASTE ELECTRODE IN AQUEOUS MEDIA

C. L. HOUSMYER*, R. L. LEWIS, Jr. and H. J. KEILY

Analytical Chemistry Department, Merrell Dow Pharmaceuticals Inc. (Subsidiary of The Dow Chemical Company), Cincinnati, OH 45215 (U.S.A.)

(Received 24th May 1982)

SUMMARY

1-[5-(Tetradecyloxy)-2-furanyl]ethanone and 5-(tetradecyloxy)-2-furancarboxylic acid as well as its esters are oxidizable at a carbon paste electrode in acetonitrile—aqueous buffer solutions. Voltammetric peak potentials for the acid decrease smoothly from 1.25 to 1.07 V vs. SCE as the electrolyte pH increases from 1.4 to 6.5. The peak potential remains constant above this pH. The remaining compounds oxidize at 1.3 V independent of pH. Controlled potential coulometry produces a transfer of two electrons at 1.3 V. The oxidative step destroys the major ultraviolet chromophore at ca. 300 nm but the products are unknown. Peak currents from wide ranging pH media are quantitatively useful. They are selective for the intact furanyl ring systems in the presence of their acid-catalyzed degradation products. The compounds are extracted into the carbon paste electrode in varying degrees in relation to their lipophilicities so that electrode contact time with sample solutions must be controlled for reasonable accuracy. In flowing streams, pre-electrolysis extraction is avoided and the carboxylic acid compound can be accurately quantified by high-performance liquid chromatography with electrochemical detection. One data set at $k' = 1.5$ showed a linear range of 1—300 ng injected, with a sensitivity of 0.295 ± 0.001 nA ng^{-1}.

Interest in a series of 2-keto-5-alkoxy furanyl compounds as pharmaceutical agents [1, 2] prompted this study of their electroanalytical characteristics. Investigations in aqueous media showed that the compounds were not reduced at a mercury electrode but were oxidized at a carbon paste electrode (CPE). Their oxidation potentials range between 1 and 1.3 V vs. SCE so that they are accessible in a variety of aqueous media for voltammetric and amperometric measurements. For comparative purposes, it can be noted that 2-furancarboxylic acid is not oxidizable under similar conditions. However, the higher potentials achievable in non-aqueous electrolytes will oxidize 2-furancarboxylic acid as well as furan [3, 4]. The oxidation potentials ($E_{1/2}$) of furan and 2,5-dimethylfuran are 1.7 and 1.2 V, respectively, at platinum in acetic acid [4]. Thus it appears reasonable to expect that 2,5-disubstituted furanyl compounds other than the subject 2-keto-5-alkoxy types may be amenable to electrochemical measurements in aqueous media.

This report provides voltammetric peak potentials and peak currents as functions of pH, peak currents as functions of concentration, coulometric data, and adsorptive–extractive behavior of the compounds at the CPE. High-performance liquid chromatographic-electrochemical detection (l.c.e.c.) data are provided for compound I. The compound structures are shown below.

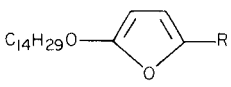

R	Compound
COOH	I
$COCH_3$	II
$COOCH_3$	III
$COOCH_2CH_3$	IV

EXPERIMENTAL

Apparatus

A PAR model 174A polarograph was used in conjunction with an isolated saturated calomel reference electrode, an isolated platinum wire auxiliary electrode, and a carbon paste working electrode of 0.5 cm^2 geometric area. The carbon paste was composed of 5% ceresin wax on SP-2 graphite in the weight ratio of 5 parts to 3 of OV-101 silicone oil. Detector signals were measured with a Houston Instruments RE0074 X-Y recorder. A PAR K-64 cell was maintained at 25°C. Ultraviolet (u.v.) spectra were recorded with a Cary 17 spectrophotometer. Liquid chromatography with electrochemical detection was accomplished with a Waters M-6000A pump, a μ Bondapak alkylphenyl column (30 cm × 0.39 cm, 10 μm packing) or a Micropak MCH column (30 cm × 0.4 cm, C-18, 10 μm packing), a Rheodyne 20-μl loop injector, and a Bioanalytical System thin-layer electrochemical detector (TL-4 cell packed with the same carbon paste as above, Ag/AgCl reference electrode, and LC-4 potentiostat).

Solutions

Electrolytes were prepared by mixing 2 ml of 0.1 M $LiClO_4$ in acetonitrile with 1 ml of an aqueous buffer. The buffers were 0.1 M solutions of glycine, citric acid, boric acid, acetic acid, or tris(hydroxymethyl)aminomethane, and 0.05 M solutions of sulfuric acid and lithium hydroxide. Sulfuric acid or lithium hydroxide was used as necessary for pH adjustment of the 0.1 M buffers. All pH values pertain to those of the electrolyte as measured with a glass electrode that had been calibrated with aqueous standard solutions.

Sample solutions for voltammetric studies were prepared by dissolving ca. 25 mg of the test species in 25 ml of acetonitrile. Solutions for l.c.e.c. studies were prepared by appropriate dilution into the mobile phase. The mobile phase for use with the alkylphenyl column was composed of 0.1 M KH_2PO_4, pH 6.25/acetonitrile/methanol in a volume ratio of 25/40/35. The mobile phase for use with the C-18 column consisted of 0.05 M $LiClO_4$ in acetonitrile/0.15 M lithium acetate, pH 6.5/water in a volume ratio of 16/4/1.

Procedures

Voltammetric data were obtained from 20 mV s^{-1} scans beginning at 0.4 V and continuing positively to the electrolyte background limit. Background curves were obtained on each electrolyte. They were used as baselines for all current measurements. Solutes were spiked into 3 ml of the electrolytes in successive 50-μl aliquots. The solutions were stirred and duplicate scans were made at fixed time intervals after addition of each aliquot. The electrode was resurfaced before use in a fresh electrolyte but not between sequential scans in the same electrolyte.

Coulometric data were obtained at fixed potential using similar solutions and equipment as for voltammetry. Total coulombs transferred were determined from manual integration of a strip-chart recorder trace. Moles of compound oxidized were determined from u.v. absorption data.

Liquid chromatography—electrochemical detection data were collected on duplicate or triplicate injections of several solutions of different concentration. Flow rates were maintained at 1 ml min^{-1} and the electrode potential was +1.1 V. Peak heights and electronic peak areas were evaluated for linearity and detection limits.

RESULTS AND DISCUSSION

Cyclic voltammetry at the CPE revealed well behaved anodic peaks and no cathodic peaks when run at 20 mV s^{-1} in acidic or basic media. In addition, scan rates up to 500 mV s^{-1} were used in pH 1.4 and 6.3 media without evidence of reversibility on the reverse scan. The anodic peaks, however, were reasonably sharp. Their peak minus half-peak potentials ($E_p - E_{p/2}$) for compound I ranged from 56 to 100 mV as the apparent pH of the electrolyte was varied between 1.5 and 11. The other compounds produced essentially constant $E_p - E_{p/2}$ values of 50—58 mV in the apparent pH range 1.5—7. The voltammograms shown in Fig. 1 are illustrative of those obtained with all the compounds.

pH effects

Peak potentials of compounds II, III, and IV do not vary with the pH of the electrolytes. These compounds oxidize at 1.28 V over the apparent pH region 1.4—7.3. However, the peak potential of compound I decreases with pH (ca. 35 mV pH^{-1}) up to the apparent pH region 5—6 (Fig. 2). This is coincident with the spectrophotometrically determined pK_a of 5.6. The carboxylate form is more easily oxidized than the carboxylic acid and because the break in the E_p vs. pH plot is at the pK_a of the acid it is apparent that this function is involved in the electron-transfer step.

Peak currents also vary with pH only in the case of compound I. The data in Fig. 2 again show a regular decrease of current constants up to the pK_a region. Beyond that, the only changes with pH seem to be specifically related to the buffers. Peak currents are enhanced in basic amine buffers compared to borate buffers. This difference in peak current constants approaches a

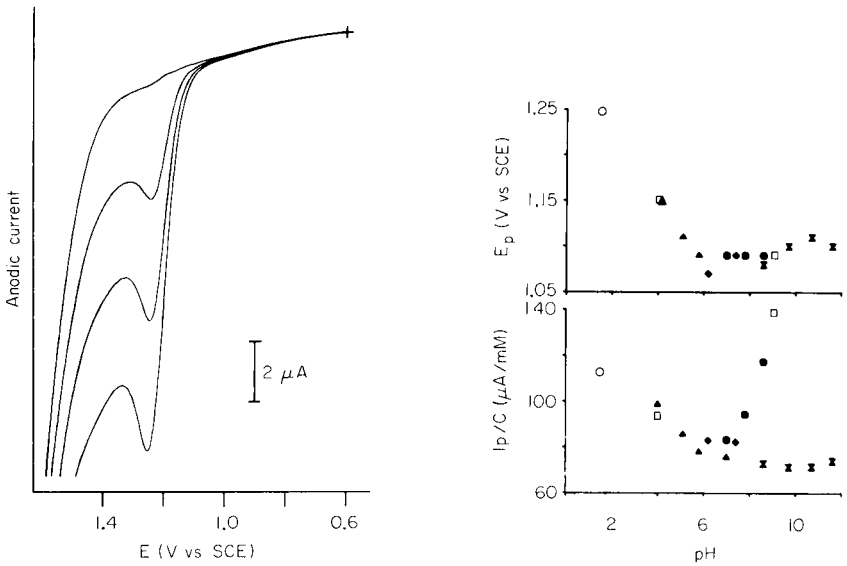

Fig. 1. Voltammograms of compound I as a function of concentration in the sulfuric acid electrolyte; background, 0.035, 0.069 and 0.10 mM, respectively.

Fig. 2. Peak potentials and peak current constants of compound I as functions of pH and electrolyte. (○) Sulfuric acid; (▲) citrate; (□) glycine; (♦) acetate; (⧗) borate; (●) tris-(hydroxymethyl)aminomethane.

factor of two and may represent a change in electrochemical mechanism. Simple increases in concentration of compound I at the electrode surface could also produce the higher currents and that possibility is not eliminated by the available data. However, it is unlikely that ion-pair formation and its potentially greater adsorption can account for the increases because they are larger at higher pH where the concentrations of amine cations are lower. These solutions were also evaluated for partitioning of solute into the CPE. Partitioning could not be demonstrated by a voltammetric scan on an electrode that had been soaked in the solution, removed and rinsed, and placed in fresh electrolyte.

Sensitivities

Ratios of peak currents to concentrations tend to increase with concentration and/or electrode–solute contact time. This effect is relatively minor for compound I but becomes progressively more significant with the other compounds as their lipophilicities increase. For example, the ratio for compound IV, the ethyl ester of I, was 16% larger at the highest concentration than it was at the lowest. Additional experiments with compound IV produced typical results for solute extraction into the CPE [5, 6]. The voltammograms show higher peak currents as the time intervals increase

between scans of a fixed concentration solution. This effect eventually reaches a steady-state equilibrium solute flux at the electrode–solution interface as shown in Fig. 3. As expected then, the plateau currents are proportional to concentration and provide lower detection limits. A similar result was reported for chloramphenicol such that its detectability approached 10^{-9} M by differential pulse voltammetry at a CPE [7]. The extraction of compound IV into the CPE was also evident by voltammetry on a CPE that had been soaked for 15 min in a 0.3 mM solution of compound IV, rinsed thoroughly, and scanned in fresh electrolyte. The first scan produced a current peak that was ca. 9% of the plateau current found for the solution of compound IV. Subsequent scans produced continually decreasing currents as the solute reservoir in the CPE was depleted.

Similar experiments with compound I in the sulfuric acid or acetate electrolytes did not produce measurable extraction when the CPE was soaked and transferred to fresh electrolyte. However, current constants from basic borate buffers were about 15% higher when the electrode-solution contact time was increased from 15 to 60 s before scans were made. It is apparent that adsorption is significant for these compounds and that their determination by these voltammetric techniques can be done accurately only by rigorous control of the experimental conditions.

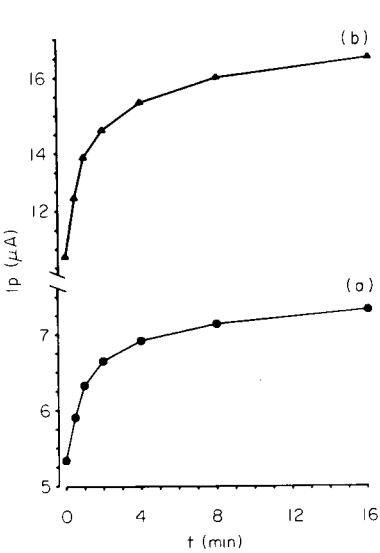

Fig. 3. Peak currents for compound IV in (a) pH 1.4 sulfuric acid and (b) pH 6.3 acetate electrolyte as a function of electrode solution contact time before scans. In sulfuric acid, IV is 3.21×10^{-5} M; in acetate, IV is 6.84×10^{-5} M.

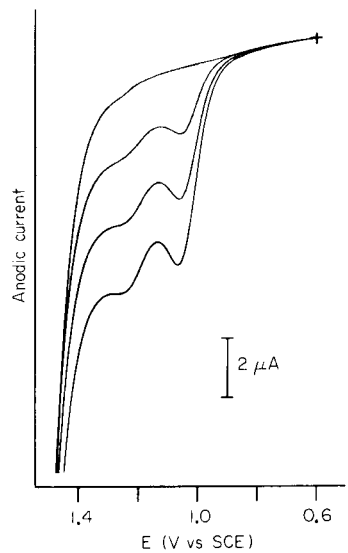

Fig. 4. Voltammograms of compound I in pH 6.3 acetate electrolyte; background, 0.027, 0.053, and 0.079 mM, respectively.

Coulometry

Controlled-potential coulometry data were obtained for compounds I, II, and IV (Table 1). The compounds transfer two electrons at 1.3 V. The anion of I, however, has an oxidation peak at 1.1 V and coulometric values under these conditions are closer to one electron. This result can be explained by voltammograms in pH 6.3, or greater, media that show a second oxidation peak at 1.3 V (Fig. 4). Because the second wave, when corrected for background, has similar symmetry and size to the first wave, it suggests sequential 1-electron oxidation steps. These results complement the voltammetric data in Fig. 2 where peak sensitivities above the pK_a are significantly lower than in strongly acidic media. The anion current constants are also about 50% of those found for compounds II, III, and IV.

The coulometric results agree with the literature on 1,5-dialkylfurans [9] insofar as they confirm a 2-electron process at suitable potential. In addition, it is well known that furanyl compounds undergo electrolysis to produce intermediates that react with nucleophiles present in the electrolyte [3, 8—12]. Many of these products are 2,5-disubstituted dihydrofurans that result from a 2-electron oxidation of the parent furan. The mechanisms are coupled electron transfer-chemical reaction and probably can be categorized as e.c.e.c. or e.c. depending on the particular compounds and the potentials used [13].

Applications

Hydrolysis studies in acidic media with 2-methoxyfuran, for example, have demonstrated first-order disappearance kinetics [14, 15]. Analogously, voltammetry of sulfuric acid—acetonitrile solutions of compounds I and II at a limited number of time points indicate pseudo-first-order kinetics for the degradation of these compounds (Table 2). In the case of compound II, solutions were independently assayed by h.p.l.c.—u.v. to assure the selectivity of the voltammetric method. No additional oxidative waves were observed

TABLE 1

Controlled-potential coulometric data

Sample	pH	Potential (V)	Time (min)	Amount oxidized (%)[a]	*n*
I	1.4	1.3	30, 60	44.4, 71.5	2.1, 2.0
	7.3	1.1	30, 90, 180	40.8, 43.9, 68.3	1.3, 1.2, 1.2
	7.3	1.3	30	57.7	1.8
II	1.4	1.3	30, 60	47.7, 71.6	1.9, 2.0
	1.4	1.25	90	69.3	1.9
	7.3	1.3	30	55.7	2.0
IV	1.4	1.25	90, 180	66.7, 88.5	2.1, 2.1

[a]Determined by u.v. absorbance loss at λ_{max} (I = 280 nm, II = 305 nm, IV = 293 nm).

TABLE 2

Hydrolysis of I and II in aqueous acid

Sample	Temp. (°C)	H_2SO_4 in CH_3CN	Percent remaining after storage[a]			
			3 h	6 h	8.25 h	24 h
I	50	0.017 M in 67%	76	59	48	12
		0.067 M in 67%	33	11	—	—
			1 h	2 h	4 h	
II	37	0.18 M in 90%	93(91)	87(85)	74(78)	

[a]Voltammetric determinations in sulfuric acid electrolyte using external standardization. Values in parentheses were determined by an independent h.p.l.c.—u.v. procedure.

in acidic solutions of either I or II which had been extensively hydrolyzed. Similar kinetic results were also found for the hydrolysis of compound I in independent experiments that utilized h.p.l.c.—u.v. for the determinations. Overall, then, these data indicate that voltammetry is selective for compounds I and II in the presence of their acid-catalyzed hydrolysis products.

The anion of compound I can be determined at low levels by l.c.e.c. with the detector operating at +1.1 V. Experiments run to generate standard curves provided linear response data up to 300 ng injected and detection limits (3 × background noise) of 2.5 ng and 1.2 ng, respectively, for h.p.l.c. systems generating k' values of 5 and 1.5. Regression analyses of the data gave

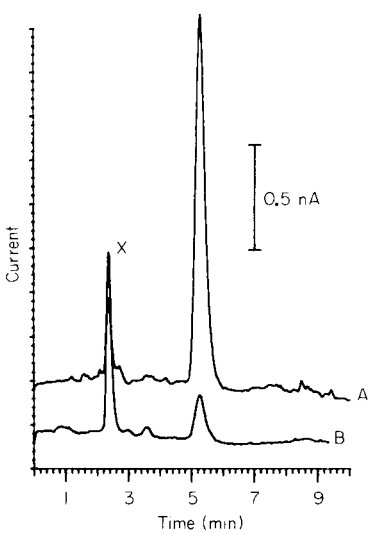

Fig. 5. Chromatograms of compound I from an alkylphenyl column: A, 9.1 ng injected; B, 1.1 ng injected; X, column void volume.

least squares equations of
I (nA) = (4.19 ± 0.086) C (ppm) + (1.5 ± 1.8) nA with s_{yx} = 5.3 nA and r = 0.997 for triplicate runs at each of 6 concentrations between 0.25 and 39.6 ppm for k' = 5, and
I (nA) = (5.91 ± 0.016) C (ppm) − (0.13 ± 0.12) nA with s_{yx} = 0.36 nA and r = 0.9999 for triplicate runs at each of 6 concentrations between 0.06 and 15.1 ppm and with k' = 1.5, in which uncertainties are quoted at ±1 s.d.

No electrode fouling was observed and there was no other evidence of significant decreases in sensitivity during several days operation. Typical chromatograms are shown in Fig. 5.

REFERENCES

1 R. A. Parker, T. Kariya, J. M. Grisar, and V. Petrow, J. Med. Chem., 20 (1977) 781.
2 R. J. Ash, R. A. Parker, A. C. Hagan, and G. D. Mayer, Antimicrob. Agents Chemother., 16 (1979) 301.
3 H. Tanaka, Y. Kobayasi, and S. Torri, J. Org. Chem., 42 (1976) 3482.
4 L. Eberson and K. Nyberg, J. Am. Chem. Soc., 88 (1966) 1686.
5 C. A. H. Chambers and J. K. Lee, J. Electroanal. Chem., 14 (1967) 300.
6 T. B. Jarbawi and W. R. Heineman, Anal. Chim. Acta, 135 (1982) 359.
7 T. B. Jarbawi, W. R. Heineman, and G. J. Patriarche, Anal. Chim. Acta, 126 (1981) 57.
8 K. Yoshida and T. Fueno, J. Org. Chem., 36 (1971) 1523.
9 K. E. Kolb and C. L. Wilson, Chem. Comm., (1966) 271.
10 A. J. Baggaley and R. Brettle, J. Chem. Soc. C, (1968) 969.
11 S. Torii, H. Tanaka, and T. Okamoto, Bull. Chem. Soc. Jpn., 45 (1972) 2783.
12 J. Froborg, G. Magnusson, and S. Thóren, J. Org. Chem., 40 (1975) 122.
13 I. Stibor, J. Šrogl and M. Janda, J. Chem. Soc. Chem. Commun., (1975) 397.
14 A. Kankaanperä and R. Aaltonen, Acta Chem. Scand., 26 (1972) 2537.
15 J. E. Garstand and G. L. Schmir, J. Org. Chem., 39 (1974) 2920.

Analytica Chimica Acta, 146 (1983) 125—134
Elsevier Scientific Publishing Company, Amsterdam — Printed in The Netherlands

MICROPROCESSOR-CONTROLLED POTENTIOSTAT FOR TWIN-ELECTRODE VOLTAMMETRY

DAVID W. PAUL,[a] THOMAS H. RIDGWAY* and WILLIAM R. HEINEMAN
Department of Chemistry, University of Cincinnati, Cincinnati, Ohio 45221 (U.S.A.)
(Received 5th July 1982)

SUMMARY

A microprocessor controlled potentiostat with independent potential control of two working electrodes is described. A 6502 microprocessor enables voltammetry to be conducted with any number of potential waveforms and current-sampling methods. A unique circuit for 60-Hz line noise elimination is used. The utility of the potentiostat is demonstrated with differential pulse anodic stripping voltammetry in a twin-electrode thin-layer cell.

The small volume capability of thin-layer electrochemical cells has been combined with the low detection limit of differential pulse voltammetry for the determination of small amounts of electroactive species [1—4]. As examples, the drug chlorpromazine has been determined to 5×10^{-9} M on 23 μl of urine by thin-layer differential pulse voltammetry [4]; and the metal ions Cu^{2+}, Pb^{2+}, Cd^{2+}, and Tl^{+} have been determined down to 30 ng ml^{-1} on a 20-μl sample by thin-layer differential pulse anodic stripping voltammetry [3].

A problem with the simultaneous determination of metal ions by thin-layer anodic stripping voltammetry is the formation of intermetallic compounds between two or more metals after their deposition in the mercury film electrode [3, 5]. Such interaction among materials which have been preconcentrated into or onto an electrode is an inherent difficulty with stripping voltammetry [6—12]. Numerous intermetallic compounds have been reported [6, 7]. The formation of such compounds can cause erroneous quantitative results because of the effect on the magnitude of the stripping current. The effect of Cu—Zn and Cu—Cd intermetallic compounds in thin-layer anodic stripping voltammetry has been investigated [3, 5]. Copper was found to interfere substantially with the determination of zinc and cadmium in the part-per-million concentration range.

A twin-electrode thin-layer cell can be used to eliminate interferences caused by intermetallic compound formation [3, 5]. The interfering metal is

---

[a]Present address: Department of Chemistry, University of Arkansas, Fayetteville, Arkansas 72701, U.S.A.

removed from the thin solution layer by selective deposition onto one of the working electrodes; the other metals are then deposited at the second working electrode and quantified by anodic stripping voltammetry. Thus, the intermetallic interference is avoided by depositing the interfering metals at different electrodes.

This concept was successfully demonstrated by using linear sweep voltammetry as the stripping technique [5]. The detection limit with this technique for thin-layer anodic stripping voltammetry is about 1 $\mu g\,ml^{-1}$. The achievement of lower detection limits by differential pulse voltammetry as the stripping technique was stymied by the unavailability of a potentiostat capable of applying the differential pulse waveform to two working electrodes with simultaneous, independent potential control. To this end, a microprocessor-controlled twin working electrode potentiostat has been developed and tested.

Computer control of the potentiostat is needed to apply the complicated waveforms and timing sequence for the twin working electrodes to eliminate the intermetallic interference. Computer control of potentiostats as a means of easily varying complicated waveforms with precisely timed current-sampling is commonly used for the implementation of such electrochemical techniques [13—25]. The main features of the new instrumentation include a unique four-electrode (reference, auxiliary, and two working) potentiostat that allows for independent potential control over each working electrode, an interface to a 6502 microprocessor that provides an unusual method of performing voltammetry with any number of potential waveforms and current sampling methods, and 60-Hz line noise elimination. This instrument and its evaluation for differential pulse anodic stripping voltammetry are described in this paper.

EXPERIMENTAL

Apparatus and reagents

The twin-electrode thin-layer cell has been previously described [5]. The bulk solution cell was constructed from a 50-ml beaker fitted with a teflon cap. Wax-impregnated graphite electrodes were prepared from POCO FXI spectroscopic graphite rods as previously described [3]. Glassy carbon electrodes (Atomergic Chemicals Co., Plainview, N.J.) were polished with successively finer grades of diamond paste (Buehler Ltd., Evanston, Ill.) Voltammograms were recorded on a Hewlett-Packard 7015A x-y recorder.

Standard solutions of Cu^{2+}, Cd^{2+}, Hg^{2+}, and Zn^{2+} were prepared by diluting Fisher Atomic Absorption Standards with appropriate amounts of 1.0 M sodium acetate—0.1 M HNO_3 or 0.1 M sodium acetate—0.01 M acetic acid. Supporting electrolyte solutions were pre-electrolyzed to reduce trace metal contamination. Preformed mercury films were deposited from a 0.006 M mercury(II) nitrate solution in 0.5 M KNO_3.

Procedure for thin-layer experiments

Glassy carbon mercury film electrodes were formed by applying a potential of −0.7 V vs. SCE for 5 min to a glassy carbon electrode immersed in a 15-ml bulk solution cell containing stirred, deoxygenated 0.006 M mercury(II) nitrate—0.5 M KNO_3 solution. After mercury film formation, the potential was stepped to +0.050 V to reoxidize any trace metals codeposited with the film. The electrode was then transferred to the thin-layer cell. Working electrode 0 (W0) was assigned to a wax-impregnated graphite electrode previously inserted into the thin-layer cell. The glassy carbon mercury film electrode was designated as working electrode 1 (W1). After the thin-layer cell had been filled with solution, the program developed for the thin-layer cell was executed. The programming stepped W0 to −0.600 V while the potential at W1 was held at +0.05 V. After exhaustive deposition of Cu^{2+} at W0, W1 was stepped to −1.4 V. When the assigned deposition time had elapsed, the potential was scanned to −0.064 V with a differential pulse waveform.

Instrument description

The system centers around an expanded KIM 1 microcomputer and the twin potentiostat interface board. The KIM 1 is a 6502 microprocessor-based computer to which was added an additional 16 K of static random access memory (RAM) and an interface to a high speed audio cassette for data and program storage. The twin potentiostat card controls the twin working electrode thin-layer cell. The operator develops programming for the acquisition of the data via a teletype in the high-level FOCAL language [26]. These programs are available on request. This programming is used to control the interface, which includes the development of potential waveforms with data acquisition and display.

A block diagram of the interface is shown in Fig. 1. The potentials applied

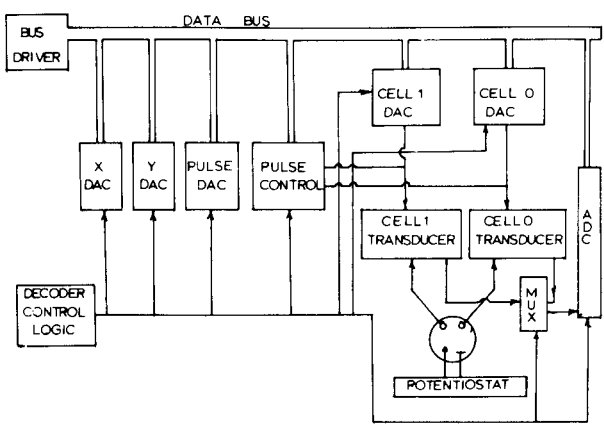

Fig. 1. Block diagram of interface between KIM 1 microcomputer and twin working electrode cell.

to the working electrodes are derived from 12-bit digital-to-analog converters (DACs) with a pulse DAC being used for pulsed mode operation. For pulse modes of operation, a second DAC applies pulses to the cell. The current resulting from the potential excitation is converted to a voltage in the cell transducers. This voltage is then converted to a binary number in the analog-to-digital converter (ADC) section and passes via an 8-bit data bus into computer memory. Control over the interface is accomplished in the decoder control logic.

One of the differences between digitally and analog controlled instrumentation is that digital control produces only discrete voltage changes so that the approximation to a linear potential ramp is a staircase waveform. The solid line in Fig. 2 shows the potential waveform and timing for staircase voltammetry. The potential is swept by updating the DAC at timed intervals. The potential excitation for differential pulse modes includes an additional potential pulse applied near the end of the staircase tread, as indicated by the dashed line in Fig. 2.

The pulse DAC (Fig. 3) is a unipolar 10-bit converter, the eight most

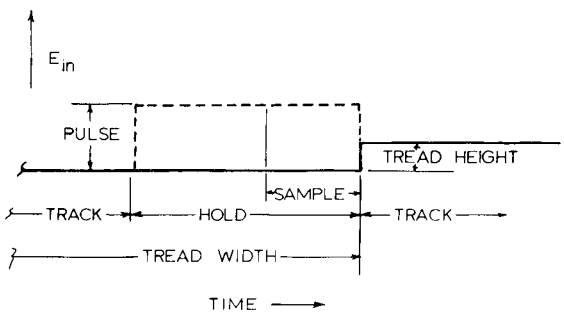

Fig. 2. Waveform for staircase differential pulse voltammetry. The dashed line shows the optional pulse.

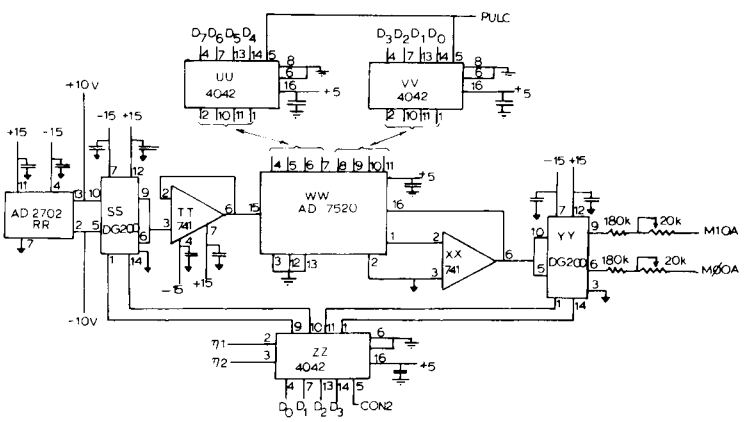

Fig. 3. Schematic diagram for pulse DAC.

significant bits of which are used. The signal and its inverse are presented to field effect transistor (FET) switches so that pulses of either polarity, or no pulse at all, can be applied. This arrangement provides an effective linearity of 11 bits. The pulse applied to the cell is in the range ±128 mV with a resolution of 0.5 mV and a linearity of ±0.063 mV.

The potentiostat, shown in Fig. 4, applies the potential to the working electrodes through the non-inverting input of the transducer amplifier. The reference electrode is held at ground potential. This arrangement allows for independent control over each of the working electrodes, which is mandatory for successful separation between the analyte metal ions and the interfering metal ion. The output of the transducer amplifier can be expressed as

$$E_o = E_{in} - i_c R_t \tag{1}$$

where E_o is the output potential of the transducer amplifier. The output potential, E_o, contains the potential applied to the cell, E_{in}, the current response from the cell, i_c, and the value of the feedback resistor, R_t, in the transducer amplifier. Subsequent circuitry removes the E_{in} component from E_o so that only the term containing i_c will reach the ADC.

Figure 5 shows the complete transducer section of the interface. Operational amplifier C converts i_c to a voltage and circuitry configured around amplifier J subtracts E_{in} from E_o. Circuitry surrounding amplifier H1 and H is used for differential modes of operation (enabling the DG508 eight-channel multiplexer G to set the differential pulse mode.) If G is disabled (non-differential modes), the output of amplifier J is $i_c R_t$.

A differential pulse experiment measures the faradaic current response arising from only the potential pulse. The commonest approach to performing the differential pulse experiment is to take one data point just before the pulse is applied and a second data point at the end of the pulse. The difference between these two values is assumed to be the faradaic current response to the pulse. This experiment yields enhanced sensitivity over regular modes of operation. There are some problems with this approach in

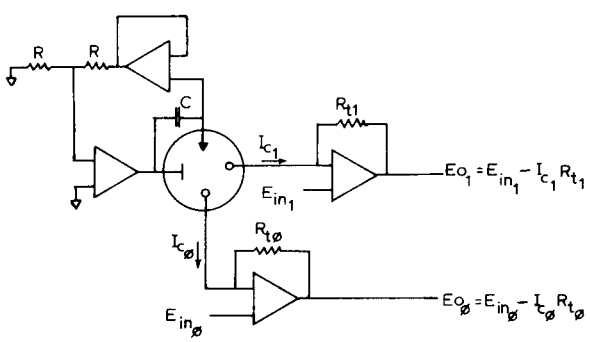

Fig. 4. Twin-working electrode potentiostat.

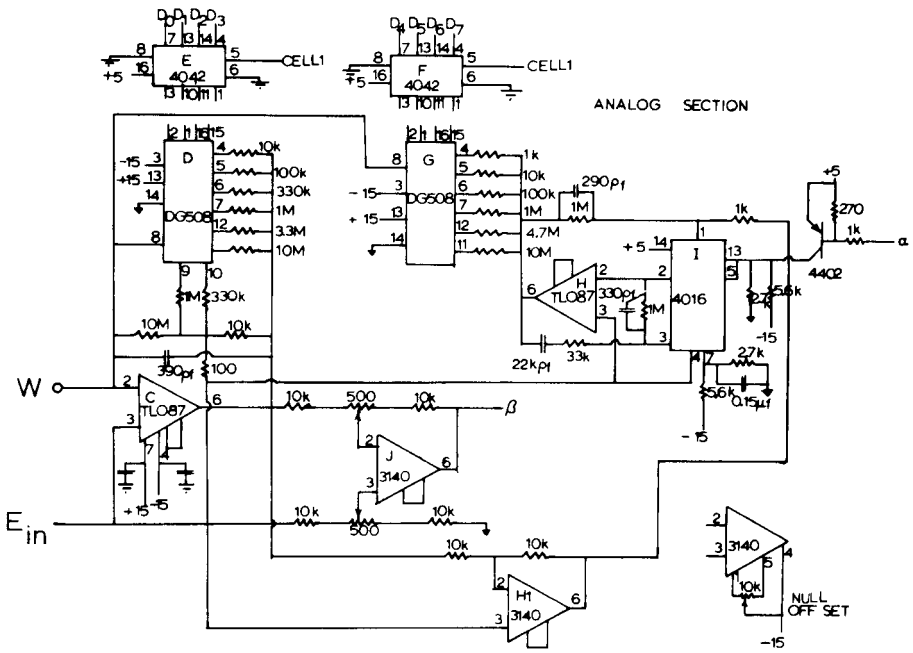

Fig. 5. Transducer section of twin-working electrode interface. Amplifier C, i to E converter; amplifier J, applied potential subtraction; amplifiers H and H1, compensation circuitry for differential pulse modes; multiplexer D, autoranging.

electrochemical systems with high background currents. In this instance, the two data points are both large and the difference between them can be small, resulting in a large relative uncertainty in the measurement.

This instrument uses analog circuitry (amplifiers H1 and H) which suppresses the current from the cell before the pulse is applied. Before the pulse is applied, the analog transmission gate, I, is closed and the output of amplifier J is driven close to zero volts. This can be expressed by

$$E_\beta = R_t i_c/(1 + R_t X/R_c) \tag{2}$$

where E_β is the potential presented to ADC, X is the gain factor for compensator H, and R_c is a compensation resistance selected by DG508.

However, when $X = 1000$, $i_c R_c \approx 1$ V, and $R_t > R_c$,

$$E_\beta = I_c R_c/X \approx 0. \tag{3}$$

These conditions have the effect of drastically reducing the output from the cell. This condition is called TRACK because the output, E_F, from the compensator amplifier H moves to the potential necessary to place E_β close to zero (see Fig. 2). A few microseconds before the pulse is applied, gate I opens and the value of E_F is held constant by the potential stored on capacitor C. This results in a continued suppression of the current that flowed through the cell just prior to application of the pulse. This condition is

called HOLD. No compensation occurs for additional current arising from the pulse causing the output of E_β to become

$$E_\beta = R_t i_p \tag{4}$$

where i_p is the current caused only by the pulse. This expression remains accurate to the extent that the current just prior to pulse application is constant through the pulse. This assumption is also made in all of the other differential methods. The result of the use of this circuit is that only the pulse-derived signal is applied to the ADC.

The ADC employed in the instrument is unusual for electrochemical instruments in that it is based upon a voltage-to-frequency converter (VFC), in conjunction with a set of counters. This method of conversion was chosen because of the inherent signal-averaging properties of a VFC. One of the prime noise components in electrochemistry is line noise (either 60 or 50 Hz). If one accumulates the counts resulting from a VFC for a time interval which is a whole multiple of the line period, then any noise components injected after the potentiostat will be essentially eliminated, and only the direct current component of the faradaic rectification signal [27] of noise injected into the potentiostat itself will be retained.

The signals from both cells are passed to a two-channel multiplexer and the selected signal is fed to a programmable gain amplifier which amplifies it by a factor of from 1 to 16 and then feeds it to the VFC. The absolute value of the signal is monitored by two comparison amplifiers so that the computer can monitor the rough magnitude of signal fed to the converter. This information is used by an auto scaling algorithm to alter the final gain stage for optimal signal level to the converter during the early stages of the pulse decay, and is then held constant during the actual conversion at the end of the pulse. The output of the converter feeds four 4-bit binary counters which are reset just prior to the conversion time (labeled SAMPLE in Fig. 2). The counts are accumulated for a fixed period (a multiple of the line period) and the count input is disabled and the results read in two 8-bit segments. The full schematic of the converter section is available from the authors on request.

RESULTS AND DISCUSSION

Bulk solution cell

The potentiostat was first evaluated by performing differential pulse anodic stripping voltammetry on cadmium(II) ions in a bulk solution cell. A stripping voltammogram for a 90 $\mu g\ l^{-1}$ Cd^{2+} solution is shown in Fig. 6. The background current suppression feature gives a good baseline and a well-defined wave for cadmium was obtained for concentrations down to 0.3 $\mu g\ l^{-1}$. The detection limit was 0.1 $\mu g\ l^{-1}$ under these conditions. Variation in pulse height from 5 to 25 mV in 5-mV increments for a 90 $\mu g\ l^{-1}$ cadmium solution gave a linear plot of peak current vs. pulse height (slope =

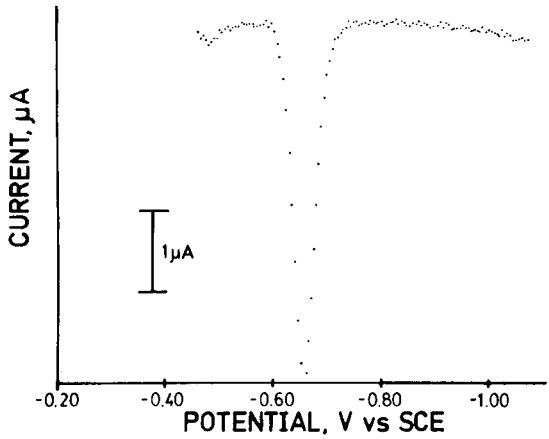

Fig. 6. Differential pulse anodic stripping voltammogram for Cd^{2+} in bulk solution cell with in situ deposited mercury film electrode. 90 $\mu g\ l^{-1}$ Cd^{2+}, 50 mg l^{-1} Hg^{2+}, 0.1 M sodium acetate, 0.01 M HNO_3. Deposition at −1.1 V vs. SCE for 5 min with stirring.

0.2218 ± 0.0082 $\mu A\ mV^{-1}$, intercept = 2.17 ± 0.14 μA, correlation coefficient = 0.998, standard error 0.017 μA). The positive intercept results from a bias current in the operational amplifier producing the pulse.

Twin-electrode thin-layer cell

Differential pulse anodic stripping voltammograms for a solution containing Zn^{2+}, Pb^{2+}, Cd^{2+}, and Cu^{2+} are shown Fig. 7. The dotted line voltammogram was obtained after all metals had been deposited on the glassy carbon mercury-film electrode at −1.4 V for 8 min. Well-defined stripping

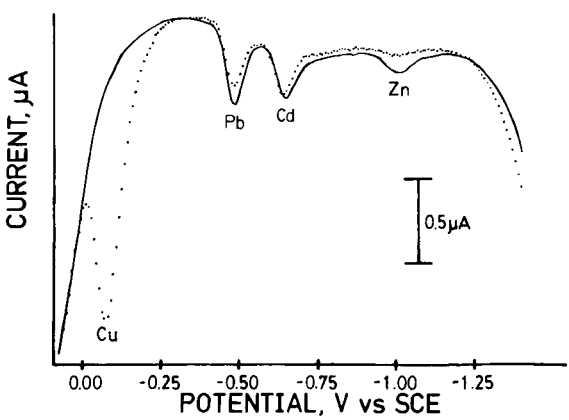

Fig. 7. Differential pulse anodic stripping voltammograms in twin-electrode thin-layer cell. 50 $\mu g\ l^{-1}$ Cu^{2+}, 50 $\mu g\ l^{-1}$ Zn^{2+}, 0.1 M sodium acetate, 0.01 M acetic acid. (---) Single electrode experiment; (——) twin-electrode experiment.

waves are evident for lead, cadmium and copper. However, the zinc wave is substantially depressed by formation of the Cu—Zn intermetallic compound; the copper wave is proportionately enhanced because zinc in the intermetallic compound is stripped at this potential. The solid line voltammogram was obtained after removal of Cu^{2+} from the thin-layer onto the wax-impregnated graphite electrode. First, W0 was stepped to −0.60 V for 10 min to deposit all copper on the wax-impregnated graphite electrode. Then W1 was stepped to −1.4 V for 8 min to deposit all Zn^{2+}, Cd^{2+}, and Pb^{2+} in the mercury-film electrode. The potential of W1 was then scanned positively with the differential pulse waveform to give the solid line voltammogram. Successful elimination of the intermetallic interference is evidenced by the absence of a peak for copper and the now present peak for zinc. Comparison of the two stripping waves for cadmium and lead shows the effect of the presence of copper on the background current.

Conclusion

The microprocessor-controlled twin-working electrode potentiostat, which avoids intermetallic interactions in thin-layer differential pulse anodic stripping voltammetry, should provide an improvement in detection limits of at least two orders of magnitude over the previously reported results with linear sweep voltammetry [5]. Virtually all voltammetric techniques can be conducted with minor changes in software. This system would be suitable for any other dual working electrode application such as rotating ring disc electrodes.

The authors thank Daryl A. Roston for many helpful suggestions. This research was supported in part by the National Science Foundation (WRH). D. P. acknowledges support by a University of Cincinnati Summer Research Fellowship.

REFERENCES

1 W. R. Heineman, T. P. DeAngelis and J. F. Goelz, Anal. Chem., 47 (1975) 1364.
2 T. P. DeAngelis and W. R. Heineman, Anal. Chem., 48 (1976) 2262.
3 T. P. DeAngelis, R. E. Bond, E. E. Brooks and W. R. Heineman, Anal. Chem., 49 (1977) 1792.
4 T. B. Jarbawi, W. R. Heineman and G. J. Patriarche, Anal. Chim. Acta, 126 (1981) 57.
5 D. A. Roston, E. E. Brooks and W. R. Heineman, Anal. Chem., 51 (1979) 1728.
6 F. Vydra, K. Stulik and E. Julakova, Electrochemical Stripping Analysis, Halsted Press, New York, 1976, pp. 58—66.
7 E. Barendrecht, in A. J. Bard (Ed.), Electroanalytical Chemistry, Marcel Dekker, New York, 1967, Vol. 2, pp. 77—78.
8 T. R. Copeland, R. A. Osteryoung and R. K. Skogerboe, Anal. Chem., 46 (1974) 2093.
9 D. G. Robbins and C. G. Enke, J. Electroanal. Chem., 23 (1969) 343.
10 M. S. Shuman and G. P. Woodward, Jr., Anal. Chem., 48 (1976) 1979.
11 S. T. Crosum, J. A. Dean and J. R. Stokely, Anal. Chim. Acta, 75 (1975) 421—30.
12 W. Kemula and Z. Kublik, Nature, 182 (1958) 1228.
13 K. F. Drake, R. P. Van Duyne and A. M. Bond, J. Electroanal. Chem., 89 (1978) 231.

14 A. M. Bond, J. Electroanal. Chem., 118 (1981) 381.
15 J. E. Anderson, R. N. Bagchi, A. M. Bond, H. B. Greenhill, T. L. E. Henderson and F. L. Walter, Am. Lab., February (1981) 21.
16 A. M. Bond and B. S. Grabaric, Anal. Chem., 51 (1979) 126.
17 J. A. Turner and R. A. Osteryoung, Anal. Chem., 50 (1978) 1496.
18 A. M. Bond and B. S. Grabaric, Anal. Chim. Acta, 101 (1978) 309.
19 T. E. Edmonds, Anal. Chim. Acta, 108 (1979) 155.
20 M. Bos, Anal. Chim. Acta, 103 (1978) 367.
21 A. M. Bond and B. S. Grabaric, Anal. Chem., 51 (1979) 337.
22 C. Yarnitzky, R. A. Osteryoung and J. Osteryoung, Anal. Chem., 52 (1980) 1174.
23 J. A. Turner, J. H. Christie, M. Vukovic and R. A. Osteryoung, Anal. Chem., 49 (1977) 1904.
24 S. C. Rifkin and D. H. Evans, Anal. Chem., 48 (1976) 2174.
25 T. R. Brumleve, J. J. O'Dea, R. A. Osteryoung and J. Osteryoung, Anal. Chem., 53 (1981) 702.
26 D. W. Paul, Ph.D. Dissertation, University of Cincinnati, Cincinnati, OH, 1980.
27 D. E. Smith, in A. J. Bard (Ed.), Electroanalytical Chemistry, Vol. 1, Marcel Dekker, New York, 1966, pp. 1—155.

Analytica Chimica Acta, 146 (1983) 135—148
Elsevier Scientific Publishing Company, Amsterdam — Printed in The Netherlands

ENZYME ELECTRODES WITH IMPROVED MECHANICAL AND ANALYTICAL CHARACTERISTICS OBTAINED BY BINDING ENZYMES TO NYLON NETS

MARCO MASCINI,* MARIO IANNELLO and GIUSEPPE PALLESCHI
Istituto di Chimica Analitica, Università di Roma, Roma (Italy)
(Received 20th May 1982)

SUMMARY

Enzyme electrodes obtained by binding enzymes on nylon net show improved mechanical and analytical characteristics. The chemical binding process is mild so that the final membrane retains a high enzyme activity. The resulting membrane also has high mechanical strength and can be assembled on the electrode surface several times without damage. Response times without nylon net are excellent. Examples with single and dual enzymes coupled with an oxygen or ammonia electrode are discussed.

Enzyme electrodes are becoming popular for the determination of specific substrates in clinical and food analysis [1, 2]. Recently, many techniques of enzyme immobilization have been described and enzyme electrodes as specific sensors have been reviewed [3—5]. Generally the techniques described for enzyme immobilization are tedious or necessitate skilled manipulation. Further, when the enzyme is fixed on the surface of the membrane electrode, the response time increases because of the extra barrier and the enzymatic reaction time. Thus an essential requisite of the enzyme electrode is to fix the minimum amount of enzyme to the electrode surface; yet it has been estimated that at least 5—10 units of enzyme should be fixed in the surroundings of the electrode surface to obtain reliable responses to the desired substrate. A compromise therefore is very often necessary. A further consideration is that the lifetime of the enzyme electrode depends strictly on the amount of enzyme fixed on the electrode surface and this parameter also influences the thickness of the enzyme layer.

An important prerequisite for wider use of enzyme electrodes is mechanical stability of the enzyme layer. As the oxygen electrode, for example, forms the basis of several enzyme sensors, the possibility of changing only the enzyme layer to obtain different sensors is of interest. When enzyme electrodes are used in flow apparatus, it is common practice to remove the probe from the flow cell for storage of the enzyme layer at low temperature when not in use; during assembly of the probe and flow cell, the enzyme layer is pressed against spacers or collars for tightness and often the enzyme layer becomes damaged. These and other problems occur when current pro-

cedures are used to fix enzymes on the electrode surfaces, e.g., cross-linking bovine serum albumin and enzyme with glutaraldehyde on the gas-sensing membrane (teflon or polypropylene) [6], binding enzymes on collagen films [7], etching the teflon gas membrane and binding the enzyme through paraformaldehyde and bovine serum albumin [8], or fixing proteins to cellulose triacetate by hexamethylene-diamine or -triamine with glutaraldehyde [9].

This paper deals with the improved analytical features obtained by fixing enzymes to nylon net. The resulting membrane shows high mechanical resistance and can be attached to, or removed from, the electrode surface several times without damage. It has an excellent response time, matching the electrode response time for the product of the enzyme reaction without nylon net. The immobilizing procedure is very simple; the chemical binding is quite mild and leads to a final membrane with high enzyme activity, which gives results comparable to, or better than, common immobilization procedures.

The enzymes investigated were mostly oxidases and the enzyme membranes were coupled with the oxygen probe; urease membranes coupled to an ammonia probe were also studied. Some bi-enzyme membranes were evaluated for the determination of sucrose, maltose, starch and lactose, by coupling an hydrolase enzyme and glucose oxidase to the oxygen electrode.

EXPERIMENTAL

Materials

Glucose oxidase (EC 1.1.3.4. from *Aspergillus niger*, 125 U mg^{-1}), urease (EC 3.5.1.5. from jack beans, 54 U mg^{-1}), amyloglucosidase (EC 3.2.1.3. from *Rhizopus mold* 10 U mg^{-1}), alcohol oxidase (EC 1.1.3.13. from *Candida boidinii* 6.1 U mg^{-1}), galactose oxidase (EC 1.1.3.9. from *Dactylium dendroides*, 90 U mg^{-1}), lactase (from *Saccharomyces fragilis*, 15 U mg^{-1}), and β-galactosidase (EC 3.2.1.23. from *Escherichia coli*, 700 U mg^{-1}) were obtained from Sigma Chemical Co. Cholesterol oxidase (EC 1.1.3.6. from *Nocardia erythropolis*, 25 U ml^{-1}), β-fructosidase (EC 3.2.1.26. from yeast, 150 U mg^{-1}) and ascorbate oxidase (EC 1.10.3.3. from *Cucurbita species*, 100 U mg^{-1}) were obtained from Boehringer (Mannheim). These enzymes and all other reagents were used without further purification. All reagents were of the highest purity commercially available. Glutaraldehyde was a 25% solution (Merck, Darmstadt); cholesterol solution (400 mg dl^{-1}) was from Farmitalia Carlo Erba (Clinical).

Nylon net. Nylon nets were obtained from A. Bozzone (Appiano Gentile, Italy) and from the Swiss Silk Bolting Cloth Mfg. Co. (CH-9425 Thal/SG, Switzerland). The nylon meshes obtained were in the range 15—120 threads/cm with thicknesses ranging from 60 to 200 μm, and free surfaces ranging from 60 to 20%. However, most of the experiments were done with a nylon net having 120 threads/cm, a thickness of 100 μm and a 35%-free surface.

Immobilization procedure for a single enzyme

The chemical procedure for immobilizing enzymes on nylon net was derived from the method of Hornby and Morris [10]. From the nylon net, small disks of 16 or 25 mm diameter were cut out and fixed around a glass rod with nylon thread for easy and rapid handling. The rod was immersed in a stoppered tube containing dimethyl sulphate and this was immersed in a simmering water bath for exactly 5 min; the tube was then transferred to an ice bath to stop the reaction. The glass rod was then immersed in a second test tube containing anhydrous methanol; in 30—40 s, a white powder formed from the nylon net and the methanol became milky. Then the glass rod was immersed in another test tube with anhydrous methanol, where it was left for about 1 min. The single disks were released from the glass rod at this stage, and immersed as soon as possible in 50 ml of 0.5 M lysine at pH 9.0 for 2 h. The lysine acts as a spacer between the nylon structure and the enzyme molecule. The disks were washed thoroughly in 0.1 M sodium chloride. The presence of lysine groups bonded to nylon net and the presence of free amino groups can be confirmed at this stage by treating the nylon net with 2,4,6 trinitrobenzenesulphonic acid. A characteristic orange colour indicates the presence of free amino groups and the extent of the previous reactions.

After being washed in 0.1 M sodium chloride, the disks were immersed in glutaraldehyde solution (12.5% in saturated (0.1 M) borate buffer) at pH 8.5 for about 45 min. After further washing they were dipped in the enzyme solution in 0.1 M phosphate buffer (pH 7.0) for 2 h at room temperature and overnight at 4°C. The disks were then washed and fixed directly to the electrode surface or stored in phosphate buffer at 4°C.

Immobilization procedure for two enzymes

For bi-enzyme preparations, three different procedures were tested. In the first, two nylon net membranes each of which held one immobilized enzyme, were fixed on the teflon gas-permeable membrane. In the second procedure, a single nylon net membrane was used on which two enzymes had been randomly co-immobilized; in this procedure, the ratio of the two enzyme activities was varied in the immobilization stage. In the third procedure, asymmetric coupling was obtained by spreading the first enzyme in lyophilized form on a microscope glass slide, laying the dry activated nylon net over it, and spreading the second enzyme in lyophilized form on the net. A second microscope slide was placed over the net and the whole was clamped together. A buffer solution was injected by a capillary into the space between the slides to dissolve the two enzymes and react with the nylon net. Generally, this third procedure gave the best results, as was indicated recently by Bertrand et al [7]. In the first and third procedures, one of the two enzymes was glucose oxidase and this membrane, or the side of the nylon net on which this enzyme had been spread, was fixed nearer the teflon gas membrane.

Apparatus and procedures

The oxygen electrode was obtained from Instrumentation Laboratory (IL) and the unit for reading the current was the IL Model 213 pO_2 analyzer. The internal solution of the oxygen electrode is 0.1 M KCl and a teflon membrane (1/4 or 1/2 mil thick) is placed against the platinum cathode. For construction of the enzyme electrodes, the nylon net with immobilized enzyme(s) was fixed over the teflon membrane, and the two membranes were secured by the same O-ring. The nylon net was very strong and proved capable of withstanding frequent assembly and dismantling of the sensor.

Experiments were done at room temperature by adding small amounts of a concentrated solution of the substrate to a buffer in which the electrode was immersed. A flow system was also used to obtain rapid responses; in this case, solutions of different concentrations were pumped for a fixed period of time (60 s) through the flow cell. The peak heights obtained were related to the concentration of the substrate.

The ammonia gas probe tested was obtained (Instrumentation Laboratory) as a pCO_2 electrode; the internal solution was replaced by 0.1 M ammonium chloride. The external membrane was a porous polypropylene membrane (Celanese Corp.). The nylon net with urease was fixed over the polypropylene membrane, and both membranes were secured with the same O-ring. The potential of the ammonia electrode was measured by an Amel recording potentiometer (Model 866).

Measurement of enzyme activities. To measure the activity of oxidases immobilized on nylon net, a single membrane was immersed in 20 ml of a 0.1 g l^{-1} solution of the relevant substrate and the decrease in oxygen concentration was monitored with an oxygen electrode, under constant magnetic stirring. A stable constant decrease was recorded from which the activity was calculated. To measure the activity of urease, an ammonia gas probe was immersed in 20 ml of 0.1 M urea solution after calibration with ammonia standard solutions at pH 8.3. When a single membrane was immersed in the solution, the reaction produced ammonia.

To measure disaccharidase membrane activities, a glucose oxidase electrode was used. The disaccharidase-treated nylon net was dipped into 10 ml of the buffer solution containing the disaccharide (1 g l^{-1}). The electrode used was an oxygen probe covered with a glucose oxidase membrane and calibrated with glucose solutions in the same buffer.

To measure the enzyme activities of the asymmetric membranes, first the glucose oxidase activity was measured by dipping the membrane in a glucose solution (1 g l^{-1}) and recording the current variation with an oxygen electrode. Then the hydrolase activity was measured by monitoring with a glucose oxidase electrode the variation of the current obtained when the nylon net holding the two immobilized enzymes was dipped in the disaccharide solution (1 g l^{-1}).

RESULTS AND DISCUSSION

The immobilization procedure

Several parameters affect the immobilization procedure. Figure 1 shows the response curves to glucose for treated nylon nets of different mesh and thickness. The change in current is plotted; the output current was leveled by using the balance gain potentiometer in the Model 213 pO_2 Analyzer. The importance of lysine as spacer was proved by Hornby and Morris [10] and reconfirmed in the present work. An important related feature is the time elapsing between the methylation of nylon and the treatment with lysine. From Fig. 2, the activity of the nylon is easily seen; even if only a few minutes pass between the washing of the membrane with methanol and the reaction with lysine solution, the amount of enzyme immobilized is drastically reduced.

The concentration of the enzyme solution was in the range 1—10 mg ml^{-1}, depending on the cost and solubility of the enzyme, and the activity of the preparation. The nylon net does not change in physical aspect or mechanical characteristics with the enzyme concentration.

Figures 1 and 2 allow the response time of the overall assembly to be estimated. Two minutes was considered as the time needed to reach steady-state response, and the calibration graphs were prepared by recording the value after this time. Figure 3 shows the response time of maltose electrodes prepared by the three procedures outlined. In contrast to the results of

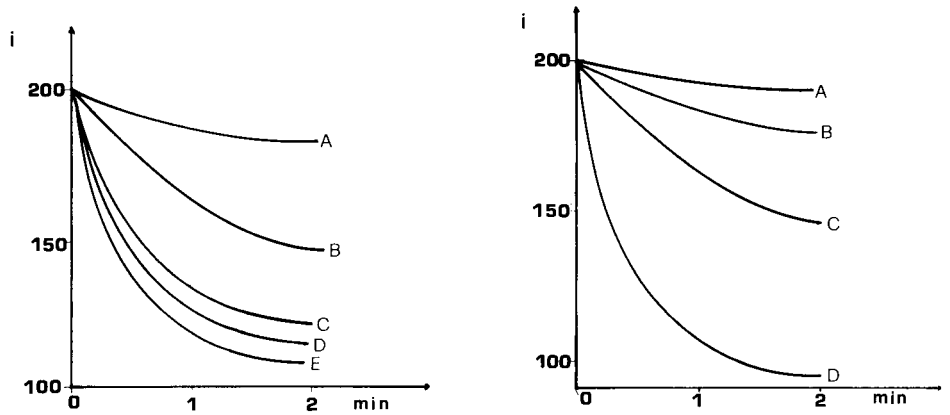

Fig. 1. Response curves of glucose oxidase electrodes prepared from nylon nets of different mesh (threads cm^{-1}) and thickness. Glucose concentration, 0.1 g l^{-1}; phosphate buffer pH 7.0. The current i (relative units) is measured. Curves: A, 15 cm^{-1}, 120 μm; B, 29 cm^{-1}, 140 μm; C, 43 cm^{-1}, 600 μm; D, 55 cm^{-1}, 100 μm; E, 108 cm^{-1}, 120 μm.

Fig. 2. Reaction of activated nylon with dimethyl sulphate. The response curves are for several enzyme electrodes obtained from the same nylon net but with decreasing periods of time between the methylation of nylon and treatment with lysine solution (0.5 M, pH 9.0). Conditions: 0.1 g l^{-1} glucose solution; phosphate buffer pH 7.0; nylon mesh, 108 cm^{-1}, 120 μm thick. Time interval: A, 20 min; B, 15 min; C, 10 min; D, 5 min.

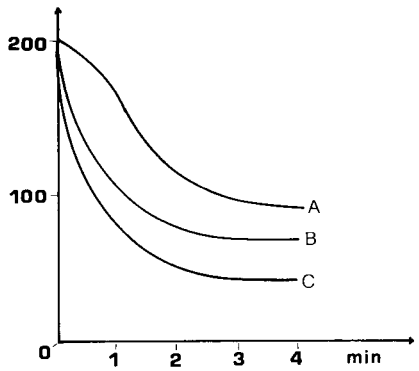

Fig. 3. Response time of dual-enzyme membranes containing amyloglucosidase and glucose oxidase. The responses were measured for a 0.3 g l^{-1} maltose solution in acetate buffer pH 4.4. Curves: A, procedure with two nylon nets; B, random immobilization; C, asymmetric immobilization.

Bertrand et al. [7], who reported variations in the response times of 10—30 min, only a small change in the response times was observed. The thickness of the teflon membrane can change the response time of the oxygen electrode and so can influence the overall response time. For the most of the present work, the porous teflon membrane was 0.5 mil thick; this has good mechanical strength and gives short response times (less than 30 s).

Table 1 lists the immobilized enzyme membranes tested; the specific immobilized activity and the lifetime of the immobilized enzyme are reported. Some of these results seem to be greatly superior to those obtained by immobilizing enzyme with collagen membrane [7, 11]. In the present experiments, all enzyme preparations were used as received; it seems obvious that the results would be improved if the enzymes were purified by column chromatography [11].

Single enzyme electrodes

Six single enzyme electrodes were assembled:

$$\text{Glucose} + O_2 \xrightarrow{\text{glucose oxidase}} \text{gluconic acid} + H_2O_2$$

$$\text{Ascorbic acid} + O_2 \xrightarrow{\text{ascorbate oxidase}} \text{dehydroascorbic acid} + H_2O_2$$

$$\text{Cholesterol} + O_2 \xrightarrow{\text{cholesterol oxidase}} \Delta^4\text{-cholestenone} + H_2O_2$$

$$\text{Alcohol} + O_2 \xrightarrow{\text{alcohol oxidase}} \text{aldehyde} + H_2O_2$$

$$\text{Galactose} + O_2 \xrightarrow{\text{galactose oxidase}} \text{galactohexodialdose} + H_2O_2$$

$$\text{Urea} + H_3O^+ \xrightarrow{\text{urease}} HCO_3^- + 2NH_4^+$$

TABLE 1

Features of immobilized enzymes on nylon net (except where stated otherwise, the medium was 0.1 M phosphate buffer, pH 7.0)

Enzyme	Activity of the starting material (Units/mg)	Specific immobilized activity (nmol min^{-1} cm^{-2})	Lifetime of the membrane
Glucose oxidase	125	100—150	Several months
Cholesterol oxidase	25[a]	600	One month
Ascorbate oxidase	100	200—300	Three months
Alcohol oxidase	6	2—3[b]	One day
Galactose oxidase	88	200	Three months
Urease	54	900—1000[c]	Several months
Amyloglucosidase	10	220 620[d]	Several months
β-Fructosidase	150	80	Fifteen days
β-Galactosidase (as lactase)	700	90	Three months

[a]Units/ml. [b]Phosphate buffer pH 8.0 was also satisfactory. [c]Phosphate buffer, pH 8.3. [d]In acetate buffer pH 4.5.

Response to glucose. The glucose oxidase electrode is the best established enzyme electrode and the present results confirm the adaptability of this enzyme to immobilization procedures. The calibration graph was linear in the range 0.004—0.2 g l^{-1}, with a correlation coefficient of 0.999 (Fig. 4, line C). The lifetime of the enzyme-treated nylon membrane was over eight months even when the net was kept at room temperature in 0.1 M phosphate buffer, pH 7.0. Some serum samples were analyzed by a flow-through cell and some results are shown in Fig. 5.

Response to ascorbic acid. An ascorbate oxidase electrode obtained by coupling ascorbate oxidase and the oxygen electrode has been reported recently [6, 11]. The enzyme was extracted and purified from the peelings of *Cucurbita* species for that work, but is now commercially available at lower activity. However, as reported in Table 1, the activity of the immobilized enzyme was very high (no information was given on the immobilized enzyme activity in the earlier papers [6, 11]) and the range of concentration measurable was 0.004—0.1 g l^{-1} (Fig. 4, line B). When this electrode is used, it is necessary to take in account the ready oxidation of the ascorbic acid. When an oxygen electrode was dipped in the phosphate buffer and ascorbic acid solution was added, the oxygen level decreased because of oxidation of the ascorbic acid by dissolved oxygen without intervention of the oxidase. The response of the ascorbate electrode was corrected for this value.

The content of vitamin C in pharmaceutical preparation was determined by dissolving tablets in a known volume of water and adding a small amount

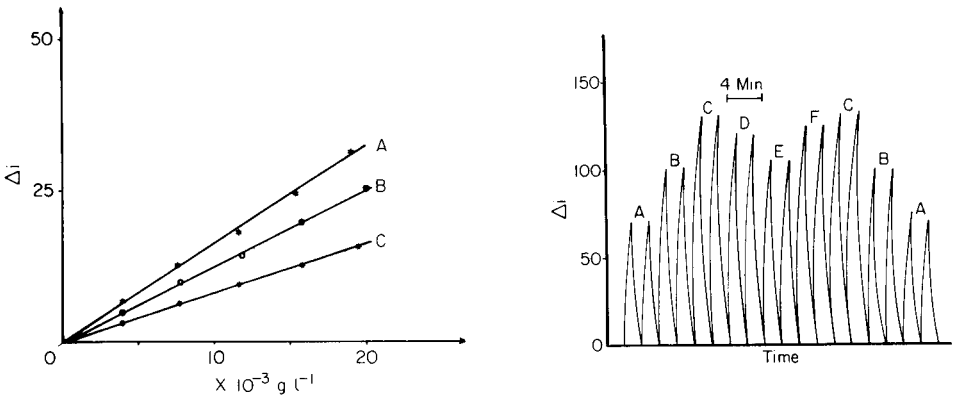

Fig. 4. Calibration graphs for different oxidase membranes and an oxygen electrode. A, Cholesterol oxidase in cholesterol solution, phosphate buffer pH 7.0 with Triton X-100 (1 ml l^{-1}). B, Ascorbate oxidase in ascorbic acid solutions, phosphate buffer pH 7.0. C, Glucose oxidase in glucose solutions, phosphate buffer pH 7.0. The change in current (Δi) on immersion of the sensor is recorded.

Fig. 5. Response to glucose in serum samples and in standard solutions with a flow technique involving 1-min sampling and 1-min wash. Serum samples were diluted 1:20 with phosphate buffer pH 7.0. Standard solutions: A, 80 mg dl^{-1}; B, 100 mg dl^{-1}; C, 120 mg dl^{-1}. D, E. F are serum samples collected from a hospital.

of the solution to a fixed volume of phosphate buffer in which the ascorbate oxidase electrode was immersed. After the addition of the sample, the current change was recorded, and a known volume of a standard solution was then added. By comparing the volumes, the current changes after background corrections, and the known concentration of the standard solution, the amounts of vitamin C in the samples were calculated. Results are reported in Table 2; the agreement with the nominal contents given by the manufacturers is considered acceptable.

Figure 6 shows the stability of the ascorbate electrode during a month of operation.

TABLE 2

Determination of vitamin C in some pharmaceutical preparations with an ascorbate oxidase electrode

Tablet	Vitamin C content (mg/tablet)	
	Nominal	Found
Vitamin C + excipients	500	480
Vitamin C + excipients	50	45.5
Multivitamin	75	71.5
Vitamin C + aspirin	240	230
Vitamin C + antibiotic	75	74.5

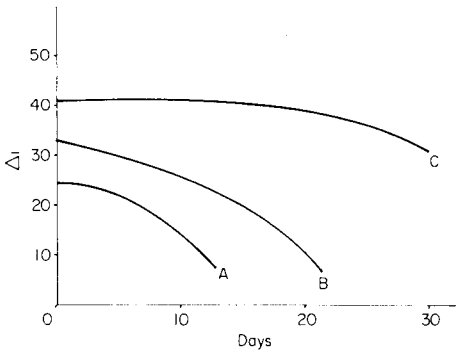

Fig. 6. Lifetime of three different nylon net membranes with immobilized enzymes, kept at room temperature. A, β-Fructosidase + glucose oxidase membrane obtained by the asymmetric procedure; the steady-state current was measured in saccharose solution (1 g l^{-1}) at pH 7.0 (phosphate). B, Cholesterol oxidase membrane for a 0.2 g l^{-1} cholesterol solution at pH 7.0 (phosphate). C, Ascorbate oxidase membrane for a 0.3 g l^{-1} ascorbic acid solution at pH 7.0 (phosphate).

Response to cholesterol. Cholesterol oxidase electrodes have been obtained by various modes of immobilizing the oxidase [12—14]. Immobilized cholesterol oxidase on nylon net was a very active preparation (Table 1). The range of determination of cholesterol concentration was 4—50 × 10^{-3} g l^{-1}, which is adequate for the determination of cholesterol in clinical samples, e.g., serum or bile after appropriate dilution. Applications in this area are under study. A calibration graph is shown in Fig. 4 (line A). The correlation coefficient was 0.998. The lifetime of the membrane was around 20 days (Fig. 6).

Response to alcohol. Attempts to immobilize alcohol oxidase on collagen membranes to give a methanol-sensitive electrode were unsuccessful [7] and the results obtained here were also not promising. The electrode showed some initial response but it degraded rapidly during the first day and after a few days the de-activation was complete. The activity of the commercial enzyme preparation was the lowest obtained and the amount immobilized on the membrane was accordingly very low.

Response to galactose. Galactose oxidase is not specific for galactose but it oxidizes galactosides and some polysaccharides containing galactose end groups [7]. However, in the absence of such compounds, an electrode could be useful for rapid screening. The linear range for the galactose concentration was 0.05—0.5 g l^{-1} (correlation coefficient, 0.997) in 0.1 M phosphate pH 7.0; this is compared with the response for lactose in Fig. 7(a). From this plot, it can be calculated that the interference of lactose is less than 3%, which could be disregarded in many cases. Application of this electrode to clinical samples is under study.

Response to urea. Urease electrodes have been prepared by immobilizing urease on the gas-permeable membrane of an ammonia sensor by binding the

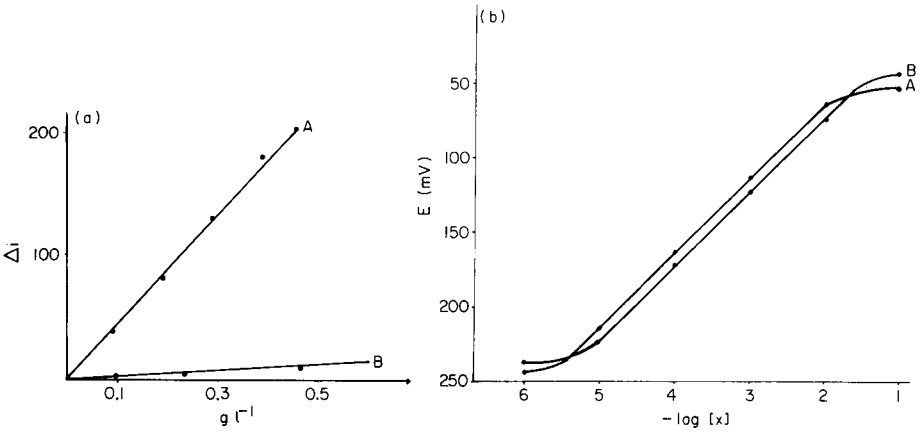

Fig. 7. Calibration graphs. (a) For the galactose oxidase nylon net with the oxygen electrode in phosphate buffer pH 7.0: (A) galactose solutions; (B) lactose solutions. (b) For the urease nylon net with the ammonia electrode in Tris buffer pH 8.3: (A) urea solutions; (B) ammonia solutions.

enzyme with bovine serum albumin solution and glutaraldehyde [15]. With the nylon net membrane, the analytical performance was similar while the mechanical strength and the lifetime were definitely improved. A calibration curve for urea with a membrane three months old in continuous operation at room temperature is reported in Fig. 7(b), where it is compared with an ammonia calibration curve. As can be seen, the calibration line for urea is higher than that for ammonia because one molecule of urea forms two ammonia molecules.

Bi-enzyme electrodes

Several disaccharides can be determined by using two or more enzymes. A disaccharidase specific for the substrate and the glucose oxidase to measure the glucose formed have been immobilized on various matrices [7, 16—18]. The immobilization procedures for two enzymes on nylon net membranes examined here were: (a) immobilization on separate nylon nets which were then stacked on the teflon membrane of the oxygen electrode; (b) co-immobilization of the two enzymes on a single net; and (c) asymmetric coupling [7, 19]. In general, the results confirmed that the asymmetric coupling yields better results. Some results for maltose determinations are summarized in Figs. 3 and 8. Similar findings were obtained for lactose and sucrose.

Table 3 summarizes the features of immobilized dual-enzyme membranes based on nylon net obtained with procedures (b) and (c). As can be seen, the specific immobilized activity does not vary much for the two immobilization procedures but the effect is clear when the membrane is coupled to the oxygen electrode (Figs. 3 and 8). The asymmetric membrane should be mounted with the disaccharidase immobilized on the outer part; with random co-immobilization, the direction of mounting is immaterial.

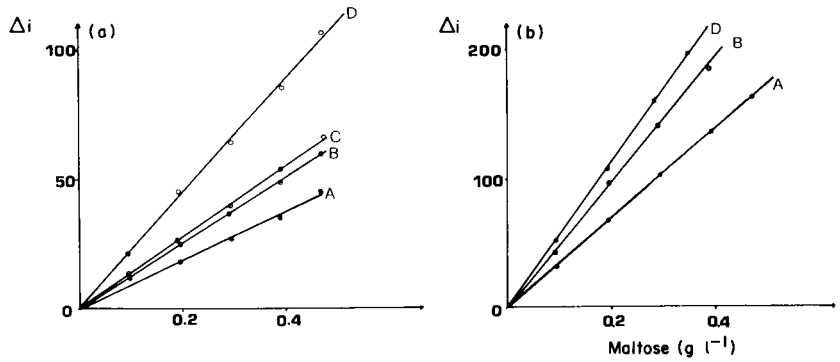

Fig. 8. Calibration graphs for maltose in (a) phosphate buffer, pH 7.0, and (b) acetate buffer, pH 4.4, with amyloglucosidase—glucose oxidase electrodes prepared by different immobilization procedures. (A) Two nylon nets stacked on teflon membrane; (B) random immobilization of glucose oxidase and amyloglucosidase activities of 250 and 20 units, respectively; (C) as for (B), but with enzyme activities of 250 and 40 units, respectively; (D) asymmetric immobilization with enzyme activities of 250 and 40 units, respectively.

Maltose and starch electrode. Glucoamylase hydrolyzes α-1,4-glucan linkages in polysaccharides, removing successive glucose units. Maltose forms two glucose molecules, and starch forms several glucose units. The calibration graphs for maltose and soluble starch are compared in Fig. 9. A change in pH has a much greater effect on the maltose calibration graphs than on the starch calibration graphs. The order of selectivity for maltose and starch is inverted at pH 7.0. The correlation coefficients for the starch and maltose

TABLE 3

Features of immobilized dual enzymes on nylon net (20°C)

Enzymes	Immobilization	Activity of enzymes GOD/ disaccharidase (units)	Buffer and pH	Specific immobilized activity (nmol min^{-1} cm^{-2})	
				As GOD	As disaccharidase
Amyloglucosidase/ glucose oxidase	Random	250/20	Acetate pH 4.4	40	70
	Asymmetric	250/40	Acetate pH 4.4	40	50
β-Fructosidase/ glucose oxidase	Random	250/1000	Phosphate pH 7.0	80	40
	Asymmetric	250/1000	Phosphate pH 7.0	70	30
β-Galactosidase/ glucose oxidase	Random	250/370	Phosphate pH 7.0	70	110
	Asymmetric	250/370	Phosphate pH 7.0	90	30

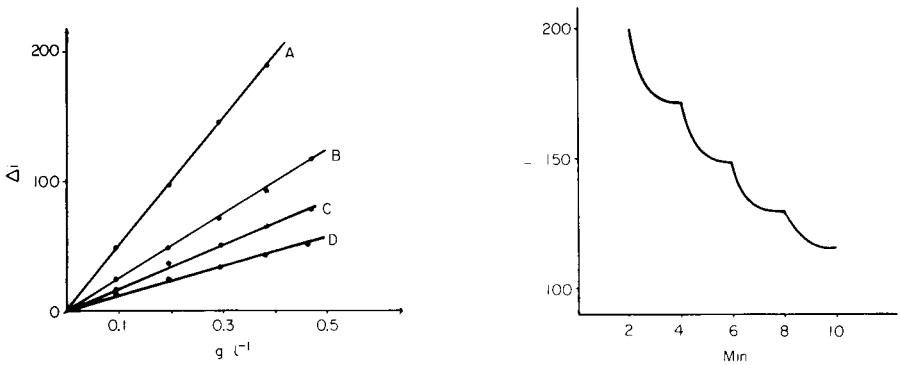

Fig. 9. Calibration graphs for maltose and soluble starch with the asymmetric amyloglucosidase/glucose oxidase membrane. (A) Maltose in acetate buffer pH 4.4; (B) soluble starch in acetate buffer pH 4.4; (C) soluble starch in phosphate buffer pH 7.0; (D) maltose in phosphate buffer pH 7.0.

Fig. 10. Response time for lactose with the β-galactosidase—glucose oxidase electrode prepared by random immobilization. Each step corresponds to addition of 0.2 ml of lactose solution (10 g l^{-1}) to 20 ml of phosphate buffer, pH 7.0.

plots were, respectively, 0.997 and 0.995; the response times were about 2 min. The lifetime of the membrane was over three months.

Figures 3 and 8 show the effect of the immobilization procedure on the electrode response. The asymmetric procedure gave the higher response at any pH. This pattern was also recorded for the other dual-enzyme electrodes reported.

Sucrose electrode. For a sucrose electrode, three enzymes should be considered: β-fructosidase to hydrolyze sucrose, mutarotase to obtain β-D-glucose from the α-D-glucose obtained, and glucose oxidase to measure the β-D-glucose formed. From the results of Bertrand et al. [7], only the β-fructosidase and glucose oxidase were immobilized and spontaneous reaction was assumed for the formation of β-D-glucose. The response time of the electrode was always around 2 min for steady-state response. The linear range of the calibration graph was 0.1—1.5 g l^{-1}, with a correlation coefficient of 0.990. The response time of the electrode obtained by immobilizing three enzymes on collagen membranes in different ways was 10—30 min [7]. Similar electrodes have been described by others [16—18]. The lifetime was only two weeks (Fig. 6), presumably because of the relative instability of β-fructosidase.

Lactose determination. Lactase, from *Saccharomyces fragilis*, was first immobilized on nylon net with glucose oxidase, but the resulting asymmetric membrane gave a very low response to lactose, perhaps because of the low activity of the preparation (15 units per mg). Better results were obtained by asymmetric immobilization of β-galactosidase and glucose oxidase. β-Galactosidase from *Escherichia coli* (Grade VIII, Sigma) has an associated lactase

activity of 100—150 units/mg; consequently, reliable results could be achieved with this combination. Calibration graphs were linear in the range 0.03—1 g l^{-1} with a steady-state response time of 1 min (Fig. 10). Figure 10 indicates a small saturation effect at the higher concentrations of lactose.

CONCLUSIONS

Nylon net membranes seem to offer a good compromise for enzyme immobilization on electrode surfaces for analytical purposes. The structure of nylon net simplifies diffusion from the surroundings of the electrode surface to the immobilized enzyme, without forming a barrier to the diffusion of the reagent or the product of the enzymatic reaction.

The procedure for immobilizing enzymes on nylon net, which is derived from the immobilization procedure of Hornby and Morris [10] for nylon tubes, is very simple and quite mild, so that a large percentage of the enzyme activity remains after the immobilization process. The mechanical strength of nylon net is virtually unimpaired by the immobilization procedure, and the membrane can be assembled or detached from the electrode surface hundreds of times, without decrease in the enzyme performance. This is not possible with the collagen membranes or with the BSA and glutaraldehyde procedures. Moreover, the results of activity obtained with nylon net membranes (Table 1) are higher than the activity obtained with other membranes (e.g. collagen or BSA) at least for the enzyme preparations so far achieved. In some cases, the method proposed failed, but the low activity of the starting enzyme preparation (alcohol oxidase and lactase) seems to be responsible for the failure. Enzyme purification could be tested in some cases to obtain higher enzyme activities for use in the immobilization procedure.

Some of the electrodes examined have given good results in practical applications, e.g., ascorbic acid, glucose, urea and lactose; others are under study. The membranes have been used with oxygen probes and, in the case of urease, with an ammonia gas probe. These systems are virtually free from interferences, because of the porous membrane that separates the sample solution from the electrode solution. In the case of systems based on the oxygen probe, the range is strictly dependent on the oxygen level of the solution, the decrease of which is measured by the electrode. The limit of detection is always limited by this concentration and is around 10^{-5} M. Of course, it would be possible to replace the oxygen probe by a hydrogen peroxide detector, to obtain lower detection limits [7], but the selectivity offered by the porous teflon membrane would then be lost or the measuring system would be complicated by a second electrode without the immobilized enzyme membrane [7]. For most practical applications, the oxygen probe must be a good choice because its selectivity is combined with the enzyme selectivity for the particular substrate.

REFERENCES

1 P. W. Cheung, D. G. Fleming, W. H. Ko and W. R. Neuman, Theory, Design and Biomedical Applications of Solid State Chemical Sensors, CRC Press, Palm Beach, FL, 1978.
2 G. J. Moody and J. D. R. Thomas, Ion Sel. Elect. Rev., 2 (1980) 219.
3 G. Guilbault, in H. H. Weetall (Ed.), Immobilized Enzymes, Antigens, Antibodies and Peptides, Dekker, New York, 1975, p. 293.
4 M. Mascini and C. Botré, Chim. Ind. (Milan), 61 (1979) 542.
5 S. Fukui, K. Sonomoto, N. Itoh and A. Tanaka, Biochimie, 62 (1980) 381.
6 P. Posadka and L. Macholan, Collect. Czech. Chem. Commun., 44 (1979) 3395.
7 C. Bertrand, P. R. Coulet and D. G. Gautheron, Anal. Chim. Acta, 126 (1981) 23.
8 S. Updike, M. C. Shults and M. Busby, J. Lab. Clin. Med., 93 (1979) 518.
9 M. Koyama, Y. Sato, M. Aizawa and S. Suzuki, Anal. Chim. Acta, 116 (1980) 307.
10 W. E. Hornby and D. L. Morris, in H. H. Weetall (Ed.), Immobilized Enzymes, Antigens, Antibodies and Peptides, Dekker, New York, 1975.
11 K. Matsumoto, K. Yamada and Y. Osajima, Anal. Chem., 53 (1981) 1984.
12 C. Bertrand, P. R. Coulet and D. C. Gautheron, Anal. Lett., 12 (1979) 1477.
13 I. Satoh, I. Karube and S. Suzuki, Biotechnol. Bioeng., 19 (1977) 1095.
14 H. S. Huang, J. C. W. Kuan and G. G. Guilbault, Clin. Chem., 23 (1977) 671.
15 M. Mascini and G. G. Guilbault, Anal. Chem., 49 (1977) 795.
16 M. Cordonnier, F. Lawny, D. Chapot and D. Thomas, FEBS Lett., 59 (1975) 263.
17 I. Satoh, I. Karube and S. Suzuki, Biotechnol. Bioeng., 18 (1976) 269.
18 A. S. Barker and P. J. Somers, in A. Wiseman (Ed.), Topics in Enzyme and Fermentation Biotechnology, Vol. 2, Ellis Horwood, Chichester, 1978, p. 20.
19 P. R. Coulet and C. Bertrand, Anal. Lett., 12 (1979) 581.

Analytica Chimica Acta, 146 (1983) 149—159
Elsevier Scientific Publishing Company, Amsterdam — Printed in The Netherlands

ACETYLCHOLINE AND CHOLINE ION-SELECTIVE MICRO-ELECTRODES

ALONSO JARAMILLO, SUSANA LOPEZ and JOSEPH B. JUSTICE, Jr.*
Department of Chemistry, Emory University, Atlanta, GA 30322 (U.S.A.)
JOHN D. SALAMONE and DARRYL B. NEILL
Department of Psychology, Emory University, Atlanta, GA 30322 (U.S.A.)
(Received 2nd July 1982)

SUMMARY

The construction and performance characteristics of ion-selective micro-electrodes for acetylcholine and choline based on their complexes with dipicrylamine are described. The micro-electrodes show near-Nernstian response over ranges of about 5×10^{-5}—10^{-2} M. The selectivity of these micro-electrodes relative to a number of amino acids, inorganic ions, neurotransmitters, and drugs is reported. Naturally occurring components of neural tissue did not interfere strongly, while many cholinergic drugs (arecholine, carbachol, atropine, scopolamine, and others) interfered. The effect of different nitroaromatic solvents on selectivity is described. Measurements in vivo are possible.

Ion-selective electrodes (i.s.e.) are finding considerable use for determination of physiologically important ionic species [1—3] and have become a useful tool for solving many analytical and bioanalytical problems [4—6]. Non-destructive methods and micro-electrode designs required for in vivo determinations have been reported [7, 8]. Of particular interest to our research group are methods for in vivo measurement of neurotransmitters [9, 10]. The voltammetric measurement of easily oxidizable components of the extracellular fluid of the brain is an area of active interest [11—13]. However, some neurotransmitters, such as γ-aminobutyric acid and acetylcholine are not easily oxidizable. While it would be very difficult to develop an adequately selective electrode for γ-aminobutyric acid, acetylcholine ion-selective electrodes have been known since the work of Baum in 1970 [14]. Baum and coworkers also reported on the characterization of a liquid-membrane ion-selective electrode for determination of the activities of acetylcholinesterase [15] and cholinesterase [16], and for the determination of the cholinesterase activity of blood-derived fractions [17]. Baum et al. [18] also developed a plasticized poly(vinyl chloride) (PVC) acetylcholine membrane electrode for the determination of acetylcholinesterase. Hopirtean and Miklos [19] studied a liquid-membrane electrode selective for acetylcholine, obtained from acetylcholine dipicrylaminate in nitrobenzene. Kina et al. [20] reported a liquid-membrane electrode selective to methacholine,

an ester of choline that was used in a potentiometric titration of methacholine chloride with sodium tetraphenylborate solution as the titrant.

Ion-selective electrodes offer the opportunity for continuous and direct monitoring of a variety of biological signals of cells and tissues. In vivo research with ion-selective micro-electrodes is typified by Thomas [7], who measured intracellular inorganic ions such as H^+, Na^+, and K^+. The medical and biological applications of ion-selective electrodes have recently been described [21].

This paper is concerned with the construction and characterization of two liquid-membrane micro-electrodes selective for acetylcholine and its metabolite, choline. Several characteristics, including stability, selectivity, and sensitivity, of both micro-electrodes are described. An in vivo application of the acetylcholine ion-selective micro-electrode in rat striatum is also presented.

EXPERIMENTAL

Chemicals and solutions

Reagent-grade chemicals were used as received. Acetylcholine chloride, choline chloride, butyrylcholine chloride, dopamine hydrochloride, L-tyrosine, tryptophan, γ-aminobutyric acid, alanine, carbamylcholine chloride, eserine and amphetamine sulphate were purchased from Sigma (St. Louis, MO). Nitrobenzene, *o*-nitroanisole, 3-nitro-*o*-xylene, 3-nitrotoluene, 2-nitrotoluene, and dipicrylamine were purchased from Aldrich (Milwaukee, WI). Sodium chloride, potassium chloride, and ammonium chloride were laboratory grade. Sodium chloride solutions (0.10 and 0.20 M) were prepared in distilled water. Solutions of acetylcholine chloride were prepared in the range 10^{-1}—10^{-6} M by serial dilution. The micro-electrodes were calibrated and the potentiometric selectivity coefficients were determined at constant ionic strength in 0.20 M NaCl or 0.10 M NaCl.

Electrochemical measurements

The membrane potential measurements were made at 25°C with a Corning Digital 110 pH meter with expanded scale connected to a McKee Pedersen MP-1027 recorder. All measurements were done in unstirred solutions. A standard calomel electrode (SCE) was used for the in vitro measurements and an Ag/AgCl micro-electrode was used for the in vivo experiment.

The electrochemical cell was Ag/AgCl|internal solution|liquid membrane|sample solution|SCE, in which the half cell, Ag/AgCl|internal solution|membrane, is the membrane electrode.

Membrane preparation. Acetylcholine dipicrylaminate was prepared by mixing equal volumes of an aqueous 0.01 M solution of acetylcholine chloride and a 0.01 M solution of dipicrylamine in acetone. The mixture was cooled in an ice-water bath and the precipitate was vacuum-filtered and dried at about 70°C for 5 min. The melting point of the complex was 127—128°C. The liquid ion-exchanger was prepared by making a solution of

the acetylcholine dipicrylaminate in each of the various solvents. Acetylcholine tetraphenylborate (ACh—TPB) and choline dipicrylaminate complexes were prepared in similar fashion. The melting points of these complexes were 184—185°C and 204—205°C, respectively.

Ion-selective micro-electrodes. Glass micropipettes were drawn with a mechanical capillary puller (Narashige PE-2) to a fine tip less than 50 μm in external diameter. The tip was dipped about 2 mm into a solution 19% (v/v) of dichlorodimethylsilane in toluene for 10 min, then washed with toluene and acetone, and stored in a desiccator with the tip upward. To fill the tip of the micro-electrode with the liquid ion-exchanger, the tip was immersed in the exchanger solution for a few seconds until the solution reached a height of 1—2 mm. By use of a long needle syringe, 3.0 M KCl was injected into the top of the micropipette shank. Micro-electrodes which had trapped air in the recess were discarded. An Ag/AgCl wire was placed in contact with the internal filling solution and a paraffin plug and/or cement was placed at the top of the micropipette to hold the Ag/AgCl wire and prevent evaporation of the aqueous solution. The internal filling solution was not presaturated with the exchanger.

Composition of the exchanger. A series of acetylcholine dipicrylaminate solutions was made up in a given solvent. The micro-electrode responses were evaluated for slope, detection limit, and stability as a function of the exchanger composition of the liquid membrane.

Selectivity coefficients. Potentiometric selectivity coefficients were determined mainly by the mixed solution method. In the cases of slightly soluble interfering substances, the separate solution method was employed. To determine the potentiometric selectivity coefficient of acetylcholine relative to choline, both the mixed and separate solutions methods were used.

Solvent studies. Once the acetylcholine ion-selective micro-electrode had been evaluated with nitrobenzene as diluent, other solvents were used in an effort to enhance the membrane properties. The following were tested: 3-nitrotoluene, 2-nitrotoluene, *o*-nitroanisole, 3-nitro-*o*-xylene, chlorobenzene, *m*-dimethoxybenzene, *m*-methylanisole, 2-nitro-*p*-cymene, toluene, and isooctane. The micro-electrodes were assessed by taking into account the values of the slope, the detection limit, the stability, the selectivity coefficients in the solvents studied, and toxicity of solvents.

In vivo recording. For in vivo recording, an adult male albino rat (Sprague Dawley) was placed under sodium pentobarbital anesthesia. The animal was given an initial dose of 50 mg kg^{-1} and then maintained under anesthesia with additional smaller doses throughout the recording session.

The acetylcholine ion-selective micro-electrode was stereotaxically placed into the anterior neostriatum [22] (AP 8.6, H 1.5, L 2.17). The reference electrode (Ag/AgCl) was placed in right parietal cortex. When a stable potential baseline was reached, a double injector for the infusion of acetylcholine and choline was lowered into the brain. The injector was made from two pieces of 30 ga stainless steel tubing connected by polyethylene tubing to

two 10-μl Hamilton syringes. The injector was lowered at an angle to within 0.5 mm of the micro-electrode tip. The injection was controlled by a Sage Instrument syringe pump while the potential from the acetylcholine electrode was recorded. After a stable baseline had been established, 1 μl of 10^{-1} M acetylcholine was injected. Fifty minutes later, 1 μl of 10^{-1} M choline was injected and recording was continued for another hour. A second choline injection (0.5 μl) was then made; and 0.5 μl of 10^{-1} M ACh was again injected.

RESULTS AND DISCUSSION

Calibration data

Calibrations were done at constant ionic strength (0.20 M). Figure 1 illustrates typical calibration curves. It is seen that the acetylcholine-selective micro-electrode can be used in the concentration range 10^{-1}—10^{-5} M where a linear relationship holds between the membrane potential and the acetylcholine concentration. For all solvents with nitro groups (Table 1), slopes approach the expected value of 0.059.

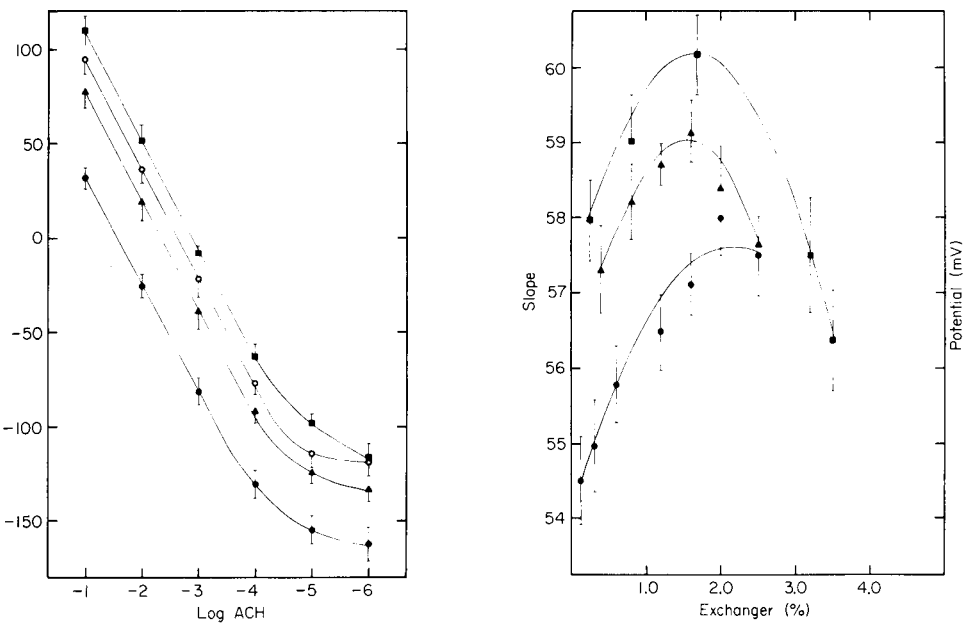

Fig. 1. Typical calibration curves of acetylcholine (ACh) ion-selective micro-electrodes with four different solvents: (■) nitrobenzene; (▲) *o*-nitroanisole; (●) 2-nitrotoluene; (○) 3-nitro-*o*-xylene.

Fig. 2. Effect of liquid ion-exchanger concentration on the slope of electrode response (mV/decade change in concentration) with three different solvents: (■) nitrobenzene; (▲) *o*-nitroanisole; (●) 2-nitrotoluene.

TABLE 1

Effect of solvent on slope and detection limit of acetylcholine dipicrylaminate electrodes

Solvent	n	Slope ± s.d. (mV/p ACh)	Detection limit (10^{-5} M)	Solvent	n	Slope ± s.d. (mV/p ACh)	Detection limit (10^{-5} M)
Nitrobenzene	22	59.4 ± 2.0	2	m-Dimethoxybenzene	5	50.2[c]	6
3-Nitro-o-xylene	6	58.4 ± 1.1	2	Toluene	5	50.6[c]	2
2-Nitrotoluene	6	57.7 ± 0.5	3	o-Nitroanisole[a]	5	51.0 ± 1.6	3
3-Nitrotoluene	5	57.8 ± 0.6	2	2-Nitro-p-cymene[a]	5	55.6 ± 1.6	5
o-Nitroanisole	15	58.8 ± 1.0	2	o-Nitroanisole[b]	11	58.5 ± 0.7	2
2-Nitro-p-cymene	5	54.4 ± 1.4	3				

[a]The complex used was acetylcholine tetraphenylborate. The dipicrylaminate gives better performance (selectivity, detection limit) to the liquid membrane in most of tne solvents studied. [b]The sample solution was dissolved in phosphate buffer saline solution at pH 7.4. [c]Data from Sullivan [23].

The response of the acetylcholine liquid-membrane sensor was evaluated for different concentrations of ion-exchanger and a series of solvents. In some of these systems, the micro-electrodes exhibited the desirable properties of rapid response, stability and near-Nernstian response. Figure 2 shows the effect of the ion-exchanger concentration on electrode slope for nitrobenzene, 3-nitro-o-xylene, and o-nitroanisole as the liquid organic phase. In each case, the slope reached a maximum at a concentration, usually about 2%, that depended on the solvent. Hence, a low concentration of the liquid ion-exchanger is desirable, but with a decrease in the exchanger concentration, the membrane resistance increases, and the transmembrane potential tends to be unstable. Subsequent studies involved exchanger concentrations in the range 0.5—2.0% (w/w).

The results obtained with the group of solvents used are shown in Table 1. The acetylcholine dipicrylaminate was insoluble in chlorobenzene, m-methylanisole, benzene, and isooctane, all having low dielectric constants. The other solvents have relatively high dielectric constants: 2-nitrotoluene (27.4), 3-nitrotoluene (23.0), 3-nitro-o-xylene ($\approx$22), o-nitroanisole (24.0), 2-nitro-p-cymene (20), and nitrobenzene (34.8) and the acetylcholine dipicrylaminate complex dissolved more readily in these solvents. It is also likely that the complex is more dissociated in these solvents. o-Nitroanisole and 2-nitro-p-cymene, both aprotic solvents, are less toxic than the other nitroaromatic solvents. 2-Nitro-p-cymene has been used for ion-selective liquid membranes [24]. In the present study, the slope was less than Nernstian (54.4) with this solvent. For in vivo measurements, o-nitroanisole is preferred to the other solvents because of its lower toxicity and faster equilibration of the liquid membrane constituents. About thirty minutes are required after these electrodes are made for the components of the electrode to reach equilibrium and before stable readings can be obtained. In addition, o-nitroanisole is expected to be a better solvent for cations because of the presence of the methoxy group.

The main parameters that govern the detection limit of an ion-selective liquid-membrane electrode are the solubility product of the complex or ion-pair in the aqueous phase and the distribution coefficient of the primary ion between the organic phase and the aqueous sample solution [6], both factors being temperature- and solvent-dependent. Deviations from the Nernst equation may arise because of time-dependent deviations between the measured activity a_i' and the intrinsic sample activity a_i. Such activity gradients are related to diffusion processes within the boundary layer of the sample solution and also contribute to the lower limit on the linear response [25]. In this study, all six solvents exhibited detection limits of about 10^{-5} M.

In general, the response time of the acetylcholine micro-electrode was 2—3 min even at low concentrations. The response time is influenced mainly by the solvent, the hydrophobicity of the micro-electrode tip, and the presence of interfering ions. The smaller the exchange current density, the longer the time required for the electrode to attain a new equilibrium. Poor exchanger conductivity results in long response times [2]. In order to study the stability of the membrane potential developed by these micro-electrodes, several experiments were conducted in which the potential response was recorded daily for the first six days then every other day for sixty days. The solvent used was 3-nitro-*o*-xylene. The electrode slope (56.4 ± 0.2) and detection limit (3.6×10^{-5}) remained constant over the sixty-day period.

Determination of selectivity coefficients

The selectivity of a dissociated liquid ion-exchange membrane depends primarily on the selectivity of the ion-exchange process at the membrane-sample solution interface, the mobilities of the ions, and hydrophobic interactions between the primary ion and the organic membrane [26]. The selectivity of the acetylcholine liquid-membrane electrode is related to the free energy of transfer of the acetylcholine ion between the aqueous and organic media [27]. Although some of the above parameters have been measured to test i.s.e. theory, simplified experimental methods are available to determine selectivity coefficients, which are in reasonable agreement with the theory. The potentiometric selectivity coefficients (k_{ij}^{pot}) of the acetylcholine and choline micro-electrodes were determined with the two methods recommended by IUPAC [28]. Although several workers [29, 30] have used the separate solution method, the mixed solution is better because the experimental conditions more closely approach the actual measurements conditions of real samples. In this work, the k_j^{pot} was calculated from the modified Nernst equation [2, 6, 28]

$$E = E^\circ + RTF^{-1} \ln (a_{ACh} + k_{AChj}^{pot} a_j) \quad (1)$$

and determined experimentally by the mixed solution method unless otherwise noted.

The polar nitroaromatic compounds used as solvents all have relatively

large dielectric constants and so have approximately the same effect on the selectivity of the micro-electrodes. For instance, Table 2 shows that the selectivity values of acetylcholine over choline at 2.5 mM are close, ranging from 0.036 to 0.050 which indicates almost the same effect on the selectivity-determining processes.

The data in Table 2 show a high selectivity of the acetylcholine i.s.e. over a series of potentially interfering ionic species. The compounds tested were chosen because they are either endogenous to the brain or are drugs often used in pharmacological studies. Acetylcholine, γ-aminobutyric acid and dopamine are neurotransmitters, while butyrylcholine is a choline ester. Amphetamine and carbachol are psychoactive drugs. The first one is an adrenergic drug associated with dopamine release, and the latter is a

TABLE 2

Potentiometric selectivity coefficients of acetylcholine electrodes prepared from different solvents and membrane compositions

Interfering species	Concentration (10^{-2} M)	Solvent	Selectivity coefficient ($\times 10^{-2}$)	Standard deviation ($\times 10^{-2}$)
Choline	5.0	Nitrobenzene	3.6	0.6
	0.5	Nitrobenzene	5.0	0.6
	5.0	3-Nitrotoluene	2.8	0.3
	0.5	3-Nitrotoluene	4.0	0.8
	0.5	2-Nitrotoluene	3.9	0.5
	5.0	*o*-Nitroanisole	3.4	0.3
	0.5	*o*-Nitroanisole	5.0	0.7
	0.5	2-Nitro-*p*-cymene	4.4	0.6
	0.5	3-Nitro-*o*-xylene	3.2[a]	0.2
	0.5	3-Nitro-*o*-xylene	3.6[b]	0.2
	0.5	3-Nitro-*o*-xylene	3.8[c]	0.5
	0.5	3-Nitro-*o*-xylene	3.6[d]	0.6
Butyrylcholine	5.0	Nitrobenzene	9.5	0.7
Dopamine	0.5	Nitrobenzene	0.62	0.01
	0.5	2-Nitrotoluene	0.62	0.07
	0.5	3-Nitrotoluene	0.66	0.1
Tyrosine[e]	0.1	Nitrobenzene	0.25	0.07
	0.1	2-Nitrotoluene	0.36	0.06
	0.1	3-Nitrotoluene	0.40	0.07
	0.1	*o*-Nitroanisole	0.27	0.02
γ-Aminobutyric acid[e]	1.0	2-Nitrotoluene	0.15	0.02
Carbachol	0.29	Nitrobenzene	3.7	0.2
	1.0	3-Nitro-*o*-xylene	2.7	0.5
d-Amphetamine	0.29	Nitrobenzene	8.6	0.2
K^+	10.0	Nitrobenzene	0.22	0.1
NH_4^+	10.0	Nitrobenzene	0.04	0.01

[a–d]Liquid ion exchanger in 3-nitro-*o*-xylene (%): (a) 0.3, (b) 0.6, (c) 1.6, (d) 2.5. [e]Separate solutions method.

cholinomimetic drug. The order of selectivity with nitrobenzene as the solvent is $NH_4^+ > K^+ >$ tyrosine > dopamine > carbachol > choline > amphetamine > butyrylcholine. For the study of choline interference, the results show that 3-nitro-*o*-xylene, the only solvent with two methyl groups, is the best solvent. Nitrobenzene, with the largest dielectric constant, is the worst solvent. This may indicate that a nitroaromatic solvent with a long alkyl chain would improve selectivity further. Koryta [4] has noted that in the case of a lipophilic anion as membrane component, the potentiometric selectivity coefficient is concentration-dependent, as is shown in Table 2. According to Tables 1 and 2, there is no direct relationship between the slope and potentiometric selectivity coefficient. The best liquid ion exchanger concentration for slope and detection limit does not necessarily give the better selectivity.

Table 3 presents the potentiometric selectivity coefficients of a choline ion-selective micro-electrode prepared from choline dipicrylaminate in nitrobenzene. An average slope of 58.0 mV per decade change in concentration and a concentration limit of 6.0×10^{-5} M were obtained from a series of different ion-exchanger concentrations (0.5%, 1.0%, 1.7%, 2.3%) in nitrobenzene. A 0.5% (w/w) concentration of the ion-exchanger gave a Nernstian response of 59.2 mV per decade change in concentration and a detection limit of 5.8×10^{-5} M. From the data in Table 3, the order of selectivity is tyrosine > tryptophan > γ-aminobutyric acid > alanine > NH_4^+ > dopamine > amphetamine > butyrylcholine > carbachol > acetylcholine. The first four compounds in the series indicate that amino acids do not interfere very much. However, the choline electrode does not discriminate very well among amphetamine, butyrylcholine, carbachol, and acetylcholine.

Table 4 shows the selectivity data obtained with a choline micro-electrode prepared from the same ion-exchanger in *o*-nitroanisole. The selectivity of the electrode relative to the drugs listed was determined because these drugs are used pharmacologically to affect the cholinergic system. Arecholine

TABLE 3

Potentiometric selectivity coefficients of a choline ion-selective micro-electrode prepared from choline dipicrylaminate in nitrobenzene

Interferent	Concentration(M)	Selectivity coefficient ± s.d.
Acetylcholine	3.3×10^{-3}	0.20 ± 0.11[a]
Butyrylcholine	5×10^{-3}	0.50 ± 0.2
Alanine	2.5×10^{-2}	$2.0 (\pm 0.4) \times 10^{-3}$
Amphetamine	1.0×10^{-3}	0.56 ± 0.12
Dopamine	8.2×10^{-3}	$6.0 (\pm 1.2) \times 10^{-2}$
Carbachol	5×10^{-3}	0.28 ± 0.10
γ-Aminobutyric acid	0.10	$3.7 (\pm 1.5) \times 10^{-4}$
Tyrosine	1×10^{-3}	$2.4 (\pm 0.7) \times 10^{-4}$
Tryptophan	1×10^{-3}	$3.2 (\pm 1.2) \times 10^{-4}$
NH_4^+	0.10	$4.2 (\pm 1.2) \times 10^{-3}$

TABLE 4

Potentiometric selectivity coefficients of a choline micro-electrode prepared from choline dipicrylaminate (1.0%) in *o*-nitroanisole

Interferent[a]	Selectivity coefficient ± s.d.	Interferent[a]	Selectivity coefficient ± s.d.
Pilocarpine	0.08 ± 0.05[b]	Atropine	0.45 ± 0.19
Mecamylamine	0.15 ± 0.08	Carbachol	0.48 ± 0.12
Apomorphine	0.36 ± 0.03	Arecholine	0.78 ± 0.13
Scopolamine	0.37 ± 0.02		

[a] 2.5×10^{-3} M.

interferes considerably with the performance of the electrode while pilocarpine has less effect. If all the selectivity data from Tables 3 and 4 are compared, it is apparent that tertiary and quaternary amines show the highest interference while primary amines interfere much less.

In vivo results and discussion

The results in Fig. 3 represent the response of the acetylcholine micro-electrode to injections of acetylcholine and choline near the electrode tip in the striatum of an anesthetized rat. An injection (1 μl) of 10^{-1} M acetylcholine caused an 88 mV change which took approximately 2 min to reach a maximum, after which the signal declined over a 30-min period. The decline in the signal evidently represents a combination of loss processes, including diffusion and metabolism. A subsequent injection of choline declined more slowly, indicating a slower rate of removal from the area of the electrode tip. The sharper decline following the first acetylcholine injection may be due to

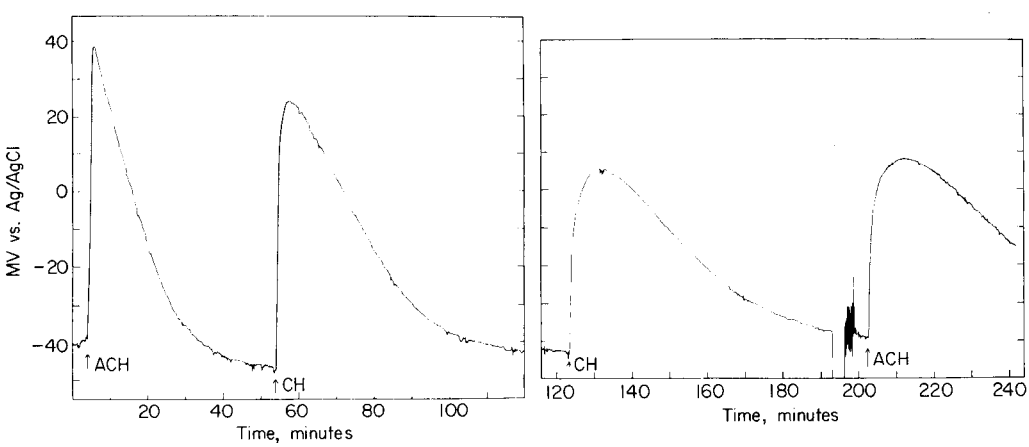

Fig. 3. Response of acetylcholine micro-electrode in anterior striatum to local injections of acetylcholine (ACH) and choline (CH) in an anesthetized rat.

metabolism of acetylcholine, but a later injection of acetylcholine also showed the slower behavior. The electrode continued to be responsive over a 4-h period as later injections of half as much choline and acetylcholine also caused a significant change in signal, although the response was broader and took longer to reach a maximum. These results indicate that in vivo recording with an acetylcholine micro-electrode is feasible.

The performance of the acetylcholine micro-electrode is comparable to those of the larger electrodes of Baum and Hopirtean and Miklos. The values of the selectivity coefficients of acetylcholine over NH_4^+, K^+, and choline according to Baum [14], determined by the separate solutions method, are respectively 1×10^{-3}, 1×10^{-3}, and 0.066. Hopirtean and Miklos [19] used acetylcholine dipicrylaminate in nitrobenzene and found the values of the selectivity coefficients for acetylcholine over the same interferents to be 5×10^{-4}, 10^{-3}, and 0.20. The acetylcholine micro-electrode described in the present paper, with nitrobenzene as solvent, has selectivities of 4.0×10^{-4}, 2.2×10^{-3}, and 0.05 for the same ions. The choline electrode may have more applicability than the acetylcholine electrode for in vivo measurements because acetylcholine is removed rapidly from the extracellular fluid, being hydrolyzed to choline and acetic acid. The choline electrode may enable an increase in extracellular choline to be observed following local release of acetylcholine from terminals of cholinergic neurons even though the choline itself is taken up to some extent for further synthesis of acetylcholine.

REFERENCES

1 G. G. Guibault, Pure Appl. Chem., 25 (1971) 727.
2 K. Cammann, Working with Ion-Selective Electrodes, Springer-Verlag, Berlin, (1979).
3 M. Kessler, L. C. Clark, D. Lubbers, I. Silver and W. Simon, Ion and Enzyme Electrodes in Biology and Medicine, University Park Press, Baltimore, (1976).
4 J. Koryta, Anal. Chim. Acta, 91 (1977) 1.
5 W. Armstrong and J. F. Carcia-Diaz, Fed. Proc., 39 (1980) 2851.
6 P. L. Bailey, Analysis with Ion-Selective Electrodes, 2nd Edn., Heyden, London, (1980).
7 R. C. Thomas, Ion-Selective Intracellular Microelectrodes, Academic Press, London, (1978).
8 J. L. Walker, Anal. Chem., 43 (1971) 89A.
9 W. S. Lindsay, J. G. Herndon, R. D. Blakely, J. B. Justice and D. B. Neill, Brain Res., 220 (1981) 391.
10 W. S. Lindsay, B. L. Kizzort, J. B. Justice, J. D. Salamone and D. B. Neill, Chem. Biomed. Environ. Instrum., 10 (1980) 311.
11 R. N. Adams, Anal. Chem., 48 (1976) 1128.
12 R. M. Wightman, Anal. Chem., 53 (1981) 1125.
13 R. F. Lane, A. T. Hubbard and C. D. Blaha, J. Electroanal. Chem., 95 (1979) 117.
14 G. Baum, Anal. Lett., 3 (1970) 105.
15 G. Baum, Anal. Biochem., 39 (1971) 65.
16 G. Baum and F. Ward, Anal. Biochem., 42 (1971) 487.
17 G. Baum, F. Ward and S. Yavarbaum, Clin. Chim. Acta, 36 (1972) 405.
18 G. Baum, M. Lynn and F. Ward, Anal. Chim. Acta, 65 (1973) 385.
19 E. Hopirtean and M. Miklos, Rev. Chim., 29 (1978) 1178.

20 K. Kina, N. Maekawa and N. Ishibashi, Bull. Chem. Soc. Jpn., 42 (1973) 2772.
21 J. Koryta, Medical and Biological Applications of Electrochemical Devices, Wiley, New York, (1980).
22 L. J. Pellegrino and A. J. Cushman, A Stereotaxic Atlas of the Rat Brain, Appleton-Century Crofts, New York, 1967.
23 T. Sullivan, Master's Thesis, Emory University, (1981).
24 T. L. Hwang and H. S. Cheng, Anal. Chim. Acta, 106 (1979) 341.
25 W. E. Morf, E. Lindner and W. Simon, Anal. Chem., 47 (1975) 1596.
26 J. Sandblom, G. Eisenman and J. Walker, J. Phys. Chem., 71 (1967) 3682.
27 J. Koryta, Ions, Electrodes, and Membranes, Wiley, New York, 1982.
28 G. Guibault, Ion-Selective Electrodes Rev., 1 (1979) 139.
29 F. Lanter, D. Erne, D. Ammann and W. Simon, Anal. Chem., 52 (1980) 2400.
30 H. Hara, S. Okasaki and T. Fujinaga, Bull. Chem. Soc., 53 (1980) 3010.
31 R. P. Buck, Anal. Chim. Acta, 73 (1974) 321.

Analytica Chimica Acta, 146 (1983) 161—169
Elsevier Scientific Publishing Company, Amsterdam — Printed in The Netherlands

PROBLEMS IN CURRENT PROCEDURES FOR ESTABLISHING RECOMMENDED VALUES OF TRACE-ELEMENT LEVELS IN BIOLOGICAL REFERENCE MATERIALS

J. J. M. DE GOEIJ*

Interuniversity Reactor Institute, Mekelweg 15, 2629 JB Delft (The Netherlands)

L. KOSTA and A. R. BYRNE

Faculty of Natural Sciences and Technology, E. Kardelj University and Jožef Stefan Institute, P.O. Box 199, 61000 Ljubljana (Yugoslavia)

J. KUČERA

Nuclear Research Institute, 25068 Řež near Prague (Czechoslovakia)

(Received 23rd April 1982)

SUMMARY

Approaches for establishing recommended values of trace-element levels in biological reference materials are discussed. Values of manganese, copper, chromium and cobalt in IAEA Milk Powder A-11 are used as an illustration. Performances of techniques currently applied in the analysis of biological materials for elements occurring at very low levels are evaluated. It is shown that statistical procedures alone are insufficient in some cases to arrive at recommended values without consideration of the analytical parameters involved.

In the analysis of biological materials for trace elements, analytical quality control is often pursued by means of reference materials, for which levels of particular trace elements are specified. Depending on the analytical and mathematical methods used, and the degree of confidence involved, this specification is presented under various names, such as overall mean, grand mean, information value, consenus value, probable value, recommended value or certified value. Although the International Organization for Standardization has defined a reference material (RM) and a certified reference material (CRM) [1], the criteria to be used in assigning values for certification have still to be set by the issuing organization.

For valid use of reference materials, they should match the samples to be analyzed with respect to levels (and ideally, in chemical properties such as valency and binding) of the trace elements of interest, as well as in matrix composition. Considering the wide variety of biological samples currently being analyzed for trace elements ranging from the microgram to the subnanogram per gram level, it is obvious that a large number of reference materials is necessary.

Standardization is not always based on analyses done in the issuing agency itself. It may depend on analytical data reported by various laboratories (one of the earliest examples of this approach is Bowen's Kale [2, 3]), sometimes collected via specially organized intercomparison studies, as in the case of IAEA materials. Obviously, the method of evaluation of the data reported for a particular reference material will have a decisive impact on the reliability of the estimates, and thus on the conclusions drawn by analysts with respect to the analytical quality of their work.

The usual philosophy in the evaluation of such data is the assumption of a model in which (i) most of the data belong to a normally distributed population, (ii) the arithmetic mean equals or comes close to the true value, and (iii) only a minor fraction of the data belongs to other populations. When this approach is applied, it is clear that the minority of outlying results should be detected and rejected before the final values and confidence limits can be calculated. For the detection and rejection of outlying results, various procedures are available [4].

In a recent study [5], the effects of various rejection methods were evaluated, using data from intercomparison studies with artificial samples obtained by spiking pure water for which the true (input) values were known. The author concluded that the results seem to indicate that a good estimate of the "true" value and a realistic evaluation of associated confidence limits can be achieved by fully objective methods, by applying specific computerized rejection methods. In addition, the author stated that some subjective, and thus necessarily arbitrary, assumptions and criteria are also needed at the stage of deciding whether or not the consensus values found can be given the status of recommended or certified values.

However, it should be realized that the first conclusion is not generally valid in trace-element intercomparisons, and is certainly not valid for many real samples with low trace element levels (nanogram per gram, and less). In such samples, sources of errors do not always result in normally distributed deviations around the true value, but may tend to systematic deviations in one direction. Therefore, it may happen that the true value will lie in the upper or lower part of the range of data reported, rather than somewhere in the middle. Consequently, the true value will hardly be recognized as such in a purely statistical approach. Hence, additional criteria should be set in the data evaluation, apart from the statistical treatment. This will be illustrated below with the help of Milk Powder A-11.

METHODS

Milk Powder A-11 was issued recently as a reference material by the International Atomic Energy Agency [6, 7] and is more or less typical of the current situation in low-level trace element determinations.

In the report on the Intercomparison [6], values are recommended with "satisfactory" or "acceptable" degrees of confidence for 14 trace elements,

while for 26 additional (trace) elements "information values only" are given. These values were obtained from intercomparison data involving 43 different laboratories which yielded single values or means of multiplicates (up to six). The analytical techniques used were: atomic absorption spectrometry (a.a.s.), electrochemical methods (e.c.), emission spectrometry (e.s.), mass spectrometry (m.s.), neutron activation analysis (n.a.a.) subdivided into radiochemical n.a.a. (r.n.a.a.) and instrumental n.a.a. (i.n.a.a.) and x-ray fluorescence or proton-induced x-ray emission (x.r.s.). The data were evaluated in the above Report [6] by pooling all data, irrespective of the analytical technique used. For detection and rejection of outliers, four different tests of discordance at the significance level $\alpha = 0.05$ were used concurrently. The tests were Dixon's test, Grubb's test, the coefficient of skewness test and the coefficient of kurtosis test [5—7].

The intercomparison data have now been re-examined for the trace elements manganese, copper, chromium and cobalt; the published data set was used. Most of the present authors participated in the original intercomparison, and additional experimental data on Milk Powder A-11 were obtained by using n.a.a. These were follow-up analyses intended to try to clear up discrepancies. For the re-examination, the intercomparison data were plotted according to increasing value, as well as to the type of analytical technique used, and statistical tests were applied to the data and subsets of data.

RESULTS AND DISCUSSION

Manganese

The thirty data for manganese are presented in Fig. 1. The intercomparison data evaluation led to rejection of nine values (above 0.733 $\mu g\ g^{-1}$), resulting in a 95% confidence interval of 0.296—0.457 $\mu g\ g^{-1}$, with an overall mean of 0.377 $\mu g\ g^{-1}$ [6]. This latter value is given as a "recommended value with a satisfactory degree of confidence". A substantial difference exists between the averages of the ten "accepted" values by a.a.s. (0.48 ± 0.06) and the nine n.a.a. results (0.30 ± 0.04). As may be seen from Fig. 1, for the a.a.s. data (N = 17) there is no plateau or even distinct inflexion point, such as should occur for a model with the majority of the data belonging to a normally distributed population. In contrast, the destructive n.a.a. data (N = 7) and instrumental n.a.a. data (N = 4) show a plateau. As well as the results rejected by statistical tests, two more seem to be outliers, viz. one at the low side and one at the high side. Only one value each was obtained by m.s. and e.s., so that an evaluation is not feasible. However, the results of both latter methods do not conflict with, but rather support, those obtained via n.a.a.

The rather large variation in the manganese levels observed is probably due to contamination, leading to a substantial positive systematic error. Apparently, for manganese in this intercomparison study, n.a.a., m.s. and e.s. are less susceptible to interferences than a.a.s. However, as two of the four instrumental n.a.a. values are outliers, instrumental n.a.a. also appears to be

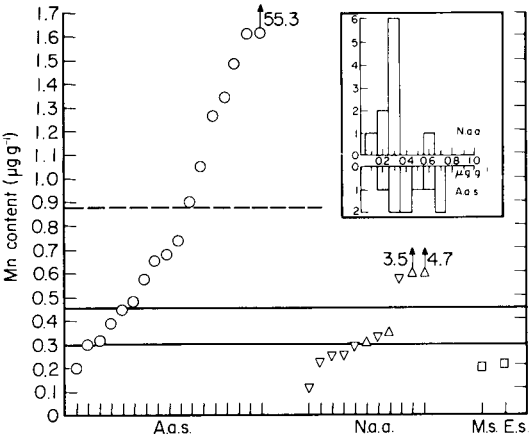

Fig. 1. Manganese levels reported for Milk Powder A-11 [6], according to the analytical method used and to increasing value. The full lines denote the 95% confidence limits [6, 7] for the recommended value of 0.377 $\mu g\ g^{-1}$, issued by the IAEA; the dashed line denotes the limit above which data were rejected. Instrumental n.a.a. is indicated by △ and destructive n.a.a. by ▽. The inset shows frequency histograms of unrejected results obtained by n.a.a. and a.a.s.

unreliable at very low manganese levels; this is probably not so much due to contamination, but rather to spectral interferences.

The likelihood of contamination as a source of positive bias was shown at an a.a.s. laboratory cooperating with two of the authors, where the a.a.s. determination was done under stringent conditions to prevent contamination, and a value of 0.32 $\mu g\ g^{-1}$ was found. A recent independent n.a.a. determination reported by Iyengar et al. [8] gave a result of 0.25 $\mu g\ g^{-1}$ based on measurements of six aliquots. In view of the differences in the a.a.s. and n.a.a. data, it seems inappropriate to pool them in deriving an overall mean. Rather, based on the original values of n.a.a. (minus four outliers), m.s. and e.s. ($N = 7 + 1 + 1$) and the new data, it appears that the concentration of manganese in Milk Powder A-11 is about 0.28 $\mu g\ g^{-1}$. Compared to this value, the recommended value is about 35% higher. It should also be noted that the 95% confidence interval of the recommended value (0.296—0.457 $\mu g\ g^{-1}$) does not cover the n.a.a. plateau, or even overlap with the inflexion point of the series of n.a.a. values.

Copper

The 37 copper data are presented in Fig. 2. The intercomparison data evaluation led to rejection of six values (above 1.87 $\mu g\ g^{-1}$, resulting in a 95% confidence interval of 0.673—1.003 $\mu g\ g^{-1}$, with an overall mean of 0.838 $\mu g\ g^{-1}$ [6]. This value is given as "recommended with an acceptable degree of confidence", although a significant difference exists between the a.a.s. (1.14 ± 0.10) and n.a.a. (0.55 ± 0.06) data. Considering Fig. 2, the a.a.s. data

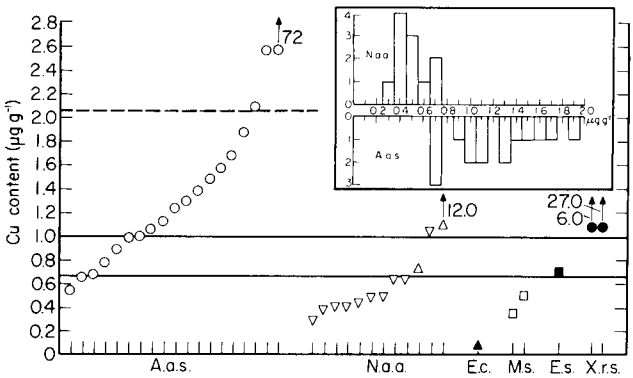

Fig. 2. Copper levels reported for Milk Powder A-11 [6], according to the analytical method used and to increasing value. The full lines denote the 95% confidence limits [6, 7] for the recommended value of 0.838 $\mu g\ g^{-1}$, issued by the IAEA; the dashed line denotes the limit above which data were rejected. Types of n.a.a. as in Fig. 1. The inset shows frequency histograms of unrejected results obtained by n.a.a. and a.a.s.

(N = 19) show wide scatter and no plateau. The data obtained by destructive n.a.a. (N = 10) and instrumental n.a.a. (N = 2) display a plateau; of the two outliers on the high side, the highest is the result of instrumental n.a.a. Four other techniques (m.s., e.c., e.s. and x.r.s. did not yield a sufficient number of values to permit an evaluation; of these both x.r.s. results were rejected as too high. However, the results of m.s. and e.s. support those by n.a.a.

For copper, as for manganese, in this intercomparison study, it seems that n.a.a. (predominantly radiochemical n.a.a.), m.s. and e.s. are less susceptible to interference than a.a.s. and x.r.s. Repeated n.a.a. determinations were done in two laboratories of the authors using different radiochemical separations [9, 10] and standards. In one laboratory, the same result (0.39 $\mu g\ g^{-1}$) was found as originally submitted, while in the other laboratory a value of 0.40 ± 0.02 $\mu g\ g^{-1}$ was obtained for a triplicate measurement. A recent independent n.a.a. determination reported by Iyengar et al. [8], gave a result of 0.374 ± 0.015 $\mu g\ g^{-1}$, based on measurement of six aliquots.

The difference of the two means, the scatter of the a.a.s. data and the fact that the compact n.a.a. group is supported by two other techniques, suggest that the true value is likely to be approximated by selective use of data. Thus, given the original values of n.a.a. (minus two outliers), m.s. and e.s. (N = 10 + 2 + 1) and the new data, the authors believe that the correct value for copper in Milk Powder A-11 is about 0.5 $\mu g\ g^{-1}$ or somewhat below. Compared to this estimate, the value recommended [6] is at least 70% higher. Here also, it should be noted that the 95% confidence interval of the latter (0.673—1.003 $\mu g\ g^{-1}$) does not cover the n.a.a. plateau, or even overlap with the inflexion point of the series of n.a.a. data.

Chromium

The 16 data for chromium are presented in Fig. 3. Concurrent use of statistical tests led to rejection of five values (above 1.3 $\mu g\ g^{-1}$) resulting in a 95%

confidence interval of 0.081—0.433 $\mu g\ g^{-1}$, and an overall mean of 0.257 $\mu g\ g^{-1}$, which is presented as an "information value only" [6].

As can be seen from Fig. 3, there is a very considerable scatter of data; for none of the analytical techniques used was a narrow cluster observed. Determination of chromium at low levels in biological materials is known to be problematic [11—13]. The n.a.a. data tend to be lower than the a.a.s. data or the data obtained by m.s., e.s. and x.r.s. This may be seen by comparing the median of the n.a.a. data (N = 6) with the corresponding value for the other techniques (N = 10); with or without the rejection of outliers, the latter is an order of magnitude higher. In such a situation it would seem sensible either not to give any suggested figure at all, or to subject the data to further selection.

On the basis of analytical factors and typical chromium levels in biological materials, it is likely that the lowest cluster of results (15—60 ng g^{-1}) better approximates the true value. In any event, it seems urgent to initiate some follow-up work on chromium in Milk Powder A-11, possibly by inviting laboratories known to be experienced in chromium determinations in the medical field.

Cobalt

In Milk Powder A-11, cobalt is certified with a "satisfactory degree of confidence". Of the twenty submitted results (18, plus 2 later values), with a dispersion of over four orders of magnitude, concurrent use of statistical tests (Dixon's, Grubbs', skewness and kurtosis) eliminated over half [6]. It is clear that in such a situation the application of statistical tests to derive a recommended value is of doubtful validity. In re-running these tests in the present work, it was also noticed that their rejection performance is very sensitive to the spacing of the data, which has a decisive effect on the position of the cut-off. In addition, Dixon's test is ineffective, while Chauvenet's criterion, which was not used in the Report [6], gave the same cut-off as the skewness and kurtosis tests.

Splitting the data according to techniques and modes (Table 1) revealed that all results for Milk Powder A-11 by atomic absorption spectrometry are on the extreme side of the outliers; this indicates that the cobalt level in A-11 is below the practical working range of a.a.s. High results by i.n.a.a. probably cannot be attributed to contamination, but more likely to counting errors and/or incorrect assignment of peaks. The likely correct value is indicated by the great consistency of results around 5 ng g^{-1}.

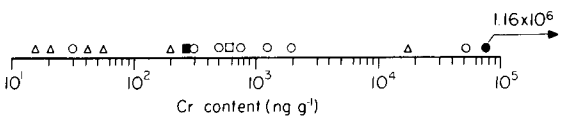

Fig. 3. Results for chromium according to increasing order of submitted averages: (△) n.a.a. involving radiochemical separations; (□) mass spectrometry; (●) x-ray fluorescence spectrometry; (○) a.a.s.; (■) emission spectrometry.

TABLE 1

Results for cobalt (ng g^{-1}) in A-11 by different techniques

i.n.a.a.	r.n.a.a.	a.a.s.	m.s.
5	4[a]	760	70[b]
5	4	1726	200[c]
6	5[d]	2000	
18	5	51500	
163	5		
536	9		
2900	15		

[a]This work. [b]Ionization m.s. [c]Chemical ionization m.s. [d]Iyengar et al. [8].

CONCLUSIONS AND SUGGESTIONS

There are no grounds for assuming that the laboratories involved in the intercomparison study of Milk Powder A-11 are less skilled than the average trace element laboratory, nor that the analysis of A-11 was conducted less accurately than normally in these laboratories. The results for Milk Powder A-11 may be considered more or less indicative of the accuracy involved in current determinations of low levels of trace elements in milk powder and related products.

From the above evidence and follow-up work by the authors and elsewhere, we believe that the recommended values for copper and manganese in the material discussed will have to be revised. This seems important because it is the only reference material of its kind and is being widely used in the current WHO/IAEA Project on Trace Elements in Human Milk, and in other studies.

Considering the techniques used, results show that n.a.a. tends to be less susceptible to laboratory-dependent systematic error than other techniques for trace element determinations, as was recently also shown by Dybczinski [14]. This is more marked when concentrations are very low as in A-11, because n.a.a. usually requires no sample treatment steps prior to irradiation, thus strongly reducing the risk of contamination as a major source of systematic error. Differences in the performance and applicability of analytical techniques are clearly shown for all four elements discussed; in the case of cobalt only n.a.a. gives reasonable values, while for copper a.a.s. is evidently positively biased. In such a case, pooling of all values may easily give rise to a result which deviates appreciably from the true value.

As shown, trace element data sets will not always meet the criteria valid for the application of a purely statistical approach (i.e., normal distribution with a minority of outliers, random rather than systematic error as the major source of scatter). While statistical tests can be applied in a fully objective manner, the criteria required (such as the maximum percentage of outliers,

the minimum number of acceptable laboratory averages, the degree of concurrence of the various analytical methods, the relative uncertainty of the overall mean, etc.) for deciding the status of the recommended value as being of a satisfactory or acceptable degree of confidence or merely an information value, are subjective. In the case of copper, some of these criteria were not met. Thus while statistical methods have a most important role to play, they need to be supported by analytical considerations such as chemical nature of the sample, likely interferences, selectivity or applicability of methods, the degree of risk of contamination, the inclusion of evidence from the upper limit values, etc. Some of these points have been discussed in relation to cadmium in A-11 elsewhere [15].

Whatever the terminology used to describe the final certified values, it is obvious that only those with narrow confidence intervals are really useful as CRM's. An "information value", if given, is valuable only if it is based on a set of consistent data which, however, cannot be given the status of a certified value because of some other failure to fulfil all the criteria required for standardization (e.g., lack of supporting data from an independent method).

Where no clear recommendation can be made from the data evaluation, it is particularly important to initiate follow-up work, probably by selected laboratories with experience of the particular element. At this stage, the use of a quality control sample sent out by the organizer in the form of a small amount of an unidentified CRM would be helpful in clarifying the issue. Recently, the intention of organizing follow-up work on the systematic differences between n.a.a. and a.a.s. for copper and manganese in Milk Powder A-11 has been announced by the IAEA [16]. Considering the importance of this particular reference material and of the trace elements discussed, it is hoped that analysts experienced in techniques applicable to these elements at the levels involved will find the uncertainty about the concentrations challenging, and will contribute additional data to permit the assignment of accurate values for Milk Powder A-11.

REFERENCES

1 International Organization for Standardization, ISO-Guide 6-1978 (E).
2 H. J. M. Bowen, At. Energy Rev., 13 (1975) 451.
3 IUPAC Commission on Analytical Radiochemical and Nuclear Materials, Pure Appl. Chem., 51 (1979) 1183.
4 V. Barnett and T. Lewis, Outliers in Statistical Data, Wiley, New York, 1979.
5 R. Dybczinski, Anal. Chim. Acta, 117 (1980) 53.
6 R. Dybczinski, A. Veglia and O. Suschny, Report on the Intercomparison Run A-11 for the Determination of Inorganic Constituents of Milk Powder, IAEA/RL/68, International Atomic Energy Agency, Vienna, Austria, 20 July 1980.
7 Information Sheet, Reference Material A-11, International Atomic Energy Agency, Vienna, Austria, 20 July 1980.
8 G. V. Iyengar, K. Kasparek, L. E. Feinendegen, Y. X. Wang and H. Weese, Sci. Total Environ., 24 (1982) 267.
9 A. R. Byrne, Radiochem. Radioanal. Lett., 40 (1979) 1.

10 J. Kučera, Radiochem. Radioanal. Lett., 24 (1976) 215.
11 J. Versieck and R. Cornelis, Anal. Chim. Acta, 116 (1980) 217.
12 R. M. Parr, in P. Brätter and P. Schramel (Eds.), Trace Element Analytical Chemistry in Medicine and Biology, De Gruyter, Berlin/New York, 1980, p. 631.
13 P. S. Tjioe, J. J. M. de Goeij and J. K. Volkers, A Routine Chromium Determination in Biological Materials; Application to Various Reference Materials and Standard Reference Materials, Report IRI-133-79-02, Interuniversity Reactor Institute, Delft, The Netherlands, 1979.
14 R. Dybczinski, J. Radioanal. Chem., 60 (1980) 45.
15 L. Kosta and A. R. Byrne, J. Radioanal. Chem., 69 (1982) 117.
16 O. Suschny, R. Dybczinski and A. Veglia, J. Radioanal. Chem., 69 (1982) 147.

Analytica Chimica Acta, 146 (1983) 171—179
Elsevier Scientific Publishing Company, Amsterdam — Printed in The Netherlands

THE DETERMINATION OF LEAD AND CADMIUM IN SOILS BY ATOM-TRAPPING ATOMIC ABSORPTION SPECTROMETRY[a]

C. M. LAU, A. M. URE and T. S. WEST*
The Macaulay Institute for Soil Research, Craigiebuckler, Aberdeen, AB9 2QJ (Gt. Britain)
(Received 12th July 1982)

SUMMARY

Atom-trapping atomic absorption spectrometry is applied to the determination of total and extractable lead and cadmium in soils. The optimum experimental parameters are described for both elements and the interfering effects of some cations present in over 500-fold amounts are reported. Extractions of twelve typical Scottish top-soils by 0.05 M EDTA and 0.5 M acetic acid were made for determination of available lead and cadmium, and total lead and cadmium were determined in aqua regia digests of these soils.

The phenomena of atom trapping have been investigated extensively [1—3]. In addition to a conventional atomic absorption spectrometer, the technique requires only a 4 mm o.d. silica tube, a tube-mounting system and appropriate connections for cold water and air. The arrangement of the tube and the connections have been described in detail [2]. By locating the tube in the flame and passing cold water through it, atomic species and their precursors present in the flame can be trapped on the cold surface of the tube. Removal of the coolant from the tube by a blast of air allows the surface of the tube to heat up rapidly and consequently the trapped material is released quickly into the flame. With a simple silica tube, severe interferences are produced by several elements, but deposition of aluminium oxide on the tube was found capable of eliminating or greatly reducing such interferences, and successful determinations of selenium in some plant materials were possible by this means [4].

For agricultural purposes, a knowledge of the plant-available trace elements in the soil is usually more important than the total values for these elements, but it is useful for geochemical, pedological and environmental studies to determine the total trace element content. Acetic acid extracts and EDTA extracts of soils are commonly used to simulate plant uptake and thus provide a guide to plant availability. Atomic absorption spectrometry (a.a.s.) has been widely used for the determination of extractable lead, cadmium and other trace elements in soils. A carbon-rod atomizer for simultaneous determinations of cadmium and lead in acetic acid extracts has been described [5]. Direct flame a.a.s. has been used for determining lead in ammonium acetate soil extracts [6, 7], while solvent extraction together with graphite-

furnace a.a.s. has been employed to determine cadmium and lead in EDTA [8] and ammonium acetate [9] extracts of soils.

The aim of the present work was to extend the atom-trapping technique to the determination of cadmium and lead in soil extracts. Concentration of the analyte within the flame instead of external preconcentration by solvent extraction saves sample preparation time as well as minimizing the risk of contamination. Interference by the matrix can be avoided by pre-coating the tube with appropriate materials.

EXPERIMENTAL

Apparatus

A Varian-Techtron model AA6 atomic absorption spectrometer equipped with a hydrogen lamp background corrector and a pen-recorder was used for atomic absorption measurements. Hollow-cathode lamp currents and slit-widths were as recommended by the manufacturer. The water-cooled silica tube was arranged as previously described [2]. Peak heights were used to calculate absorbances. Background correction was made to eliminate non-atomic absorption and scattering effects.

Optimization of instrumental parameters. In addition to the usual experimental parameters involved in conventional a.a.s. such as the hollow-cathode lamp current, slit-width and the absorption line, the position of the silica tube in the flame as well as the composition of the flame are additional factors which determine the sensitivity of the atom-trapping a.a.s. method.

The tube position has to be optimized with respect to both the light path and the flame. This is done by varying its distance from the burner head or the light path, one at a time, and measuring the signal from a standard solution in each position until the maximum signal is obtained. The optimum flame stoichiometry was chosen by altering the fuel flow rate and measuring the absorbance from a standard solution at each flame condition. The flame composition chosen for each element was that which gave the largest signal.

Standard solutions

Lead and cadmium stock solutions of concentration 1000 μg ml^{-1} were prepared from cadmium sulphate and lead nitrate (both analytical-reagent grade). Cadmium and lead standard solutions were freshly prepared from them in 0.06 M hydrochloric acid for aqua regia digests, and in 0.05 M EDTA or 0.5 M acetic acid for the corresponding soil extracts. Appropriate amounts of sodium and, where necessary, aluminium or iron were added to match the matrix of the sample solutions.

Sample preparation and spectrometry

The soil samples were air-dried, <2 mm, top-soils collected from different locations in Scotland and included a wide range of parent materials.

The aqua regia digestion procedure consisted of adding 10 ml of aqua regia (1 + 3 redistilled nitric acid—6 M redistilled hydrochloric acid) to 1 g of finely ground (<150 μm) soil sample and taking to dryness on a steam bath. This procedure was repeated three times and then once with 6 M hydrochloric acid. The sample solution was finally prepared by treating the residue with 0.06 M hydrochloric acid, filtering and diluting to 25 ml with this dilute acid.

The EDTA extraction was carried out by shaking 15 g of air-dried, <2 mm, soil with 75 ml of 0.05 M EDTA for one hour to achieve equilibrium [10]. The solution was filtered into a conical flask and then transferred to a polyethylene sample tube for storage before the measurements.

For acetic acid extraction, the soil sample (20 g) was weighed, transferred to a 1-l bottle and shaken overnight in an end-over-end shaker with 800 ml of 0.5 M acetic acid. The resulting mixture was filtered and the filtrate stored in a 500-ml polyethylene bottle for a.a.s. measurement.

Sample and standard solutions were analysed by atom-trapping a.a.s. using an aluminium oxide-coated tube [4]. In cases where the sodium and iron contents of the extracts were high (>10 μg ml^{-1}), it was necessary first to coat the aluminium oxide-coated tube with iron oxide by pre-aspirating a 5000 μg ml^{-1} iron solution for 15 s, and then to match the sample and standard solutions approximately in iron concentration. The latter was found necessary for the aqua regia digests and EDTA extracts because of the high concentration of sodium and iron extracted, but was not required for the acetic acid extracts.

RESULTS AND DISCUSSION

Optimization of experimental parameters

The optimum cadmium signal was obtained when the tube was placed 7 mm above the burner head and the burner-tube combination was set at a height at which the upper surface of the tube obscured some 50% of the light from the hollow-cathode lamp. For lead, the tube had to be closer to the burner head, ca. 5 mm, and again set to achieve 50% obscuration of the light (Table 1). In both cases, the highest signals were obtained when the light path was close to the tube surface.

Cadmium and lead were measured at different conditions of flame stoichiometry achieved by altering the fuel flow rate with a fixed oxidant flow rate. While an oxidizing flame gave better cadmium signals, a reducing flame was found to be more suitable for lead as shown in Fig. 1. In the latter case, the richness of the flame was restricted to prevent soot from depositing on the tube surface.

Calibration curves for both cadmium and lead were constructed for different collection times from several sets of standard solutions. A straight line was obtained for cadmium up to a concentration of 0.1 μg ml^{-1} after a 30-s collection. Curvature occurred with higher concentrations or longer

TABLE 1

The effect of the height of the silica tube with respect to the optical path on the absorbance signal for 1 μg ml^{-1} Pb and 0.2 μg ml^{-1} Cd solutions
(Collection for 30 s; tube (base)-to-burner height at optimum, i.e., 5 mm for Pb and 7 mm for Cd.)

Cadmium			Lead		
Height[a] (mm)	Obscuration (%)	Absorbance	Height[a] (mm)	Obscuration (%)	Absorbance
2	—	0.077	2	—	0.128
1	—	0.095	1	—	0.088
0	—	0.189	0	—	0.064
−1	25	0.320	−1	25	0.150
−1.5	37.5	0.369	−1.5	37.5	0.178
−2	50	0.397	−2	50	0.203

[a]Height of optical path above top of silica tube.

collection times. For lead, the calibration graph was straight in the range 0.01—0.5 μg ml^{-1} after a 1-min collection (Fig. 2). Collection of low concentrations of cadmium and lead (0.01 μg ml^{-1} Cd and 0.1 μg ml^{-1} Pb) for 2 min yielded relative standard deviations of 7.4% and 6.8% and characteristic concentrations (sensitivity) for 1% absorption of 0.0004 and 0.0029 μg ml^{-1} for cadmium and lead, respectively. The corresponding detection limits were 0.0001 μg ml^{-1} Cd and 0.0005 μg ml^{-1} Pb. These sensitivities could be further improved with longer collection times.

Interference studies

The interference effects of more than ten elements on the determination of selenium by trapping on a silica tube have already been examined [4]. Very rarely was the interference by the concomitant elements directly due

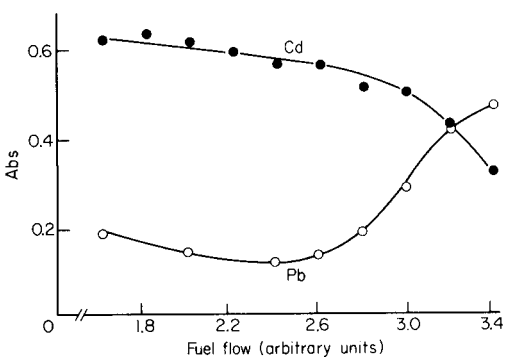

Fig. 1. The effects of the flame stoichiometry on the sensitivities of lead and cadmium signals by varying only the fuel flow rate. 1.0 μml^{-1} Pb; 0.2 μg ml^{-1} Cd; 30 s collection.

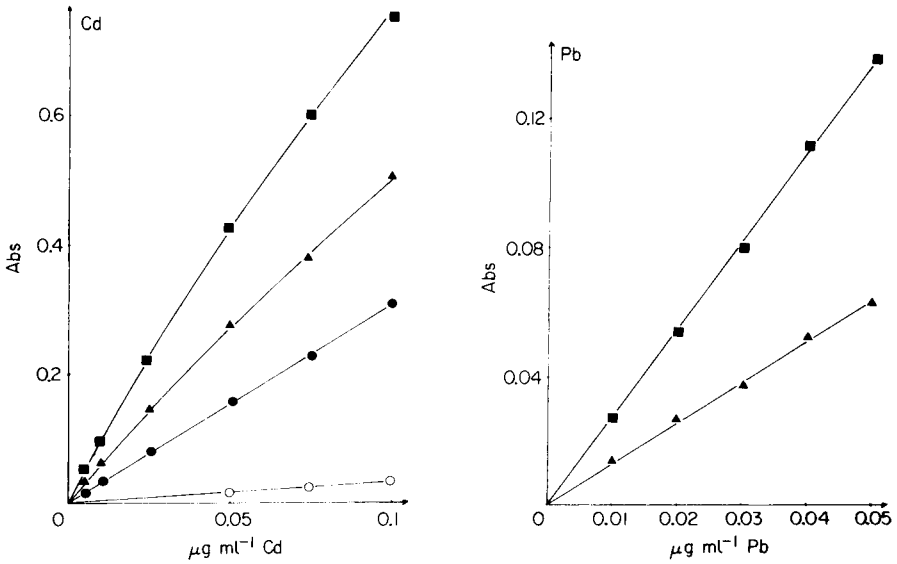

Fig. 2. Calibration graphs for cadmium and lead by the atom-trapping technique with different collection times: (■) 2 min; (▲) 1 min; (●) 0.5 min. (○) Conventional a.a.s.

to chemical interaction with selenium, but rather to physical alteration of the tube surface as a result of deposition or of chemical attack on the silica, which influenced the efficiency of trapping selenium. It was found that a coating of aluminium oxide formed on the tube by aspirating a concentrated (5000 μg ml^{-1}) solution of aluminium (as aluminium chloride) would minimize interferences to a very large extent and that consistent interference-free signals could usually be obtained. The behaviour of this coating as a means of eliminating interference was examined for lead and cadmium, with specific regard to those elements that would be present in major amounts in soil extracts.

The effects of the presence of Al, Ca, Fe, Mg, Na, Ni and Zn on the determination of lead and cadmium by collecting on the aluminium oxide-coated tube were studied. The aluminium oxide coating was prepared by aspirating a 5000 μg ml^{-1} aluminium solution for 5 min, with the water-cooled silica tube located in the appropriate position of a stoichiometric air—acetylene flame. To examine the effects of a particular cation as a possible interference, various amounts of the element concerned were added to the cadmium and lead solutions. The solutions were then collected for 30 s to 2 min. In this way the effects of up to 500 μg ml^{-1} levels of the cations mentioned on 0.4 μg ml^{-1} Pb and 0.05 μg ml^{-1} Cd were investigated.

Effect of sodium on lead. Absorbance measurements were made successively (30-s collection times) on a solution containing 0.4 μg ml^{-1} lead alone and on solutions containing 0.4 μg ml^{-1} lead with increasing concentrations of sodium (as $NaNO_3$); the results are shown in Table 2. The presence of low concentra-

TABLE 2

The effect of sodium (as sodium nitrate or sodium chloride) on the lead and cadmium signals by successive 30-s collections on an Al_2O_3-coated tube

Effect on Pb signal from $NaNO_3$		Effect on Cd signal from NaCl	
Solution ($\mu g\ ml^{-1}$)	Absorbance	Solution ($\mu g\ ml^{-1}$)	Absorbance
0.4 Pb	0.200	0.05 Cd	0.193
0.4 Pb + 10 Na	0.209	0.05 Cd + 10 Na	0.205
0.4 Pb + 50 Na	0.210	0.05 Cd	0.195
0.4 Pb + 100 Na	0.205	0.05 Cd + 50 Na	0.217
0.5 Pb + 500 Na	0.270	0.05 Cd	0.200
0.4 Pb	0.270	0.05 Cd + 100 Na	0.213
0.4 Pb + 10 Na	0.260	0.05 Cd	0.140
0.4 Pb + 50 Na	0.260	0.05 Cd + 500 Na	0.148
0.4 Pb + 100 Na	0.270	0.05 Cd	0.055
0.4 Pb + 500 Na	0.265		

tions of sodium did not affect the lead signal but, when the sodium concentration was more than 100 $\mu g\ ml^{-1}$, a drastic increase in lead signal was recorded so that at 500 $\mu g\ ml^{-1}$ sodium, the absorbance increased by 35%. However, when the experiment was repeated on the same tube, the presence of sodium in concentrations ranging from 0 to 500 $\mu g\ ml^{-1}$ no longer affected the lead signal significantly. Further collection of the same solutions on the same tube for 1-min and 2-min periods confirmed this. The effects of sodium as sodium chloride were essentially the same. Thus provided that the aluminium oxide-coated tube is preconditioned by exposure to 500 $\mu g\ ml^{-1}$ sodium solutions, freedom from sodium interference effects is obtained.

Effect of iron on lead. The effect of iron on lead was investigated experimentally in the same way as for sodium. When iron was present at low concentrations (10 $\mu g\ ml^{-1}$) it had no effect on the lead absorbance. At concentrations of 50 $\mu g\ ml^{-1}$ iron, the lead signal was 30% depressed but at 100 $\mu g\ ml^{-1}$ no depression was observed. As for sodium, it was found that once the aluminium oxide-coated tube had been exposed to iron solutions, and thus pre-coated with iron oxide, the lead signals were independent of variations in iron concentration in sample solutions, and the tube sensitivity was similar to that obtained with pure lead solutions and tubes freshly coated with aluminium oxide not exposed to iron solutions. In practice, where samples containing iron as a major constituent were to be analysed, the tube was additionally pre-coated with iron oxide by nebulizing a 5000 $\mu g\ ml^{-1}$ iron ($FeCl_3$) solution for 15 s.

Effect of other elements on lead. The effect of nickel on sensitivity is exceptional. Depressive effects on sensitivity were observed even at 10 $\mu g\ ml^{-1}$ nickel in solution and increased rapidly to about 50—60% depression at 100 $\mu g\ ml^{-1}$ nickel. Even after exposure to about 100 $\mu g\ ml^{-1}$ nickel solution, the tube exhibited considerable variations in sensitivity with nickel concentration.

None of the other elements tested (calcium, magnesium, zinc) showed any significant effects on lead.

Effect of elements on cadmium. The interferences of the above elements, at various concentrations, on cadmium were studied in the same way and, apart from the depressive effects of sodium described below, no significant effects were observed. At low sodium concentrations ($\leqslant 50$ μg ml^{-1}), no significant effects were observed. At higher concentrations cadmium absorbance was depressed considerably in the presence of sodium, and the sensitivity was markedly dependent on the sodium concentration despite exposure to several cycles of sodium-containing solutions, as shown in Table 2.

For the determination of cadmium in solutions containing sodium at concentrations more than 100 μg ml^{-1}, matching of standard and sample solutions is necessary. It is preferable, where sodium concentrations in the samples are high and variable, to use an aluminium oxide-coated tube which has been coated with iron oxide, as described above for measurements of lead. With such a pretreated tube the effects of sodium were very small and this procedure was used for cadmium determinations in the aqua regia digests and EDTA extracts of soils presented below. This additional iron coating also served to eliminate any interference by iron in the determination of cadmium.

In general, pretreatment of the tubes with the matrix elements sodium and iron provides freedom from interference. Approximate matching of standards and samples in iron and sodium concentration is a useful precaution and ensures that conditioning of the tube surface is maintained throughout an analytical series. Some of the elements tested produce, at high concentrations, temporary changes in sensitivity with a new aluminium oxide-coated tube which do not persist once the tube has been exposed to them even for short periods (ca. 30 s). It is useful, therefore, with samples of unknown major element composition to precondition the tube surface with the sample matrix by a preliminary cycle of collection and release using the sample itself for this purpose.

Analysis of top-soils

Aqua regia digests. The total cadmium and lead contents of twelve Scottish top-soils were assessed by atom-trapping a.a.s. using an aqua regia digestion procedure which dissolves more than 80% of the total soil cadmium and lead contents. The contents were also measured, in the same digests, by conventional a.a.s. with the same instrument. Whereas the conventional technique was just capable of determining the lead content, it was not sensitive enough for cadmium in these digests. Table 3 demonstrates that the contents determined by atom trapping are in as good agreement with those by conventional a.a.s. as is consonant with the poor detection limits of the latter.

EDTA extracts (0.05 M). Both the cadmium and lead contents of the 0.05 M EDTA extracts of the twelve top-soils were measured. Slight depression of the lead signal from the sample solution was found, however, when

TABLE 3

The cadmium and lead content in aqua regia digests of some top-soil samples by conventional a.a.s. (A) and the atom-trapping technique (B) (Results are given as $\mu g\ g^{-1}$ in the air-dried soil.)

Sample	Cd content		Pb content		Sample	Cd content		Pb content	
	(A)	(B)	(A)	(B)		(A)	(B)	(A)	(B)
1	<0.25	0.21	16.0	15.8	7	<0.25	0.14	14.0	13.8
2	<0.25	0.10	9.3	8.5	8	<0.25	0.28	26.5	27.3
3	<0.25	0.28	14.0	14.5	9	<0.25	0.16	22.0	23.0
4	<0.25	0.18	55.0	52.0	10	0.25	0.25	22.0	23.0
5	0.25	0.32	29.0	29.0	11	<0.25	0.21	24.5	24.8
6	<0.25	0.21	23.3	25.5	12	<0.25	0.25	21.0	21.8

the aluminium oxide coating was used for collection. This difference was probably due to the presence of some iron in the extract but not in the standards. Deposition of some iron(III) oxide on top of the aluminium oxide layer eliminated this effect. Conventional a.a.s. and the atom-trapping technique were applied to the extracts; the results obtained are presented in Table 4. In general, results by the two methods agree well.

Acetic acid extracts (0.5 M). The same set of soil samples was studied for lead and cadmium by using 0.5 M acetic acid as the extractant. Because the concentrations were much lower than in the EDTA extracts, their determination by conventional a.a.s. was impossible and even with atom-trapping a.a.s., longer collection times were necessary, 2 min for lead and 3 min for cadmium. Both standard and sample solutions were measured before and after the samples to take account of any changes of the surface with time. Results were checked by measuring the recovery of cadmium and lead as shown in Table 5.

TABLE 4

A comparison of the 0.05 M EDTA-extractable cadmium and lead contents in twelve Scottish top-soils, determined by conventional a.a.s. (A) and by the atom-trapping technique (B) in the same extract (Results are given as $\mu g\ g^{-1}$ in the air-dried soil.)

Sample	Cd content		Pb content		Sample	Cd content		Pb content	
	(A)	(B)	(A)	(B)		(A)	(B)	(A)	(B)
1	0.10	0.12	3.3	3.4	7	0.08	0.10	2.6	2.8
2	0.04	0.04	2.0	2.2	8	0.12	0.20	5.4	6.1
3	0.10	0.12	1.9	1.9	9	0.11	0.14	4.8	5.3
4	0.08	0.10	12.0	14.0	10	0.15	0.20	7.4	7.9
5	0.20	0.29	6.7	7.6	11	0.10	0.11	3.8	4.3
6	0.12	0.14	3.2	3.8	12	0.10	0.13	3.0	3.2

TABLE 5

The determination of 0.5 M acetic acid-extractable contents of cadmium and lead in the twelve Scottish top-soils by atom-trapping a.a.s. and the recovery of 2.5 $\mu g\ g^{-1}$ Pb and 0.2 $\mu g\ g^{-1}$ Cd, added to the soils before extraction

Samples	Cd found[a] ($\mu g\ g^{-1}$)	Recovery of Cd (%) added	Pb found[a] ($\mu g\ g^{-1}$)	Recovery of Pb (%) added
1	0.08	103	1.16	95
2	0.02	100	1.00	96
3	0.09	98	0.92	108
4	0.07	106	2.84	104
5	0.16	111	1.32	110
6	0.10	100	1.00	102
7	0.06	96	1.24	105
8	0.10	107	1.64	110
9	0.19	111	1.12	98
10	0.14	93	1.12	96
11	0.03	109	1.24	105
12	0.07	95	1.04	106

[a]By atom-trapping a.a.s. with collection for 3 min (Cd) or 2 min (Pb).

Conclusions

Both cadmium and lead showed a sensitive response to the atom-trapping technique. Collection of dilute cadmium and lead solutions for 2 min resulted in a 30-fold signal enhancement for both elements compared to conventional a.a.s. Experimental conditions for optimum signals were different for the two elements, and the degree of interference by different cations also varied. While coating the tube with aluminium oxide itself reduced interference effects, it was necessary for both lead and cadmium in the presence of high sodium and iron concentrations to coat the tube additionally with iron oxide. Successful application of this technique was demonstrated by determining the total and extractable lead and cadmium content of twelve Scottish top-soil samples.

REFERENCES

1 C. Lau, A. Held and R. Stephens, Can. J. Spectrosc., 21 (1976) 100.
2 J. Khalighie, A. M. Ure and T. S. West, Anal. Chim. Acta, 107 (1979) 191.
3 J. Khalighie, A. M. Ure and T. S. West, Anal. Chim. Acta, 117 (1980) 257; 131 (1981) 27; 134 (1982) 271.
4 C. M. Lau, A. M. Ure and T. S. West, Anal. Chim. Acta, 141 (1982) 213.
5 A. M. Ure, H. P. Hernandez-Artiga and M. C. Mitchell, Anal. Chim. Acta, 96 (1978) 37.
6 H. L. Kahn, F. J. Fernandez and S. Slavin, At. Absorpt. Newsl., 11 (1972) 37.
7 F. Beavington, Austr. J. Soil. Res., 11 (1973) 27.
8 B. Peterson, M. Willems and S. S. Jorgensen, Analyst, 105 (1980) 119.
9 I. I. Petrov, D. L. Tsalev and A. I. Barsev, Anal. Spectrosc., 1 (1980) 47.
10 A. M. Ure and M. L. Berrow, Anal. Chim. Acta, 52 (1970) 247.

Analytica Chimica Acta, 146 (1983) 181—190
Elsevier Scientific Publishing Company, Amsterdam — Printed in The Netherlands

THE TRANSIENT OXIDATION OF BRUCINE IN SOLUTION AS A TOOL FOR THE DETERMINATION OF CHROMIUM(VI) AND BRUCINE

TAKESHI YAMANE[a] and HORACIO A. MOTTOLA*
Department of Chemistry, Oklahoma State University, Stillwater, OK 74078 (U.S.A.)
(Received 29th July 1982)

SUMMARY

The oxidation of the alkaloid brucine by chromium(VI) in sulfuric acid medium in the presence and absence of oxalic acid is described. Photometric monitoring of a red intermediate (λ_{max} = 525 nm) permits determinations of both chromium(VI) and brucine at low concentrations (Cr(VI), 0—7.5 μg ml^{-1}; brucine, 0—197 μg ml^{-1}) in an unsegmented continuous-flow system by direct injection of the sample into the detection area. Detection limits are 0.1 μg ml^{-1} for chromium and 4 μg ml^{-1} for brucine. Other alkaloids structurally related to brucine (e.g., strychnine, yohimbine and corynanthine) do not give intermediates with the high molar absorptivity exhibited by brucine. Determination of chromium in water samples and standards is described.

A novel approach to fast, continuous kinetic-based determinations using an unsegmented continuous-flow system in closed-loop configuration and transient oxidation-reduction signals was introduced by Dutt and Mottola in 1975 [1]. All necessary reagents are contained in a single reservoir solution which is continually circulated, at constant flow, through the cell into which an aliquot of the sample containing the sought-for species is injected. The species to be determined participates in a rapid redox reaction which by generation of a product or consumption of a reactant perturbs the baseline signal. A subsequent but slower reaction restores the signal level to its original baseline value. The height of the recorded transient peak (or its area) is proportional to the amount of sought-for species in the sample. A kinetic model based on consecutive first-order processes has been proposed to describe the transient signals obtained in such situations [2].

Oxidations of several organic species by chromium(VI) produce unstable intermediates that fit the characteristics just described. Some of these oxidations are affected by the presence of promoting agents such as oxalic acid. The alkaloid brucine, and some analogs, are among these organic species oxidized by chromium(VI) with the generation of a transient intermediate. Brucine is readily available commercially and has been used as a redox indicator [3]. Under rather mild oxidizing conditions it is converted to

[a]Permanent address: Department of Chemistry, Faculty of Education, Yamanashi University, Takeda-4, Kofu-shi, Japan.

bruciquinone which is bright red. In presence of oxalic acid (or at high sulfuric acid concentrations), the red intermediate is converted to a colorless species. Because this sequence of events occurs even when the oxidizing agent is not in excess, oxidation of the quinonoid ring seems improbable (although it cannot be ruled out totally) and the possibility of reversible conversion to brucine, with its analytical implication for repetitive determinations of chromium(VI) and brucine in an unsegmented continuous-flow system (closed-loop configuration), prompted the studies reported here.

EXPERIMENTAL

Apparatus

The experimental set-up basically followed the schematic concept of the one proposed originally [1]. A Gilson Minipuls 2 peristaltic pump (Gilson Medical Electronics, Middleton, WI) was used for solution(s) recirculation. The photometric system was custom-assembled and consisted of: a 6-V tungsten lamp (Chicago Miniature Lamp Works No. 1493) operated by an MP-1026 regulated power supply (Pacific Precision Instruments, Concord, CA), a H-10 Jobin Yvon concave holographic grating monochromator, a specially designed cell holder accommodating a 1-cm flow cell [4] and equipped with a magnetic stirring system consisting of a miniature d.c. motor (0.35—2.5 V, minimum current for operation 25 mA; Edmund Scientific, Barrington, NJ) operated by an Energel 6-V rechargeable battery (Radio Shack, Ft. Worth, TX), and an HUV-4000B pin photodiode-operational amplifier combination (EG & G Electro-Optics, Salem, MA) operated by a 915 Dual Power Supply, ±15 V, 25 mA (Analog Devices, Norwood, MA). The read-out unit was a model 2D-2 X-Y recorder (F. L. Moseley Co., Pasadena, CA). Viton tubing (3 mm i.d.) was used in the pump head and silicone rubber (3 mm i.d.) tubing was used for solution transport. Injection of sample was manual and with the aid of a gas-tight modified B-D Yale 1.00-cm^3 tuberculin syringe.

Reagents and solutions

All reagents used were of analytical grade. Chromium(VI) stock solution was prepared by dissolving potassium dichromate in water (12.5 μg Cr ml^{-1}); more dilute solutions were prepared by direct dilution of aliquots of the stock solution. Brucine solutions were prepared by dissolution of brucine sulfate (Mallinckrodt); these solutions were stable for about a week. The water used was purified by distilling deionized water in a borosilicate still equipped with a quartz-covered immersion heater.

Experimental procedures

Detection of chromium(VI). A 0.02-ml aliquot of the test solution is mixed with 0.01 ml of 5.4 M sulfuric acid, 0.04 ml of 0.020 M oxalic acid, and 0.04 ml of 0.0025 M brucine solution in the depression of a spot plate.

A pink color (which disappears in a few minutes) develops within a few seconds of mixing in the presence of as little as 0.025 μg of Cr(VI) in the sample.

Detection of brucine. A 0.02-ml aliquot of the test solution is mixed with 0.02 ml of 9 M sulfuric acid, 0.02 ml of 0.10 M oxalic acid and 0.01 ml of 0.0030 M dichromate solution in the depression of a spot plate. A development of a pink color in a few seconds which rather rapidly disappears indicates the presence of brucine. A positive test is observed with 0.4 μg or more of brucine.

Batchwise determination of chromium(VI). A sample aliquot (up to 2 ml) containing chromium(VI) in the range 0.1—1.2 μg is mixed with 0.5 ml of 0.020 M oxalic acid and 0.5 ml of 3.6 M sulfuric acid inside a 1-cm glass photometric cell and the mixture is diluted to a total volume of 3.0 ml. The reaction is initiated by injection of 0.20 ml of a 0.0025 M brucine solution with effective stirring. The increase in absorbance is monitored at 525 nm and the change in absorbance (fixed-time procedure) in the first 8 s of reaction, a measure of the reaction rate, is directly proportional to the Cr(VI) concentration in the sample. Measurements beyond 8 s or at higher Cr(VI) concentrations yielded working curves deviating from linearity.

Batchwise determination of brucine. A sample aliquot of up to 2 ml, and containing between 10 and 200 μg of brucine is mixed with 0.12 ml of 0.020 M oxalic acid and 0.5 ml of 3.6 M sulfuric acid. The resulting solution is mixed in a 1-cm glass cell and water is added to obtain a final volume of 3.0 ml. The reaction is initiated by injecting 0.20 ml of 3.0×10^{-4} M dichromate solution and the increase in absorbance is monitored at 525 nm. Brucine is determined in a manner like that described for chromium.

Continuous-flow determination of chromium(VI) or brucine. The reservoir solution for Cr(VI) determination contained 2.5×10^{-3} M brucine, 7.5×10^{-2} M oxalic acid, and 0.56 M sulfuric acid. The same solution for brucine determination consisted of 2.0×10^{-4} M dichromate, 3.0×10^{-2} M oxalic acid, and 2.3 M sulfuric acid. The injected sample size in both cases was 0.20 ml.

RESULTS AND DISCUSSION

The oxidation of brucine by chromium(VI) in sulfuric acid media proceeds by at least two consecutive reactions:

$$\text{Brucine} + \text{Cr(VI)} \xrightarrow{k_1} \text{red intermediate} + \text{Cr(III)} \quad (1)$$

$$\text{Red intermediate} \xrightarrow{k_2} \text{product(s)} \quad (2)$$

The red intermediate is postulated as bruciquinone. Brucine in 5.6 M sulfuric acid solution shows absorption in the near u.v. region of the spectrum with maximum absorption at 300 nm (molar absorptivity = 9.0×10^3 l mol^{-1} cm^{-1}).

The absorption spectrum of the solution after completion of reactions (1) and (2) is similar to that of brucine before oxidation, suggesting the regeneration of brucine, but a slight decrease in absorbance at the wavelength of maximum absorption after each addition of chromium(VI) and the accumulation of a faint yellow product (which turns to orange as the concentration of Cr(VI) is increased) suggest the modification of reaction (2) as follows:

$$\text{Red intermediate} \xrightarrow{k_2} \text{brucine} + \text{faint yellow product} \qquad (3)$$

These observations are valid in the presence as well as in the absence of oxalic acid as a promoter. This partial regeneration of brucine encouraged the exploration of the closed-loop continuous-flow system with direct injection into the detection area. The rate of reaction (1), represented by the change in absorbance during the first eight seconds after mixing, is affected in a pronounced manner by the concentration of sulfuric acid. Figure 1 shows such dependence both in presence and absence of oxalic acid as promoter. In both cases a significant increase in rate is observed as the sulfuric acid concentration increases; in the absence of oxalic acid, however, negligible, if any, effect was observed below 0.84 M H_2SO_4. Relatively high concentrations of sulfuric acid need to be avoided because of an increase in the viscosity of the medium that introduces optical artifacts upon injection of the sample, complicated by slow mixing. A sulfuric acid concentration of 0.56 M, in the presence of sufficient oxalic acid, provides satisfactory condi-

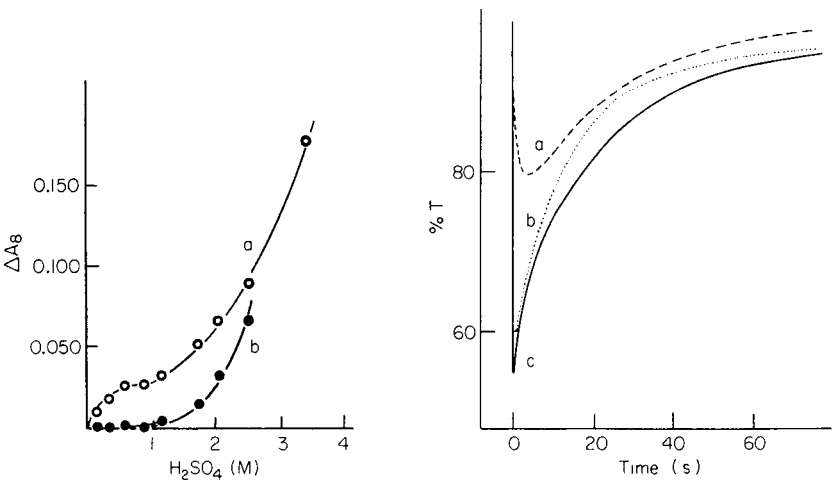

Fig. 1. Effect of sulfuric acid concentration on the rate of oxidation of brucine by chromium(VI): (a) in presence of oxalic acid; (b) in absence of oxalic acid. Conditions: 9.4×10^{-6} M $K_2Cr_2O_7$, 6.2×10^{-4} M oxalic acid, 1.6×10^{-4} M brucine. ΔA_8 is the change in absorbance after the 8-s reaction.

Fig. 2. Effect of sulfuric acid concentration on the transient signal profile. Sulfuric acid concentration: (a) 0.56 M; (b) 2.3 M; (c) 4.5 M. Conditions: 3.12×10^{-5} M brucine, 7.8×10^{-3} M oxalic acid, 1.9×10^{-4} M $K_2Cr_2O_7$.

tions for chromium(VI) determination. At relatively low concentrations of chromium, brucine and oxalic acid, the following experimentally derived rate dependence was observed:

$$\text{Rate} = k_1 [\text{Cr(VI)}]_0[(\text{COOH})_2]_0[\text{brucine}]_0 \quad (4)$$

with $[\ ]_0$ denoting initial concentrations. For brucine determination, the sulfuric acid concentration must be higher, to compensate for the decrease in brucine concentration. Figure 2 shows the effect of sulfuric acid when the determination of brucine is contemplated. The need for higher sulfuric acid concentration when brucine is determined is also dictated by the fact that at 0.56 M H_2SO_4, an increase in oxalic acid concentration, although enhancing the rate of decolorization of the bruciquinone intermediate, only slightly affects the rate of color production. Figure 3 shows the effect of oxalic acid on the combined operation of reactions (1) and (3). It is evident that oxalic acid affects the rate of both reactions (1) and (3), and as such, a compromise concentration has to be used to retain the needed condition of $\text{Rate}_1 \gg \text{Rate}_3$ for good sensitivity but Rate_3 must still be high enough to allow a relatively short time for regeneration; this is of relevance in the number of injections that can be accommodated per hour in continuous-flow sample processing. The effect of brucine concentration is shown in Fig. 4. As expected, brucine affects both reactions, and concentrations higher than 3.1×10^{-3} M did not enhance the peak height significantly to be of value in the determination of chromium(VI).

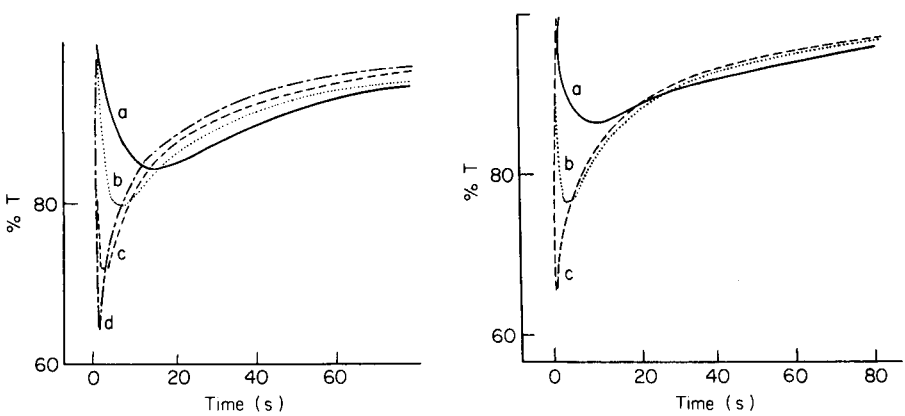

Fig. 3. Effect of oxalic acid concentration on the transient signal profile. Oxalic acid concentration: (a) 7.8×10^{-4} M; (b) 3.1×10^{-3} M; (c) 1.6×10^{-2} M; (d) 1.6×10^{-1} M. Conditions: 1.56×10^{-3} M brucine, 0.56 M H_2SO_4, 3.75×10^{-6} M $K_2Cr_2O_7$.

Fig. 4. Effect of brucine concentration on the transient signal profile. Brucine concentration: (a) 7.8×10^{-5} M; (b) 3.1×10^{-4} M; (c) 3.1×10^{-3} M. Conditions: 3.1×10^{-2} M oxalic acid, 0.56 M H_2SO_4, 3.75×10^{-6} M $K_2Cr_2O_7$.

Determination of chromium(VI)

Figure 5 shows typical signal traces obtained by repetitive injection of chromium(VI) into a reservoir solution as described in the Procedure. The peak height (area) and time for return to baseline are important parameters because they dictate the method sensitivity and the rate of determination [2]. Both parameters are potentially affected by the flow rate employed; such dependence is illustrated in Fig. 6. Because under the experimental conditions employed here, the rate for reaction (1) is many times the rate of reaction (3), no significant change in signal height was observed when the flow was changed between 5 and 20 ml min^{-1}. The time for return to baseline, however, steadily decreases, indicating that the highest possible flow rate affordable appears as the one to be used to improve the injection rate. At a flow rate of 15 ml min^{-1} an injection rate of 180 h^{-1} is estimated. Use of a reservoir solution of 50 ml gave no significant change in peak height after 31 repetitive injections of 0.20-ml samples containing 4.5×10^{-5} M dichromate. A gradual drift in baseline was observed, however, because of the accumulation of the faint yellow product. A linear relationship was observed between the dichromate concentration (up to 7.5×10^{-5} M) and the peak height (use of peak area instead of peak height did not improve the working curves). As expected, increasing the sample size improves sensitivity but samples larger than 0.20 ml show negative deviation from linearity in the working curves. Injection of 0.20 ml of purified water produced a very small signal easily distinguishable from that of chromium(VI) injection. The water signal is a single sharp trace lacking the width characteristic of the chromium(VI) signals.

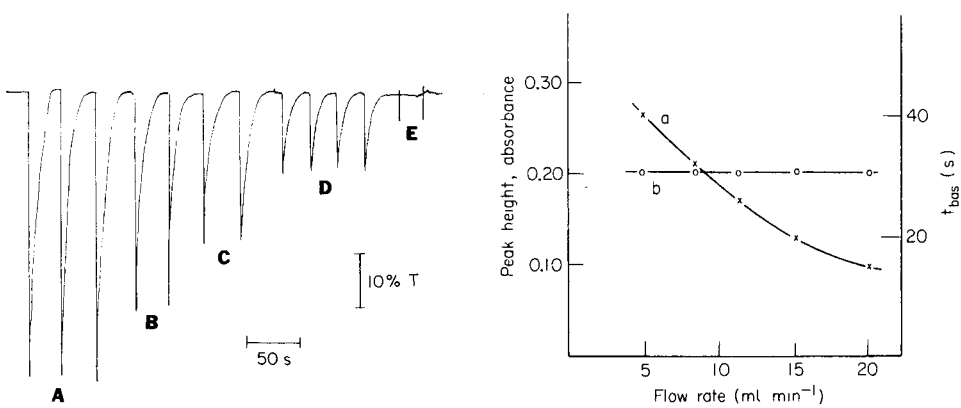

Fig. 5. Typical signal profiles for chromium(VI) determination. Dichromate concentration: (A) 7.5×10^{-5} M; (B) 4.5×10^{-5} M; (C) 3.0×10^{-5} M; (D) 1.5×10^{-5} M; (E) none (peak corresponds to injection of 0.20 ml of water). Conditions: 2.5×10^{-3} M brucine, 0.56 M H_2SO_4, 7.5×10^{-2} M oxalic acid.

Fig. 6. Effect of flow rate on (a) the time for return to baseline (t_{bas}), and (b) the peak height. Injected sample was 0.20 ml of 4.5×10^{-5} M dichromate run as under procedure.

The experimentally determined limit of detection for dichromate is 1×10^{-6} M. A relative standard deviation of 2.5% was observed for 31 repetitive injections of samples containing dichromate at the 4.5×10^{-5} M level.

The method sensitivity for chromium is reduced to 70—80% of its original value after injection of a few chromium samples if the resulting reservoir solution is let stand at room temperature for six or more hours. No effect on the method sensitivity is observed if the freshly prepared reservoir solution (without chromium in it) is allowed to stand for comparable lengths of time.

The effects of interferences on the chromium(VI) determination are summarized in Table 1. Iodide, nitrite, lead and uric acid (all capable of reaction with Cr(VI)) interfere seriously. Vanadium(V) and arsenic(III) show slight positive and negative effects, respectively, when present in 100-fold molar excess with respect to chromium. A three-fold molar excess of these species can be tolerated. Chromium(III) does not interfere, and the method is selective for the chromium(VI) oxidation state in solution. No interference was observed when nitric acid was added up to a 1 M concentration; at larger concentrations, nitric acid oxidizes brucine and interferes. Concentrations of sodium chloride as high as 0.80 M had no deleterious effect.

Determination of brucine

The general observations made for chromium(VI) determination apply for the brucine determination. The number of injections per hour, in the case of brucine, is about 280 with a flowrate of 20 ml min^{-1}. Linear calibration graphs were obtained up to 5×10^{-4} M brucine. A 2% relative standard deviation was observed for 18 repetitive injections of 0.20-ml samples of brucine (2.5×10^{-4} M) and the limit of detection was estimated as 1×10^{-5} M brucine.

Analogs of brucine (strychnine, yohimbine and corynanthine), when oxidized by chromium(VI) slowly give solutions which are light orange-red, light brown and light brown, respectively. The rates of color development did not seem to be affected by the presence of oxalic acid. In the determination of 2.5×10^{-4} M brucine, as much as 1.0×10^{-2} M strychnine, 4.1×10^{-5} M yohimbine and 4.1×10^{-5} M corynanthine can be tolerated. It is of interest to note that corynanthine and yohimbine exert a negative effect on the brucine peak although they developed color (positive effect) when present alone.

Application to some relevant samples

Municipal digested sludge. A U.S. Environmental Protection Agency sample (Sample No. 2402, Date 976) was treated and chromium was determined in the corresponding digests. Three different digestion procedures were employed. The first was the one recommended in EPA Manual (EPA-74, 4.1.3.) except that final dissolution was with hydrochloric acid. In the other two procedures of sample preparation, hydrogen peroxide was used to oxidize organic matter, and Cr(III) to Cr(VI). The EPA method and one of

TABLE 1

Effect of foreign species on the determination of chromium (3.48 $\mu g\ ml^{-1}$)
(Results are based on the effect of 31 injections of the amount added.)

Species added	Amount added ($\mu g\ ml^{-1}$)	Added as	Relative error (%)
Fe(III)	134	$FeNH_4(SO_4)_2 \cdot 12H_2O$	−1.2
Cu(II)	610	$CuSO_4$	−0.6
Mn(II)	142	$MnCl_2 \cdot 4H_2O$	−3.2
	71		0
Co(II)	566	$Co(NO_3)_2 \cdot 6H_2O$	0.6
Zn(II)	628	$ZnSO_4 \cdot H_2O$	0
Cr(III)	500	$KCr(SO_4)_2 \cdot 12H_2O$	0
Mo(VI)	922	$Na_2MoO_4 \cdot 2H_2O$	0
W(VI)	1760	$Na_2WO_4 \cdot 2H_2O$	23
	441		0
Ag(I)	1040	$AgNO_3$	0.6
Al(III)	259	$AlK(SO_4)_2 \cdot 12H_2O$	0
Se(IV)	760	Na_2SeO_3	0
Cd(II)	1080	$Cd(NO_3)_2 \cdot 4H_2O$	0
Hg(II)	1920	$HgCl_2$	0
Ca(II)	1150	$Ca(NO_3)_2 \cdot 4H_2O$	0.6
Mg(II)	468	$MgSO_4 \cdot 7H_2O$	0
Ni(II)	560	$NiSO_4 \cdot 6H_2O$	0
Pb(II)	100	$Pb(CH_3COO)_2 \cdot 3H_2O$	—[a]
	2.5		−0.5
Cl^-	2700	NH_4Cl	0
F^-	365	NaF	0
I^-	12	KI	−32
NO_2^-	440	$NaNO_2$	−100
NO_3^-	2400	$NaNO_3$	−0.6
PO_4^{3-}	912	$Na_3PO_4 \cdot 12H_2O$	0
Glucose	1720		−1.2
Uric acid	2		−23
EDTA	4800		−1.0
As(III)	24	As_2O_3	−12.8
	8		−2.6
V(V)	196	NH_4VO_3	38
	5		0

[a]Precipitation.

the hydrogen peroxide oxidation procedures gave no signal indicating that the Cr(III) was not oxidized to Cr(VI). The other procedure using hydrogen peroxide, however, was satisfactory for determining chromium in the sludge sample; a value of 121 mg Cr kg^{-1} was obtained; this value is within the 95% confidence level (115—294 mg Cr kg^{-1}) for an average of 204 as reported by EPA for the given sample. Application of the method of standard addition yielded good linear dependence with calibration graphs of the same slope as the working graphs obtained with potassium dichromate standards. In the

successful method, 0.5 g of sludge sample was transferred to a beaker and 3 ml of concentrated nitric acid was added. The mixture was evaporated to dryness on a hot plate with due care. After the residue had cooled to room temperature, 2 ml of 9 M H_2SO_4 was added and the mixture was heated until it became dark. After cooling again to room temperature, 0.5 ml of 30% H_2O_2 was added and the mixture was heated, with additional peroxide being added as needed until digestion was complete. After the watch glass and walls of the beaker had been washed down with deionized-distilled water, the solution was filtered to remove any insoluble matter. Potassium hydroxide solution was added to the filtrate to adjust the pH to ca. 12 and then 1 ml of 30% H_2O_2 was added, and the solution was evaporated to dryness to remove the excess of peroxide. The residue was dissolved in a small volume of water and 9 M H_2SO_4 was added to adjust the pH to 1, with final dilution to 50 ml in a volumetric flask. Aliquots (0.20 ml) of this solution were used for the continuous-flow injection determination of chromium(VI).

Water pollution quality control samples. Attempts to quantify chromium in U.S. Environmental Protection Agency water quality control samples (Concentrate 3) as received were unsuccessful even on application of the standard addition method. Oxidation of the samples with hydrogen peroxide in basic medium provided satisfactory results; a value of 14.0 ± 0.6 μg Cr ml^{-1} was obtained; the EPA reported value was 14.6 ± 1.3. This concentrate contained the following metals (in μg ml^{-1}): Al (70), As (20), Be (75), Cd (5), Co (50), Cu (25), Fe (60), Pb (25), Mn (35), Hg (0.75), Ni (25), Se (4), B (75) and Zn (20). Although the continuous-flow procedure lacks the limit of detection for direct application to levels expected in typical water samples, it is reliable for the determination of chromium (as Cr(VI)), after appropriate sample preparation in a variety of samples. It is of interest to note that EPA's Concentrate 3 without hydrogen peroxide oxidation contains species capable of interfering with the chromium(VI) oxidation of brucine, or else the chromium is all as chromium(III).

Steel. Two samples of steel, a low-alloy steel (BCS/SS No. 403) and a 13% manganese steel (BCS/SS No. 495) provided by the British Chemical Standards (Bureau of Analysed Samples) were analyzed. Sample treatment consisted of dissolution with (1 + 3) nitric acid followed by heating on a hot plate. After complete dissolution, the solution was boiled for a few minutes to expel oxides of nitrogen. After it had cooled to room temperature, 2 ml of a 0.8% (w/v) silver nitrate solution and 2 g of ammonium persulfate were added and the solution was boiled for 15—30 min to oxidize chromium to the hexavalent state and destroy the excess of persulfate. After the persulfate had been removed, the solution was allowed to cool to room temperature and made to appropriate volume depending on the chromium content. Aliquots (5 ml) were finally diluted to 50 ml and 0.20 ml of the resulting solution was used for the chromium measurement.

The low-alloy steel gave satisfactory results, 0.41% Cr compared to a reported value of 0.42% Cr. The method failed to give satisfactory results

for the 13% manganese steel sample. A batch of determinations gave only 30% chromium recovery. By repeating the oxidation and boiling with persulfate as much as 70% of the chromium present was recovered, but sulfur deposits built up and the silver content, if the process was to be repeated, could reach interferent levels. It should be noted that manganese has a slight interfering effect (Table 1) on the chromium determination when its concentration is close to 100 times (molar level) the dichromate concentration.

The work reported here was supported by a National Science Foundation grant (CHE-7923956).

REFERENCES

1 V. V. S. Eswara Dutt and H. A. Mottola, Anal. Chem., 47 (1975) 357.
2 H. A. Mottola and A. Hanna, Anal. Chim. Acta, 100 (1978) 167.
3 J. M. Ottaway, in E. Bishop (Ed.), Indicators, Pergamon, Oxford, 1972, p. 519.
4 V. V. S. Eswara Dutt, A. Eskander-Hanna and H. A. Mottola, Anal. Chem., 48 (1976) 1207.

Analytica Chimica Acta, 146 (1983) 191—200
Elsevier Scientific Publishing Company, Amsterdam — Printed in The Netherlands

CONCENTRATION OF METAL IONS BY COMPLEXING WITH *N*-METHYLFUROHYDROXAMIC ACID AND SORPTION ON XAD-4 RESIN

INTISAR A. AL-BIATY and J. S. FRITZ*
Ames Laboratory, Iowa State University, Ames, IA 50011 (U.S.A.)
(Received 18th June 1982)

SUMMARY

N-Methylfurohydroxamic acid (*N*-MFHA) has been synthesized and shown to be an excellent chelating reagent for a number of metal ions. Considerable selectivity is achieved by pH adjustment. Metal ions can be separated into groups or concentrated from very dilute solutions by complexation with *N*-MFHA and sorption on a small column containing XAD-4 resin. The metal complexes are readily eluted with hydrochloric acid in acetone for subsequent measurement by atomic spectrometry or absorption spectrophotometry.

Hydroxamic acids, and *N*-phenylbenzohydroxamic acid in particular, have found extensive use as precipitants [1, 2], color-forming reagents [3, 4] and as complexing agents [5—7] for separation of metal ions by solvent extraction. Chelating resins containing the functional group ArC(OH)N(OH)R have been prepared and found to retain a number of metal cations selectively at different pH values [8—10]. Metal ion complexes are stable at more acidic pH values when R = CH_3 than when R = C_6H_5 or H [11]. These chelating resins are useful for separation and concentration of a variety of metal ions, although in some instances the complex is so strong that rapid, quantitative elution of the metal ion becomes a problem.

The purpose of the present work was to prepare a hydroxamic acid monomer suitable for concentration of metal ions by complexation and subsequent sorption of the metal complexes on a small resin column. The sorbed complexes are eluted from the column by an organic solvent. This approach has been used successfully with 8-quinolinol as the complexing reagent [12]. The sequence of complexation, sorption and elution has several advantages over the complexation and solvent-extraction procedures that are so widely used for concentration prior to measurement of metal ions by atomic spectrometry or other methods. One is that sorption can provide larger concentration factors than those obtained by solvent extraction. Also, manipulation is reduced and water-miscible organic solvents can be used in the complexation and sorption procedure.

For separation and concentration of metal ions by sorption, the molecule of the chelating reagent should be designed to include the desired chelating group but with certain solubility and sorption characteristics in mind. Both the reagent and the metal complex should be soluble in water (at least at fairly low concentrations) but the metal complex should be strongly sorbed by an appropriate resin. The metal ion complexes of existing reagents often are insoluble in water, causing the resin column to become plugged and the filtration to become very slow.

After several hydroxamic acid reagents had been synthesized and tested, *N*-methylfurohydroxamic acid (*N*-MFHA) was selected as the most promising for further study. It is easily prepared and its metal complexes are soluble in water at low concentrations but can be sorbed by XAD-4 resin. A procedure has been developed that is extremely effective for concentrating metal ions prior to their measurement.

EXPERIMENTAL

Synthesis of N-*methylfurohydroxamic acid*

N-Methylfurohydroxamic acid (*N*-MFHA) was prepared by the following reaction sequence:

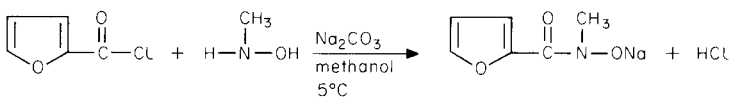

To a solution of 3.56 g (0.04 mol) of *N*-methylhydroxylamine in 50 ml of methanol, 4.5 g (0.04 mol) of anhydrous sodium carbonate was added. The solution was stirred and chilled in an ice bath. 2-Furoyl chloride (4.5 ml) was added dropwise under constant stirring. The temperature was maintained below 5°C through the reaction time (90 min). The solution was stirred for another 30 min after the completion of the reaction. The solution was filtered by suction, and the residue was washed with methanol. The combined filtrates were evaporated to dryness on a steam bath. The product was dissolved in a solution of sodium hydroxide in methanol (1.6 g/20 ml). The filtrate was acidified with acetic acid and evaporated to remove methanol. The residue was recrystallized from 1:1 methanol—water solution. *N*-Methylfurohydroxamic acid was separated as light-yellow crystalline needles.

The product is soluble in organic solvents such as acetone and methanol, but it is slightly soluble in water at room temperature. It dissolves readily in water at 40°C. The reagent is stable in light and air and in acids such as hydrochloric and sulfuric acids. It can be stored for months without decomposition. It was analyzed for carbon, hydrogen, and nitrogen by a Perkin-

Elmer analyzer; for $C_6H_7NO_3$ (m. w. = 141.32) theoretical results are 51.1% C, 5.0% H, 9.9% N, and the results found were 51.1% C, 5.2% H, 9.9% N. The presence of the hydroxamic acid group in the final product was confirmed qualitatively by the formation of a violet solution of iron (III) hydroxamate, and a yellowish solution of titanium(IV) hydroxamate in acidic medium.

Reagents

Solutions of metal ions were in general prepared from reagent-grade nitrate or perchlorate salts and made up in dilute hydrochloric acid. Zirconium(IV) solution was prepared by dissolving $ZrOCl_2 \cdot 8H_2O$ in the minimum amount of concentrated hydrochloric acid and diluting to a final concentration of 3 M HCl. Acetate-buffered solutions were used for studies at pH 5.0 and triethanolamine buffers for experiments at pH 8. Hydrochloric acid in acetone was prepared by diluting the concentrated acid with 7 volumes of acetone.

Break-through curves

The sorption column was prepared by adding a slurry of 100 mg of XAD-4 resin (100—200 mesh; Rohm & Haas) to a 2 mm × 100 mm glass column. The column was washed with 1.0 M hydrochloric acid in acetone, and then with distilled water. The test solutions of metal complexes were pumped through this column at the desired flow rate. The fractions were collected at 42-min intervals and the mean volume of the fractions was calculated (about 8.0 ml). The progress of adsorption was shown qualitatively by the development of a colored zone at the top of the column, and quantitatively by measuring the concentration of metal ion in each fraction by atomic absorption spectrometry or by solution spectrophotometry. The break-through curves were obtained by plotting the percentage extraction against the volume of effluent. The capacity was obtained by calculating the millimoles of complexed metal ion solution passed at the point of 50% extraction.

The effect of reagent concentration was studied by adding appropriate volumes of 0.001 *N*-MFHA to 1.0×10^{-4} M solutions of various metal ions so that reagent:metal ion ratios of 1:1, 2:1, 3:1, 6:1, 10:1 and 15:1 were obtained. The effect of pH was studied by adjusting the pH of the complexed metal ion solutions to 0.5, 3.0, 5.0 and 9.0. The effect of low concentrations of organic solvents was studied by adding the solvent to the complexed, buffered metal ion solutions.

After elution from the XAD-4 column, the metal ion content was determined by atomic absorption spectrometry or by standard spectrophotometric procedures.

Separation and preconcentration of metal ions

A gravity column (5.0 mm i.d. × 50 mm) was packed with 1.0 g of XAD-4 resin (100—200 mesh). This was equilibrated with 1.0 M hydrochloric acid in acetone overnight and then washed thoroughly with deionized water.

Separation of metal complexes. An excess of *N*-MFHA reagent was added to solutions of metal ions to be separated, and the mixture was buffered to the desired pH and diluted to exactly 25.00 ml with deionized water. Then 10.00 ml was passed through the XAD-4 column at a flow rate of 2.0 ml min^{-1}. The column was washed with deionized water, the complexed metal ions were eluted with 5 ml of hydrochloric acid in acetone, and the column was washed with distilled water. The eluate was collected in a 10- or 25-ml volumetric flask, depending on the constituents and on the method of final measurement by standard spectrophotometric methods or by atomic absorption spectrometry.

Purification of reagents. Concentrated solutions (5% or 10%) of calcium nitrate and other salts were spiked with enough of a second metal ion to prepare a solution of 10^{-4} M in the trace metal. The solution was made 10^{-3} M in the *N*-MFHA reagent (a 10-fold molar excess over the trace metal ion) and the pH was adjusted to the desired value. Then 10 ml of the test solution was passed through the XAD-4 column at a flow rate of 2.0 ml min^{-1}. The column was washed several times with distilled water. Then the retained metal complexes were eluted with 5.0 ml of hydrochloric acid in acetone as above and measured by atomic absorption or by spectrophotometric methods.

Effect of anions on copper(II) recovery. An aqueous solution of 5% (w/v) disodium hydrogenphosphate was spiked with 10^{-4} M copper(II). A 10-fold excess of *N*-MFHA was added and the pH was adjusted to 5.0. A small amount of ascorbic acid (1 mg) was added to reduce any iron(III) that might be present. A 10-ml aliquot of this solution was passed through the XAD-4 column, and eluted with HCl in acetone as before. Similar experiments were done with other anions.

Preconcentration of trace metal ions. In this experiment trace metals were concentrated separately or in groups, depending on the pH of complexation reactions and on the method of final measurement. A gravity column which contained XAD-4 resin to a depth of 5 cm was used. The column was washed several times with 1 M HCl and then with deionized water. All glassware was soaked in (1 + 1) nitric acid overnight, and then rinsed thoroughly with deionized water. All solutions used including buffers, acids and bases were prepared in deionized water.

A solution (1 l) which was 10^{-6} M in metal ion was prepared by successive dilution of stock solution. Excess of reagent was added so that the final concentration was $0.5—1.0 \times 10^{-3}$ M. The mixture was buffered and the pH was adjusted to the desired value. The solution was added to a 1-l round-bottom flask which was attached to the top of the column by a 24/40 joint. The flow rate was adjusted to 1.0 ml min^{-1}, and the adsorptions of metal complexes were indicated by the development of a colored band at the top of the bed. The column was washed with deionized water several times, and the metal ions were eluted with 5.0 ml of the HCl/acetone solution, except for molybdenum(VI) which was eluted with 5.0 ml of 1 M ammonia solution followed by 3.0 ml of acetone. The eluate was collected in a 25- or 10-ml

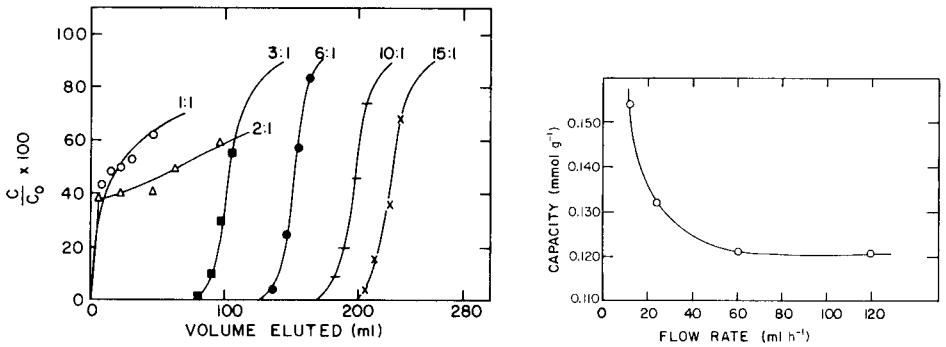

Fig. 1. Break-through curves of copper methylfurohydroxamate (pH 5.0) at different molar ratios of reagent to metal.

Fig. 2. Effective capacity for copper methylfurohydroxamate as a function of flow rate at pH 5.0.

volumetric flask, and the concentrations of sorbed metals were quantified by atomic absorption or by colorimetric methods.

RESULTS

Break-through curves

The effect of various parameters on the recovery of metal ions was studied by means of break-through curves. A 10^{-4} M solution of metal ion, complexed with excess of *N*-MFHA reagent and buffered at a fixed pH value, was pumped through a small column filled with XAD-4 resin until break-through occurred. Further fractions were collected and their metal ion content was measured so that an entire curve of percentage uptake vs. effluent volume could be plotted.

A break-through curve for copper(II) as a function of reagent:metal ion ratio is shown in Fig. 1. Break-through occurs quite early at low reagent:

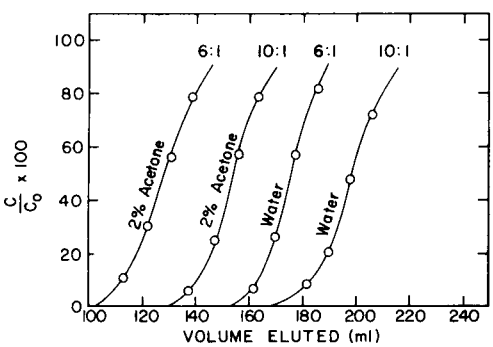

Fig. 3. Break-through curves of copper methylfurohydroxamate (pH 5.0) in 2% acetone and in aqueous solution at different molar ratios of reagent to metal.

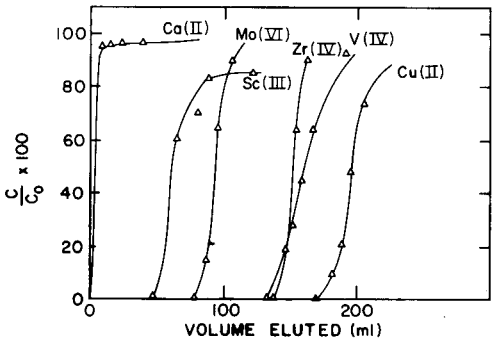

Fig. 4. Break-through curves of the methylfurohydroxamates of scandium(III), molybdenum(VI), zirconium(IV), vanadium(IV), copper(II), and calcium(II) at pH 5.0.

metal ion ratios, but good retention is indicated at ratios of 3:1 and above. The efficiency of uptake continues to improve as the reagent:metal ion ratio is increased. From this and similar curves for other metal ions, a 10:1 molar ratio of reagent to metal ion was selected for most of the later experiments.

The effect of flow rate through the XAD-4 column was studied. The effective capacity for copper(II) is plotted as a function of flow rate in Fig. 2. Variations are probably due to kinetic factors, with greater uptake at slower

TABLE 1

Capacity for metal—methylfurohydroxamate complexes on XAD-4 resin (Conditions: 10^{-4} M metal ion complexed with 10^{-3} M reagent at varying pH values; flow rate 12 ml h^{-1})

Metal ion	Capacity (μmol g^{-1})			
	pH 0.5	pH 3.0	pH 5.0	pH 9.0
Fe^{3+}	20[a]	291		
Ti^{4+}	32[a]	690		
Sn^{4+}	84	—		
Zr^{4+}	92	—	154	
Sc^{3+}	132	—	60	
Mo(VI)	340	—	92	
Cu^{2+}	0	14	199	
Th^{4+}	0	24	450	
Al^{3+}	0	0	355	
Ni^{2+}	0	0	0	24
Mn^{2+}	0	0	0	26
Pb^{2+}	0	0	0	32
Cd^{2+}	0	0	0	—
Co^{2+}	0	0	0	56
Zn^{2+}	0	0	0	69
La^{3+}	0	0	0	—
Lu^{3+}	0	0	7.0[a]	418

[a]Incomplete adsorption.

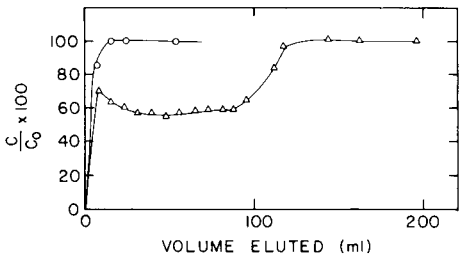

Fig. 5. Break-through curves of copper acetohydroxamate (○) and copper phenylbenzohydroxamate (△) at pH 5.0.

flow rates. However, later work indicated that for purposes of trace metal concentration, a much faster flow rate could be used with a column of larger diameter (see below).

Figure 3 shows the effect of small amounts of acetone on the sorption of copper(II) at two different molar ratios of reagent to metal ion. Although the curves are shifted to lower values by only 2% acetone in the solvent, the results indicate that a certain amount of organic solvent can be tolerated.

The capacity of XAD-4 resin was studied at four pH values for several metal ions. Break-through curves for several metal ions at pH 5.0 are shown in Fig. 4. The results of these studies are summarized in Table 1. Calcium, magnesium, sodium and lithium ions were not adsorbed at the pH values used.

The sorption of copper(II) complexes of *N*-phenylbenzohydroxamic acid (*N*-PBHA) and acetohydroxamic acid on a column of XAD-4 resin was also studied. All of the complexing and sorption conditions were the same as those used for the studies with the *N*-methylfurohydroxamic acid (*N*-MFHA). The results, shown in Fig. 5, indicate rapid break-through with the *N*-PBHA and acetohydroxamate complexes, although some of the copper complex of *N*-PBHA is retained. These results may be attributed to the lower solubility of these complexes or to a different structure which might not be suitable for sorption on the hydrophobic XAD-4 resin. The *N*-methylfurohydroxamic acid clearly is more suitable for sorption of metal complexes, at least on the particular resin used.

TABLE 2

Separation of a 10^{-4} M metal ion from higher concentrations of other metal ions

Ion separated	Other ions present[a]	pH	Recovery (%)
Zr(IV)	Co^{2+}, Cd^{2+}, Cu^{2+}, Zn^{2+}, Al^{3+}	0.5	100
Mo(VI)	Mn^{2+}, Ni^{2+}, Zn^{2+}	1.0	100
Fe(III)	Cd^{2+}, Co^{2+}	3.0	100
Th(IV)	La^{3+}	4.0	100
Cu(II)	Cd^{2+}, Pb^{2+}	4.0	100

[a]Each metal was present at a concentration of 10^{-3} M.

Separation and preconcentration of metal ions

The break-through data in Table 1 indicate that selective retention of metal ions should be possible by selective complexation with *N*-MFHA reagent at different pH values. Accordingly, several quantitative experiments were run in which a small amount of a strongly complexed metal ion was mixed with higher concentrations of several metal ions that are only complexed at a more alkaline pH. The results, listed in Table 2, show excellent recovery in every case and demonstrate the practicality of analytical separations based on selective complexation with *N*-MFHA at an appropriate pH with subsequent sorption on a small resin column.

The ability to recover copper(II) from concentrated sodium or potassium salts of various anions was also demonstrated. All solutions contained 6.35 mg l^{-1} copper(II), excess of *N*-MFHA reagent, and 1 mg of ascorbic acid to mask iron impurities, and the pH was adjusted to 5.0. Excellent recoveries of copper(II) were obtained from 5% disodium hydrogenphosphate, 5% potassium chloride, 1% potassium fluoride and 0.1 M sodium tartrate. However, only 31% of the copper was recovered from 0.1 M sodium citrate, a stronger complexing agent than tartrate. Negligible copper blanks were found for the salt solutions with no copper added.

Sometimes it is necessary to remove trace amounts of metal ion impurities from various salt solutions. The ability to purify salt solutions by *N*-MFHA chelation and sorption on XAD-4 resin was demonstrated for 5% and 10% calcium nitrate, 10% aluminum chloride and 5% sodium acetate (see Table 3). Good to excellent recovery of the trace metal ion was noted in every case except for nickel(II) in 5% calcium nitrate. However, recovery of nickel(II) from 1% calcium nitrate was fairly satisfactory. The method used for purification could of course be used as an analytical procedure for determining the amounts of certain trace metals in various solutions.

TABLE 3

Removal of 10^{-4} M metal ion impurity added to a concentrated salt solution

Salt	Conc. (%)	Volume (ml)	Metal added	pH	Recovery (%)
$Ca(NO_3)_2 \cdot 4H_2O$	5	10.0	Fe(III)	5.0	100
$Ca(NO_3)_2 \cdot 4H_2O$	10	100.0	Fe(III)	5.0	95
$Ca(NO_3)_2 \cdot 4H_2O$	5	10.0	Zn(II)	9.0	100
$Ca(NO_3)_2 \cdot 4H_2O$	5	10.0	Mn(II)	9.0	100
$Ca(NO_3)_2 \cdot 4H_2O$	5	10.0	Co(II)	9.0	90
$Ca(NO_3)_2 \cdot 4H_2O$	5	10.0	Ni(II)	9.0	40
$Ca(NO_3)_2 \cdot 4H_2O$	1	10.0	Ni(II)	9.0	90
$Al(Cl)_3 \cdot 6H_2O$	10	10.0	Zr(IV)	0.5	100
$CH_3COONa \cdot 3H_2O$	5	10.0	Cu(II)	5.0	100.5

Preconcentration of trace metal ions

Perhaps the most important aspect of this work is to demonstrate that *N*-MFHA complexing and subsequent sorption on XAD-4 resin can be used to concentrate trace amounts of metal ions prior to their measurement by atomic spectrometry or other appropriate techniques. Very dilute solutions (10^{-6} M) of several metal ions were prepared, excess of hydroxamate reagent was added and the pH was adjusted to 0.5, 3.0, 5.0, or 9.0, depending on the metal ions taken. The test solution (1 l) was passed through a XAD-4 resin column. Then the sorbed metal complexes were eluted with 5 ml of hydrochloric acid in acetone and the individual metal ions were determined by atomic absorption spectrometry or spectrophotometry. Considering the very dilute solutions taken and the error inherent in the measurement methods, the recoveries reported in Table 4 are generally quite good. Only tin(IV) and thorium(IV) gave recoveries as much as 10% low. Negligible blanks were obtained in all cases. It is interesting that good recovery for chromium(III) was obtained because considerable difficulty was experienced in retaining chromium(III) with a chelating resin [13].

TABLE 4

Preconcentration of metal ions from 1 l of 10^{-6} M solution by adding *N*-MFHA and sorbing on XAD-4 resin

Metal	Sorption pH	Added ($\mu g\ l^{-1}$)	Found ($\mu g\ l^{-1}$)	Recovery (%)
Sn(IV)	0.0	118.0	106.2	90.0
W(VI)	0.0	184	193.2	105.0
Mo(VI)	0.5	96.0	93.1	97.0
Zr(IV)	0.5	91.0	91.0	100.0
Ti(IV)	3.0	48.0	47.0	97.9
Al(III)	5.0	27.0	29.0	110.0
Bi(III)	5.0	208.0	208.0	100.0
Cr(III)	5.0	52.0	54.6	105.0
Cu(II)	5.0	64.5	60.2	93.3
Fe(III)	5.0	55.9	55.9	100.0
Sc(III)	5.0	45.0	48.0	106.6
Th(IV)	5.0	232.0	211.1	91.0
U(VI)	5.0	238.0	238.0	100.0
V(IV)	5.0	51.0	51.0	100.0
Cd(II)	9.0	112.0	112.0	100.0
Co(II)	9.0	59.0	54.9	93.0
Eu(III)	9.0	152.0	152.0	100.0
La(III)	9.0	139.0	150.1	108.0
Lu(III)	9.0	175.0	179.4	102.5
Mn(II)	9.0	54.9	52.2	95.0
Ni(II)	9.0	58.7	55.8	95.0
Pb(II)	9.0	207.0	196.7	95.0
Zn(II)	9.0	65.4	62.2	95.0

Selective preconcentration of certain metal ions is possible by operating at acidic pH values. For example, at pH 0.5 a very good recovery of 10^{-6} M zirconium(IV) was obtained without retaining any of the europium(III), cobalt(II), copper(II), or zinc(II) also present in the sample.

The only drawback of this preconcentration procedure under the conditions used is its slowness with samples as large as one liter. When the work was nearly complete, recovery experiments with copper(II) complexed with *N*-MFHA at pH 5.0 were done in which 1.0 g of XAD-4 resin was packed into a column of 25 mm i.d. to a depth of only 10 mm. Even at a flow rate of 34 ml min^{-1} (17 times the previous flow rate), the copper complex from a 1-l sample was retained as a thin green band at the top of the column. Subsequent elution with hydrochloric acid in acetone gave 100% recovery for the copper.

The Ames Laboratory is operated for the U.S. Department of Energy by Iowa State University under contract no W-7405-ENG-82. Partial financial support for this research was provided by the Director of Energy Research Office of Basic Energy Sciences, WPAS-KC-03-02-03.

REFERENCES

1 B. Das and S. C. Shome, Anal. Chim. Acta, 40 (1968) 338.
2 V. A. Kulumbegashvili and E. A. Ostroumove, Zh. Anal. Khim., 35 (1980) 1246.
3 O. R. Zmieuskaya and V. I. Fadeeva, Zh. Anal. Khim., 35 (1980) 909.
4 C. E. Meloan, P. Hokeboer and W. W. Brandt, Anal. Chem., 32 (1960) 791.
5 A. D. Shendrikar, Talanta, 16 (1969) 51.
6 G. Grossi and F. Baroncelli, 2nd Proc. Int. Solvent Extr. Conf. (1977) 640-4.
7 H. Forster and K. Schwabe, Anal. Chim. Acta, 45 (1969) 511.
8 G. Petrie, D. Locke and C. E. Meloan, Anal. Chem., 37 (1965) 919.
9 F. Vernon and H. Eccles, Anal. Chim. Acta, 79 (1975) 229.
10 F. Vernon and H. Eccles, Anal. Chim. Acta, 83 (1976) 187.
11 R. J. Phillips, Ph.D. Dissertation, Iowa State University, IA (U.S.A.), 1980.
12 R. E. Sturgeon, S. S. Berman and S. N. Willie, Talanta, 29 (1982) 167.
13 R. E. Sturgeon, S. S. Berman and A. DeSauliniers, Talanta, 27 (1980) 85.

Analytica Chimica Acta, 146 (1983) 201—209
Elsevier Scientific Publishing Company, Amsterdam — Printed in The Netherlands

EXTRACTION OF MONOVALENT AND DIVALENT CATIONS BY POLYETHER-BASED POLYURETHANE FOAM

ANJUM S. KHAN, W. G. BALDWIN and A. CHOW*
Department of Chemistry, University of Manitoba, Winnipeg, Manitoba R3T 2N2 (Canada)
(Received 3rd June 1982)

SUMMARY

The extraction of silver(I), thallium(I), barium(II) and lead(II) ions by polyether-based polyurethane foam from aqueous picrate solution is described. The extraction equilibrium constants and the ion-pair formation constants for the picrate systems containing the four ions are reported. The sorption of these ion-pairs by polyether foam can be explained in terms of cation chelation.

It is now well understood that macrocyclic compounds containing repeating ethylene oxide units (—O—CH_2—CH_2—) give stable complexes with alkali and alkaline earth metal cations. The complexing ability of the compounds containing ethylene oxide units is not limited to the cyclic derivatives. Complexes of ethylene glycol with some cations (e.g. Hg^{2+} [1] and Ba^{2+} [2]) were known before Pedersen [3] reported the synthesis and the complexing ability of crown ethers. However, it is only recently, in connection with the present interest in the chemistry of macrocyclic polyethers, that systematic investigations have been made to explore further the complexing ability of noncyclic polyethers.

Chaput et al. [4] have reported the stability constants of Na^+, K^+, Cs^+ and Tl^+ complexes with ethylene glycol and its derivatives in methanol. The stability constant of Pb^{2+}/2,2′-bis-(2-methoxyethoxy)ethyl ether in aqueous solution has also been reported [5]. Vogtle and Weber [6] have reported the synthesis and complexing ability of several noncyclic polyethers. It has been shown that the complexing power of these polyethers depends on the average molecular weight of the polyether and the nature of the end-group attached to the chain.

Yanagida et al. [7] have published the results, obtained by solvent extraction and n.m.r. techniques, of a study on the interactions of alkali and alkaline earth metals with polyethylene oxide and its derivatives. More recently, Fujita et al. [8] reported the synthesis of polyethylene oxide resin beads and demonstrated the use of these beads for the extraction and separation of alkali metal salts. Vanura et al. [9] have reported the extraction of strontium in the presence of polyethylene glycol.

It is clear from these reports that, like cyclic polyethers, noncyclic polyethers are also able to form complexes with several cations, although to a lesser extent [4, 10]. It might be expected therefore, that polyether-based polyurethane foam would also be capable of complexing some cations. Extraction was selected as a convenient method for investigating this possibility as it had been already widely used in similar studies for cyclic [11] as well as noncyclic polyethers [12]. The main object of the present study was to assess the complexing ability of polyether-based polyurethane for monovalent and divalent cations from the distribution of these cations between water and polyurethane foam in the presence of picrate ion.

EXPERIMENTAL

Apparatus and reagents

A Perkin-Elmer model 306 atomic absorption spectrometer and Baird-atomic model 530 A single-channel γ-ray spectrometer fitted with a Harshaw well-type NaI(Tl) crystal were used to quantify the cations. The former was used for silver, thallium, and lead; the radioactive tracer technique was used for barium.

Silver nitrate, thallium chloride, barium nitrate, and lead nitrate were of reagent grade. 8-Anilino-1-naphthalene sulphonic acid (ANS) as the magnesium salt was obtained (Eastman Kodak Co.). A 0.05 M solution of picric acid hydrate (BDH reagent-grade) was standardized potentiometrically against standard sodium hydroxide using a glass electrode. Barium-133 was obtained from New England Nuclear Canada Ltd. A sheet of commercial flexible polyurethane foam was used. In this study, polyether-based polyurethane foam was used unless otherwise stated. In general, flexible foams are prepared from polyols of moderately high molecular weight and low degree of branching and thus have a low cross-link density. The polyols (polyethylene oxide or polypropylene oxide) most commonly used in the production of polyether-based polyurethane foam have approximately 10—40 monomeric units per chain of prepolymer.

Procedures

Polyurethane foam was cut in cubes of approximately 0.3 g each, soaked in 0.5 M HNO_3 for 12 h, washed several times with distilled water until free from acid, washed with acetone in a Soxhlet apparatus for 6 h, and finally air dried.

For each experiment, 100 ml of sample solution was equilibrated with the foam cube for 6—8 h in the extraction cell. The squeezing was done at 25.0 $\pm$ 0.01°C by a thermostated automatic squeezing apparatus [13] which is capable of handling up to 10 samples at a time.

The percentage of metal ion extracted was determined by measuring the concentration of the metal in sample solution before and after extraction. The distribution coefficient for metal ion is given by the ratio of the concentration on the foam to the concentration in the solution at equilibrium

$$D = \frac{\%\text{ of metal on the foam}}{\text{wt. of foam}} \times \frac{\text{volume of solution}}{\%\text{ of metal left in solution}}$$

So defined, D has units of volume per weight.

In preliminary experiments, the extractibility of several monovalent and divalent cations by polyether foam from aqueous picrate solution was checked. The results indicated that only Ag^+, Tl^+, Ba^{2+}, Hg^{2+}, and Pb^{2+} were effectively extracted; no detectable amount of Li^+, Na^+, K^+, Rb^+, Cs^+, or Mg^{2+} was extracted even from 5×10^{-2} M picric acid solution. Experiments also showed no extraction of any of the metal ions in the absence of picric acid. Measurements of the extraction as a function of time indicated that equilibrium was achieved in about 4 h. For further studies, the foam cubes were squeezed for 6—8 h in order to ensure the establishment of equilibrium.

Treatment of the data

The equilibrium between an aqueous solution containing the monovalent metal cation M^+, the picrate anion A^- and polyether based polyurethane foam can be written as:

$$M^+ + A^- \overset{K_{ex}}{\rightleftharpoons} MA_f \; ; K_{ex} = [MA]_f/[M^+][A^-] \tag{1}$$

where MA denotes the ion-pair, the subscript "f" indicates the foam phase and the absence of subscript denotes the aqueous phase. The overall extraction equilibrium can be analyzed in terms of the following constituent equilibria.

Since the ion-pair formation constants have been reported for the alkali metal picrate systems [14], it is quite reasonable to assume ion-pair formation of Ag^+ or Tl^+ with picrate in aqueous solution:

$$M^+ + A^- \overset{K_1}{\rightleftharpoons} MA \; ; K_1 = [MA]/[M^+][A^-] \tag{2}$$

The extraction of the ion-pairs into foam can be represented by

$$MA \overset{K_{1ex}}{\rightleftharpoons} MA_f \; ; K_{1ex} = [MA]_f/[MA] \tag{3}$$

Considering the low polarity of the organic phase (foam), equilibria such as dissociation and aggregation of the ion-pair in the foam have been ignored.

Using the definition for the distribution coefficient "D" for metal and substituting Eqns. (2) and (3)

$$D = [MA]_f/([M^+] + [MA]) \tag{4}$$

Substituting for $[MA]_f$ and $[MA]$ from the definitions of K_1 and K_{1ex} yields

$$D = K_1K_{1ex}[M^+][A^-]/([M^+] + K_1[M^+][A^-])$$

$$D = K_1K_{1ex}[A^-]/(1 + K_1[A^-])$$

$$\text{or } D(1 + K_1[A^-]) = K_1K_{1ex}[A^-] \tag{5}$$

Similarly for divalent cations

$$D(1 + K_1[A^-] + K_1K_2[A^-]^2) = K_1K_2K_{2ex}[A^-]^2 \quad (6)$$

At high concentrations of anion one can assume that $[MA] \gg [M^+]$ and eqn. (4) can be written as $D \approx [MA]_f/[MA]$ or $D \approx K_1K_{1ex}[M^+][A^-]/K_1[M^+][A^-]$, i.e., $D \approx K_{1ex}$.

Analogously, it is reasonable to assume that at low concentration of anion, $[M^+] \gg [MA]$, and thus eqn. (4) can be approximated to $D \approx [MA]_f/[M^+]$ or $D \approx K_1K_{1ex}[M^+][A^-]/[M^+]$, i.e., $D \approx K_1K_{1ex}[A^-]$.

Thus a plot of D vs. $[A^-]$ for monovalent cation should, at low A^- concentration, be a straight line with a slope equal to the product of K_1K_{1ex}, and at high A^- concentration be independent of anion concentration with $D \approx K_{1ex}$. Similarly for divalent cations, a plot of D vs. $[A^-]$ yields the value of K_{2ex} at very high concentration of anion and the value of K_1K_2 from the slope of a plot D vs. $[A^-]^2$ at low anion concentrations.

Extraction equilibrium constants

The extraction of metal cations was studied as a function of initial picrate concentration. The concentration of picric acid was varied from 2.5×10^{-4} to 2.5×10^{-2} M for monovalent cations and from 2.5×10^{-3} to 5×10^{-2} M for divalent cations. Results are shown in Figs. 1 and 2, where it is clear that for each cation, extraction increases with the increase of picric acid up to a certain concentration and then levels off. This extraction behaviour of the metal cations is consistent with the ion-pair extraction of metal picrate by polyether-based polyurethane foam as predicted above.

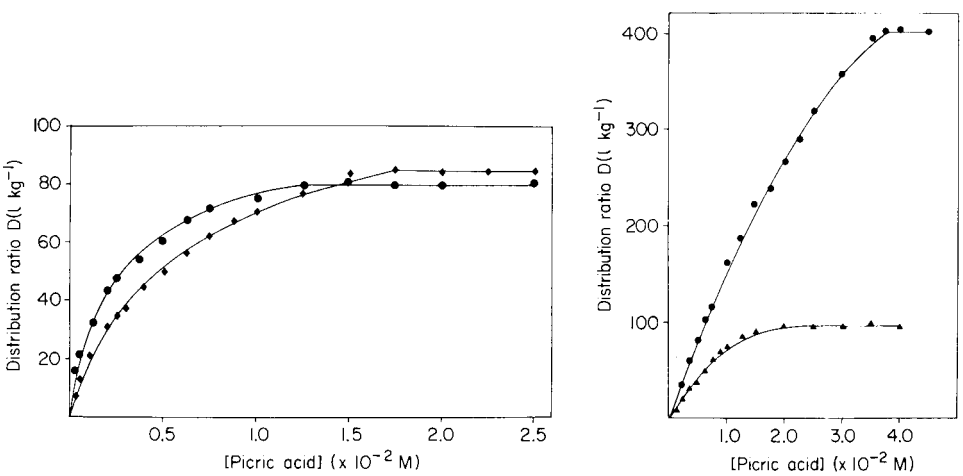

Fig. 1. Effect of varying the initial concentration of picric acid on the extraction of monovalent cations: (•) Ag^+; (♦) Tl^+. Conditions: 0.4 g of foam, 100 ml of solution, 1×10^{-4} M in cations.

Fig. 2. Extraction of divalent cations: (▲) Ba^{2+}; (•) Pb as a function of initial concentration of picric acid. Conditions as in Fig. 1.

The effect of some other anions on the extraction of thallium(I) was also studied. No detectable extraction of Tl^+ was observed either from 0.01 M solution of nitrate ion, or from aqueous 0.004 M solution of 2,4- or 2,6-dinitrophenolate ions. However, the extraction of Tl^+ improved significantly in the presence of the bulkier ANS. In Fig. 3, curves a and b show the plot of D vs. the initial concentrations of picric acid and of ANS for the extraction of thallium(I). The increase in distribution coefficient from picrate ion to ANS is most likely due to the decreasing hydration of the anion in the aqueous phase. Higher extraction from an aqueous solution of ANS than from an aqueous solution of picric acid was also observed for other cations (Ag^+, Ba^{2+} and Pb^{2+}).

Extraction of metal picrates by polyether foam was also studied as a function of initial picric acid concentration for three different initial concentrations of metal cation. The results of such a study for silver are shown in Fig. 4. The plots of D vs. initial picric acid concentration for three different initial concentrations of silver ion are coincident. Similar results were obtained for other metal ion/picrate systems, indicating that extraction of these ion-pairs is independent of metal ion concentration under these conditions.

The effect of silver ion concentration on the distribution coefficient was also studied at constant initial picrate ion concentration. The results are shown in Fig. 5. As can be seen, D values remain practically constant up to 7×10^{-4} M initial concentration of silver ion. The D values start to decline above this concentration with a resulting slope of 0.4. Such a small value of slope can be attributed neither to the dissociation of the extracting species (Ag^+ Pic^-) in the polyether foam, nor to the capacity of the foam. This drop in the D values may, however, be due to the continuous decrease in the metal ion to picrate ratio with the increase of metal concentration. This idea is further substantiated by the fact that when a similar experiment was done

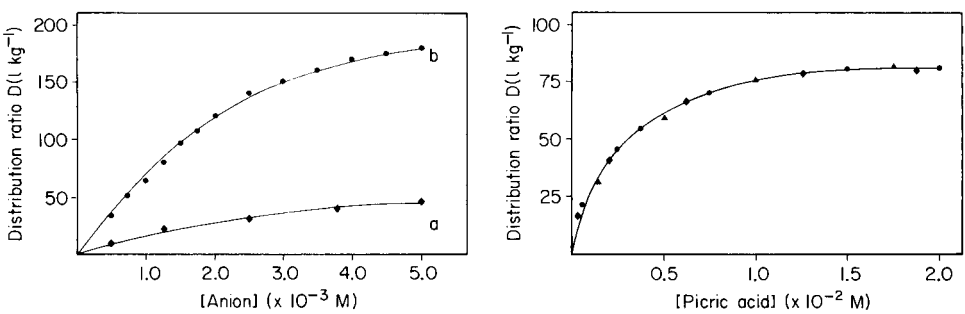

Fig. 3. Extraction of Tl^+ as a function of initial concentration of anion: of (♦) picric acid; (●) ANS. Conditions as in Fig. 1.

Fig. 4. Distribution ratio as a function of initial concentration of picric acid for different concentrations of Ag^+: (♦) 5×10^{-5} M; (▲) 1×10^{-4} M; (●) 2.5×10^{-5} M. Other conditions as in Fig. 1.

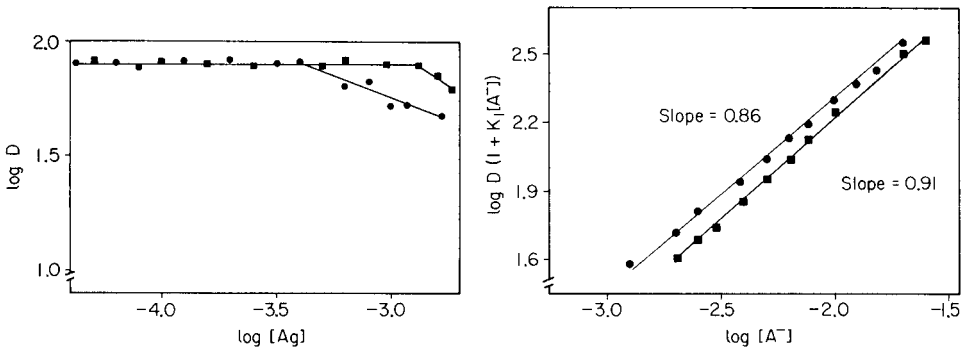

Fig. 5. Plot of log D vs. log $[Ag^+]$ in equilibrium aqueous phase. Conditions as in Fig. 1 except for picric acid concentration: (•) 2×10^{-2} M; (▪) 3×10^{-2} M.

Fig. 6. Plots of log D $(1 + K_1[A^-]$ vs. log $[A^-]$ for monovalent metal picrate systems: (•) Ag^+; (▪) Tl^+.

with higher initial concentration of picric acid, the D values remained constant up to a higher concentration of silver.

The values of K_1 and K_{1ex} for monovalent cations and K_1K_2 and K_{2ex} for divalent cations were determined from the data presented in Figs. 1 and 2, respectively. From the reported value of K_1 for Ba^{2+}/picrate system [15] and the "best fit" for Pb^{2+}/picrate, the values of K_2 have also been estimated and are given in Table 1. Because in all experiments the initial anion concentration is always greater than the initial cation concentration, it is reasonable to assume that $[A^-]$ is approximately equal to the initial anion concentration. If the assumptions used are reasonable, the plots of log D $(1 + K_1[A^-])$ vs. log $[A^-]$ for Ag^+ and Tl^+ and the plots of log D $(1 + K_1[A^-] + K_1K_2[A^-]^2)$ vs. log $[A^-]$ for Ba^{2+} and Pb^{2+} should be straight lines with slopes of one and two, respectively. Such plots (Figs. 6 and 7) are indeed straight lines with slopes close to unity for Ag^+ and Tl^+ cations and with a slope of nearly two for Pb^{2+} and Ba^{2+}, thus confirming the validity of these assumptions.

TABLE 1

Equilibrium constants, K, for the extraction of metal picrates into polyether-based polyurethane foam

Cation	K_1 ($l\ mol^{-1}$)	K_2 ($l\ mol^{-1}$)	K_{1ex} ($l\ kg^{-1}$)	K_{2ex} ($l\ kg^{-2}$)	K_{ex}[a]
Ag^+	195	—	80	—	1.56×10^4
Tl^+	155	—	85	—	1.32×10^4
Ba^{2+}	3980	2.8	—	100	1.11×10^6
Pb^{2+}	1038	3.0	—	400	1.25×10^6

[a]Units of K_{ex} for monovalent cations are $l^2\ mol^{-1}\ kg^{-1}$ and for divalent cations are $l^3\ mol^{-2}\ kg^{-2}$.

DISCUSSION

It seems unlikely that the polarity of the foam is playing any significant role in the extraction of these ion-pairs. Under similar conditions, little or no extraction ($D \ll 1$) has been observed for these cations by a variety of organic solvents ranging in polarity from pentane to methylene chloride. Additional evidence is also obtained by comparing the extraction of these ion-pairs by polyether and polyester foams. It was observed that each metal cation is better extracted by polyether foam. These results are opposite to that expected on the basis of polarity. Because esters are more polar than ethers, it seems most likely that the same is true for their polymeric analogues. Furthermore, the higher extraction of the smaller Pb^{2+} (1.2 Å) compared to that of the larger Ba^{2+} (1.35 Å) cannot be explained by the general rules of ion-pair extraction, according to which the increase in size should lead to an increase in extraction [16].

The sorption of Hg^{2+} (1.1 Å) from the aqueous picrate in solution into polyether foam was also studied and a distribution coefficient of 190 ± 10 was obtained for Hg^{2+}/picrate ion system. This D value is higher than that obtained for the larger Ba^{2+} (D = 100 ± 5) but lower than that of the medium sized Pb^{2+} (D = 400 ± 18). This order of distribution coefficient is not easily explained by the simple ion-pair extraction mechanism.

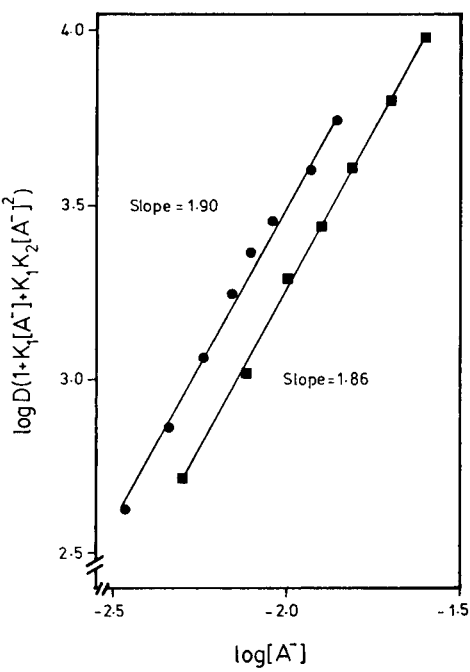

Fig. 7. Plots of log D ($1 + K_1[A^-] + K_1K_2[A^-]^2$) vs. log [$A^-$] for divalent metal picrate systems: (•) Ba^{2+}; (■) Pb^{2+}.

TABLE 2

Equilibrium constants for the interaction of metal ion with 18-crown-6 at 25° C

Cation	K_e[a]	K_f[b]
Ag^+	2.7×10^4 l^2 mol^{-2}	32 l mol^{-1}
Tl^+	2.0×10^6	186
Ba^{2+}	5.2×10^9 l^3 mol^{-3}	7.4×10^3
Pb^{2+}	5.6×10^{11}	1.9×10^4

[a] K_e for the extraction into benzene [18, 19]: $M^{n+}(aq) + n\text{Pic}^-(aq) + L(org) \rightleftharpoons M(\text{Pic})_n\text{-}L(org)$.
[b] K_f for the reaction [20]: $M^{n+}(aq) + L(aq) \rightleftharpoons ML^{n+}(aq)$.

The extraction of these metal cations from the aqueous solution of a bulky anion, e.g., picrate, may be rationalized by the cation-chelation mechanism [17]. According to this mechanism, polyether-based polyurethane foam, like cyclic and linear polyethers, possesses the unique ability to chelate effectively, but certainly not equally, many metal cations. The chelation of the cation, M^+, is most likely a result of the ability of the polyether chains to adopt a helical configuration in which 6 to 10 or so inwardly directed oxygen atoms constitute a "solvent sheet" around the cation. Based on this, the extraction of these ion-pairs by polyether-based polyurethane foam is a result of the effective solvation of the cations by the polyol segment of the foam. The extent of the ion-pair sorption depends not only on the complexing affinity for the cation of the polyether chain (which is mainly influenced by size and the charge of the cation) but also on the solubility of the counter anion.

Based on the cation-chelation mechanism, extraction of metal ions from aqueous solution into polyether based polyurethane foam is analogous to the extraction of metal ions into an organic solvent containing a macrocyclic polyether. The polyether 18-crown-6 is considered a reasonable model compound; some extraction results for 18-crown-6 are shown in Table 2. The data in Table 2, while not strictly comparable to those of Table 1, suggest that for monovalent cations, polyurethane foam is comparable to 18-crown-6 in its efficiency of extraction. Divalent cations are less effectively extracted, perhaps because it is more difficult to arrange two anions near the cation in the rigid foam than in the organic solution of 18-crown-6.

This work was supported by Natural Science and Engineering Research Council of Canada.

REFERENCES

1 A. A. Blumberg, S. S. Pollack and C. A. Hoeve, J. Polym. Sci., Part A-2, 6 (1964) 2499.
2 R. J. Levins and R. M. Ikeda, Anal. Chem., 37 (1965) 671.
3 C. J. Pedersen, J. Am. Chem. Soc., 89 (1967) 7017.

4 G. Chaput, G. Jeminet and J. Juillard, Can. J. Chem., 53 (1975) 2240.
5 M. Kodama and E. Kimura, Bull. Chem. Soc. Jpn., 49 (1976) 2465.
6 F. Vogtle and E. Weber, Angew. Chem. Int. Ed. Engl., 18 (1979) 753.
7 S. Yanagida, K. Takahashi and M. Okahara, Bull. Chem. Soc. Jpn., 50 (1977) 1386; 51 (1978) 1294, 3111.
8 H. Fujita, S. Yanagida and M. Okahara, Anal. Chem., 52 (1980) 869.
9 P. Vanura, J. Rais, P. Selucky and M. Kyrs, Collect. Czech. Chem. Commun., 44 (1980) 157.
10 H. K. Frensdorff, J. Am. Chem. Soc., 93 (1971) 600.
11 C. J. Pedersen, Fed. Proc., Fed. Am. Soc. Exp. Biol., 27 (1968) 1305.
12 A. M. Y. Jabber, G. J. Moody and J. D. R. Thomas, J. Inorg. Nucl. Chem., 39 (1977) 1689.
13 R. F. Hamon, Ph.D. Thesis, 1981, Univ. of Manitoba, Canada.
14 M. Yamane, T. Iwachido and K. Toei, Bull. Chem. Soc. Jpn., 44 (1971) 745.
15 G. Kortum and K. Andrussow, Z. Phys. Chem. (Leipzig), 25 (1969) 433.
16 R. M. Diamond and D. G. Tuck, Progress in Inorganic Chemistry Vol. 2: F. A. Cotton (Ed.), Interscience, New York, 1960, pp. 109—192.
17 R. F. Hamon, A. S. Khan and A. Chow, Talanta, 29 (1982) 313.
18 Y. Takeda and H. Goto, Bull. Chem. Soc. Jpn., 52 (1979) 1920.
19 T. Takeda and H. Kato, Bull. Chem. Soc. Jpn., 52 (1979) 1027.
20 R. M. Izatt, R. E. Terry, B. L. Haymore, L. D. Hansen, N. K. Dalley, A. G. Avondet and J. J. Christensen, J. Am. Chem. Soc., 98 (1976) 7620.

Analytica Chimica Acta, 146 (1983) 211—217
Elsevier Scientific Publishing Company, Amsterdam — Printed in The Netherlands

THE DETERMINATION OF DIALKYLLEAD, TRIALKYLLEAD, TETRAALKYLLEAD AND LEAD(II) IONS IN WATER BY CHELATION/EXTRACTION AND GAS CHROMATOGRAPHY/ATOMIC ABSORPTION SPECTROMETRY

Y. K. CHAU*

National Water Research Institute, Canada Centre for Inland Waters, Burlington, Ontario L7R4A6 (Canada)

P. T. S. WONG and O. KRAMAR

Great Lakes Fisheries Research Branch, Canada Centre for Inland Waters, Burlington, Ontario L7R4A6 (Canada)

(Received 19th May 1982)

SUMMARY

The highly polar and solvated dialkyllead, trialkyllead and lead(II) ions are quantitatively extracted into benzene from aqueous solution after chelation with dithiocarbamate. The lead species are butylated by Grignard reagent to the tetraalkyl form, $R_nPbBu_{(4-n)}$(R = CH_3 or C_2H_5) and Bu_4Pb, all of which can be quantified by a gas chromatography—atomic absorption spectrometry method. Molecular covalent tetraalkyllead species, if present in the sample, are also extracted and quantified simultaneously. A detection limit of 0.1 $\mu g\ l^{-1}$ lead can be achieved with one litre of water. Other metals co-extracted by the chelating agent do not interfere.

In the study of the environmental fate and toxicity of organolead compounds, determination of the ionic organolead species, namely, dialkyllead and trialkyllead (R_2Pb^{2+}, R_3Pb^+; R = Me, Et), is of paramount importance in understanding their pathways and toxicity. It has been shown that inhalation or absorption of tetraalkyllead compounds resulted in the formation of trialkyllead in the fluids and tissues of rats [1], humans (2), and fish [3]. Tetraalkyllead in the aquatic ecosystem also undergoes slow degradation to the trialkyllead and dialkyllead forms and finally to inorganic lead ion [4]. The toxic effects of tetraalkyllead to mammals have been attributed to the trialkyl species [5]. Monoalkyllead compounds are extremely unstable and their existence has not been established.

Methods available for the determination of dialkyl- and trialkyl-lead ions include spectrophotometric measurements of their dithizonates in chloroform at different wavelengths [6], and of their dialkyllead complexes with 4-(2-pyridylazo)resorcinol after conversion of the trialkyllead to dialkyllead with iodine monochloride [7]. Gas chromatographic methods with electron capture detector [8], with microwave-plasma emission detection [9], and

atomic absorption detection (g.c.—a.a.s.) [10] have been used after extraction of the lead compounds from aqueous solution. Direct aqueous sample injection into a g.c.—a.a.s. system has also been reported in a study of tetraethyllead and triethyllead equilibrium in sea water [11].

Recently, two electrochemical methods have been developed. By using anodic stripping voltammetry (a.s.v.) at different plating potentials, the alkyllead species can be determined after extraction from biological materials [12]. This method, however, determines the dialkyl and trialkyllead only as a class without identification of the alkyl groups. The other method also employs different plating potentials together with selective extraction to achieve separation and identification of R_4Pb, R_3Pb^+, R_2Pb^{2+} and Pb^{2+} compounds (R = CH_3 or C_2H_5) in water [13]. The latter procedure is lengthy and involves many steps of calculation by difference. All the above methods suffer either from lack of sensitivity or selectivity for low level environmental samples. None of the methods have achieved quantitative extraction of all the ionic alkyllead species.

Most alkyllead compounds are thermally unstable and some are known to decompose even below their boiling points [14]. Chromatographic separation of these compounds is preferably conducted at the lowest possible temperatures. Both the dialkyl- and trialkyl-lead compounds can be readily alkylated to the tetraalkyl states which have adequate boiling points for gas chromatographic separation. Another advantageous feature of the tetraalkyllead formation is that these derivatives decompose easily in an electrothermal atomizer thus providing good sensitivity for atomic absorption detection. The present study describes the quantitative chelation/extraction of the dialkyl- and trialkyllead species and the conversion to their butyl derivatives for g.c.—a.a.s. The method determines all the alkyllead species in the same forms as they are present in the sample.

EXPERIMENTAL

Equipment and chemicals

The details of the g.c.—a.a.s. system have been described previously [15]. The sample extract was introduced directly to the chromatographic column by a syringe. The chromatographic column was of glass, 1.8 m long, 6 mm diameter, packed with 10% OV-1 on Chromosorb W, (80—100 mesh) with a carrier gas (N_2) flow rate of 65 ml min^{-1}. The injection port and transfer line were at 150 and 160°C, respectively; the column was programmed from 80°C to 200°C at a rate of 5°C min^{-1}. The 217.0 nm line from a lead electrodeless discharge lamp operated at 10 W was used with an electrically heated quartz furnace at 900°C, with hydrogen flowing at 85 ml min^{-1} and a deuterium lamp was used for background correction. Peak areas were integrated with an Autolab Minigrator (Spectra-Physics, CA).

The lead compounds used were dimethyllead chloride, diethyllead chloride (both from Associated Octel Co., S. Wirrel, Gt. Britain), tetramethyllead,

tetraethyllead (both from Alfa Chemicals, Danver, MA, U.S.A.) and mixed tetraalkyllead compounds (Ethyl Corp., Ferndale, MI, U.S.A.). The commercial trialkyllead salts are reasonably pure whereas the dialkyllead compounds generally contained trialkyllead and other lead(II) impurities. A convenient procedure based on the reaction of trialkyllead and iodine monochloride can be used to synthesize dialkyllead if pure compounds are not available [7]. Trialkyllead compounds can also be synthesized, if required, by the reaction of iodine and tetraalkyllead [16].

Standard dialkyllead solutions (100 μg Pb ml^{-1}) were prepared by first dissolving 0.0149 g and 0.0162 g, respectively, of dimethyllead chloride and diethyllead chloride in small amounts of methanol and diluting to 100 ml with distilled water. Standard trialkyllead solutions (100 μg Pb ml^{-1}) were prepared by dissolving 0.0152 g and 0.0171 g, respectively, of trimethyllead acetate and triethyllead acetate in 100 ml of water.

Sample storage

All the ionic alkyllead compounds slowly degrade in the presence of light. However, lake water samples enriched with dimethyllead chloride and trimethyllead acetate at 100 μg l^{-1} level are stable over a period of at least one month in the laboratory when stored in the dark and refrigerated. There is no need to add any preservative to the sample. Storage in a cold dark room is recommended. Alternatively, the samples can be extracted, butylated and dried over anhydrous sodium sulfate.

Procedure

To 1 l of water are added 50 ml of aqueous 0.5 M sodium diethyldithiocarbamate (NaDDTC), 50 g of sodium chloride and 50 ml of benzene, and the mixture is shaken for 30 min. The benzene phase is then carefully evaporated in a rotary evaporator to 4.5 ml in a 10-ml centrifuge tube to which 0.5 ml of butyl Grignard reagent is added. The mixture is gently shaken for 10 min, and washed with 5 ml of 0.5 M sulfuric acid to destroy the excess of Grignard reagent. About 2—3 ml of the organic phase is pipetted into a small vial and dried with anhydrous sodium sulfate. Appropriate amounts (5—10 μl) are injected into the g.c.—a.a.s. system.

RESULTS AND DISCUSSION

Extraction of ionic alkyllead species from aqueous solution

Because several methods [2, 7, 12, 17, 18] have proven inadequate for the quantitative extraction of alkyllead compounds, the use of chelating agents was examined. For these tests, 100-ml portions of distilled water were spiked with 20 μg of each of Me_3Pb^+, Me_2Pb^{2+}, Et_3Pb^+, Et_2Pb^{2+} and Pb^{2+}, individually and in a mixture, and extracted with 5 ml of benzene in the presence of tropolone [19] (0.5% in benzene) or NaDDTC (0.5 M). The benzene phase was separated and butylated as described in the

following section and the alkyllead species were separated and quantified by the g.c.—a.a.s. method.

Tropolone is satisfactory for the extraction of alkyltin species [19] but did not effectively extract alkyllead. Dithiocarbamate is well known to form lead(II) complexes which can be extracted by organic solvents [20]. It was found in this investigation that the ionic alkyllead species, $R_nPb^{(4-n)+}$, were quantitatively extracted into benzene in the presence of sodium diethyldithiocarbamate (Table 1). Although the reaction mechanisms are beyond the scope of this study, it is known that alkyllead salts form coordination compounds with many chelating agents [14].

A small amount of sodium chloride (5 g/100 ml) was found desirable in the extraction of water to facilitate rapid phase separation and also to provide a uniform ionic strength for extraction of various natural waters with different salt contents.

Butylation of alkyllead compounds

The alkyllead species, after extraction into benzene, react readily with butyl Grignard reagent to form $R_nPbBu_{(4-n)}$ similar to that reported earlier for alkyltin compounds [19]. The butylation reactions are spontaneous. There is no increase in yield on shaking the reaction mixture from two minutes to one hour, nor on increasing the amount of Grignard reagent. The reaction yield is quantitative as indicated by comparison of the total lead content in the organic phase with that in the original aqueous phase. Special precaution against water is not particularly necessary although Grignard reagents are unstable in the presence of moisture. Drying the reaction products with anhydrous sodium sulfate increased the storage life of the butyl-alkyllead. Standards prepared in this manner were kept at ambient conditions for several months without noticeable deterioration.

When the retention times of the butylated dialkyl- and trialkyl-lead were measured, only one well-defined peak was found for each compound,

TABLE 1

Extraction efficiency of dialkyllead, trialkyllead, and lead(II) ions species from water[a]

Medium	Extraction efficiency (%)[b]				
	Me_2Pb^{2+}	Me_3Pb^{+}	Et_2Pb^{2+}	Et_3Pb^{+}	Pb(II)
NaCl (sat.)	10(3)	40(4)	14(4)	95(3)	0
NaCl (sat.) + KI (40 g)	45(3)	100(5)	58(6)	112(8)	5(4)
Tropolone	17(4)	25(4)	20(7)	15(7)	20(6)
NaDDTC	109(8)	97(6)	105(9)	94(5)	94(8)
NaDDTC + NaCl (sat.)	98(5)	100(7)	97(6)	98(6)	93(5)

[a]Distilled water, 100 ml; lead compounds, 20 μg each species; volume of benzene in all cases, 5 ml; tropolone (0.5% in benzene), 5 ml; NaDDTC (0.5 M), 5 ml.
[b]Average of two results with average deviation in parentheses.

indicating that no decomposition had occurred on the column or at the heated transfer line. It was found that Pb^{2+} was also extracted by this procedure.

Tetraalkyllead compounds (typically Me_4Pb, Me_3EtPb, Me_2Et_2Pb, $MeEt_3Pb$, Et_4Pb) have high vapor pressures and are seldom found in water unless they are adsorbed on sediments or particulate matter [21]. If these compounds are present in the water sample, they can be extracted into benzene and included in the determination. The butylation reaction has no effect on the tetraalkyllead. A chromatogram showing the separation of five tetraalkylleads, four ionic alkyllead and Pb^{2+} species in a synthetic sample is illustrated in Fig. 1.

Calibration

Peak areas for equal quantities of all the alkyllead species expressed as Pb are identical. Lead(II) ion, after butylation, gave a broader peak shape and smaller peak area when compared to equivalent amounts of alkyllead species. Reasons for this behavior were not established.

The trialkyllead compounds are more stable and were therefore chosen as standards. The method can be calibrated by processing samples containing 10 μg of trimethyllead acetate and 20 μg of Pb^{2+} in 1.0 l of distilled water. Calibration graphs for all the dialkyl- and trialkyl-lead compounds are linear

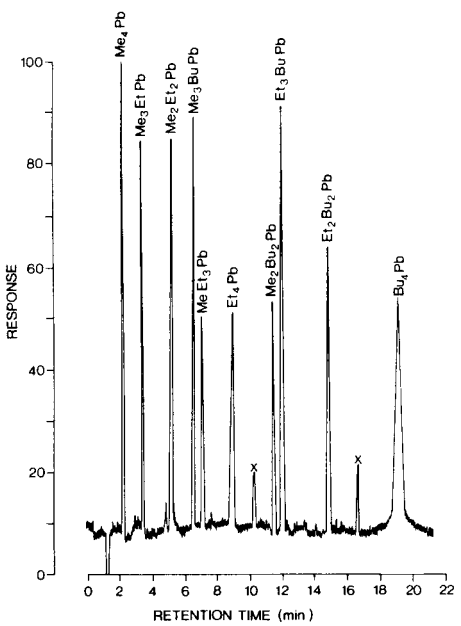

Fig. 1. Gas chromatography—atomic absorption spectrometry of five tetraalkyllead compounds (10 ng each); four butyl derivatives of dialkyl- and trialkyl-lead (8 ng each) and Pb^{2+} (15 ng). x, unidentified lead compounds.

for 1—100 ng, above which overlapping of component peaks occurs. If a single alkyllead is present in the sample, the linear range can be extended much further until the atomization furnace is saturated.

Precision, recovery, and interferences

The precision of the method was evaluated by determining ten replicate samples from 100 ml of Lake Ontario water enriched with 10 μg of each of the alkyllead and Pb^{2+} species. The relative standard deviation for the four alkyllead and Pb^{2+} compounds at this level varied from 5.4% for Me_3Pb^+ to 9.5% for Pb(II). Recovery was assessed by adding different levels of alkyllead compounds to 100 ml of Lake Ontario water which had been pre-extracted with NaDDTC/benzene to strip off its lead content. The recoveries (Table 2) for the alkyllead and Pb^{2+} varied from 90% to 114% in the range 5—30 μg.

Calibration graphs run in distilled water and lake water showed no difference in slopes. Thus, no serious matrix interferences are expected. Acidic water (pH 1—2) lowered the extraction efficiency to about 10%; therefore, samples should be adjusted to pH 6—7 before extraction. Many metals are extracted by NaDDTC [20], but those extracted and likewise butylated to the tetraalkyl-metal forms are tin(IV) and germanium(IV). When tetramethyltin and tetramethylgermanium were tested, there was no response whatsoever in the a.a.s. detection system, set at 217.0 nm.

The reagent blank showed no detectable alkyllead and only traces of Pb^{2+}, which can be easily corrected with a reagent blank.

Detection limit

The absolute detection limit (a signal twice the baseline noise) corresponding to organolead in the g.c.—a.a.s. system is 0.1 ng. With 1 l of water sample, a detection limit of 0.1 $\mu g\ l^{-1}$ can be achieved with 5-μl injections from a final volume of 5 ml of extract. With the deuterium arc background correction, as much as 20 μl of solvent can be tolerated in the furnace without background interferences. Thus, the detection can be further enhanced by a factor of 4.

TABLE 2

Recovery of dialkyllead, trialkyllead and lead(II) ions from lake water[a]

Amount added (Pb, μg)	Recovery (%)[b]				
	Me_2Pb^{2+}	Me_3Pb^+	Et_2Pb^{2+}	Et_3Pb^+	Pb^{2+}
5	101(5)	110(7)	90(4)	92(5)	91(6)
10	95(2)	98(4)	92(5)	95(6)	93(3)
20	101(4)	102(6)	94(4)	97(3)	90(4)
30	93(4)	114(10)	95(6)	92(4)	107(9)

[a] Lake Ontario water, 100 ml; 5 ml of NaDDTC, 5 ml of benzene, 5 g of NaCl.
[b] Average of two results with average deviation in parentheses.

If required, the detection limit can be substantially lowered by increasing the volume ratio of the aqueous and organic phases or by reducing the volume of the resulting organic extract before the butylation step. The benzene phase can be evaporated to smaller volume without loss of the dialkyl- and trialkyl-lead. This would facilitate processing of larger samples if necessary. However, some low boiling tetraalkyllead species (e.g., tetramethyllead) were lost during evaporation. If the tetraalkyllead species are to be determined, the extract should not be evaporated.

REFERENCES

1 J. E. Cremer, Br. J. Industr. Med., 16 (1959) 191.
2 W. Bolanowska, J. Piotrowski and H. Garczyncki, Arch. Toxikol., 22 (1967) 278.
3 C. Botre, E. Malizia, P. Melchiorri, A. Stacchini, G. Tiravanti and C. De Zorsi, European Soc. Toxicol. 19th Meeting, Copenhagen, 1977.
4 J. R. Grove, in M. Branica and Z. Konrad (Eds.), Lead in the Marine Environment, Pergamon Press, Oxford, 1980, p. 45 ff.
5 P. Grandjean and T. Nielson, Resid. Rev., 72 (1979) 97.
6 S. R. Henderson and L. J. Snyder, Anal. Chem., 33 (1961) 1172.
7 F. G. Noden, in M. Branica and Z. Konrad (Eds.), Lead in the Marine Environment, Pergamon Press, Oxford, 1980, p. 83 ff.
8 K. Hayakawa, Jap. Hyg., 26 (1971) 377.
9 S. A. Estes, P. C. Uden and R. M. Barnes, Anal. Chem., 53 (1981) 1336.
10 Y. K. Chau and P. T. S. Wong, in G. G. Leppard (Ed.), Trace Element Speciation in Surface Waters and Its Ecological Implications, Plenum Publ., New York, in press.
11 J. W. Robinson, E. L. Kiesel and I. A. L. Rhodes, J. Environ. Sci. Health, A14 (1979) 65.
12 S. E. Birnie and D. J. Hodges, Environ. Tech. Lett., 2 (1981) 433.
13 M. P. Colombini, G. Corbini, R. Fuoco and P. Papoff, Annal. Chim. (Rome), 71 (1981) 609.
14 H. S. Shapiro and F. W. Frey, The Organic Compounds of Lead, Wiley, New York, 1968, pp. 288, 298.
15 Y. K. Chau, P. T. S. Wong and P. D. Goulden, Anal. Chim. Acta, 85 (1976) 421.
16 L. Newman, J. F. Philip and A. R. Jensen, Ind. Eng. Chem., Anal. Ed., 19 (1947) 451.
17 H. R. Potter, A. W. P. Jarvie and R. N. Markall, Wat. Pollut. Control, (1977) 123.
18 A. W. P. Jarvie, R. N. Markall and H. R. Potter, Environ. Res., 25 (1981) 246.
19 Y. K. Chau, P. T. S. Wong, G. A. Bengert and O. Kramar, Anal. Chem., 54 (1982) 246.
20 J. Stary, The Solvent Extraction of Metal Chelates, Pergamon Press, Oxford, 1964, pp. 156—161.
21 Y. K. Chau, P. T. S. Wong, O. Kramar, G. A. Bengert, R. B. Cruz, J. O. Kinrade, J. Lye and J. C. Van Loon, Bull. Environ. Contam. Toxicol., 24 (1980) 265.

Analytica Chimica Acta, 146 (1983) 219—226
Elsevier Scientific Publishing Company, Amsterdam — Printed in The Netherlands

FULLY AUTOMATED LIQUID CHROMATOGRAPHIC SYSTEM FOR THE DETERMINATION OF HYDROCHLOROTHIAZIDE IN BLOOD PLASMA AND SERA

ROBERT WEINBERGER* and TONY PIETRANTONIO
Technicon Industrial Systems, Tarrytown, NY 10591 (U.S.A.)
(Received 23rd March 1982)

SUMMARY

A fully automated high-performance liquid chromatographic system for the determination of hydrochlorothiazide in sera or plasma is described. The technique is based on segmented-stream, continuous-flow sample preparation coupled to a liquid chromatograph. The sample preparation involves solvent extraction of plasma with chloroform/isopropanol/ethyl acetate (2:1:1). The extract is evaporated to dryness, reconstituted in aqueous solvent, and injected into the chromatograph. Separation is achieved by paired-ion non-polar stationary phase chromatography on a C_8 column. The mobile phase is 20% acetonitrile in pH 7.5, 0.01 M phosphate buffer with 0.005 M tetrabutylammonium hydroxide, with a flow rate of 2.5 ml min^{-1}. Detection is at 272 nm. Relative standard deviations of 2.3—10.1% were obtained for drug concentrations in the range 1000—50 ng ml^{-1}. The limit of detection is less than 10 ng ml^{-1}. The throughput rate is 10 samples/h, and only 0.5 ml of sample is required for each assay.

Hydrochlorothiazide has been one of the most frequently prescribed diuretic and anti-hypertension agents for over two decades. In spite of its long history of use, it is often necessary to perform comparative bio-availability studies in humans to insure the continuing quality and efficacy of the tablet dosage form. Several methods have been used to quantify the drug in biological fluids: colorimetry [1], thin-layer chromatography [2], gas chromatography [3], and more recently, various forms of high-performance liquid chromatography [4—8]. All of these methods have in common substantial sample preparation steps prior to the final quantitative measurement. The liquid chromatographic assays do not employ the selectivity of secondary equilibria, thus necessitating multiple extractions to obtain clean chromatograms.

Segmented-stream, continuous-flow systems have been used as sample preparation devices for the liquid chromatograph for quantifying theophylline [9], anti-convulsant drugs [9], and tricyclic anti-depressants [10] in sera. Factors influencing the precision of these systems have been described [11,

*Present address: Department of Chemistry, Seton Hall University, South Orange, NJ 07079, U.S.A.

0003-2670/83/0000-0000/$03.00

12]. This paper reports an application of this technology for quantifying hydrochlorothiazide in plasma or sera. The method utilizes solvent extraction, evaporation to dryness, and paired-ion chromatography on a non-polar stationary phase, with all parts linked together in an integrated system. Substantial improvements in both the sampling methodology and the chromatography of thiazides are provided. A bio-availability profile utilizing the new technique is reported.

EXPERIMENTAL

Apparatus

A Technicon FAST · LC System consisting of sample preparation and high-performance liquid chromatographic (h.p.l.c.) modules was utilized. The sample preparation portion required a liquid Sampler IV, Proportioning Pump III, Evaporation-to-Dryness Module and a sample processing cartridge, the design of which is shown in Fig. 1. The output from the cartridge flows to a six-port pneumatically activated valve equipped with a 500-μl loop. The chromatograph was equipped with a 15-cm, 4.6-mm i.d. non-polar stationary (reverse) phase column (Tricyclics C_8). A variable wavelength ultraviolet detector, operated at 272 nm, was used to monitor the column effluent. The entire system was synchronized with the microprocessor-based FAST · LC Programmer.

Solutions and reagents

Mobile phase. The mobile phase consisted of 20% acetonitrile and 80% 0.1 M phosphate buffer (pH 7.5) with 0.005 M tetrabutylammonium hydroxide (TBAH). The flow rate was 2.5 ml min^{-1}.

Pickup reagent for evaporation-to-dryness module. A variation of the mobile phase containing 10% acetonitrile was used to redissolve the residue

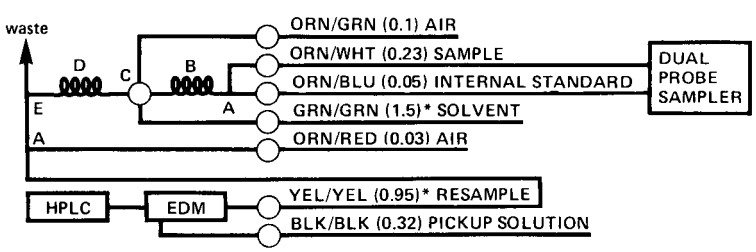

Fig. 1. Simplified flow diagram of sample treatment system. A, 1-mm i.d. glass T; B, 1-mm i.d. 5-turn coil; C, PT 16 fitting; D, 90-turn 0.86-mm i.d. polyethylene coil; E, 3.2-mm i.d. polypropylene T phase separator. Acidflex pump tubing is asterisked; other tubes are tygon. Numbers in parentheses refer to flow rates in ml min^{-1}. The hydraulic connections to the h.p.l.c. sampler and evaporation-to-dryness module (EDM) wash stations are not shown.

after the evaporation step. This facilitated "solvent focusing", thereby reducing band broadening from the large (0.5 ml) injection.

Reagents. Hydrochlorothiazide was obtained from Merck and Company, Rahway, New Jersey. Hydroflumethiazide was from Ayerst, Rousses Point, New York. Chloroform, ethyl acetate, isopropanol, acetonitrile and methanol were h.p.l.c. grade (Fisher Scientific) or Photrex (J. T. Baker). Bromocresol purple, dipotassium hydrogenphosphate and TBAH (40% in water) were from Baker. The extracting solvent consisted of 25% ethyl acetate, 25% isopropanol and 50% chloroform. All water was deionized. A 5% sodium hypochlorite solution (Chlorox) was used for cleaning the cartridge.

Internal standard preparation. A stock solution (0.5 mg ml^{-1}) of the internal standard hydroflumethiazide was prepared in methanol. This solution was further diluted with water to the working concentration of 5 $\mu g\ ml^{-1}$.

Standard preparation. Plasma standards were prepared from a primary stock solution containing 200 $\mu g\ ml^{-1}$ hydrochlorothiazide. Secondary stock solutions, 40-fold more concentrated than the working solutions were prepared in water. The final standards were prepared by adding 250 μl of the secondary stock solutions to 9.75 ml of plasma. Plasma standards containing 0—1000 ng ml^{-1} were prepared in this manner.

Bio-availability profile. A volunteer was administered orally, one 50-mg tablet of Hydrodiuril (Merck & Co.). Blood samples were drawn at intervals of 0, 1, 2, 3, 4, 5, 6 and 24 h post dosage and collected in Red-Top and Purple-Top Vacutainers and centrifuged. The resulting plasma and sera were stored frozen for processing on the following day.

Procedure

The temperature and vacuum controls of the evaporate-to-dryness module are adjusted to establish complete evaporation of solvent and the system is allowed to equilibrate for at least 20 min. To ensure injection into the h.p.l.c. at the proper time, the lag time of the system, from sample pick-up to the time when the extract reaches the injection loop, must be measured. This phasing is done visually by following the color of a 0.2% bromocresol purple solution as it travels through the system. Once this time is known ($\approx$9 min), it is entered into the injection feature of the system programmer. The internal standard solution, which is dispensed along with the sample, is phased in a similar fashion except that a water-soluble ink solution is employed and the length of the transmission tubing is adjusted to provide for mixing with the sample prior to entry into the cartridge. Note that two cups and two probes are used for each assay to contain the sample and internal standard.

Standards and samples are run at the rate of 10 h^{-1}, with a sample-to-wash ratio of 1:2 (sample time is 2 min). The peak height ratio of hydrochlorothiazide to hydroflumethiazide is used for all calculations.

The system is cleaned at the end of the daily run with hypochlorite by pumping the reagent through all lines for 10 min, with subsequent rinsing of the solvent line with methanol and other lines with water.

RESULTS

Typical chromatograms for the quantification of hydrochlorothiazide in human plasma are shown in Fig. 2. The chromatograms of plasma samples to which a standard amount of hydrochlorothiazide was added indicate no interference from endogenous plasma constituents and baseline resolution of all important peaks. The regression equation for plasma calibration data is $R = (1.52 \pm 0.003)C$ (pg ml^{-1}) + 0.0006 ± 0.002 with SE = 0.00297 and r = 0.999 where R is the peak height ratio, C is the hydrochlorothiazide concentration, SE is the standard error of estimate and r is the correlation coefficient.

The relative standard deviations (RSD) over a wide range of concentrations were as follows. For plasma concentrations of 1000, 500, 100 and 50 ng ml^{-1} hydrochlorothiazide, RSDs of 2.3, 4.3, 8.1 and 10.1% were obtained, respectively, for combined day-to-day and within-day imprecision. This corresponds to respective uncertainties of 23, 21.5, 8 and 5 ng ml^{-1} throughout the concentration range. The limit of detection for hydrochlorothiazide in plasma is less than 10 ng ml^{-1}.

Absolute recovery of material is difficult to define with certainty because of the potential for several non-stoichiometric operations during the course of the sample preparation. These include incomplete recovery of the organic phase after the extraction (necessary to prevent aspiration of aqueous waste), and incomplete removal of material from the moving wire of the evaporation-

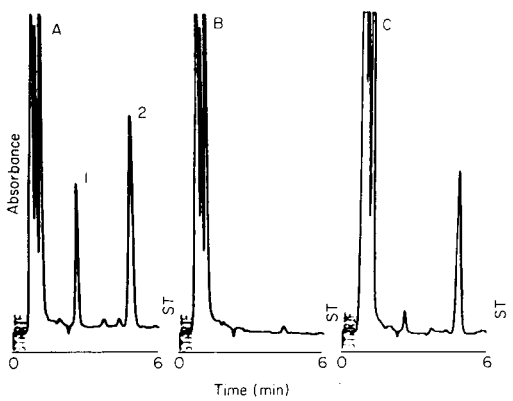

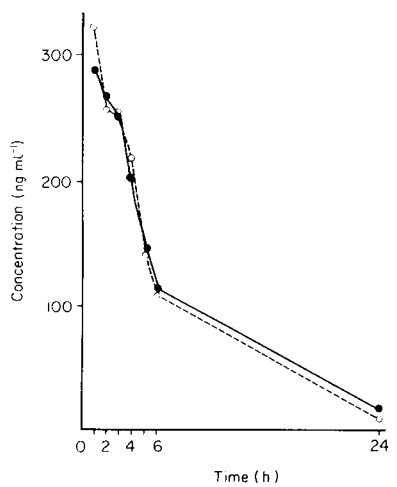

Fig. 2. Representative chromatograms: A, 400 ng ml^{-1} hydrochlorothiazide in plasma; B, plasma blank; C, 100 ng ml^{-1} hydrochlorothiazide in plasma. (1) hydrochlorothiazide; (2) hydroflumethiazide.

Fig. 3. Hydrochlorothiazide levels in the plasma and serum of a human volunteer after oral administration of a 50-mg dose: (○) plasma level; (●) serum level.

to-dryness module. Experience has shown that these potential sources of error are unimportant, as samples and standards are treated identically by the automated system with a repeatability that would be impractical to accomplish by manual techniques. To compensate for non-stoichiometry and to increase precision and reliability, the selection of an appropriate internal standard is necessary. It was found that hydroflumethiazide had similar extractive and chromatographic properties as hydrochlorothiazide, which recommended its selection as the internal standard. Recovery of hydrochlorothiazide and hydroflumethiazide from plasma versus aqueous external standards was 85 and 87%, respectively. The system thus configured provides for complete compensation of recovery owing to matrix uniformity and the presence of the internal standard in all standard and sample preparations.

A bio-availability profile of hydrochlorothiazide in a human volunteer was obtained for both plasma and serum samples. The results of this study (Fig. 3) were consistent with those previously reported [2, 7, 8, 13]. There were no significant differences between the plasma and sera results.

DISCUSSION

Sample preparation

Conventional manual h.p.l.c. methods for hydrochlorothiazide in plasma rely on a hydrocarbon clean-up, followed by an ethyl acetate extraction. Because the reliability of automated systems is enhanced by simplicity, a single extraction step was developed. This necessitated chromatographic improvements because some selectivity might be lost.

The scheme used consisted of a single solvent extraction with a ternary mixture of 2:1:1, chloroform/ethyl acetate/isopropanol. These solvents were chosen to employ the favorable properties of each. Pure ethyl acetate cannot be pumped with conventional peristaltic pump tubes as it attacks all common materials. Chloroform served to dilute the ethyl acetate and raised the density of the blend which facilitated phase separation. The isopropanol served to reduce and disperse the protein precipitate and, being miscible in both phases, enhanced mass transport. Such solvent blends seem to have been under-utilized in solvent extraction.

Manifold materials were chosen and connected to prevent the protein precipitate from adhering to surfaces. The coils and phase separator were made from polyolefins, which remained free of protein coating. The fitting where sample and solvent were mixed had a dead volume in the microliter range; thus the sample and solvent mixture entered the extraction coil before precipitation could occur. The system as described operated for eight hours without requiring clean-up.

The evaporation step is performed with a commercially available module, the design and operation of which has been described [9]. Extract is deposited on the moving wire at a rate of 0.92 ml min^{-1} and the residue is redissolved with the pick-up reagent at a flow rate of 0.32 ml min^{-1}. However, the

degree of concentration is not necessarily three-fold because of dispersion within the pick-up station. This dilution effect is minimized by providing for solvent flow countercurrent with the motion of the moving wire.

If additional sensitivity is required, the moving wire can be temporarily stopped to allow sample to build up in a concentrated band, and then restarted. Preliminary studies have yielded a three-fold increase in response without any other changes. This feature is limited by lipid build-up, which would eventually prevent dissolution of the solute at the pick-up station.

Chromatography

The chromatographic properties of hydrochlorothiazide and other thiazides have not been adequately explored. Previous studies [4, 8, 13] have concentrated primarily on the sample preparation steps to obtain clean chromatograms. It was thought that additional selectivity could be obtained by optimizing the separation, and the results of these studies are shown in Table 1. The experiments focused on how mobile-phase modifiers and ion-pairing reagents influence the chromatographic capacity factor, k', of hydrochlorothiazide.

When a mobile phase of 20% acetonitrile was used, more retention was obtained than with 10% methanol. This was surprising but could be rationalized on inspection by the fact that the sulfonamide group on hydrochlorothiazide is highly polar and an excellent hydrogen bonder. With a good proton donor such as methanol as the mobile-phase modifier, it is likely that its interaction with hydrochlorothiazide inside the stationary phases decreases the partition coefficient of the drug. Acetonitrile, being aprotic, has decreased interaction with hydrochlorothiazide, and competes less strongly for hydrochlorothiazide compared with the stationary phase, resulting in increased retention. Once the appropriate mobile-phase modifier was chosen, additional selectivity was sought by using paired-ion chromatography.

TABLE 1

Effect of mobile-phase modifier and ion-pairing agent on the capacity factor of hydrochlorothiazide

Mobile-phase modifier	Ion-pair reagent	Capacity factor
10% methanol	None	1.7
	Octanesulfonic acid	1.7
20% acetonitrile	None	2.4
	Octanesulfonic acid	2.4
	TBAH	3.2
	TBAH[a]	3.2
	HDTMAB	4.2
	HDTMAB[a]	5.8
	HDTMAB[a]	6.5

[a]Replicate injection immediately after previous run.

With octanesulfonic acid as the ion-pairing agent at pH 3, no increase in retention was noted with either mobile phase. Based on the sulfonamide group, ion-pairing at pH 7.5 with quaternary ammonium salts was attempted. Increased retention with tetrabutylammonium hydroxide (TBAH) and hexadecyltrimethylammonium bromide (HDTMAB) was noted. Although greater selectivity from plasma excipients was found with HDTMAB, TBAH was chosen because the equilibration time was short. This was due to substantial retention of HDTMAB with 20% acetonitrile while TBAH was essentially unretained. Although the extra selectivity could have been advantageous, it was unnecessary for the determination of hydrochlorothiazide. However, HDTMAB might be better suited to the determination of chlorothiazide, a thiazide that is poorly retained. The mobile phase can be adjusted for highly lipophilic thiazides such as trichloromethiazide simply by increasing the acetonitrile content.

An appropriate internal standard was sought. The order of elution of the drugs studied was chlorothiazide, hydrochlorothiazide, hydroflumethiazide, methyclothiazide and trichloromethiazide, which is consistent in terms of the structural properties of each drug. The hydroflumethiazide window was free from artifacts and was well resolved from hydrochlorothiazide. The dual-probe mode of addition of the internal standard was automatic and provided for system reliability by dispensing the standard simultaneously with the sample.

Because this totally automated procedure was designed for bio-availability studies, extensive drug interference studies were not done; such studies are generally undertaken on healthy individuals not on other medications. However no interferences were found for xanthines such as theophylline or caffeine.

The authors thank Professor L. J. Cline Love of Seton Hall University for her invaluable critique and suggestions towards this manuscript. This work was presented in part at the American Pharmaceutical Association Academy of Pharmaceutical Sciences, 31st National Meeting in Orlando, Florida, November 1981.

REFERENCES

1 H. Sheppard, T. F. Mowles and A. H. Plummer, J. Am. Pharm. Assoc. Sci. Ed., 49 (1960) 722.
2 M. Schofer, H. G. Geissler and E. Mulshler, J. Chromatogr., 143 (1977) 615.
3 E. Redalieu, V. V. Tienis and W. E. Wagner, Jr., J. Pharm. Sci., 67(5) (1978) 727.
4 M. J. Cooper, A. R. Sinaiko, M. W. Anders and B. L. Mirkin, Anal. Chem., 48(8) (1976) 1110.
5 P. A. Tisdall, T. P. Moyer and J. P. Anhalt, Clin. Chem., 26(6) (1980) 702.
6 J. D. Henion and G. A. Maylin, J. Anal. Toxicol., 4 (1980) 185.
7 W. T. Robinson and L. Cosyns, Clin. Biochem., 11(4) (1978) 172.
8 R. H. Barbhaiya, T. A. Phillips and P. G. Welling, J. Pharm. Sci., 70(3) (1981) 291.

9 J. W. Dolan, Sj. van der Wal, S. J. Bannister and L. R. Snyder, Clin. Chem., 26 (1980) 871.
10 S. J. Bannister, Sj. van der Wal, J. Dolan and L. R. Snyder, Clin. Chem., 27 (1981) 849.
11 L. R. Snyder and Sj. van der Wal, Anal. Chem., 53 (1981) 877.
12 Sj. van der Wal and L. R. Snyder, Clin. Chem., 27 (1981) 1233.
13 S. J. Soldin, E. Hach, A. Pollard and A. G. Logan, Therapeutic Drug Monitoring, 1 (1979) 3

Analytica Chimica Acta, 146 (1983) 227—236
Elsevier Scientific Publishing Company, Amsterdam — Printed in The Netherlands

THE DETERMINATION OF TOLUENE DIISOCYANATE IN AIR BY HIGH-PERFORMANCE LIQUID CHROMATOGRAPHY WITH ELECTROCHEMICAL DETECTION

STEPHEN D. MEYER[a] and DENNIS E. TALLMAN*
Department of Chemistry, North Dakota State University, Fargo, ND 58105 (U.S.A.)
(Received 19th July 1982)

SUMMARY

A rapid method is described for determining toluene diisocyanate in air, based on a simultaneous collection/derivatization step followed by reverse-phase, high-performance liquid chromatography with electrochemical detection of the derivatized toluene diisocyanate. The toluene diisocyanate is derivatized using *p*-aminophenol and the separated products are detected amperometrically in the oxidative mode at a Kel-F—graphite composite electrode. Whereas the recovery of toluene diisocyanate from dynamic air samples is comparable to that obtained by other reported methods (75—80%), the chromatographic step is characterized by a detection limit of 94 pg of toluene diisocyanate injected, a linear working range to beyond 12 ng of toluene diisocyanate injected, and a relative standard deviation of less than 2%. The procedure described represents an improvement in detection limit with reduced sample handling, compared to other reported methods, and readily lends itself to an automated continuous monitoring approach.

Polyurethanes produced from toluene diisocyanate monomers are used extensively in the coatings and plastics industry. Very low atmospheric concentrations of such monomers can cause sensitization that may lead to respiratory deficiencies even when exposure is below the recommended time-weighted average concentration limit, and prolonged exposure may cause death [1]. The development of improved methods for determination of atmospheric toluene diisocyanate is, therefore, a worthwhile goal.

The current method of atmospheric sampling and quantitation of toluene diisocyanate recommended by the National Institute for Occupational Safety and Health involves the prior decomposition of toluene diisocyanate to its respective ureas [1], accomplished by drawing a specified volume of air through a glass impinger containing a nitro absorber solution. This absorber solution is then dried and the residue is dissolved in dichloromethane which is subsequently injected into a liquid chromatograph with a u.v. detector for quantitation of the derivatized toluene diisocyanate. This method provides an upper limit of determination dependent on the concentration of nitro reagent and a detection limit of 2 ng/injection for toluene diisocyanate.

[a]Present address: 3M Center, Building 260-6A, St. Paul, MN 55144 U.S.A.

Many other methods for sampling and quantitation of toluene diisocyanate have been summarized [1].

Electrochemical detectors have produced some of the lowest detection limits yet reported for high-performance liquid chromatography (h.p.l.c.). However, only those compounds can be detected which display electroactivity within the accessible potential range, which in turn is generally established by choice of electrode, eluent, and electrolyte. Frequently, compounds which lack electroactivity can be readily converted to electroactive compounds either before being applied to the column or after elution from the column but prior to entering the detector. Because detector potential can be adjusted to be insensitive to certain eluates which might otherwise interfere, lower column efficiency can often be tolerated which can result in reduced separation/measurement time. Liquid chromatography with electrochemical detection (l.c.e.c.) has been used to determine a variety of analytes at the nanogram to picogram level [2—7].

A recent report by Warwick et al. [7] suggested the use of 1-(2-methoxyphenyl)piperazine as a derivatizing agent for the l.c.e.c. determination of toluene diisocyanate (and other isocyanates) in air. While their approach yields a lower limit of detection (0.2 ng/injection) than the official method [1], the procedure still requires rather extensive sample handling prior to the l.c.e.c. step.

This report describes preliminary results of a promising method for determining toluene diisocyanate in air based on a simultaneous collection/derivatization step followed by reverse-phase separation and electrochemical measurement of the derivative. The toluene diisocyanate is derivatized with *p*-aminophenol and the chromatographed products are detected amperometrically in the oxidative mode at a Kel-F—graphite electrode [8—10]. This procedure reduces the detection limit and sample handling compared to other reported methods.

EXPERIMENTAL

Reagents

Reagent-grade *p*-aminophenol was sublimed at 0.7 mtorr and 110°C and stored under nitrogen at 5°C. The 2,4-toluene diisocyanate (Mondur TDS Grade II, >99%; Mobay Chemical Corporation, Polyurethane Division, Pittsburgh, PA) was used without further purification. Acetonitrile (Burdick and Jackson, Muskegon, MI) was u.v.-pure h.p.l.c. grade. Water was prepared as described previously [10]. Sodium dihydrogenphosphate (analytical-reagent grade) was dried at 120°C.

Mobile phases were prepared by dissolving an appropriate amount of the dihydrogenphosphate in water and diluting with acetonitrile to yield the desired percent acetonitrile in 0.05 M NaH_2PO_4.

The absorber solution was prepared by dissolving 0.0109 g of *p*-aminophenol (0.1 mmol) in 100 ml of acetonitrile. This solution was stable for at least a week with no special precautions taken.

Standard solutions of derivatized toluene diisocyanate were prepared by first dissolving 6.1 mg of 2,4-toluene diisocyanate in 10 ml of acetonitrile and then adding a 10-μl aliquot of this solution to 10 ml of absorber solution, yielding a solution containing the equivalent of 610 mg ml^{-1} toluene diisocyanate. Further dilutions with the absorber solution were made to give a series of standards covering the range 4.7—610 ng ml^{-1} toluene diisocyanate.

Equipment

The liquid chromatograph consisted of a Milton Roy Model 396 pump, a Rheodyne Model 70-10 injector with a 20-μl sample loop, a stainless steel Bourdon tube pulse dampener, a Rheodyne Model 7037 pressure release valve, a Rheodyne 7302 inline filter, a 0-5000 psi pressure gauge, and an Altex 15 cm × 4.6 mm i.d. Ultrasphere-octyl column with 5-μm particles. The electrochemical detector cell incorporated a 15% Kel-F—graphite (Kelgraf) working electrode as described elsewhere [8—10]. The potentiostat, constructed in-house, was a standard difference amplifier controller design. Chromatograms were recorded on a Fisher Recordall Series 5000 strip-chart recorder.

Cyclic voltammograms were recorded by using the potentiostat, a PAR 175 programmer (EG & G Princeton Applied Research, Princeton, NJ), an Omnigraphic 2000 recorder (Houston Instruments, Austin, TX), and a 15% Kelgraf working electrode [10] with a Pt counter electrode. All potentials in this work are reported vs. Ag/AgCl/3.5 M KCl.

Procedures

Air samples containing toluene diisocyanate were generated using the apparatus shown schematically in Fig. 1. Compressed air adjusted to a flow rate of 1 l min^{-1} was passed through Tygon tubing to two impingers placed in series. A suitable dilution of toluene diisocyanate in acetonitrile was injected by means of a hypodermic syringe into the apparatus through the Tygon tubing at point D (Fig. 1). The air stream passing over the small volume of

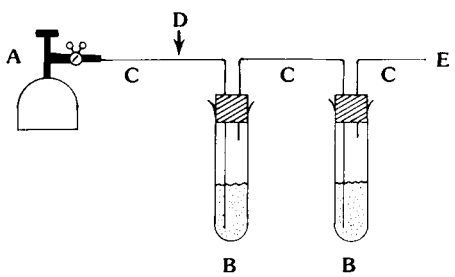

Fig. 1. Dynamic atmosphere generator and impinger system. A, Compressed air cylinder with flow regulator; B, 16 mm × 150 mm impinger tube with 5 mm o.d. inlet tube tapering to 1 mm i.d. near bottom of impinger tube, 5 mm o.d. outlet tube, rubber stopper; C, interconnecting 4.8 mm i.d. Tygon tubing; D, approximate location at which appropriate dilutions of toluene diisocyanate in acetonitrile are injected through the Tygon tubing; E, to vent.

this solution deposited on the inside wall of the tubing promoted slow and apparently complete vaporization of the toluene diisocyanate which was then carried to the impingers where it was trapped and derivatized by the absorber solution. For example, 5 μl of injected solution containing 3.0 μg of toluene diisocyanate requiring a flow of 10 l of air for complete vaporization would correspond to a dynamic air sample containing 300 $\mu g\ m^{-3}$ toluene diisocyanate.

The trapping efficiency of the absorber solution was determined by generating a toluene diisocyanate air sample at the 150 $\mu g\ m^{-3}$ level and passing this sample at a flow rate of 1 l min^{-1} to the two impingers in series, each impinger containing 10 ml of absorber solution. The sample flow was continued for 10 min after which the derivative in the solution in each impinger was quantified. This approach permitted an assessment of the extent of breakthrough of toluene diisocyanate from the first impinger to the second.

Impinger solutions were prepared by transferring the solution (originally 10 ml in volume, but now reduced in volume as a result of solvent evaporation during sampling) to a 10-ml volumetric flask, rinsing the impinger with 1 ml of acetonitrile which is added to the volumetric flask, and diluting to 10 ml with acetonitrile. Derivatized toluene diisocyanate in the resulting solution was determined by l.c.e.c. (20-μl injection) after calibration of the equipment with standard solutions prepared as described above. A detector potential of 1.25 V was used throughout.

RESULTS AND DISCUSSION

Existing methods for determination of atmospheric toluene diisocyanate require somewhat extensive sample handling, often including a rather slow evaporation to dryness step [1, 7]. Our initial efforts were directed towards developing a simplified, faster method for this determination which would be amenable to automation for eventual routine monitoring of industrial atmospheres. The relatively low cost of l.c.e.c. instrumentation combined with the potential for high analytical selectivity and low detection limits was attractive.

Because toluene diisocyanate is not electroactive under the experimental conditions used, it must be converted to an electroactive compound. Furthermore, it would be highly desirable if toluene diisocyanate could be stripped from the air sample and derivatized in one step. Amines are known to react rapidly with isocyanates [11, 12] and phenols have been shown to be amenable to l.c.e.c. detection [10]. Thus, *p*-aminophenol appeared to be an excellent candidate for a stripping/derivatization agent.

The nature of the p-*aminophenol derivative*

The electrochemical activities of *p*-aminophenol and the toluene diisocyanate adducts were investigated by cyclic voltammetry (c.v.); the results are displayed in Fig. 2. Alone, *p*-aminophenol exhibits a single oxidation peak (Fig. 2b) on the forward scan at 0.38 V and a reduction peak on the

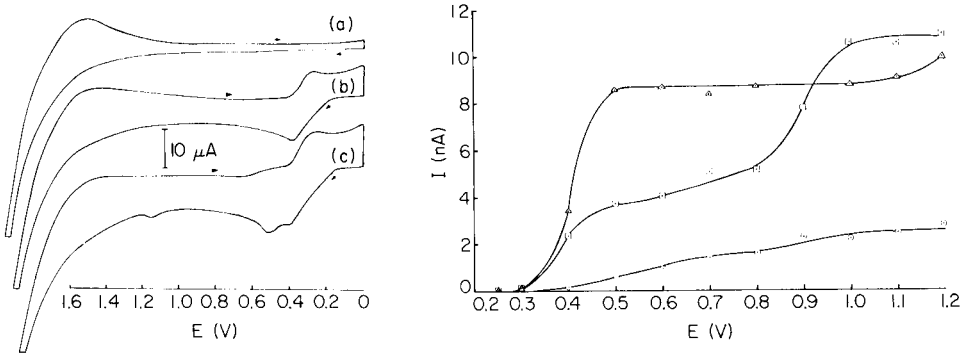

Fig. 2. Cyclic voltammetry of *p*-aminophenol and the adducts with toluene diisocyanate. Single scan starting at 0 V, 100 mV s^{-1} scan rate, 15% Kelgraf electrode. All solutions contained 0.05 M NaH_2PO_4, 30% acetonitrile. (a) Blank; (b) 1 mM *p*-aminophenol; (c) reaction mixture containing initially 1 mM *p*-aminophenol and 0.1 mM toluene diisocyanate.

Fig. 3. Hydrodynamic voltammetry of the adducts at a 15% Kelgraf electrode. Eluent composition 30% acetonitrile, 0.05 M NaH_2PO_4; flow rate 1.1 ml min^{-1}; 36 ng of total toluene diisocyanate (in 1 mM *p*-aminophenol) per 20-μl injection; curves correspond to chromatographic peaks of Fig. 4 as follows: (△) peak 1; (□) peak 2; (○) peak 3.

reverse scan with a ΔE_p of 110 mV. Further oxidation of *p*-aminophenol is not observed, even for potentials exceeding 1.50 V. Addition of toluene diisocyanate to the *p*-aminophenol solution gives rise to two new oxidation peaks (Fig. 2c) at 0.51 and 1.15 V in addition to the peak at 0.38 V attributed to excess of the phenol. In the absence of *p*-aminophenol toluene diisocyanate shows no electrochemical activity over the range of potential accessible in the solvent system used in this study. The two oxidation peaks which appear upon addition of toluene diisocyanate to *p*-aminophenol are believed to originate from at least two of the four predicted adducts which could result from the ability of toluene diisocyanate to react with either the —OH or the $-NH_2$ group of *p*-aminophenol. The structures of the four predicted adducts are displayed in Table 1. The high reactivity of toluene diisocyanate towards amines and alcohols [11, 12] and the large excess of *p*-aminophenol in these solutions should insure derivatization of both isocyanate groups while minimizing formation of molecules containing two or more toluene diisocyanate moieties. The peak at 0.51 V is assigned to oxidation of the phenolic substituents of adducts I and II while the smaller peak at 1.15 V is consistent with the oxidation of the substituted anilines or aryl carbamates [13, 14] of II and III. The observation of only two additional c.v. peaks following derivatization suggests that certain of the four adducts are not present at levels high enough to be observed by c.v. and/or the oxidations of the two substituents on each derivatized toluene diisocyanate occur independently of one another.

TABLE 1

Proposed structures and chromatographic peak assignments of derivatization products

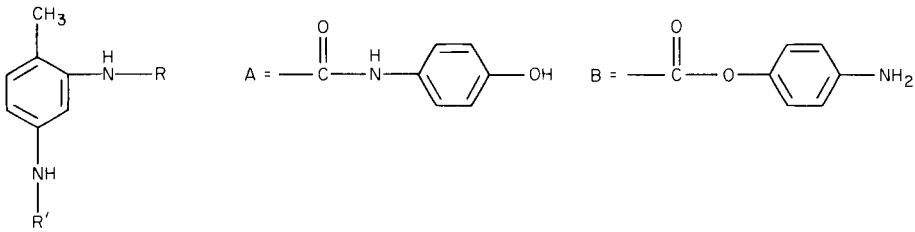

Compound[a]		R	R'	Chromatographic peak assignment[b]
I	2,4-Diamino-2*N*, 4*N*-bis(4-hydroxyphenylcarbamoyl)toluene	A	A	1
IIa	2,4-Diamino-2*N*-(4-hydroxyphenylcarbamoyl)-4*N*-(4-aminophenylcarboxyl)toluene	A	B	2[c]
IIb	2,4-Diamino-2*N*-(4-aminophenylcarboxyl)-4*N*-(4-hydroxyphenylcarbamoyl)toluene	B	A	3[c]
III	2,4-Diamino-2*N*,4*N*-bis(4-aminophenylcarboxyl)toluene	B	B	n.d.[d]

[a]In the text, compounds are referred to by number. [b]These numbers refer to the peaks in the chromatogram of Fig. 4. [c]These tentative assignments are based on the higher reactivity, hence lower selectivity, of the 4-position of toluene diisocyanate relative to the 2-position [11]. [d]n.d. not detected, see text.

The above interpretation of the c.v. results is corroborated by hydrodynamic voltammetry. Figure 3 illustrates the results obtained from multiple injections of a toluene diisocyanate—*p*-aminophenol standard; each chromatogram was recorded at a different detector potential and the chromatographic peak height for each of the three observed chromatographic peaks (see Fig. 4) was plotted against detector potential. Peak 1 (longest retention time) is characterized by a single wave with a plateau potential of ca. 0.5 V, believed to represent the independent oxidation of the two phenolic substituents of adduct I. Chromatographic peak 2 (and possibly 3) exhibits two waves (Fig. 3) with plateau potentials of ca. 0.5 V and 1.1 V, attributed to the oxidation of the 4-hydroxyphenylcarbamoyl and 4-aminophenylcarboxyl substituents, respectively, of the two isomeric forms of adduct II. These plateau potentials by hydrodynamic voltammetry are consistent with the previously assigned c.v. peak potentials. The smallness of peak 3 and its proximity to the solvent front preclude a reliable interpretation of its origin.

The higher reactivity of toluene diisocyanate with amines than with alcohols [12] might lead one to predict only very low yield of adduct III. Yet, the excess of *p*-aminophenol may serve to base-catalyze the reaction of

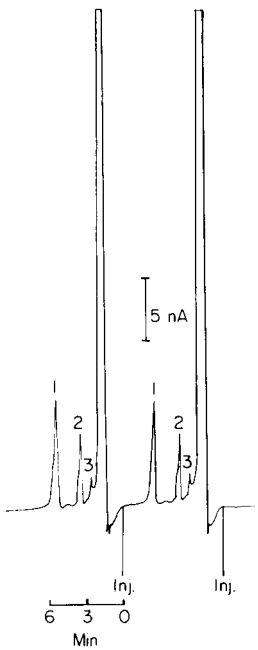

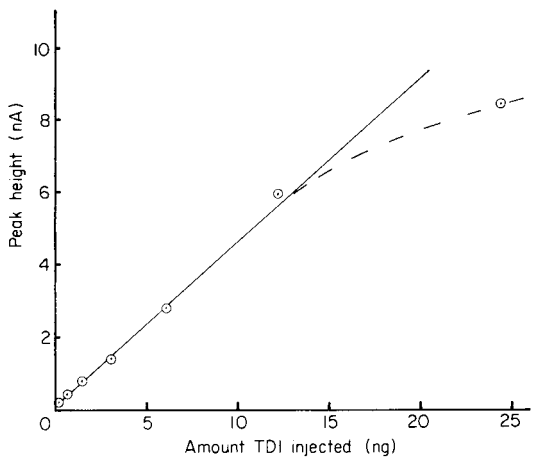

Fig. 4. Replicate chromatograms of the toluene diisocyanate—*p*-aminophenol absorber solution. Ultrasphere column; 0.05 M NaH_2PO_4, 30% acetonitrile; 1.1 ml min^{-1} flow rate, 1300 psi; E_{app} = 1.25 V, 15% Kelgraf electrode; 24.4 ng of toluene diisocyanate (total, all derivatized forms) injected. See text for proposed peak assignments.

Fig. 5. Calibration curve for peak 1 of the chromatogram. Chromatographic conditions as in Fig. 4.

toluene diisocyanate with the —OH group of *p*-aminophenol, giving rise to higher yields of adducts II and III than might otherwise be expected. The failure to observe a chromatographic peak which could be attributed to adduct III may be due to low yield of this derivative or may result from elution of this derivative with the solvent front. Indeed, the *p*-amino groups of the phenol and of adducts II and III will be extensively protonated under the elution conditions used, which explains the observed elution of the excess of *p*-aminophenol with the solvent front (Fig. 4). It would, therefore, be reasonable to expect adduct I to exhibit the longest retention, adduct II a somewhat shorter retention, and adduct III (the highest charged) the shortest (perhaps negligible) retention.

To assess the effect of water on the derivatization reaction, a 1 mM *p*-aminophenol absorber solution was made 120 mM in water and the chromatographic peak heights obtained from derivatization of 6.1 μg of toluene diisocyanate added directly to this absorber solution were compared to those obtained with water-free absorber solution. No significant difference in peak height for any of the three peaks in the chromatogram was observed. The

same ratios of chromatographic peak heights were obtained whether a given amount of toluene diisocyanate was added directly to the absorber solution as in preparation of the standard solutions or carried to the absorber solution by the air stream of the air sample generator, although all three peaks are somewhat reduced in amplitude for the latter approach (see later discussion).

Chromatography of absorber solutions

A detector potential of 1.25 V was used throughout this study to permit observation of all three chromatographic components with maximum sensitivity. However, for routine application of this method, only peak 1 attributed to adduct I need be detected and the detector potential could then be reduced to 0.6 V (see Fig. 3). The eluent conditions used were judged to be optimal in terms of peak separation and minimum time. As mentioned earlier, the excess of *p*-aminophenol exhibits negligible retention under these conditions and is eluted with the solvent front (Fig. 4). The separation between the *p*-aminophenol peak and the adduct peaks is sufficient to permit direct chromatography of the *p*-aminophenol absorber solutions, a distinct advantage over existing methods which require additional sample manipulations prior to chromatography [1, 7].

Chromatographic peak 1 was found to give the greatest linear working concentration range and the lowest detection limit and was used for quantifying toluene diisocyanate. A working curve based on this peak is displayed in Fig. 5. A limit of detection of 94 pg of toluene diisocyanate injected, based on a signal/noise ratio of two, is the lowest yet reported in spite of the formation of multiple derivatives and is adequate for routine quantitative work. The onset of nonlinearity in the working curve results from variation in the ratio of the adducts formed when derivatization is done at increasingly higher concentrations of toluene diisocyanate with a constant concentration of *p*-aminophenol. However, it should be emphasized that, when the procedure outlined herein is used, the linear portion of the working curve (<0.1 to >10 ng of toluene diisocyanate) encompasses the toluene diisocyanate levels most likely to be encountered in industrial air samples, and samples containing unusually high levels can be brought into the linear range by collecting a smaller volume of the sample. The precision of the determination over the range displayed in Fig. 5 is characterized by a relative standard deviation of 1.9%. The detector working electrode was routinely removed, inspected, and polished after each month of continuous use. In spite of the relatively high level of *p*-aminophenol injected into the l.c. no evidence of fouling was observed, suggesting that the detector could function unattended for periods of several weeks.

Determination of toluene diisocyanate in laboratory-generated air samples

The trapping efficiency of the *p*-aminophenol absorber solution for toluene diisocyanate was assessed by using two impingers in series. Three air samples, each containing the equivalent of 150 $\mu g\ m^{-3}$ toluene diisocyanate, were

generated and sampled as described earlier. In none of the three cases was toluene diisocyanate detected in the second impinger, indicating that the trapping efficiency of the first impinger is essentially 100%, and only one impinger would be required for collection in the field.

The percent recovery of toluene diisocyanate from air samples at the 30—300 $\mu g\ m^{-3}$ level was typically 75—80%. Similar recoveries from isocyanate atmospheres have been reported elsewhere [7] and the less than quantitative recovery has been attributed to reaction of toluene diisocyanate with water vapor in the air and/or to adsorption of the diisocyanate onto surfaces of the generation/collection apparatus [7]. It should be noted that reaction of toluene diisocyanate with atmospheric water vapor is not inconsistent with the earlier observation that water introduced into absorber solutions has no observable effect on distribution of derivatization products. Isocyanates are known to react with water but at a much lower rate than with amines or alcohols [11]. Thus the reaction of toluene diisocyanate vapor with atmospheric moisture is a kinetically favorable process (no competing reactions) whereas the reaction with water in the absorber solution is not. As in earlier studies [7], no attempt was made to dry the air used in generating the air samples because samples collected in the field would generally contain some moisture. The reaction of toluene diisocyanate with atmospheric moisture would produce the corresponding mono- or di-aminotoluene which would most likely elute with the solvent front under the chromatographic conditions used here. The detection of these products is under investigation.

For a 10-l air sample, the detection limit of this method is 5 $\mu g\ m^{-3}$ toluene diisocyanate. This detection limit is comparable to that obtained from methods which require preconcentration steps combined with h.p.l.c. and u.v. detection [1, 7] and is only a factor of about two higher than that (2 $\mu g\ m^{-3}$) obtained with another l.c.e.c. approach but also using a ten-fold preconcentration step [7].

Conclusions

The well established reaction chemistry of isocyanates with amines and alcohols [11], the observed distribution and chromatographic behavior of the reaction products, and the voltammetric data all strongly support our assignment of the derivatization products. The method described above should be applicable to the determination of other isocyanates in air and work in this area is continuing in this laboratory. A disadvantage of the approach is the formation of multiple derivatives which might lead to somewhat more complex chromatograms than obtained with existing methods applied to mixed isocyanate atmospheres. Most commonly, however, industrial air samples contain only one or perhaps two major isocyanates, and proper choice of elution conditions and detector potential should provide quantitatively useful chromatograms.

The principle advantage of the method compared to existing methods [1, 7] is considerably reduced sample handling prior to the chromatographic

step, without significant sacrifice in sensitivity. The simplicity of the method is attributed to the one-step stripping/derivatization reaction that is very rapid and complete and to the fact that unreacted *p*-aminophenol does not interfere in the subsequent chromatographic step.

The authors express their appreciation to Peter Markusch and Mobay Chemical Corporation for supplying the toluene diisocyanate used in this work.

REFERENCES

1 Occupational Exposure to Diisocyanates, Publication No. 78-215, U.S. Dept. of Health, Education and Welfare, Public Health Service, Center for Disease Control, National Institute for Occupational Safety and Health, Cincinnati, OH, 1978.
2 P. T. Kissinger, C. Refshauge, R. Dreiling and R. N. Adams, Anal. Lett., 6 (1973) 465.
3 C. Bollet, P. Oliva and M. Caude, J. Chromatogr., 149 (1978) 625.
4 D. N. Armentrout, J. D. McLean and M. W. Long, Anal. Chem., 51 (1979) 1039.
5 A. N. Strohl and D. J. Curran, Anal. Chem., 51 (1979) 1050.
6 K. Štulík and V. Pacáková, J. Electroanal. Chem., 129 (1981) 1.
7 C. J. Warwick, D. A. Bagon and C. J. Purnell, Analyst, 106 (1981) 676.
8 J. E. Anderson, D. E. Tallman, D. J. Chesney and J. L. Anderson, Anal. Chem., 50 (1978) 1051.
9 D. J. Chesney, J. L. Anderson, D. E. Weisshaar and D. E. Tallman, Anal. Chim. Acta, 124 (1981) 321.
10 D. E. Weisshaar, D. E. Tallman and J. L. Anderson, Anal. Chem., 53 (1981) 1809.
11 J. H. Saunders and K. C. Frisch, Polyurethanes: Chemistry and Technology, Part I, Chemistry, Interscience, New York, 1962.
12 S. G. Entelis and O. V. Nesterov, Russ. Chem. Rev., 35 (1966) 917.
13 D. J. Chesney and J. L. Anderson, Anal. Chem., 52 (1980) 2156.
14 G. E. Batley and B. K. Afghan, J. Electroanal. Chem., 125 (1981) 437.

Analytica Chimica Acta, 146 (1983) 237—241
Elsevier Scientific Publishing Company, Amsterdam — Printed in The Netherlands

SOLVENT EXTRACTION EQUILIBRIA OF URANIUM WITH 7-DODECENYL-8-QUINOLINOL

LIN ZHU[a] and HENRY FREISER*
Department of Chemistry, University of Arizona, Tucson, AZ 85721 (U.S.A.)
(Received 18th June 1982)

SUMMARY

Solvent extraction equilibrium constants in the system uranyl—7-dodecenyl-8-quinolinol (HL) in chloroform are reported. A mixed ligand complex is formed in the presence of acetate ion, $UO_2(OAc)L \cdot HL$, which adversely affects the extraction. In the absence of acetate, the extracted species is the self-adduct, $UO_2L \cdot HL$. The extraction is enhanced by 1,10-phenanthroline (phen) which forms $UO_2L_2 \cdot$ phen.

The study of the metal extraction equilibria of the higher molecular weight analogs of metal chelating extractants not only provides an interesting comparison with the parent compounds that sheds light on the role of the substituents in affecting reagent behavior, but also is essential in evaluating the efficacy of the reagents themselves in both micro and macro scale separations.

This report concerns the equilibria involved in the extraction of uranyl ion by 7-dodecenyl-8-quinolinol (DDQ). The study is part of a systematic evaluation of chelating extractants for the separation of individual lanthanides and actinides [1—6]. An earlier study, devoted to the behavior of DDQ with representative lanthanides [4], revealed that the high-molecular-weight extractant exhibited a marked decrease in self-adduct formation.

EXPERIMENTAL

7-Dodecenyl-8-quinolinol [7-(1-vinyl-3,3′,6,6′-tetramethylhexyl)-8-quinolinol; DDQ] is commercially known as Kelex 100 (Ashland Chemicals). It was purified by washing with 1 M hydrochloric acid [4]. The purity of DDQ was determined by converting it to its copper complex and determining the copper content by atomic absorption spectrometry.

To prepare uranyl stock solution, 1.004 g of $UO_2(NO_3)_2\,6H_2O$ (analytical reagent) was dissolved in a few milliliters of 6 M hydrochloric acid and the solution was evaporated to dryness. A few drops of concentrated hydrochloric acid was added and evaporation was continued until fuming was com-

[a] On leave from Sichuan University, Chengdu, Sichuan, People's Republic of China.

0003-2670/83/0000-0000/$03.00

plete. The residue was dissolved in 0.01 M HCl, and then diluted to 100 ml with 0.01 M HCl. The concentration of the uranyl solution was determined gravimetrically.

Chloroform (analytical grade) was purified by washing with water and distilling. All other reagents used were of analytical reagent purity.

An Eberbach box shaker with a shaking speed of 280 oscillations/min was employed to equilibrate the extraction mixtures which were contained in 50-ml screwcap glass vials fitted with polyethylene stoppers and plastic screwcaps. Absorbance measurements were made in a Gilford Model 2400 spectrophotometer and pH measurements were made using an Orion 701 pH meter. The experimental procedures for extraction were as previously described [4].

RESULTS AND DISCUSSION

The distribution of uranyl ion between aqueous buffer and DDQ in chloroform was examined as a function of the concentrations of uranyl ion UO_2^{2+}, pH, acetate ion, and DDQ. The distribution ratio was found to be independent of metal ion concentration in the range $10^{-3.5}$—$10^{-4.5}$ M, demonstrating the monomeric character of the extracted complex. In the range $10^{-1.8}$—$10^{-2.6}$ M DDQ, the slope of the log D vs. log $[DDQ]_0$ plot was constant at 2.1. The corresponding log D vs. pH plot from pH 5.5 to 6.5 had a slope of only 1.08, rather than the value of two expected from the formation of a simple 2:1 DDQ—UO_2^{2+} chelate. This problem was clarified by the observation of the dependence of D upon the acetate concentration. The adverse effect of acetate ion on the extraction can be explained by the formation of a series of uranyl acetate complexes from $UO_2(OAc)^+$ to $UO_2(OAc)_3^-$. Such complexing can be taken into account by utilizing the fraction of aquated uranyl ion concentration, α_U,

$$\alpha_U = \{1 + \sum_{i=1}^{3} \beta_i [OAc^-]^i\}^{-1} \quad (1)$$

where $\beta_1 = 10^{2.61}$, $\beta_2 = 10^{4.9}$, and $\beta_3 = 10^{6.23}$ [7], to correct the distribution ratio D. A plot of log D/α_U vs. log $[OAc^-]$ was approximately linear with a slope close to unity, demonstrating that a single acetate was incorporated in the extracted species. The extraction data are consistent with the following formulation of the reaction:

$$UO_2^{2+} + OAc^- + 2HL(0) \overset{K_{ex}}{\rightleftharpoons} UO_2(OAc)L \cdot HL(0) + H^+ \quad (2)$$

where HL represents DDQ.

The experimental results are summarized in Table 1. The good agreement of values of the extraction constant, (log $K_{ex} = 2.50 \pm 0.05$) calculated from all the data according to Eqn. (2), is seen to validate this formulation.

Extraction equilibria of uranium by DDQ in the absence of acetate exhibited different linear relationships. The slopes of log D vs. pH and log $[DDQ]_0$

TABLE 1

Extraction equilibria in presence of acetate buffer

Plot coordinates	Slope	log K_{ex}
Log D vs. log C^0_{HL}	2.1 ± 0.07	2.54 ± 0.08
Log D vs. pH	1.1 ± 0.02	2.43 ± 0.02
Log D vs. log C_M	0.0 ± 0.02	2.54 ± 0.03
Log D/α_v vs. log [OAc^-] (pH 6.04)	0.84 ± 0.07	2.53 ± 0.02
Log D/α_v vs. log [OAc^-] (pH 5.80)	0.74 ± 0.05	2.49 ± 0.02
		Mean 2.50 ± 0.05

were found to be close to 2.0 and 3.0, respectively (Table 2). Thus, the extraction equation

$$UO_2^{2+} + 3HL(0) \overset{K'_{ex}}{\rightleftharpoons} UO_2L_2 \cdot HL(0) + 2H^+ \quad (3)$$

satisfactorily explains the data, as seen by the low variability of the extraction constant (log $K' = -2.56 \pm 0.02$).

It is interesting to note that while the extraction of uranyl by DDQ occurs at a much lower pH in the absence of acetate, the value of K'_{ex} is lower than that of K_{ex}. In comparing uranium extraction in the presence and absence of acetate, it is useful to remember the composite nature of the extraction constant. It can be shown [6] that for K_{ex} of Eqn. (2),

$$K_{ex} = \beta_{(2)} K_{DC(2)} K_a / K^2_{DR} \quad (4)$$

where $\beta_{(2)}$ and $K_{DC(2)}$ represent the formation and distribution constants of the species UO_2 (OAc)L · HL, respectively, and K_a and K_{DR} are the acid dissociation and distribution constants of the reagent, respectively. Similarly, for K'_{ex} of Eqn. (3),

TABLE 2

Extraction equilibria in unbuffered solutions

Plot coordinates	C_{HL} or pH	Slope	$-\log K'$
Log D vs. pH	C_{HL}: 0.05 M	2.1 ± 0.03	2.56 ± 0.02
	0.04	2.0 ± 0.09	2.54 ± 0.03
	0.03	1.9 ± 0.17	2.60 ± 0.06
	0.02	1.8 ± 0.15	2.55 ± 0.05
Log D vs. log C^0_{HL}	pH: 3.80	2.9 ± 0.11	2.54 ± 0.06
	3.60	3.0 ± 0.10	2.57 ± 0.03
	3.40	3.0 ± 0.07	2.56 ± 0.02
			Mean 2.56 ± 0.02

$$K'_{ex} = \beta_{(3)} K_{DC(3)} K_a^2 / K_{DR}^3 \quad (5)$$

where $\beta_{(3)}$ and $K_{DC(3)}$ represent the formation and distribution constants of the species $UO_2L_2 \cdot HL$, respectively.

If Eqn. (3) is subtracted from Eqn. (2), the reaction

$$UO_2L_2 \cdot HL(0) + H^+ + OAc^- \overset{K_{(6)}}{\rightleftharpoons} UO_2(OAc)L \cdot HL(0) + HL(0) \quad (6)$$

is characterized by an equilibrium constant, $K_{(6)}$, given by

$$K_{(6)} = K_{ex}/K'_{ex} = [\beta_{(2)} K_{DC(2)}/\beta_{(3)} K_{DC(3)}] [K_{DR}/K_a] = 10^{5.06} \quad (7)$$

The large positive value of $K_{(6)}$ is, nevertheless, far smaller than that of K_{DR}/K_a for DDQ which is $10^{15.9}$ [4], signifying that the βK_{DC} product for the acetate-containing extractive species is lower than the other by a factor of $10^{10.8}$. A good part of this ($10^{7.4}$) can be explained by the difference between the formation constants of the uranyl complex of acetate ($\beta_1 = 10^{2.6}$) and DDQ (assumed to be close to that of 8-quinolinol, $\beta_1 = 10^{10}$), with the rest of the difference ($10^{3.4}$) attributable to the reasonable assumption tht the DDQ anion contributes more to the value of K_{DC} than does acetate anion.

In contrast to the behavior of DDQ with the lanthanides, the presence of the large 7-substituent does not eliminate the formation of self-adduct complexes [4]. For further comparison with the behavior of the lanthanides with DDQ, extractions were repeated in the presence of 1,10-phenanthroline (phen). In order to correlate the observed increase in extent of extraction obtained with phen, the entire increase in the value of D was attributed to the extraction of a mixed ligand complex. This increase, ΔD, was then subjected to the same slope analysis technique, i.e., $\log \Delta D$ vs. pH, $\log [HL]_0$, or phen to define the stoichiometry and equilibrium constant of the new species. As can be seen from a summary of the experimental data in Table 3, the following reaction expresses the results

$$UO_2^{2+} + 2HL(0) + phen(0) \overset{K''_{ex}}{\rightleftharpoons} UO_2L_2 \cdot phen(0) + 2H^+ \quad (8)$$

The value of this extraction constant, $10^{-2.50}$, is very close to that of the self-adduct complex, making it appear as if replacing the DDQ as monodentate adduct by the probably bidentate phen has no advantage. Thus, the equilibrium constant $K_{(9)}$, of the exchange reaction,

$$UO_2L_2 \cdot HL(0) + phen(0) \overset{K_{(9)}}{\rightleftharpoons} UO_2L_2 \cdot phen(0) + HL(0) \quad (9)$$

is given by $K_{(9)} = K''_{ex}/K'_{ex} = 10^{-0.06}$. Analysis of K''_{ex} and K'_{ex}, however, gives

$$K_{(9)} = K''_{ex}/K'_{ex} = [\beta_{(8)} K_{DC(8)}/\beta_{(3)} K_{DC(3)}] [K_{D(P)}/K_{DR}] \quad (10)$$

where the ratio of the distribution constants of phen ($K_{D(P)}$) and DDQ (K_{DR}) has a value of 10^{-2}. Inasmuch as the distribution constant of the phen complex is either equal to or less than that of the DDQ self-adduct, the value of $\beta_{(8)}$ is, therefore, at least $10^{2.5}$ times greater than $\beta_{(3)}$, indicating the bidentate

TABLE 3

Extraction equilibria in presence of phenanthroline

Plot coordinates		Slope	$-\log K$
Log D vs. pH (C^o_{phen} = 0.02 M) C^o_{HL}:	0.03	2.0 ± 0.14	2.39 ± 0.03
	0.02	1.6 ± 0.18	2.55 ± 0.04
	0.01	1.7 ± 0.20	2.40 ± 0.04
Log D vs. C^o_{HL} (C^o_{phen} = 0.02 M) pH:	4.0	2.0 ± 0.16	2.52 ± 0.06
	3.8	1.9 ± 0.16	2.44 ± 0.06
Log D vs. pH (C^o_{HL} = 0.02 M) C^o_{phen}:	0.03	1.6 ± 0.38	2.56 ± 0.05
	0.02	1.6 ± 0.18	2.55 ± 0.04
	0.01	1.8 ± 0.42	2.57 ± 0.07
Log D vs. C^o_{phen} (C^o_{HL} = 0.02 M) pH:	4.0	1.1 ± 0.06	2.59 ± 0.02
	3.8	1.2 ± 0.12	2.53 ± 0.04
			Mean 2.51 ± 0.07

binding of 1,10-phenanthroline to uranium. It should be further noted that, by using a 5- or 7-alkyl substituted phenanthroline which would result in a larger $K_{D(p)}$ without any significant change in $\beta_{(8)}$, then, in accord with Eqn. (10), the value of $K_{(9)}$, i.e., the advantage of the use of the alkyl-1,10-phenanthroline in this system, would increase substantially.

This project was supported by a grant from the Department of Energy.

REFERENCES

1 T. Hori, M. Kawashima and H. Freiser, Separ. Sci. Technol., 15 (1980) 861.
2 M. Kawashima and H. Freiser, Anal. Chem., 53 (1981) 902.
3 O. Tochiyama and H. Freiser, Anal. Chem., 53 (1981) 909.
4 E. Yamada and H. Freiser, Anal. Chem., 53 (1981) 2115.
5 O. Tochiyama and H. Freiser, Anal. Chim. Acta, 131 (1981) 233.
6 G. H. Morrison and H. Freiser, Solvent Extraction in Analytical Chemistry, Wiley, New York, 1957.
7 R. M. Smith and A. E. Martell, Critical Stability Constants, Plenum Press, New York, 1975.

Analytica Chimica Acta, 146 (1983) 243—248
Elsevier Scientific Publishing Company, Amsterdam — Printed in The Netherlands

APPLICATION OF PYROELECTRIC DETECTORS IN DIFFERENTIAL THERMAL ANALYSIS

HAMID RAHNAMAI*

The Moore School of Electrical Engineering, University of Pennsylvania, Philadelphia, PA 19104 (U.S.A.)

(Received 4th May 1982)

SUMMARY

The differential thermal detector described is based on a low-frequency, alternating-current heated pyroelectric crystal. The heat reduction from the sample electrode is measured during vaporization of a thin liquid film of sample. Equations are developed to represent the relationship between the measured signal and the properties of the material. The recorded thermogram is explained qualitatively. The detection limit of the device is estimated as about 1 microcalorie.

Differential thermal analysis (d.t.a.) provides a wide range of qualitative and quantitative information on material and chemical properties. Various aspects of d.t.a. have been studied extensively [1, 2]. In general, the sensor is a thermocouple which measures the temperature change resulting from heat generated or lost from the specimen. For a given specimen size, the accuracy of the differential signal and the detailed thermograms depend on such factors as the nature of the thermocouple, the sample holder, the rate of temperature rise, the thermal properties of the specimen, etc. While these instruments have been developed remarkably in many ways, they are not suitable for thermal measurements on extremely small (microgram size) specimens or thermal processes involving changes of the order of microcalories or less. Although d.t.a. of microgram samples is possible with a thermocouple [3], its applications are limited. Pyroelectric materials are suitable for this purpose. The extremely high sensitivity of these materials to changes in temperature provides useful devices for various applications [4—6].

The high temperature resolution ($<10^{-6}$ °C [3]) and the low noise equivalent power of the pyroelectric materials (10^{-8} W $Hz^{-1/2}$ [7]) in conjunction with the response to the time derivative of the temperature are the central features for the operation of the pyroelectric differential thermal detector. It is well known that the derivative technique of thermal analysis provides more detailed information than the conventional differential technique [2].

*Present address: INTELSAT, 490 L'Enfant Plaza, S.W., Washington, DC 20024, U.S.A.

Because the response of the pyroelectric material is proportional to the time derivative of the temperature, the pyroelectric detector actually provides results equivalent to the derivative thermal technique.

In the present study a differential thermal detector is fabricated with a lithium tantalate pyroelectric crystal. The heat exchange from the evaporation of a thin liquid film placed on the sample electrode is tested, and the detection limit of the device is assessed. Results are interpreted to find the relationship between the pyroelectric signal and the properties of the material.

EXPERIMENTAL

The pyroelectric material used was Czochralski-grown, z-cut lithium tantalate, obtained as plates with one side polished. The sample area was 5 × 8 mm^2 and the thickness of the plate was 0.099 mm. A mechanical evaporation mask was prepared by means of standard photolithography for the evaporation of nichrome electrodes and heater films. The films were 1 μm thick. A similar film 0.1 μm thick was evaporated onto the back surface to provide a ground contact for the pyroelectric charge measurement. The heater film resistance was about 300 Ω, and the electrode-heater separation distance was 0.25 mm. Aluminum wires were used to make electrical contacts by means of air-drying silver paste. Figure 1(a) shows a top view of the device and Fig. 1(b) shows the device mounted on two support wires.

For the measurements, an audio-frequency, low-power signal generator (Interstate Electronics Corporation) was used to supply the a.c. voltage to the heater resistor. The electrode signals were fed into a low-noise, high input impedance differential preamplifier, the output of which was connected to a lock-in amplifier. Because the frequency of the heat flow was twice the frequency of the applied voltage, the reference signal in the lock-in amplifier was set to the $2f$ mode.

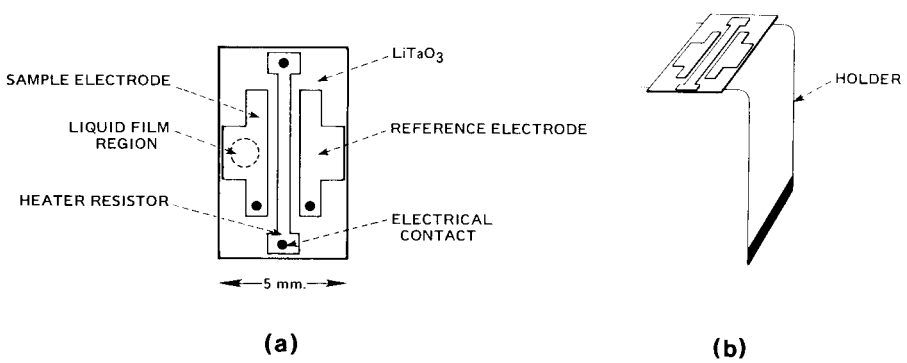

Fig. 1. Schematic diagram of the device: (a) top view; (b) holder assembly.

PRINCIPLE OF OPERATION

The thin film resistor evaporated on the surface of the pyroelectric plate serves as the heat source. The electrodes located symmetrically on either side of the heater serve as the sample electrode and reference electrode, respectively. An a.c. voltage at a frequency, f_0, applied to the heater resistor produces an alternating current with $2f_0$ frequency at the center of the pyroelectric plate. This heat diffuses symmetrically toward the electrodes. If the thermal diffusion time constant of the pyroelectric plate is smaller than $1/2f_0$, then the electrode temperature and so the pyroelectric plate voltage will vary with frequency $2f_0$. Experimentally, it was found that for $f_0 < 5$ Hz, the above condition was valid; for $5 < f_0 < 15$ Hz, the pyroelectric signal showed a complex time-dependence, and for $f_0 > 15$ Hz there was no signficant signal. The frequency dependence of the pyroelectric signal was similar to the frequency of lithium tantalate obtained from chopped thermal radiation [8].

In general, an exact theoretical treatment of the problem of heat exchange between the sample and the electrode is rather complex. A special case is considered below, however, in which the sample is a thin liquid film on the electrode, covering a small area of the electrode surface. When the sample evaporates, it removes heat from the electrode, thereby producing a corresponding signal.

The temperature of the pyroelectric plate, T_0, is considered to vary as follows:

$$T_0 = T + T_1 \sin \omega t \tag{1}$$

where ω is the angular frequency and t is time; T and $T_1 \sin \omega t$ are the d.c. and a.c. components of the temperature, respectively. For simplicity, the temperature variation across the plate under the sample is neglected here; this is valid if the sample size or the area of the liquid film is sufficiently small. When the liquid sample evaporates, the d.c. and a.c. components of temperature under the sample are reduced. (The temperature, T_0, is assumed to be low enough so that the film does not boil, i.e., there is no vapor layer at the film/electrode interface.) If the temperature at the interface with the liquid is T_i, and the temperature of the upper surface of the liquid film is T_d, it is assumed that T_i is greater than T_d. It is also assumed that the film is sufficiently thin that in the film region, $\partial T/\partial d \approx (T_i - T_d)/d$, where d is the film thickness; and furthermore, that the pyroelectric element has a sufficiently low thermal time constant, τ, that $\partial T/\partial t \approx (T_0 - T_i)/\tau$. With these assumptions, the heat flux transferred into the liquid is roughly

$$Q_1 = [A' k_1 (T_i - T_d)]/d \tag{2}$$

where k_1 is the thermal conductivity of the liquid and A' is the area of the liquid film. The heat flux lost from the pyroelectric element is roughly

$$Q_2 = [H(T_0 - T_i)]/\tau \tag{3}$$

where $H = A'b\rho c$ is the heat capacity of the pyroelectric element under the film; b, ρ and c are the thickness, density and specific heat of the pyroelectric material, respectively. The heat-balance condition at the interface requires that $Q_1 = Q_2$, or

$$[A'b\rho c\,(T_0 - T_i)]/\tau = [A'k_1\,(T_i - T_d)]/d \tag{4}$$

This equation, after substitution of the value of T_0 from Eqn. (1), yields

$$T_i = (T + T_1 \sin \omega t + \alpha T_d)/(1 + \alpha) \tag{5}$$

where $\alpha = (\tau k_1)/(b\rho cd)$. These equations are written for the initial state of evaporation, but are also valid for any instant during the period of evaporation.

The pyroelectric voltage response is given [8] by $V = (Pb/\epsilon\epsilon_0)\bar{T}$, where P is the pyroelectric coefficient, ϵ and ϵ_0 are the permittivity and the permittivity in vacuum, respectively, and $\bar{T}$ is the average temperature variation of the pyroelectric plate. With the measurement technique described above, only the a.c. component of the temperature, T_i, produces the pyroelectric signal. Thus, from Eqn. (5), $\bar{T} = T_1 \sin \omega t/(1 + \alpha)$, and the pyroelectric voltage is given by

$$V = (Pb/\epsilon\epsilon_0)\,[T_1 \sin \omega t/(1 + \alpha)] \tag{6}$$

This equation shows the relationship between the measured signal and the properties of the material. At the instant when the liquid film begins to evaporate, the film thickness, d, is a maximum, the value of α is a minimum, and consequently, V from Eqn. (6) is a maximum. Experimentally, when the sample droplet is placed on the electrode, the maximum signal is expected to appear a few seconds later. This time delay is due to the time needed for formation of the liquid film and due to the time, τ, necessary to remove heat from the electrode.

Equation (6) is useful if the magnitude of α (for the initial film thickness) is not much less than one. Otherwise, $(1 + \alpha)$ in Eqn. (6) will be approximately equal to one and so the signal, V, will have a constant value that is independent of sample properties. Thus, for a given set of device parameters (τ, b and c) and thermal conductivity of the liquid film (k_1), Eqn. (6) is beneficial if the initial film thickness is equal or less than the magnitude of $\tau k_1/b\rho c$.

RESULTS

Isopropanol was chosen for testing because it does not react with the lithium tantalate or the deposited nichrome film, it gives very low residues after vaporization (0.00005%), and it vaporizes rapidly at low temperatures. Isopropanol droplets were placed on the sample electrode (Fig. 1) with a microliter syringe. The input voltage applied to the heater resistor was set to a fixed value during the experiment. The initial temperature of the isopropanol

was 24°C and the initial electrode temperature after the input voltage had been applied was about 32°C.

Figure 2 shows the recorded differential signal vs. time for a 0.6-μl droplet and an input voltage of 2 V at a frequency of 2 Hz. The device sensitivity, defined as the ratio of the peak voltage to the total heat transferred from the sample electrode, was 3.6 V cal^{-1}. Because a differential signal as low as 1 μV was measurable, the minimum detectable amount of heat removed from the sample electrode was estimated to be 1 μcal. Although the data in Fig. 2 for 0.6-μl samples were reproducible, the peak area for smaller samples ($\leqslant$0.2 μl) varied slightly. The variation is attributed to the uncertainty in the volume of sample added rather than to the pyroelectric device.

In Eqn. (6), $T_1/(1 + \alpha)$ represents the time dependence of the signal amplitude. The initial value of α for the sample used here can be estimated. For a 0.6-μl sample, the diameter of the liquid film was about 2 mm. Therefore, the initial value for d is 1.9×10^{-2} cm. The initial value for τ is assumed to be 1 s (an approximate value for lithium tantalate wafers [8]), and $k_1 = 3.6 \times 10^{-4}$ cal s^{-1} cm^{-2} (K cm^{-1}) for isopropanol [9] $c = 3.19$ J cm^{-3} K^{-1} for $LiTaO_3$ [10], and $b = 9 \times 10^{-3}$ cm. When these values are used, the equation $\alpha = (\tau k_1)/b\rho cd$ gives $\alpha = 2.48$, which satisfies the requirements of Eqn. (6).

According to a theory developed by Toda [11], the liquid film thickness during the evaporation varies as $d = d_0(1 - t/\tau^*)^{1/2}$, where τ^* is the time necessary to evaporate the liquid film to dryness. Furthermore $\tau^* = d_0^2\lambda[2a_1 c_1(T_i - T_d)]^{1/2}$, where c_1 and λ are the specific heat at constant pressure and the latent heat of vaporization, respectively, and a_1 is the thermal diffusivity. Because $\alpha \gg 1$ during the evaporation, Eqn. (6) predicts that V is inversely proportional to α. (It is assumed that T_1 and τ do not change significantly during the evaporation). From this theory [11], the pyroelectric

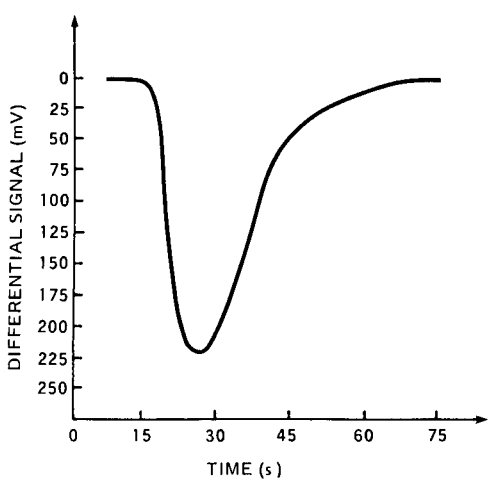

Fig. 2. Differential signal vs. time for 0.6 μl of isopropanol specimen. The input voltage to the heater resistor is 2 V and the frequency is 2 Hz.

signal, V, will be proportional to $(1 - t/\tau^*)^{1/2}$. The experimental result shown in Fig. 2 qualitatively agrees with this theory.

DISCUSSION

The evaluation of the device and comparison with existing d.t.a. equipment obviously require further study, but some aspects of the device and design considerations may be discussed. The pyroelectric detectors used in infrared technology have, in general, excellent reliability and their stability is comparable with that of semiconductor detectors. However, because of the ionic nature of most pyroelectric crystals, the integrity of pyroelectric detectors at elevated temperatures for d.t.a. applications may be unsatisfactory. If the material is unstable during extended use at higher temperatures, then the application of these devices in d.t.a. is limited to low and moderate temperatures.

The structure described in this study is useful if the width of the electrode is small and the temperature variation across the electrodes can be neglected. In such a case, the specimen size should be small. If, however, the heater resistor film is deposited on the whole back surface and the two electrodes remain on the top surface of the pyroelectric plate, the resistor will produce uniform heat across the entire plate. Consequently, the area of the electrode can be made large enough to accommodate larger specimens. Various design considerations and differential arrangements employed in d.t.a or differential scanning calorimeter instruments are also applicable to the pyroelectric-based system. The use of a uniform heat source over the entire plate has further advantages. The data obtained from the detector should be easily analyzed, because the heat transfer problem is much simpler and a theoretical equation can be derived easily.

Finally, the pyroelectric detectors must be operated at temperatures below the Curie temperature of the material (618°C for lithium tantalate [7]). The temperature limitation of these devices in d.t.a. is certainly a disadvantage. The advantages of the lithium tantalate device over other thermal detectors employed in d.t.a., are the high temperature sensitivity, the short response time, and the simplicity of device fabrication using integrated circuit technology.

REFERENCES

1 P. D. Garn, Thermoanalytical Methods of Investigation, Academic Press, New York, 1965.
2 W. W. Wendlandt, Thermal Methods of Analysis, 2nd edn., Wiley—Interscience, New York, 1974, p. 202.
3 C. Mazieres, Anal. Chem., 36 (1964) 602.
4 S. B. Lang and F. Steckel, Rev. Sci. Instrum., 36 (1965) 1817.
5 H. Rahnamai and J. N. Zemel, Sensors and Actuators, 2 (1981) 3.
6 H. Rahnamai, Anal. Chem., 54 (1982) 142.
7 H. P. Beeman, Infrared Phys., 15 (1975) 225.
8 C. B. Roundy and R. L. Byer, J. Appl. Phys., 44 (1973) 929.
9 Handbook of Chemistry and Physics, 60th edn., CRC Press, Cleveland, 1979, p. E-4.
10 S. T. Liu and D. Long, Proc. IEEE, 66 (1978) 14.
11 S. Toda, Heat Transfer, Jpn. Res., 3 (1974) 1.

Analytica Chimica Acta, 146 (1983) 249—253
Elsevier Scientific Publishing Company, Amsterdam — Printed in The Netherlands

Short Communication

UREA SENSOR BASED ON IRIDIUM DIOXIDE ELECTRODES WITH IMMOBILIZED UREASE

ROBERT M. IANNIELLO and ALEXANDER M. YACYNYCH*

Department of Chemistry, Rutgers, The State University of New Jersey, New Brunswick, NJ 08903 (U.S.A.)

(Received 28th May 1982)

Summary. An iridium dioxide electrode with immobilized urease is useful as a potentiometric detector for pH changes resulting from hydrolysis of urea at the electrode surface. Electrodes constructed by urease entrapment in a poly(vinyl chloride) film are superior to electrodes with urease covalently immobilized to the oxide layer via a cyanuric chloride linkage. Logarithmic response is obtained for the dip-coated electrode over the range 5×10^{-5}—5×10^{-3} M urea with a slope of −51 mV/decade. The slope remains constant for approximately 12 days. Recoating a stripped electrode with PVC-urease has essentially no effect on the slope.

Enzyme-coated potentiometric sensors are now well established. Immobilization procedures based on physical entrapment and cross-linking [1] as well as direct covalent attachment [2—4] have been used on a variety of electrode materials. It has been demonstrated [5] that an electrode can be fashioned by coating an antimony wire with urease. Such electrodes are attractive because of their simplicity of construction and potential for miniaturization.

Recently, pH sensors have been constructed by coating metal or glass substrates with oxides of palladium [6], tin [7], and iridium [8]. This communication reports the use of an iridium dioxide-coated metal as a pH-responsive electrode for monitoring enzyme-catalyzed reactions that produce pH changes. As an example, urease (EC 3.5.1.5) is immobilized on titanium thinly coated with iridium dioxide. The enzyme is immobilized by either physical entrapment in a poly(vinyl chloride) (PVC) film or direct covalent attachment via a cyanuric chloride linkage [4]. Changes in pH, caused by the enzyme-catalyzed hydrolysis of urea near the electrode surface, yield potentiometric response with logarithmic variation of urea concentration.

Experimental

Apparatus. A Corning Model 135 pH/ion meter connected to a Fisher Recordall Series 5000 strip-chart recorder was used for all potentiometric measurements. A single-junction saturated calomel electrode (SCE) served as the reference electrode. A calibrated glass combination electrode was used for pH measurements. The iridium dioxide electrodes were constructed from titanium rods (4 mm diameter, 5 cm long; Alfa Ventron, Danvers, MA)

sealed in glass tubing with Devcon "5 minute" epoxy cement. For electrical contact, mercury was placed between a copper wire lead and the electrode. All solutions were kept at 25.0 ± 0.1°C by immersion in a thermostated water bath during potentiometric measurements.

Reagents. Urease (Type IX, 85 I.U. mg^{-1}) and urea (crystalline) were obtained from Sigma Chemical Co. Poly(vinyl chloride) (secondary standard), tetrahydrofuran (Gold Label, 99.9%), and iridium(III) chloride trihydrate (99.9%) were obtained from Aldrich Chemical Co. Cyanuric chloride (purum grade; Tridom Chemical Co., Hauppauge, N.Y.) was used as received. Acetone was distilled from anhydrous potassium carbonate and stored over 4Å molecular sieve. Stock solutions of Tris-HCl buffer (0.1 M, pH 7.0) were prepared from reagent-grade materials. A series of Clark-Lubs buffer solutions [9] was used in the IrO_2—pH response experiments. Distilled, deionized water was used throughout. All other chemicals were of reagent grade.

Preparation of iridium dioxide electrodes. Segments of titanium rod (5 cm long) were machined to a diameter of 4 mm, primarily to remove any titanium oxide coating. The segments were then washed sequentially with hexane, distilled water, 6 M HCl, and distilled water and dried with a tissue. The segments were heated to 90°C and sprayed with a fine mist of iridium trichloride in distilled water. This film was allowed to dry, and the segments were heated at 400°C in air for 10 min. This procedure was repeated ten times after which the final layer was annealed at 400°C for 3 h. The resulting layer was black when dry and blue-black in aqueous solution, in accordance with the physical appearance of iridium(IV) oxide [10].

Preparation of urease—IrO_2 electrodes. Urease was immobilized onto the IrO_2-coated electrodes by two distinct procedures. Physical immobilization was accomplished by immersing the electrode in a stirred PVC—THF solution (20 mg of PVC/3 ml of THF) which contained 200 mg of finely powdered urease. The coating was dried for 10 min by rotating in a stream of nitrogen. This procedure was repeated ten times. Before use, the electrode was soaked in 5 mM, pH 7.0 Tris—HCl buffer for 1 h. When not in use, the electrode was stored dry at 2°C.

Covalent attachment of the enzyme was achieved by cyanuric chloride activation [4] of the IrO_2 layer. The electrode was first placed in stirred 2 M NaOH for 1 h, then treated with a solution of cyanuric chloride in acetone (0.5 g ml^{-1}) for 1 h, and washed three times each with cold anhydrous acetone, cold distilled water, and cold anhydrous acetone again. It was then treated with 50 ml of urease solution (6 mg of urease per ml of 0.1 M, pH 8.0 phosphate buffer) for 30 min, and washed with distilled water, 1 M NaCl and 0.1 M, pH 7.0 Tris—HCl buffer. The electrode was soaked in 5 mM, pH 7.0 Tris—HCl buffer (0.1% EDTA) for 30 min before use.

Standard solutions. A stock solution of 0.1 M urea was prepared fresh daily and used for preparation of all urea standard solutions by serial dilution. Unless otherwise stated, the working buffer was 5 mM, pH 7.0 Tris—HCl buffer, containing 0.1 M NaCl.

Standard solutions (50 ml) were allowed to reach thermal equilibrium by immersion in the water bath for 10 min. The urease electrode was then immersed in the quiescent solution and millivolt readings were recorded when steady state was obtained (3—5 min for the dip-coated electrode; 1—2 min for the chemically-modified electrode). Between trials, the electrode was rinsed with distilled water and immersed in the working buffer. Testing of the standard urea solutions was done only after the electrode potential had returned to its original (urea-free) value (2—3 min for the dip-coated electrodes; 1—2 min for the chemically-modified electrode). This procedure resulted in a total measurement time of approximately 10 min per sample.

Results and discussion

The method of preparation of the iridium dioxide layer is similar to that described by Ardizzone et al. [8]. In this study, however, aerosol deposition of iridium trichloride proved superior to dip-coating in that it was possible to obtain a thin layer. This is an important consideration in order to avoid slow equilibration due to diffusion of ions through the oxide layer. Thermogravimetric curves of $IrCl_3 \cdot 3H_2O$ show that rapid decomposition (oxide formation) occurs at temperatures above 600°C. However, oxide layers prepared at elevated temperatures are not homogeneous ("cracked" layers) [8, 11]. This is avoided when lower temperatures are used for oxide formation.

The potentiometric response of the IrO_2 electrode to solutions with pH between 3 and 12 was evaluated. The response was linear with a least-squares equation of E (mV) = $-(66.2 \pm 0.8)$ pH + (830.1 ± 0.5) mV with $r = 0.999$ and standard error of estimate of 8.7 mV. Potential readings were recorded at steady state, which was about 1—2 min for all solutions tested. The magnitude of response is similar to that observed previously [8]. However, the response time of the IrO_2 electrode in this study is much faster, presumably because of the thin, homogeneous oxide coating.

Calibration data for the urease electrodes prepared by both dip-coating and covalent attachment are shown in Fig. 1. Dip-coated electrodes displayed logarithmic response for urea concentrations in the range 5×10^{-5}—5×10^{-3} M. The response was linear with a least-squares equation of E (mV) = $-(51.0 \pm 3.6)$ log C + (29.3 ± 12.5) mV with $r = 0.988$ and standard error of the estimate of 5.8 mV. The covalently bonded urease electrode displayed less sensitive response [E (mV) = $-(23.2 \pm 0.8)$ log C + (157.3 ± 2.6) mV with $r = 0.996$ and standard error of estimate of 1.64 mV] over a slightly wider range (5×10^{-5}—1×10^{-3} M urea). These calibration curves represent the combined responses of five series of standard solutions for each electrode. The relative standard deviation (r.s.d.) of the response is about 1% (dip-coated electrode) to 5% (chemically-modified electrode). Potential drift for the dip-coated and chemically-modified electrodes was —0.1 to —0.2 mV min^{-1} and —0.3 to —0.5 mV min^{-1}, respectively. The reduced sensitivity of the dip-coated urease electrode compared to the bare IrO_2 electrode (77%) is

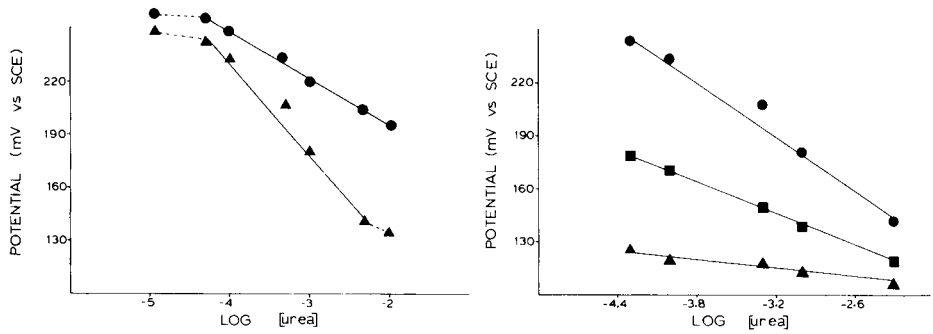

Fig. 1. Potentiometric response of the urease-coated electrodes to urea: (▲) PVC-coated; (●) covalently attached with cyanuric chloride.

Fig. 2. Potentiometric response of the dip-coated urease electrode to urea at different pH values: (●) pH 7.0; (■) pH 8.0; (▲) pH 9.0. Tris—HCl buffer (5 mM, 0.1 M NaCl) used for all solutions. Electrode slopes at pH 7, 8 and 9 are −51.0 ± 0.9, −30.2 ± 0.4, and −10.2 ± 0.9, respectively. The corresponding standard errors of estimate are 5.8, 0.7, and 1.9, respectively.

probably due to non-stoichiometric conversion of urea to ammonium ions caused by the thickness of the PVC membrane. In the case of the cyanuric chloride-modified electrode, however, the drastically lower sensitivity (35%) is most likely due to the blocking or consumption of a significant portion of the pH-active sites on the oxide layer by cyanuric chloride. As the linking agent reacts with available hydroxyl groups (or their salt form, —ONa) to effect the covalent linkage to the IrO_2 layer, those sites responsible for the pH response are probably consumed. The thin nature of the layer itself is actually a drawback (in terms of response magnitude) in the case of covalent enzyme attachment because of the limited amount of oxide present. Yet the thin enzyme layer has certain advantages in terms of better response and recovery times. Because of the relatively small response, however, covalent attachment is not advantageous here and was not investigated further.

The influence of pH on the potentiometric response of the dip-coated electrode was examined (Fig. 2). Maximum response is observed at pH 7.0, with severe attenuation at higher pH values. Experiments at pH $<$ 7.0 were not conducted because of the reduced activity of the enzyme in acidic solution [12]. The reduced response at pH $>$7.0 is probably due to two factors: urease displays maximum activity in the pH range 7.0—7.5 [12], and there would be some buffering effect from the presence of a basic solution at the electrode surface.

The effect of buffer concentration (pH 7.0) on the electrode response was evaluated for urea standards in 5 mM, 10 mM, and 100 mM Tris buffers. Drastic attenuation of the response was observed at buffer concentrations $>$5 mM (90% reduction in slope relative to 5 mM). As the ionic strength of all solutions was about the same (0.1 M NaCl), enzyme inhibition by salt

effects [13] cannot be considered as the cause of decreased response at elevated buffer concentrations. Clearly, buffer concentrations in excess of 5 mM negate the pH change at the electrode surface because of the increased buffer capacity of the solutions.

The feasibility of re-using the coated electrode as a potentiometric sensor was evaluated by stripping an enzyme-coated electrode (by immersion in THF) and recoating with urease—PVC. Recoated electrodes were also tested after 12 days storage (dry at 2° C). In all cases, the slopes and curve shapes were about the same, but shifted along the potential axis by ca. 15 mV. As the enzyme-recoating process did not significantly alter the response slope, the THF treatment cannot have destroyed the integrity of the oxide layer. While retention of enzyme activity under the defined storage conditions is indicated, the electrode lost its response after 8 days of storage in the working buffer. This may be due to enzyme denaturation and/or leaching from the PVC film. This is not a serious drawback, however, because of the ease of recoating of the oxide layer with enzyme.

A. M. Y. thanks Biomedical Research Support Grants, National Institutes of Health (grant GM 28125-01), and the National Science Foundation (grant CHE-8022237) for research support, and Rutgers University for a Junior Faculty Fellowship. R. M. I. is the recipient of the Joseph W. Richards Fellowship of the Electrochemical Society and acknowledges this financial support.

REFERENCES

1 P. W. Carr and L. D. Bowers, Immobilized Enzymes in Analytical and Clinical Chemistry, Wiley—Interscience, New York, 1980.
2 N. Yamamoto, Y. Nagasawa, M. Sawai, T. Sudo and H. Tsubomura, J. Immunol. Methods, 22 (1978) 309.
3 C. R. Lowe, FEBS Lett., 106 (1979) 405.
4 R. M. Ianniello and A. M. Yacynych, Anal. Chim. Acta, 131 (1981) 123.
5 P. W. Alexander and J. P. Joseph, Anal. Chim. Acta, 131 (1981) 103.
6 W. T. Grubb and L. H. King, Anal. Chem., 52 (1980) 270.
7 H. A. Laitinen and T. M. Hseu, Anal. Chem., 51 (1979) 1550.
8 S. Ardizzone, A. Carugati and S. Trasatti, J. Electroanal. Chem., 126 (1981) 287.
9 V. E. Bower and R. G. Bates, J. Res. Nat. Bur. Stand., 55 (1955) 197.
10 J. P. Hoare, The Electrochemistry of Oxygen, Wiley—Interscience, New York, 1968, p. 59.
11 G. Lodi, G. Zucchini, A. De Battisti, E. Silvieri and S. Trasatti, Mat. Chem., 3 (1978) 179.
12 N. D. Jespersen, J. Am. Chem. Soc., 97 (1975) 1662.
13 G. G. Guilbault, Enzymatic Methods of Analysis, Pergamon Press, Oxford, 1970, p. 17.

Analytica Chimica Acta, 146 (1983) 255—259
Elsevier Scientific Publishing Company, Amsterdam — Printed in The Netherlands

Short Communication

DETERMINATION OF α- AND β-LACTOSE IN DAIRY PRODUCTS BY TOTALLY AQUEOUS LIQUID CHROMATOGRAPHY

J. M. BEEBE and R. K. GILPIN*

IBM Instruments Inc., PO Box 332, Orchard Park, Danbury, CT 06810 (U.S.A.)

(Received 1st July 1982)

Summary. In the proposed method, the mobile phase is pure water and sample preparation requires only dilution and centrifugation steps. A total determination requires 15 min including sample handling. Total and anomeric ratios of lactose were determined in samples of yoghurt, milk, dry milk, and ice cream. The method variability was evaluated by using five milk samples, randomly selected from the same dairy; for each sample, 3—5 replicate chromatograms were obtained. The mean total lactose in these milk samples was 4.50% with a pooled standard deviation of 0.132%.

Lactose, which occurs naturally only in milk products, is currently of interest to the food industry as a natural sweetener. Successful determinations of lactose in milk products (milk, ice cream, and yoghurt) by both gas and liquid chromatography have been reported [1—9]. The major disadvantages of current methods are the time and complexity of sample preparation.

Lactose exists naturally in two forms, the α- and the β-anomers. Of the two anomers, the β-form is desirable because it is more soluble and sweeter. Lactose converts totally to the β-form if recrystallized at over 93.5°C [10]. Although the resolution of the α- and β-anomers of lactose has been reported [8], the procedure is time-consuming, including extraction and derivatization steps prior to gas chromatography.

The method described here has several advantages over those reported previously. First, glucose, β-lactose, α-lactose, maltose, and sucrose (in order of elution) are resolved in 13.5 min. The resolution of these sugars is important because glucose occurs as a decomposition product in the sample matrix; sucrose is added routinely to samples such as ice cream; and maltose is employed as the internal standard. The second, and perhaps most significant advantage, is that sample preparation requires only dilution with water followed by centrifugation. Lastly, the method is versatile and has been applied to a variety of different sample types (milk, yoghurt, ice cream, and dry milk) with little or no interference from matrix materials.

Experimental

Apparatus. The liquid chromatograph included an IBM Instruments Model LC/9521 isocratic modular pump and Model LC/9525 refractive index detector which was thermostated at 35°C with a Haake FE circulating bath. The

0003-2670/83/0000-0000/$03.00

mobile phase was 100% water at a flow rate of 0.7 ml min^{-1}. Samples were injected from a Model 7125 Rheodyne valve equipped with a 20-μl loop. For the separations, two octadecyl columns (IBM Instruments; 4.5 mm i.d. × 25 cm) were coupled and thermostated at 3.8° C with a Neslab Model EX-300 temperature bath and a Model DCR-1 digital controller. The samples were centrifuged on a Brinkman Eppendorf Model 5412 centrifuge.

Reagents. Acetonitrile (u.v. grade; Burdick and Jackson Laboratories) and other chemicals (Sigma) were used as received. All water was obtained from a Barnstead 4-module Nanopure purification system.

Procedure. Solutions for the standard calibration graphs were prepared by weighing accurately 100, 75, 50 and 25 mg of both lactose and sucrose into four 50-ml volumetric flasks. To each of these flasks, 5 ml of a 10 mg ml^{-1} maltose internal standard solution was added. The total volume was then brought up to 50 ml with water. In this manner, lactose and sucrose standards of 2.0, 1.5, 1.0 and 0.5 mg ml^{-1} were prepared. Each of these contained an internal standard (maltose) concentration of 1.0 mg ml^{-1}.

Samples of dry milk, yoghurt, cow's milk, and ice cream were prepared by accurately weighing 500 mg of each into 50-ml volumetric flasks. Next, 5 ml of maltose internal standard solution was added, and the total volume was brought up to 50 ml with water. After dilution, an aliquot (1 ml) of the sample solutions was placed in a tube and centrifuged at 15 000 rpm for 1 min. After centrifugation, 20 μl of the supernatant liquid was injected.

Column conditioning and regeneration. Initially, two columns in series were conditioned at room temperature with 50 ml of acetonitrile followed by approximately 100 ml of water. Ambient temperature was employed to facilitate conditioning speed. After conditioning, the columns were placed in the temperature bath and allowed to reach thermal equilibrium at 3.8° C; about 30 min was allowed for this. After about 50 assays, a residue formed on the leading frit of the first column. This deposit caused the system pressure to build slowly. When the system pressure reached an unacceptable level, the first frit was cleaned or replaced, and the columns were reconditioned as described above.

Results and discussion

Lactose exists in two mutarotational forms. If dissolved in solution, α-lactose and β-lactose interconvert to establish steady-state concentrations. The thermal dependency of the kinetics of this mutarotation was studied by using the above procedure. At temperatures near 0° C, the conversion was found to be sufficiently slow that it does not affect significantly, within the time frame of the reported chromatographic separations, the quantitative ratio of the isomeric forms.

Sample data. Representative chromatograms of the carbohydrate standards and samples of milk, yoghurt, and ice cream are shown in Fig. 1(a—d). The elution order and retention times for the sugars of interest are β-lactose at 8.5 min, α-lactose at 9.0 min, maltose, the internal standard, at 9.9 min,

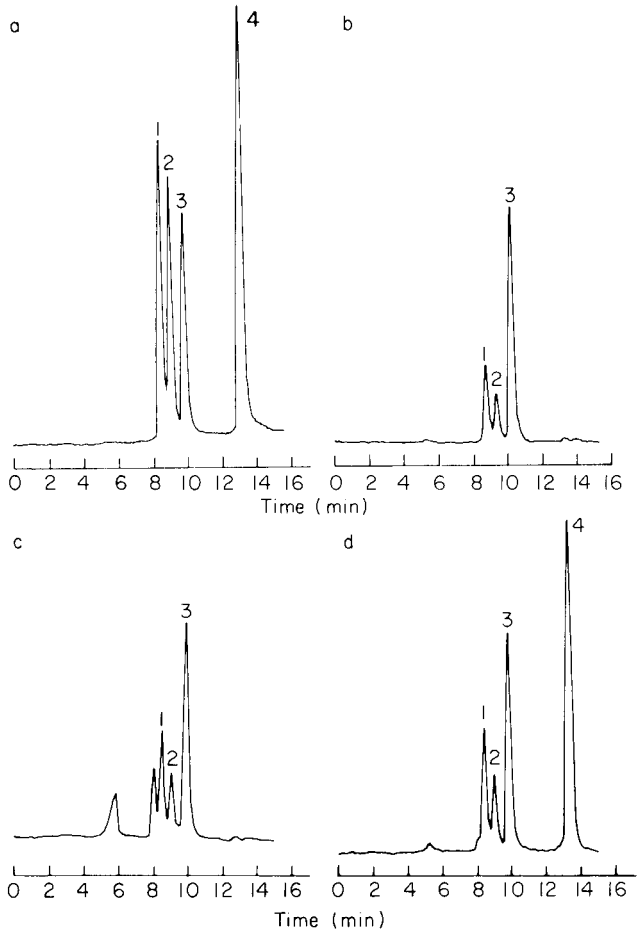

Fig. 1. Representative chromatograms from different samples: (a) standard mixture; (b) milk; (c) yoghurt; (d) ice cream. Peaks: (1) β-lactose; (2) α-lactose; (3) maltose (internal standard); (4) sucrose.

and sucrose at 13.5 min. In Fig. 1(b) is a typical chromatogram obtained from a milk sample. As expected, this sample contained only α- and β-lactose. The yoghurt sample (Fig. 1c) also contained α- and β-lactose, as well as two unidentified peaks, one eluting at 5.8 min and the second eluting at 8.0 min. The second peak is attributed to glucose and galactose, hydrolysis products of lactose. This is reasonable because glucose and galactose co-elute at a retention time of 8.0 min, and so do not interfere with the carbohydrates of interest. The sample of ice cream (Fig. 1d) contained α-lactose, β-lactose, and sucrose; sucrose is added routinely by the manufacturer to enhance product flavor. Of the four types of dairy products examined, only ice cream contained sucrose.

Levels of α-lactose, β-lactose, and sucrose in the various sample types were determined from the mean values of 3—5 replicates. The value of 4.48% total lactose for the milk sample is consistent with a literature range of 4.5—4.8% [7, 10]. Additionally, in milk, the β-form of lactose predominates over the α-form in a 3:2 ratio which is consistent with determined values of 62.2% and 37.8%, respectively. The 4.84% total lactose in yoghurt is in agreement with reported data ranging between 4.81 and 6.23% [9]. Likewise, the 6.12% lactose in ice cream is consistent with literature values of 6.0—6.7% (w/w) [6, 11]. When a sample of dry milk was analyzed, a value of 14.0% (w/w) lactose was obtained for the undiluted product. When the "instant dry" milk was prepared as recommended by the manufacturer, a solution containing 1.4% lactose resulted.

Method development. During the initial kinetic studies, the detector responses for α-lactose and β-lactose were found to be equal. This was based on the observation that the total integrated peak area for α- and β-lactose remained constant as the isomeric ratio varied. Shown in Fig. 2 are plots of area ratio using maltose as the internal standard versus (a) total lactose and (b) sucrose. The curves for both disaccharides were similar with slopes of 1.043 ± 0.036 (S_{yx} = 0.024) and 1.102 ± 0.054 (S_{yx} = 0.020), respectively. Likewise, the intercepts for these curves were nearly zero (0.051 ± 0.07 and 0.062 ± 0.102, respectively). The responses for both disaccharides were linear up to at least 2.0 mg ml^{-1}, which was the maximum concentration studied.

The method variability was evaluated by using five different milk samples selected at random from the same dairy over a period of 11 days, with 3—5 replicate determinations on each sample. The total lactose values ranged from 4.20 ± 0.06 to 4.62 ± 0.11% with a mean value of 4.50% and a pooled standard deviation of 0.204% for a total of nineteen trials.

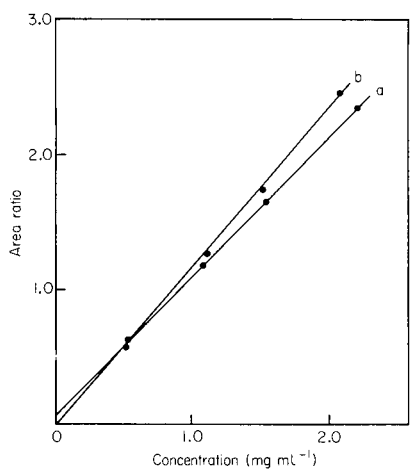

Fig. 2. Calibration graphs for area ratio vs. concentration: (a) lactose $y = (1.043 \pm 0.036)x + (0.051 \pm 0.07)$ with $S_{yx} = 0.024$ and $r = 1.000$; (b) sucrose $y = (1.102 \pm 0.054)x + (0.062 \pm 0.102)$ with $S_{yx} = 0.020$ and $r = 1.000$.

REFERENCES

1 J. R. Euber and J. R. Brunner, J. Dairy Sci., 62 (1979) 685.
2 J. S. Hobbs and J. G. Lawrence, J. Sci. Food Agric., 23 (1972) 45.
3 W. J. Hurst, R. A. Martin, Jr. and B. L. Zoumas, J. Food Sci., 44 (1979) 892.
4 H. O. Jaynes and T. Asan, J. Milk Food Technol., 36 (1973) 333.
5 J. G. Lawrence, Chimia, 29 (1975) 367.
6 J. J. Warthesen and P. L. Kramer, J. Food Sci., 44 (1979) 626.
7 S. Adachi and A. Yamagi, J. Dairy Res., 45 (1978) 127.
8 D. F. Newstead and I. K. Gray, N.Z. J. Dairy Sci. Technol., 7 (1972) 262.
9 L. Mouillet, F. M. Luquet and J. F. Boudier, Lait, 1 (1977) 37.
10 Merck Index, Merck, Rahway, NJ, 9th edn., 1976, p. 5192.
11 L. J. Iverson and M. P. Bueno, J. Assoc. Off. Anal. Chem., 64 (1981) 139.

Analytica Chimica Acta, 146 (1983) 261—266
Elsevier Scientific Publishing Company, Amsterdam — Printed in The Netherlands

Short Communication

APPLICATIONS OF ION CHROMATOGRAPHY FOR DETERMINATION OF SELECTED ELEMENTS IN COAL AND OIL SHALE

R. A. NADKARNI* and D. M. POND

Analytical Research Laboratory, Exxon Research and Engineering Company, PO Box 4255, Baytown, TX 77520 (U.S.A.)

(Received 26th May 1982)

Summary. Ion chromatography is used to separate and quantify halogens, nitrogen, and sulfur in coal and oil shale samples after combustion in a Parr oxygen bomb. Accuracy and precision of the results as determined with NBS standards are ±10 and ±5%, respectively. Other applications of ion chromatography include the determination of sulfur species in wastewaters and leachates from coal.

Coal and oil shale are major fossil fuels. For processing purposes, and for assessing the environmental impact of coal and shale conversion, it is important to quantify the trace element levels in the source materials as well as in the end- and by-products. Anionic species have been determined in the past by miscellaneous techniques for individual elements [1]. With the availability of ion chromatography (i.c.) techniques, many of the anionic species in coal and oil shale related materials can be simultaneously determined with a single sample preparation. This communication describes the applications of ion chromatography for the determination of halogens, nitrogen, sulfur, and some other heteroatoms in coal and oil shale derived materials.

Experimental

Equipment. A Dionex ion chromatograph model IC-14, with 4 × 50-mm anion concentrator, 4 × 250-mm anion separator, and 9 × 100-mm anion suppressor columns, was used. The injection loop was 100 μl and ions were detected with a conductivity meter. The most commonly used eluent was 2.4 mM Na_2CO_3 + 3.0 mM $NaHCO_3$ at a flow rate of 2.30 ml min^{-1}, but considerable variations from this were used when necessary for specific separations.

Oxygen bombs (Parr Instrument Company, Moline, IL) were used for sample decomposition [1]. Other instruments used included an ion meter (Orion Instruments), ion-selective electrodes, a polarograph (Princeton Applied Research), and an x-ray fluorescence system (Phillips).

Reagents and materials. Ultra high-purity reagents were used wherever possible. Water from a MilliQ deionizer (≈16 Mohm resistance) was used in all experiments. Stock solutions of anions (1 mg ml^{-1}) were diluted as

required. National Bureau of Standards and U.S. Geological Survey coal and oil standards were dried at 110° C in an air-oven for 4 h.

Combustion procedure. The procedure for combustion of coal and other organic materials in an oxygen bomb was as described earlier [1]. The coal or shale sample is mixed with white oil as a combustion aid and is burned in a bomb containing 5 ml of water and pressurized to 30 atm. of oxgyen. The washings from the bomb are diluted to 50 ml. Coal samples can be burned without the combustion aid but oil shales are essentially non-combustible and need the white oil.

Sulfur forms in coal were determined by the ASTM procedure [2]. The coal leachability test was done as specified by the U.S. Environmental Protection Agency [3].

Results and discussion

Evaluation of columns. Two types of anion separator columns are available from Dionex for ion chromatographic separations: the "normal" S1 columns and the more recent S3 columns which are fast flowing. Only small variations in the calibration from day to day or over a period of seven months were observed. Thus, in principle, daily calibration is unnecessary, but in practice, the system was calibrated at least twice a day. The retention time of the S3 columns is about the same as that of S1 columns for rapidly eluting anions (fluoride, chloride, and nitrite) but is much shorter for slowly eluting anions (phosphate, bromide, nitrate, and sulfate). Overall, about two complete separations can be completed with S3 columns in the time needed for one separation with S1 columns. The S3 columns have sensitivity similar to S1 columns for fluoride, chloride, and phosphate, but much higher sensitivity for nitrite, bromide, and sulfate. For the rest of this work, fast S3 columns were used.

Oxygen bomb combustion. This procedure was evaluated earlier for organic-based materials with satisfactory results [1]. Water and dilute sodium carbonate solution are equally good as the absorbing medium in the bomb combustion of coal or oil shale. When bromine or iodine is determined, 100 mg of hydrazine is added to the absorbing solution, to reduce all the bromine and iodine species to bromide or iodide, respectively. Without hydrazine, disproportionation reactions may cause low bromine and iodine results. A serious difficulty encountered in the i.c. separation of nitrate from the decomposed samples was an exceedingly large blank. This excessive nitrate resulted from the oxidation of nitrogen in the air trapped in the Parr bomb. Purging of the bomb with high-purity oxygen for 10 min reduced the blank to an insignificant level that did not interfere with the determination of true nitrate or sulfate content.

Comparison of ion chromatography with other techniques. Before the advent of ion chromatography, various anions in the fuel matrices were determined in this laboratory by other procedures. Table 1 compares the i.c. data with ion-selective electrodes, polarography, and x-ray fluorescence

TABLE 1

Comparison of ion chromatography with ion-selective electrodes (i.s.e.), polarography (pol.) and x-ray fluorescence (x.r.f.)

Sample	Fluorine ($\mu g\ g^{-1}$)		Bromine		Chlorine ($\mu g\ g^{-1}$)	
	I.c.	I.s.e.	I.c.	I.s.e.	I.c.	I.s.e.
Tetrabromobenzene	—	—	66.9%	67.2%	—	—
Dibromonaphthalene	—	—	55.3%	55.9%	—	—
1632A Coal	252	200	61 ppm	60 ppm	789	770
1632 Coal	71	90	—	—	915	930

	Sulfite ($\mu g\ ml^{-1}$)		Sulfate ($\mu g\ ml^{-1}$)	
	I.c.	Pol.	I.c.	Pol.
Coal Leachate 1	19	17	20	27
Coal Leachate 2	7540	7532	9032	9010

	Phosphorus ($\mu g\ ml^{-1}$)		Sulfur (%)	
	I.c.	X.r.f.	I.c.	X.r.f.
Coal Leachate 1	20	19	—	—
1632A Coal	—	—	1.37	1.48

measurements for six anions in coal, coal leachates, and organic compounds. Except for the coal leachates, all samples were prepared by Parr bomb combustion. Agreement between results from i.c. and other techniques tested is good, confirming that i.c. can be used as a replacement for more time-consuming techniques.

Analysis of fuel standards. Table 2 gives some typical results obtained by the Parr oxygen bomb combustion/chromatography procedure for three NBS standard coals, one fuel oil, and two USGS standard oil shales. The results are in fair agreement with available certified or published values for these standards. There are inadequate data published on fluorine values to make meaningful comparisons. Agreement for chlorine in coal standards is good. Agreement for nitrogen and sulfur is satisfactory. From the replicate runs indicated in Table 2, the average imprecision of the present results appears to be about 6% for fluorine, chlorine, and nitrogen, and about 2% for sulfur. The precision for shale samples is poorer than that for coal samples, probably reflecting the difficulty in complete combustion of the shale samples.

Determination of sulfur species in coal. The difficulties in the ASTM determination can be overcome by using the ion chromatographic determination of sulfate. Normally, with fast anion columns and the standard eluent of 0.003 M $NaHCO_3$ + 0.0024 M Na_2CO_3, the retention time for sulfate is 10 min. However, this time can be reduced to 5 min by using different eluents, such as 0.006 M Na_2CO_3, or 0.005 M Na_2CO_3 + 0.004 M NaOH.

TABLE 2

Results for coal and oil shale

Sample	Fluorine (ppm)		Chlorine (ppm)		Nitrogen (%)		Sulfur (%)	
	Present	Found	Present	Found	Present	Found	Present	Found
Coal: NBS-1632	90 [4]	71	962 [4]	915	1.3 [4]	1.01	1.35 [4]	1.22
Coal: NBS-1632A[a]	—	210 ± 10	784 [5]	743 ± 46	1.27 [5]	1.72 ± 0.06	1.62 ± 0.03 [6]	1.37 ± 0.01
Coal: NBS-1635[b]	—	77 ± 1	26 [5]	28 ± 2	1.0 [5]	0.95 ± 0.01	0.33 ± 0.03 [6]	0.33 ± 0.01
Fuel oil: NBS-1634A[b]	—	—	—	—	—	1.23 ± 0.02	2.14 ± 0.02 [6]	2.12 ± 0.01
Shale: USGS-SGR[c]	—	—	—	—	—	—	1.90 [7]	1.71 ± 0.05
Shale: USGS-SCO[c]	—	—	—	—	—	—	1.64 [8]	
							0.12 [9]	0.052 ± 0.001
							0.06 [7, 8]	

[a] 5 replicates. [b] 3 replicates. [c] 4 replicates.

TABLE 3

Sulfur species in coal standards[a] by ion chromatography and i.c.p.e.s.

Standard	Sulfate sulfur (%)		Pyritic sulfur (%)		
	Certified	I.c.	Certified	I.c.	I.c.p.e.s.[b]
AR-773	0.02	0.01	0.07	0.097	0.072
AR-778	0.03	0.03	0.49	0.62	0.60
AR-779	0.02	0.03	0.68	0.68	0.85
AR-780	0.13	0.15 ± 0.01[c]	0.74	0.52	0.84
AR-782	0.06	0.05	1.19	1.40	1.27
Illinois 6	0.53	0.57	0.63	0.56	0.66

[a]Standards were obtained from Alfa Resources. Certified results were obtained by the ASTM procedure. [b]Calculated from iron values determined by i.c.p.e.s. [c]Average of three measurements.

The sulfate peak is resolved quite well from the chloride and nitrate peaks when the concentrations of these three ions are roughly the same. However, when the amount of chloride or nitrate present is much larger than that of sulfate, the signal-to-noise ratio for sulfate is poor. Use of silver acetate to precipitate silver chloride, or a halide suppressor column, did not reduce this problem. It is still feasible to use the chloride evaporation step from the

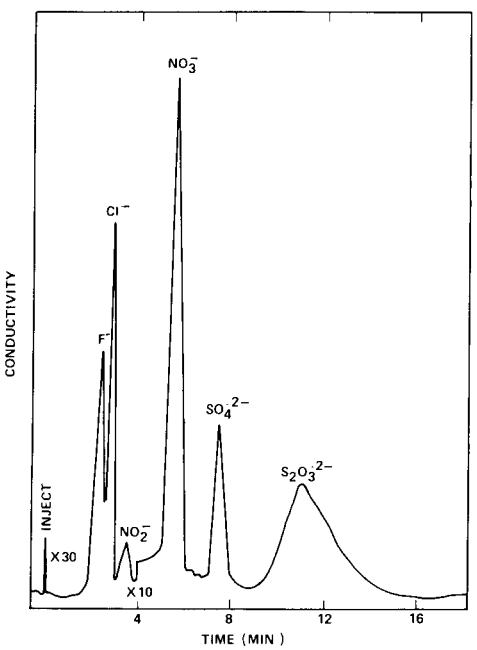

Fig. 1. Ion chomatograph of Green River oil shale Fischer Assay water. Eluent: 2.4 mM Na_2CO_3 + 3 mM $NaHCO_3$.

ASTM procedure before the sample is subjected to ion chromatography; this removes most of the chloride from the sample.

Conventionally, the pyritic sulfur in coal is determined after the nitric acid extraction by measuring the attached iron by atomic absorption or inductively-coupled plasma emission spectrometry (i.c.p.e.s.). However, ion chromatography of the nitric acid extract was found to give results equivalent to the certified or i.c.p.e.s. results within the uncertainty allowed by the ASTM. The results for sulfur in coal standards are given in Table 3. Agreement between the present results and the certified values is good. The results for pyritic sulfur are also in close agreement.

Oil shale products. Ion chromatography is well suited for the identification of anions in shale wastewaters. Figure 1 shows an ion chromatogram of wastewater obtained by subjecting Green River oil shale to Fischer assay retorting. Oil shale and kerogen require Parr bomb combustion; shale leachates and wastewaters require only a simple dilution.

The authors thank R. B. Williams for his encouragement and keen interest in this work.

REFERENCES

1 R. A. Nadkarni, Am. Lab., August (1981) 22.
2 Am. Soc. Test. Mater., Book No. 26, D-2492 (1981).
3 U.S. Environmental Protection Agency, Federal Register, 43 (1978) 243.
4 R. A. Nadkarni, Anal. Chem., 52 (1980) 929.
5 M. P. Failey, D. L. Anderson, W. H. Zoller, G. E. Gordon and R. M. Lindstrom, Anal. Chem., 51 (1979) 2209.
6 National Bureau of Standards Certificate of Analysis.
7 B. P. Fabbi and L. F. Espos, USGS Prof. Paper 840 (1976) 89.
8 K. L. Evans, J. G. Tarter and C. B. Moore, Anal. Chem., 53 (1981) 925.
9 L. G. Schultz, H. A. Tourtelot and F. J. Flanagan, USGS Prof. Paper 840 (1976) 21.

Analytica Chimica Acta, 146 (1983) 267—270
Elsevier Scientific Publishing Company, Amsterdam — Printed in The Netherlands

Short Communication

THE DETERMINATION OF URANIUM, THORIUM, YTTRIUM, ZIRCONIUM AND HAFNIUM IN ZIRCON

N. KORTE*, M. KOLLENBACH and S. DONIVAN

Bendix Field Engineering Corporation (Contractor to U.S. Department of Energy), Grand Junction Area Office, Grand Junction, CO 81502 (U.S.A.)

(Received 19th July 1982)

Summary. Inductively-coupled plasma emission spectrometry is used for the determination of selected elements in zircon separates. Zirconium, hafnium and yttrium can be determined directly. Thorium is measured after an extraction/concentration step with tri-n-octylphosphine oxide, and back-extraction into dilute sulfuric acid. Uranium was more easily determined by the fused-pellet fluorimetric method. This scheme proved to be very successful, yielding results with apparent imprecision and inaccuracy of 2—6%.

The elemental content of zircon separates from whole rock provides the geochemist with considerable information. For example, elevated concentrations of uranium and thorium are an indication of a more highly differentiated magma and a better source rock for uranium deposits [1]. The yttrium content can be related to the isostructural relationship of xenotime and zircon [2]. Zirconium/hafnium ratios can be used as a differentiation index for intrusive rocks [3]. For these reasons, determinations of U, Th, Y, Zr and Hf in zircons are important. These are difficult determinations because of the refractory nature of the mineral. Techniques based on multiple extractions and ion exchange [4] are possible but are exceedingly tedious. Methods involving x-ray fluorescence [5], mass spectrometry [6, 7], and neutron activation [8] all have one or more serious limitations. This report describes the use of a digestion procedure coupled with an inductively-coupled plasma emission spectrometric (i.c.p.e.s.) system for quantifying Th, Y, Zr and Hf and with a fluorescence method for uranium [4].

Experimental

Whole rock samples were collected from various locations in the Western United States by company geologists. The zircon separates were obtained by the petrology laboratory using standard methods [9].

Digestion. Sodium hydroxide solution (1 ml, 25% w/v) is dried in a platinum dish to provide an even coating of sodium hydroxide. Up to 0.25 g of zircon is added and mixed with 0.85 g of sodium peroxide. The dish is heated in a furnace at 490°C for 2.5 h, cooled, and added to a beaker of water to stand overnight. Then 10 ml of concentrated nitric acid is added, and the

beaker is heated on a hot plate for about 15 min. The dish is then removed, and heating is continued until the volume is reduced to approximately 35 ml. The solution is cooled, diluted to 50 ml, and transferred to a plastic bottle.

Uranium. An aliquot (1 ml) of sample solution, 1 ml of 2 M HNO_3, 20 ml of saturated aluminum nitrate solution, 1 ml of ammonia liquor, and 5 ml of ethyl acetate are added to a glass vial in that order. The vial is capped and shaken for 2 min. An aliquot (250 μl) of the organic phase is pipetted into a 2-cm diameter platinum dish, dried, and fused with 0.5 g of 98% NaF/2% LiF at 1000°C for 3.5 min using a rotary fusion burner (EDA, What Ridge, CO). The fluorescence of the pellet is then measured and compared to standards in a Jarrell-Ash Model 32-000 fluorimeter.

Thorium. To a centrifuge tube are added 0.5 g of axalic acid, 20 ml of sample solution, 10 ml of 2 M HNO_3, and 5 ml of 2% tri-n-octylphosphine oxide in cyclohexane, in that order. The tube is capped and shaken for about 2 min. The organic phase is transferred to another tube containing 10 ml of 0.3 M H_2SO_4. The extraction is repeated and the organic phases are combined. The thorium is back-extracted for 5 min and quantified in the aqueous phase by i.c.p.e.s.

Zirconium, hafnium and yttrium. An aliquot (2 ml) of sample solution is diluted to 10 ml with 2 M HNO_3. The elements are quantified directly by i.c.p.e.s.

Inductively-coupled plasma emission spectrometry. All measurements were made with a Perkin-Elmer Model 5000 inductively-coupled plasma spectrometer with a cross-flow nebulizer and demountable torch [10]. The wavelengths used were: Th, 353.96; Zr, 357.68; Hf, 277.34; and Y, 371.03 nm. Argon pressures were set according to the manufacturer's instructions. All measurements were taken at a viewing height of 15 mm with a 1-s integration. Slight baseline shifts were encountered for thorium and yttrium, hence background corrections were made by subtracting the readings 0.05 nm above the thorium line and 0.05 nm below the yttrium line. The most prominent thorium lines suffered from uranium, zirconium, and titanium interferences. The line at 353.96 nm is less intense than was required; hence the extraction was designed to provide both a cleaner matrix and a factor of two concentration of thorium.

Because uranium has no strong emission lines, even with a plasma source, the fluorimetric method was used to quantify uranium.

Results and discussion

Sample decomposition. Zircon is not appreciably attacked by mineral acids. It can be dissolved by fusion with lithium metaborate [11]. However, the flux-to-sample ratio could not be decreased below twenty without requiring fusion times of several hours. In addition, the relatively low solubility of lithium metaborate required more dilution. Although the dilution was not a problem for Zr and Hf, it was undesirable for the other elements. The method finally chosen was reported by Bock [12] and employs both

sodium hydroxide and peroxide to decompose the sample. At 490°C, the attack on the platinum ware was slight.

Thorium determinations. Because the nine most prominent thorium lines all have direct spectral overlaps with one or more elements likely to be present in zircons, tri-n-octylphosphine oxide was used to separate thorium from the principal interferences, namely Ti, Fe, Zr and rare earths [14]. Oxalic acid was added to inhibit the extraction of Zr [4]. The efficiency of the extraction and back-extraction was studied with synthetic zircon solutions and standard additions. Recovery was always within an experimental error of 100% when a double extraction was performed.

Accuracy. It was difficult to check the accuracy by comparison with standard reference materials. There are no standard zircon samples, and standard rock samples containing similar amounts of the elements being determined are rare. Table 1 displays results for some standard reference materials having quantities of some of the elements similar to that of zircons. The Zr and Hf contents are significantly less than in the zircons but were the highest available. There samples do represent a wide variety of sample types. In every case, the method yielded results within 3% of the expected value.

Precision. The imprecision associated with the method was evaluated by processing five Precambrian Granite samples. Concentrations and standard deviations obtained for U (ppm), Th (ppm), Y (ppm), Hf (%) and Zr (%) were 968 ± 57, 364 ± 8, 987 ± 36, 1.18 ± 0.03 and 41.4 ± 1.4, respectively. Some Laramie Granite samples collected 25 miles apart on separate sampling trips gave similar deviations for Hf and Zr, and substantially larger deviations for U, Th and Y.

These results show that the i.c.p.e.s. method is relatively straightforward for determining some refractory elements in a difficult sample matrix.

The petrological separations were performed under the direction of M. Eatough. The authors also thank S. M. Rush for helpful suggestions and discussions. This work was supported by the Grand Junction, Colorado, Office of the U.S. Department of Energy for the Uranium Resource Assessment Program.

TABLE 1

Results for standard reference materials[a]

Sample	Type	Source	U		Th		Y		Zr		Hf	
Dh-1	Uranium/thorium ore	CANMET	1764	(1770)	1062	(1040)	195	(180)	—		—	
BL-4	Uranium ore	CANMET	1674	(1730)	—		—		—		—	
SY-3	Syenite	CANMET	682	(640)	996	(980)	734	(740)	—		—	
GSE	Glass	USGS	446	(470)	—		492	(490)	467	(480)	506	(500)
STM-1	Nepheline syenite	USGS	—		—		—		1227	(1260)	—	
NBS-696	Bauxite	NBS	—		—		—		1092	(1036)	—	

[a]All results are given in ppm ($\mu g\ g^{-1}$). The certified values are given in parentheses.

REFERENCES

1 R. K. Nishimori, P. C. Ragland, J. J. W. Rogers and J. K. Greenberg, U.S. DOE Open-File Report GJBX-13, 1977.
2 W. A. Deer, R. A. Howie and J. Zussman, An Introduction to the Rock Forming Minerals, Longmans, London, 1966.
3 J. R. Butler and A. J. Thompson, Geochim. Cosmochim. Acta, 29 (1965) 165.
4 A. I. Busev, V. G. Tiptsova and V. M. Ivanov, Handbook of the Analytical Chemistry of the Rare Elements, Ann Arbor-Humphrey Science Publishers, Ann Arbor, 1970.
5 V. V. Lyakhovich and I. D. Shevaleyevskii, Geokhimiya, 5 (1962) 440.
6 H. Nagasawa, Earth Planet Sci. Lett., 9 (1970) 359.
7 R. V. Gentry, T. J. Sworski, H. S. McKown, D. H. Smith, R. E. Eby and W. H. Christie, Science, 216 (1982).
8 P. A. Dalheim and R. J. Kuryvial, U.S. DOE Open-File Report GJBX-103, 1980.
9 G. Müller, Methods in Sedimentary Petrology, Hafner Publishing Company, New York, 1967.
10 G. F. Wallace, V. V. Pirc and R. D. Ediger, Winter Conference on Plasma Spectrochemistry, Orlando, FL, January 1982, Paper No. 81.
11 N. Korte, M. Hollenbach and S. Donivan, At. Spectrosc., 3 (1982) 3.
12 R. Bock, A Handbook of Decomposition Methods in Analytical Chemistry, International Textbook Co., London, 1979.
13 R. K. Winge, V. J. Peterson and V. F. Fassel, Appl. Spectrosc., 33 (1979) 3.
14 J. C. White and W. J. Ross, Separations by Solvent Extraction with Tri-n-octylphosphine Oxide, National Research Council, Nuclear Science Series, NAS-NS-3102, 1961.

ANALYTICA CHIMICA ACTA, VOL. 146 (1983)

AUTHOR INDEX

Vol. 146

ACA announcements

ANNOUNCEMENTS OF MEETINGS

20th ANNIVERSARY OF THE INTERNATIONAL SYMPOSIUM ON ADVANCES IN CHROMATOGRAPHY

The 20th Anniversary of the International Symposium on Advances in Chromatography will be held on Oct. 3–6, 1983, in Amsterdam, The Netherlands. The scope of the meeting will cover papers and informal discussion groups by outstanding researchers from throughout the world in all fields of chromatography. In particular, new developments in gas, liquid, and high-performance thin-layer chromatography will be included. There will also be a commercial exhibition of the latest instrumentation and books. Participation in the symposium will be on the basis of invited papers as well as unsolicited contributions. Authors desiring to present papers must submit 200-word abstracts by April 1, 1983. Complete manuscripts of accepted authors will be due on Oct. 3, 1983, at the meeting in Amsterdam. Special separate intensive two-day short courses on high resolution capillary columns, HPLC, GC–MS, and computer chromatography will be available on Friday and Saturday, Sept. 30 and Oct. 1, just prior to the meeting. All correspondence pertaining to the symposium, short courses, and exhibition space should be directed to: Professor A. Zlatkis, Chemistry Department, University of Houston, Houston, TX 77004, U.S.A.

8th INTERNATIONAL SYMPOSIUM ON COLUMN LIQUID CHROMATOGRAPHY

The 8th International Symposium on Column Liquid Chromatography will be held in New York City at the New York Statler Hotel on May 20–26, 1984. This will be the eighth of a symposium series that deals with recent developments in high-performance liquid chromatography and related techniques. These symposia are organized annually and alternately in the United States and a European country.

The scientific program of the symposium will consist of invited and contributed lectures and posters. Emphasis will be placed on the fundamentals and applications of HPLC in various areas of the life sciences and in industry.

An exhibition of modern liquid chromatographic equipment and accessories will be held concurrently with the symposium.

Requests for the first circular and inquiries should be directed to the Chairman of the symposium, Professor Cs. Horváth, Yale University, Department of Chemical Engineering, P.O. Box 2159, Yale Station, New Haven, CT 06520, U.S.A. Tel: (203) 436-1271.

4th INTERNATIONAL SYMPOSIUM ON ISOTACHOPHORESIS – ITP 84

The above-mentioned symposium will be held on Sept. 2–5, 1984, at the Pharmaceutical Faculty of the Charles University, Hradec Králové, Czechoslovakia, under the auspices of the Czechoslovak Chemical Society, the Institute of Organic Chemistry and Biochemistry and Institute of Analytical Chemistry of the Czechoslovak Academy of Sciences, the Faculty of Natural Sciences of the Charles University and the Chemical Institute of the University of Komenský.

The scientific program will comprise plenary lectures and communicated papers and/or posters on the fundamental aspects of isotachophoresis and related methods, their application in biochemical, clinical, environmental, pharmaceutical, physical and industrial (agriculture, food industry, etc.) fields. An exhibition of isotachophoretic equipment will be included. In addition, an intensive course on isotachophoresis, covering fundamental and practical aspects, will be held during the symposium.

The deadline for registration is February 1, 1984. For further information contact: ITP 84, Dr. Z. Prusik, C.Sc., Institute of Organic Chemistry and Biochemistry ČSAV, Flemingovo nám. 2, CS-166 10 Praha 6, Czechoslovakia.

BIOCHEMICAL ANALYSIS PRIZE 1984

The German Society for Clinical Chemistry awards the Biochemical Analysis Prize every two years at the Biochemische Analytik Conference in Munich, G.F.R. The prize of DM 10.000,- - is donated by Boehringer Mannheim GmbH for outstanding and novel work in the field of biochemical analysis or biochemical instrumentation or for significant contributions to advancement in experimental biology especially relating to clinical biochemistry. Competitors for the 1984 prize (to be awarded at the 1984 conference, which will take place on April 10–13, 1984) should submit papers concerning one theme (either published or accepted for publication between Oct. 1, 1981, and Sept. 30, 1983) before November 15, 1983, to: Prof. Dr. Dr. I. Trautschold, Secretary of the Biochemical Analysis Prize, Medizinische Hochschule Hannover, Konstanty-Gutschow-Strasse 8, 3000 Hannover 61, G.F.R.

Continued from outside back cover)

Elsevier Scientific Publishing Company, 1983

Printed in The Netherlands.

CONTENTS

Abstracted, Indexed in: Anal. Abstr.; Biol. Abstr.; Chem. Abstr.; Curr. Contents Phys. Chem. Earth Sci.; Life Sci.; Index Med.; Mass Spectrom. Bull.; Sci. Citation Index; Excerpta Med.)

(Continued on inside back cover)